The role of mitochondria in defence mechanisms of human endothelial cells

Dr James Richard Wilkinson

A thesis submitted for the Degree of Doctor of Philosophy in University College London

July 2010

Declaration of ownership

I, James Richard Wilkinson, declare that this thesis is the result of my own work. All help and advice has been acknowledged and primary and secondary sources of information have been properly attributed.

Dr James Richard Wilkinson

BSc. (Hons), MB BS, MRCP (UK)

Abstract

Introduction: Mitochondria are considered to be the powerhouse of the cell being the primary generators of ATP, they also have numerous other important functions including; being the main generator of reactive oxygen species (ROS) and a central role in apoptosis. As the main intracellular source of ROS, many people believe that mitochondria play a significant role in ageing. Senescence is associated with ageing and has been associated with atherosclerotic vascular disease. The concept of human cells lacking functional mitochondria (Rho 0 cells) is not new and was first described by Attardi et al in 1989. However, most of this work has been done on immortalised cell lines.

Aims: To see if it is possible to generate and characterise Rho 0 human endothelial cells. To use these cells as a tool to investigate the mechanisms by which they respond to stress and whether differences in ROS production and/or antioxidant defences account for any differences observed.

Methods: Human Umbilical Vein Endothelial Cells (HUVEC) were grown in media supplemented with glucose and uridine in the presence of low dose ethidium bromide. Rho 0 status of the cells was confirmed by auxotrophy for uridine, quantitative PCR for mitochondrial-encoded gene expression and western blots for mitochondrial-encoded proteins.

Results: The Rho 0 status of the cells was confirmed by; auxotrophy for uridine (Rho 0 cells die in medium lacking uridine), absence of mitochondrial-encoded genes (subunit-1 of complex IV and subunit-6 of subunit V) and lack of expression of the mitochondrial-encoded protein subunit-1 of complex IV. Rho 0 cells are resistant to both stress-induced senescence and apoptosis. They produce less ROS and have upregulated antioxidant defences.

Conclusions: It is possible to grow Rho 0 HUVEC. These cells are a useful tool for studying the role of mitochondria in senescence and apoptosis in the cardiovascular system.

Acknowledgements

I am most indebted to my lovely wife Olive and our two beautiful daughters Annabelle and Rebecca for their love and endless support. I hope they will forgive me for the substantial family time we did not spend together because of my working on this project. I am deeply grateful to my parents and family for their continued support throughout this work and my career.

I am very grateful to all of Salvador's group and everyone in the Pharmacology department (2.3) at the Wolfson. I am very grateful to Neale Foxwell for his ongoing support throughout this work, especially with tissue culture. I am exceptionally grateful to Sergio Colombo for his supervision and for teaching me molecular biology so well and inspiring me. I am very grateful to Ying Hong, Ana Gutierrez Del Arroyo and Joaquim Hernandez-Martin for their help and support throughout this work. Catherine Panayiotou and Chris Skene thank you both for your moral support, friendship and advice throughout my time in research.

A very special thanks to Professor Salvador Moncada for informally overseeing my work in the final year, truly inspiring me and teaching me the highest standards of basic science.

Thanks to Professor Chris Boshoff for being my second supervisor. Finally thank you to Professor Jorge Erusalimsky for supervising me, teaching me meticulous attention to detail, rigorous scientific discipline and editing my thesis with great care.

Publications arising from this work

Work described in this thesis has contributed to or given rise to the following manuscripts:

1) Marisol Quintero, Sergio L. Colombo, Andrew Godfrey and Salvador Moncada (2006). Mitochondria as signalling organelles in the vascular endothelium. Proceedings of the National Academy of Science of the United States of America. **103** (14): 5379-5384.

The Rho 0 cells that were supplied for the experiments in this paper were provided by my work. I undertook all the work preparing the Rho 0 cells, described in the Materials and Methods under the subheading 'Cells and Reagents'. This paper constitutes the first published description of Rho 0 endothelial cells in the literature. Jorge Erusalimsky (my supervisor) was acknowledged for his critical reading of the paper. However, I was not acknowledged for my contribution to this paper.

2) **James R. Wilkinson**, Sergio L. Colombo, Jorge Erusalimsky (2006). Characterisation of human endothelial cells lacking mitochondrial DNA (Rho0 cells): a model system to study the involvement in mitochondria in cellular senescence. European Heart Journal. **27** (supplement 1): 875.

Oral presentation. World Congress of Cardiology, Barcelona, Sept 2006.

Table of contents

Table of abbreviations

$\Delta\psi_m$	- Mitochondrial membrane potential
γ-GCS	- Gamma-glutamylcysteine synthetase
ρ^0 cell	- Rho 0 cells, lacking functional mitochondrial DNA
ρ^+ cell	- Cells with functional mitochondrial DNA
ACE	- Angiotensin converting enzyme
Acetyl CoA	- Acetyl coenzyme A
ADP	- Adenosine Diphosphate
AIF	- Apoptosis-inducing factor
ALDHA1	- Aldehyde dehydrogenase
AMPK	- AMP-dependent protein kinase
AMP	- Adenosine 5'-monophosphate
ANT	- Adenine nucleotide translocator
ANOVA	- Analysis of Variance
Apaf-1	- Apoptotic protease-activating factor-1
APO-1	- Fas or CD95
APO-2	- TNF-related apoptosis-inducing ligand
APS	- Ammonium Persulphate
ARB	- Angiotensin receptor blockers
ARE	- Antioxidant responsive element
ARF	- Alternate reading frame
ATII	- Angiotensin II
ATP	- Adenosine 5'-triphosphate
ATPase	- Adenosine Triphosphate synthase
AU	- Arbitrary units

Bad	- Bcl-2/Bcl-X_L-associated death promoter
Bax	- Bcl-2–associated X
BCA	- Bicinchoninic acid
Bcl-2	- B-cell lymphoma 2
BH3	- Bcl-2 homology-3
Bid	- BH3 interacting domain death agonist
BrdU	- 5-bromo-2'-deoxyuridine
BSA	- Bovine serum albumin
BSO	- Buthionine sulfoximine
CcO	- Cytochrome C oxidase
cGMP	- Cyclic guanosine 3',5'-monophasphate
CMV	- Cytomegalovirus
CPD	- Cumulative population doubling
CT	- Cycle threshold
Cu_A	- Binuclear centre
CuZnSOD	- Copper-zinc superoxide dismutase
CVD	- Cardiovascular disease
Cys	- Cysteine
dATP	- Deoxyadenosine triphosphate
DCF	- Dichlorofluorescein
DCFH	- Non-fluorescent dichlorofluorescein
dCTP	- Deoxycytidine triphosphate
DEAE	- Diethylaminoethyl
dGTP	- Deoxyguanosine triphosphate
DiI-Ac-LDL	-1,1'-dioctadecyl-3,3,3',3'-tetramethyl-indocarbocyanine perchlorate labelled acetylated-low density lipoprotein

DISC - Death-induced signalling complex

DNA - Deoxyribonucleic acid

DNA POLG - DNA polymerase gamma

dNTP - Deoxynucleotide phosphate

DOG - Deoxy-D-glucose

DMSO - Dimethyl Sulfoxide

DTNP - 5,5'-dithiobis-2-nitrobenzoic acid

dNTP - Deoxynucleotide phosphate

DPI - Diphenyleneiodonium chloride

DTT - DL-Dithiothreitol

EB - Ethidium Bromide

ECL - Enhanced chemiluminescence

EDRF - Endothelium-derived relaxing factor

EGF - Endothelial growth factor

ETC - Electron transport chain

EDTA - Ethylenediamine-Tetraacetic acid

EGM-2 - Endothelial Growth Medium-2

ELISA - Enzyme-Linked ImmunoSorbent Assay

eNOS - Endothelial nitric oxide synthase

FACS - Fluorescence-activated cell sorting

$FADH_2$ - Reduced flavin adenine dinucleotide

FAD - Flavin adenine dinucleotide

FADD - Fas receptor associated death domain

Fas - Apoptosis-stimulating fragment

FCCP - 4-trifluoromethoxyphenylhydrazone

FCS - Foetal calf serum

FGF - Fibroblast growth factor

FMN - Flavin mononucleotide

FCS - Foetal Calf Serum

GPx - Glutathione peroxidase

GSH - γ-glutamylcysteinylglycine or reduced glutathione

GSSG - Oxidised form of glutathione

GSTP1 - Glutathione transferase P1

GTP - Guanosine 5'-triphosphate

H^+ - Proton

H^+_N - Protons from negative side of matrix

H^+_P - Protons from positive side of matrix

H_2DCFDA - 2′,7′-dichlorodihydrofluorescein diacetate

HEK-293 - Human embryonic kidney-293

HIV - Human immunodeficiency virus

HMG-CoA - Hydroxy methylglutaryl coenzyme A

HO-1 - Heme-oxygenase-1

HUVEC - Human Umbilical Vein Endothelial Cells

ICAM-1 - Intercellular adhesion molecule-1

IGF-1 - Insulin growth factor-1

IL-1β - Interleukin 1 beta

IHD - Ischaemic heart disease

iNOS - Inducible nitric oxide synthase

LB - Luria broth

M2VP - 1-methyl-2-vinylpyridiniumtrifluoromethanesulfonate

mA - Milliampere

MnSOD - Manganese superoxide dismutase

mtDNA - Mitochondrial DNA

mtROS - Mitochondrial ROS

MTP - Mitochondrial permeability transition pore

NAC - N-Acetyl Cysteine

NAD^+ - Oxidised form of NADH

NADH - Nicotinamide adenine dinucleotide

NADPH - Nicotinamide adenine dinucleotide phosphate

NCBI - National Centre for Biotechnology Information

ND - NADH dehydrogenase

NF-κB - Nuclear factor kappa-light-chain-enhancer of activated B cells

nNOS - Neuronal nitric oxide synthase

NOS - Nitric oxide synthase

Nox - NADPH oxidase

Nrf2 - Nuclear factor-erythroid 2-related factor 2

NS-GPxs - Nonselenium GPx-like proteins

$OH^{\bullet}$ - Hydroxyl radical

O_2^{2-} - Peroxy derivative

PBS - Phosphate Suffered Saline

PCR - Polymerase chain reaction

PD - Population doublings

PGC1α - Peroxisome-proliferator-activated receptor γ co-activator 1α

PGI_2 - Prostaglandin I_2

PMOR - Plasma membrane oxidoreductase

POD - Peroxidase

PS - Phosphatidylserine

·Q - Ubisemiquinone

Q	- Ubiquinone
QH_2	- Ubiquinol
qPCR	- Quantitative PCR
RFU	- Relative fluorescence units
RNA	- Ribonucleic acid
ROS	- Reactive oxygen species
RPE	- R-phycoerythrin
RPM	- Revolutions per minute
RT-PCR	- Reverse Transcriptase Polymerase Chain Reaction
SA-β-gal	- Senescence-associated β-galactosidase
SDM	- Site-Directed Mutagenesis
SDS-PAGE	- Sodium Dodecyl Sulphate Polyacrylamide Gel Electrophoresis
SEM	- Standard error of mean
sGC	- Soluble guanylate cyclase
siRNA	- Small interfering RNA
SIRT1	- Sirtuin-1
SOD1	- Copper-zinc superoxide dismutase
SOD2	- Manganese superoxide dismutase
SIPS	- Stress-induced premature senescence
STASIS	- Stress or aberrant signalling-induced senescence
TAE	- Tris-Acetate Sodium EDTA
Taq	- *Thermus aquaticus*
TB	- Terrific Broth
*t*BHP	- *Tert*-butyl hydroperoxide
TBS-T	- Tris-Buffered Saline Tween-20
TEMED	- N,N,N',N'-Tetramethylenediamine

TMRM - Tetramethylrhodamine

TNF - Tumour necrosis factor

TNS - Trypsin neutralising solution

tPMET - Transplasma membrane electron transport

TRADD - TNF receptor associated death domain

TRAIL - TNF-related apoptosis-inducing ligand

TRF - Telomere repeat binding factor

Tris-HCl - Tris(hydroxymethyl)aminomethane hydrochloride

TRX - Thioredoxin

Tris-HCl - Tris(hydroxymethyl)aminomethane hydrochloride

TTP - Thymidine triphosphate

Tween - Polyoxyethylene-sorbitan monolaurate

VCAM-1 - Vascular-cell adhesion molecule-1

VWF - Von Willebrand Factor

WIBR - Wolfson Institute for Biomedical Research

WT - Wild Type

List of figures

List of tables

1 Introduction

1.1 ATP and respiration- an overview

Adenosine 5'-triphosphate (ATP) was first discovered and characterised by Fiske and SubbaRow (Fiske and SubbaRow 1929) and first proposed to be the main energy-transfer molecule of the cell by Fritz Lipman in 1941 (Lipman 1941). The hydrolysis of a phospholanhydride bond of ATP, leads to the release of a phosphate group and the production of adenosine diphosphate (ADP), releasing free energy. ATP is the main source of energy in the cell, is essential to most metabolic pathways, and could be considered to be the 'currency of life'. ATP is produced in the process of cellular respiration where up to 32 molecules can be generated from the oxidation of one molecule of glucose to carbon dioxide (CO_2) and water, in the presence of oxygen (O_2) (Rich 2003). The metabolic pathways of respiration can be seen overleaf in figure 01.

Gustav Embden and Otto Meyerhof are first credited with elucidating the full glycolysis pathway in the 1930s (Kresge, Simoni et al. 2005). Glycolysis is the process whereby one molecule of glucose is reduced, through a series of enzymatic steps, to yield two molecules of pyruvate, the reduced form of Nicotinamide adenine dinucleotide (NADH) and two molecules of ATP. In the absence of O_2, each molecule of pyruvate and NADH combine to form the by-product of lactic acid regenerating NAD^+ (the oxidised form of NADH, which is needed to drive glycolysis) and giving a net yield of two molecules of ATP. This process is referred to as anaerobic respiration.

Figure 01 Overview of the reactions of Glycolysis and Kreb's cycle. NADH and reduced flavin adenine dinucleotide (FADH2) donate electrons to the electron transport chain, leading to the production of ATP. In the absence of O2 pyruvate forms lactic acid (anaerobic respiration) giving a net yield of two molecules of ATP.

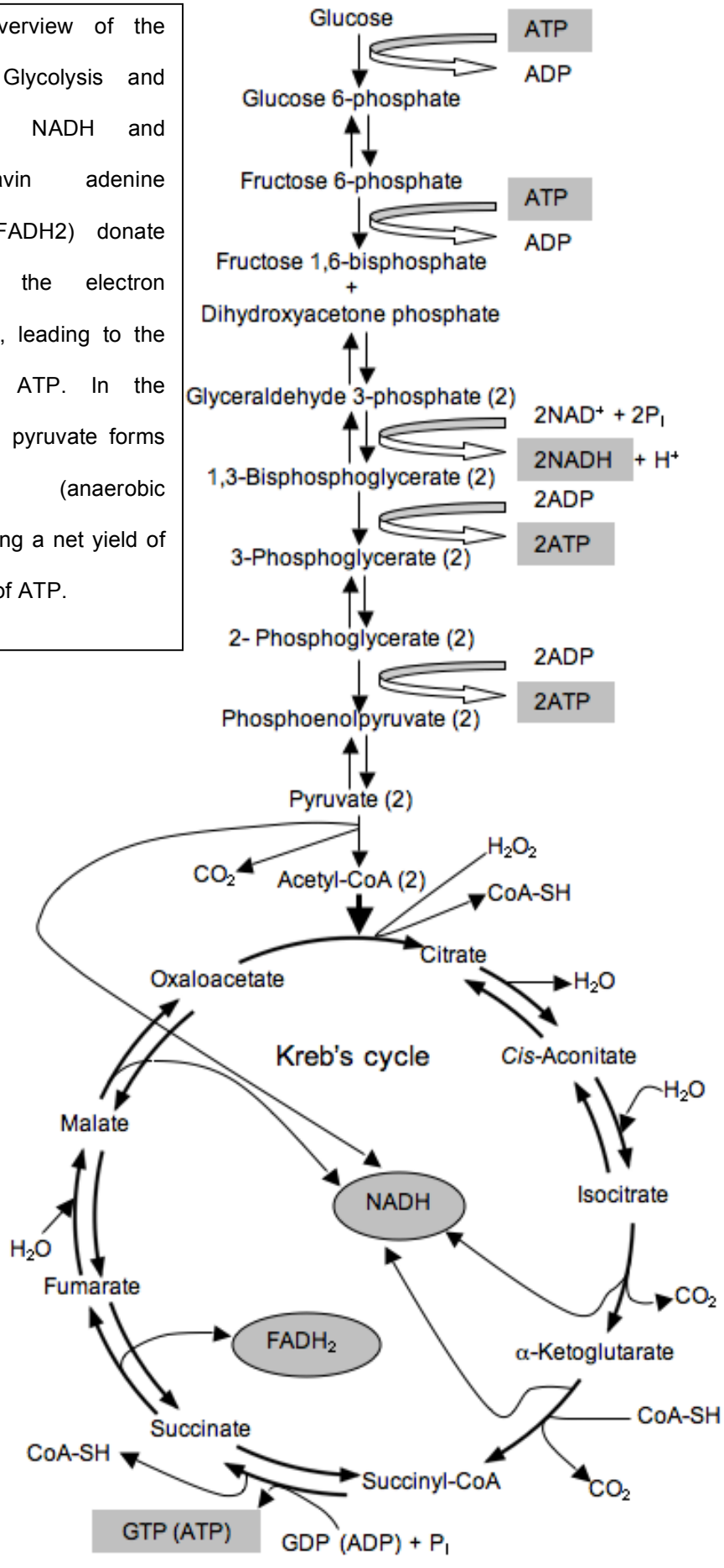

In the presence of O_2 aerobic respiration can occur, where each molecule of pyruvate can be degraded in the mitochondria to acetyl coenzyme A (Acetyl CoA) yielding a molecule of NADH. Alternatively fatty acids can be broken down to acetyl CoA, via the ß-oxidation pathway, to form a supply of acetyl CoA for the citric acid cycle, otherwise known as Krebs cycle, first characterised by Sir Hans Krebs in 1937 (Krebs and Johnson 1937). Acetyl CoA, either from glycolysis or ß-oxidation, is then able enter the citric acid cycle where the carbon atoms of the Acetyl CoA are completely oxidised to yield: CO_2, three molecules of NADH, one molecule of $FADH_2$ and one molecule of guanosine triphosphate (GTP). GTP is able to transfer its terminal phosphate group to ADP yielding one molecule of ATP. NADH and $FADH_2$ are both carriers of high-energy electrons, which are used by the process of oxidative phosphorylation to produce 2.5 and 1.5 molecules of ATP respectively.

1.2 Mitochondria

1.2.1 Overview

Eukaryotes rely on aerobic respiration for a majority of their bioenergetic demands and because this occurs within the mitochondrion they are often thought of as the ‘powerhouse of the cell’. Approximately 1500 million years ago the first ancestral eukaryotic cells developed, these cells were entirely dependent on anaerobic respiration. However as the demands of the cell could not be met the cells had to adopt alternative means of energy supply. Initially they endocytosed aerobic bacteria and developed an endosymbiotic relation with them. Eventually some of the bacterial genes migrated to the genome and the

eukaryotic cells became fully capable of aerobic respiration, as we know them (Brown and Doolittle 1997).

1.2.2 Mitochondrial structure

Mitochondria are mobile, plastic organelles that are 0.5 – 1 µm in diameter and occupy a substantial portion of the cytoplasm. They contain a highly convoluted inner membrane, which contains the enzymes responsible for oxidative phosphorylation (complexes I to IV of the electron transport chain (ETC) and ATPsynthase) and an outer membrane. (see figure 02).

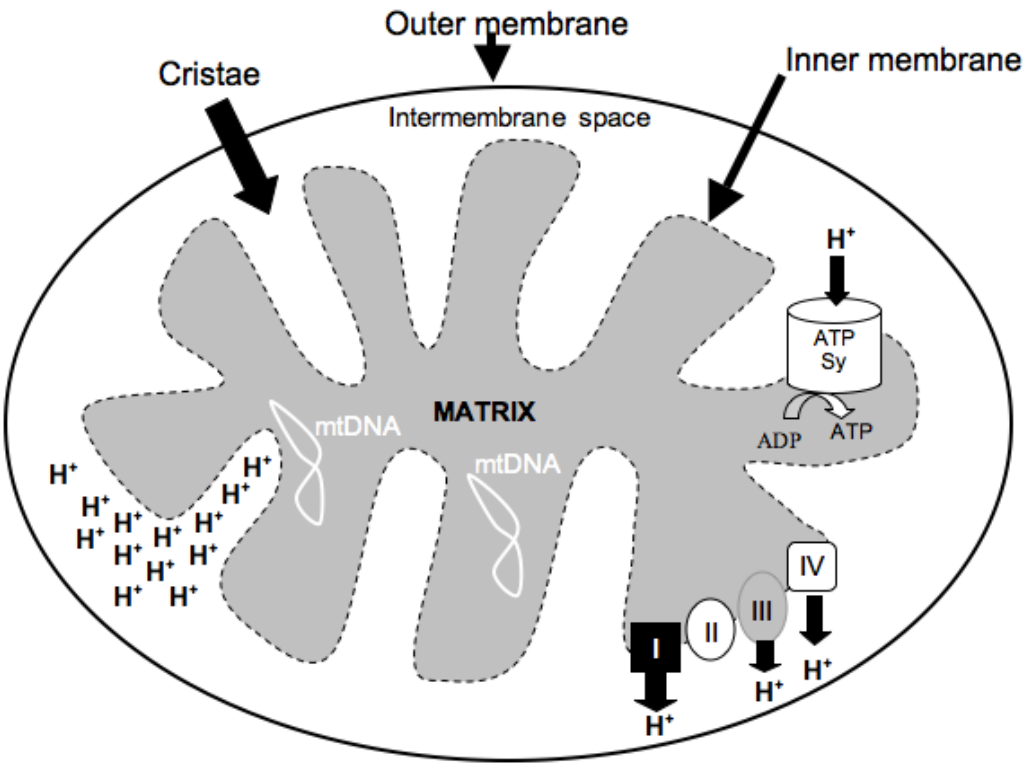

Figure 02 – schematic cartoon of mitochondrion showing components I-IV of the electron transport chain and ATP synthase. Cristae are formed by infolding of the inner membrane.

The matrix contains the enzymes responsible for the oxidation of pyruvate and fatty acids to acetyl CoA and the enzymes responsible for the citric acid cycle. The electron transport chain pumps protons (H^+ ions) through the inner mitochondrial membrane, which is impermeable to protons, and these subsequently pass back through ATP synthase driving the production of ATP (Rich 2003).

1.2.3 The electron transport chain

The electron transport chain is a series of proteins tightly bound to the inner mitochondrial membrane. A schematic diagram of the ETC is shown below in figure 03.

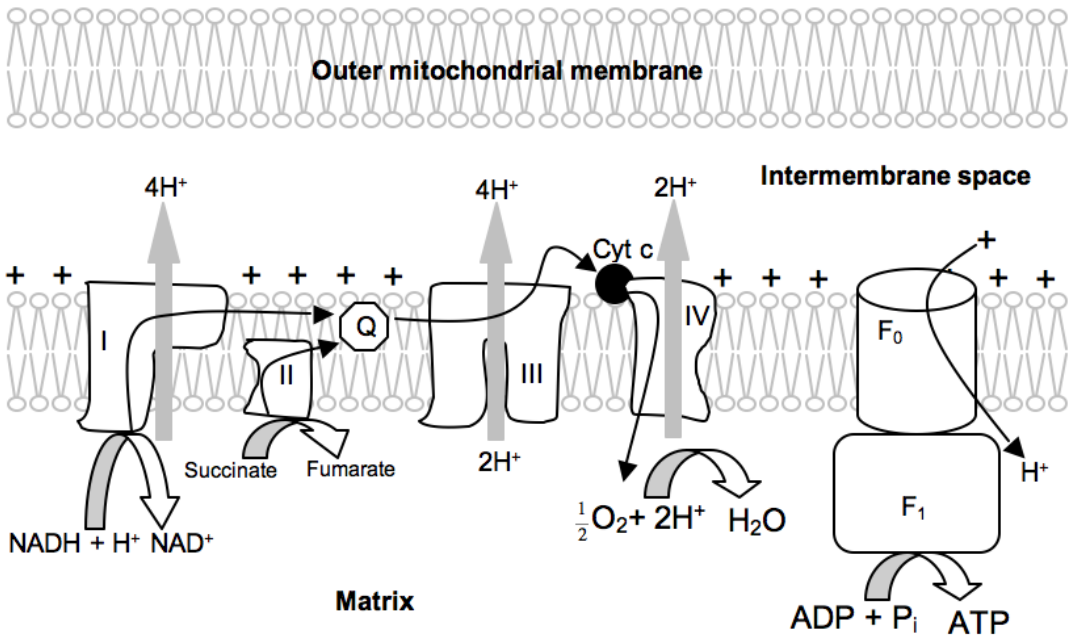

Figure 03 – schematic cartoon of ETC showing components I-IV of the ETC, situated on the inner mitochondrial membrane, and flow of electrons though chain driving proton gradient. The proton gradient drives ATP synthase to produce ATP.

The ETC proteins accept high-energy electrons from NADH and $FADH_2$, which are transferred down the chain. This electron flow maintains a proton gradient across the inner mitochondrial membrane, which drives ATP synthase leading to the formation of ATP and H_2O. NAD+ or FAD respectively are regenerated during this process. The ETC is composed of the following enzyme complexes: complex I (NADH dehydrogenase), complex II (succinate dehydrogenase), complex III (cytochrome *c* reductase) and complex IV (cytochrome c oxidase) (Schultz and Chan 2001).

1.2.3.1 Complex I

Complex I otherwise known as NADH dehydrogenase or NADH: ubiquinone oxidoreducase is a large L-shaped enzyme consisting of at least 45 subunits and having a molecular weight of greater than 900 kDa (Schultz and Chan 2001; Galkin and Moncada 2007). The majority of electrons enter the ETC via this complex. Complex I catalyses the transfer of a hydride ion (the equivalent of a proton and two electrons) from NADH to flavin mononucleotide (FMN), regenerating NAD^+ in the process. The two electrons are passed through a series of iron-sulphur (Fe-S) centers to the Fe-S protein N-2. The electrons are then passed to Ubiquinone (Q, otherwise known as coenzyme Q), which combines with two H^+ ions and is, as a result, reduced to Ubiquinol (QH_2), which diffuses to complex III. This reaction drives the expulsion of four protons into the intermembrane space and is written as the equation:

$$NADH + 5H^+_N + Q \rightarrow NAD^+ + QH_2 + 4\ H^+_P$$

Where H^+_N are protons from the negative side (matrix) and H^+_P are protons from the positive side (intermembrane space).

1.2.3.2 Complex II

Complex II, known as succinate dehydrogenase is much smaller than the other complexes in the ETC. It has 4 subunits and a molecular weight of 125 kDa (Schultz and Chan 2001; Rustin and Rotig 2002). It is the only membrane-bound enzyme in the Kreb's cycle and during the reduction of succinate to fumarate $FADH_2$ is generated, which passes its electrons through a series of Fe-S centers. This eventually leads to the reduction of ubiquinone to QH_2, which subsequently diffuses to complex III.

1.2.3.3 Complex III

Complex III otherwise known as cytochrome bc_1 complex or ubiquinone: cytochrome *c* oxidoreducase consists of 11 subunits and has a molecular weight of 240 kDa (Iwata, Lee et al. 1998; Schultz and Chan 2001). It consists of two cytochromes: cytochrome *b* with its two hemes (b_L and b_H) and cytochrome c_1. Compex III couples the transfer of electrons from QH_2 to cytochrome *c* with the transport of protons from the matrix to the intermembrane space, it achieves this via the Q cycle.

QH_2 carries two electrons but the cytochromes can only accept one. The Q cycle is a two-step process, the net reaction allows QH_2 to be oxidised to Q with two molecules of cytochrome *c* becoming reduced and four protons being transferred to the intermembrane space.

The first reaction involves QH_2 being reduced to Q with two protons being transported to the intermembrane space. Then one electron passes to the Fe-S complex via cytochrome c_1 to cytochrome *c*. The second electron passes via cytochrome b_L and cytochrome b_H to Q which is reduced to ubisemiquinone ($\cdot Q^-$). The reaction equation is:

QH_2 + cyt c_1 (oxidised) $\rightarrow \cdot Q^-$ + $2H^+_P$ + cyt c_1 (reduced)

The second reaction involves QH_2 being reduced to Q with two protons being transported to the intermembrane space. Then one electron passes to the Fe-S complex via cytochrome c_1 to cytochrome *c*. The second electron passes via cytochrome b_L and cytochrome b_H to $\cdot Q^-$ which is reduced, with the addition of two protons to ubiquinol (QH_2). The reaction equation is:

QH_2 + $\cdot Q^-$ + $2H^+_N$ + cyt c_1 (oxidised) $\rightarrow$ QH_2^- + $2H^+_P$ + Q + cyt c_1 (reduced)

The net equation for the Q cycle is:

QH_2 + 2 cyt c_1 (oxidised) + $2H^+_N \rightarrow$ Q + 2 cyt c_1 (reduced) + $4H^+_P$

1.2.3.4 Complex IV

Complex IV is known as cytochrome *c* oxidase and consists of 13 subunits, it has a molecular weight of approximately 200 kDa (Denis 1986; Schultz and Chan 2001). It carries electrons from cytochrome *c* to molecular oxygen. Subunits I, II and III are the most important and are responsible for electron transfer. Two molecules of reduced cytochrome *c* each donate an electron to a binuclear centre consisting of two copper (Cu) ions complexed with the SH-groups of two cysteine (Cys) residues of a binuclear centre (Cu_A). From here the electrons are passed to

a second binuclear centre, consisting of heme a_3 and another copper ion (Cu_B), and transfers them to O_2 bound to heme a_3 resulting in the peroxy derivative (O_2^{2-}). Delivery of two more electrons from cytochrome *c* with the consumption of four protons results in the production of two molecules of water. In addition four protons are pumped from the matrix to the intermembrane space. The equation for the overall reaction of complex IV is:

$$4 \text{ cyt } c \text{ (reduced)} + 8H^+_N + O_2 \rightarrow 4 \text{ cyt } c \text{ (oxidised)} + 4H^+_P + 2H_2O$$

1.2.3.5 ATP Synthase

ATP synthase is an F-type ATPase and is a member of the diphosphate bond hydrolysis-driven transporter family. It is known as an F-type ATPase because it consists of an F_0 subunit (so called because it is inhibited by oligomycin), which sits in the inner mitochondrial membrane and an F_1 subunit (so called because it was the first of the two units discovered), which sits in the matrix. Flow of protons through the F_0 subunit causes “rotational catalysis” whereby protons cause the rotation of F_0 relative to F_1 leading to the generation of ATP. The whole reaction is reversible so ATP can be hydrolysed to drive protons out of the matrix. P-type ATPases are plasma membrane ion transporters and V-type ATPases produce gradients of protons across intracellular membranes, including plant vacuolar membranes, neither of these are discussed in more detail in this thesis.

1.2.4 Mitochondrial deoxyribonucleic acid (DNA)

Mitochondria are unique in that as a result of their evolution from aerobic bacteria their components are encoded by both their own mitochondrial DNA (mtDNA) and nuclear DNA. Mitochondrial DNA contains 37 genes that encode 13 subunits of the electron transport chain, 22 transfer ribonucleic acids (RNAs) and 2 ribosomal RNAs. Mitochondrial DNA is a covalently closed circular DNA that is expressed and replicated within mitochondria (Sato, Nakada et al. 2006). Mitochondrial DNA is a lot simpler in structure than nuclear DNA and is not supercoiled, contains no protective histones, is devoid of introns and has a limited repair capacity (Singh 2006). Mitochondrial DNA is inherited maternally (Cummins 1998). A representative map of mitochondrial DNA, with the components of the respiratory chain encoded by it, is shown in figure 04 (DiMauro and Schon 2003).

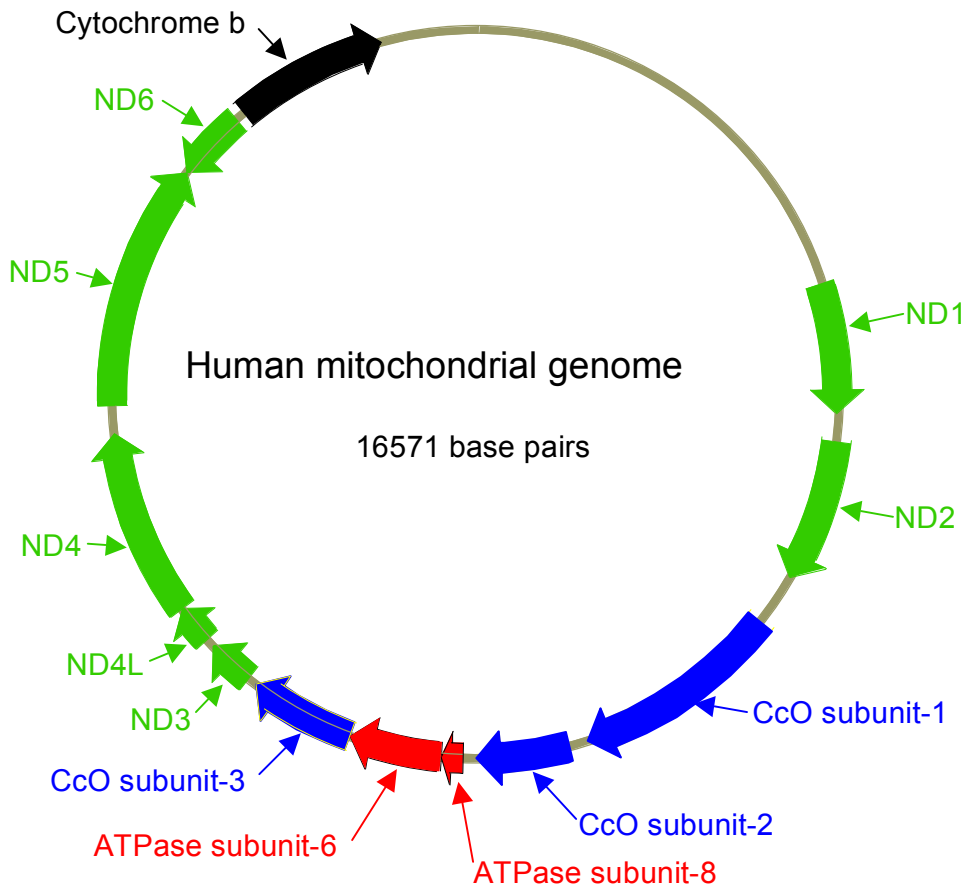

Figure 04 – The human mitochondrial genome encodes: 7 subunits of complex I (NADH dehydrogenase - ND); The cytochrome b subunit of complex III (cytochrome c reductase); 3 subunits of complex IV (cytochrome C oxidase - CcO) and 2 subunits of complex V (ATPase). Figure adapted from DiMauro and Schon 2003.

1.2.5 Other functions of mitochondria

Although the main role of mitochondria is the generation of ATP more recently they have been implicated (as being involved) in several other intracellular processes. These include being the major intracellular source of reactive oxygen species (ROS); regulation of metabolism; regulation of calcium homeostasis; cell-cycle control; development; antiviral responses and cell death (McBride, Neuspiel et al. 2006). Two of these will be discussed in more detail because they play an

integral role in deciding a cells fate when exposed to an insult. Firstly apoptosis because when cells are exposed to a stressor they may undergo apoptosis and apoptosis has been implicated in cardiovascular pathology (Fadeel and Orrenius 2005). Secondly ROS generation because this has been implicated as the major source of oxidative stress, which has been implicated in both cardiovascular disease and aging (Harman 1956; Passos, Zglinicki et al. 2006; Forstermann 2008).

1.2.5.1 The role of mitochondria in apoptosis

1.2.5.1.1 An overview of apoptosis

Apoptosis, otherwise known as programmed cell death, was first described by Kerr et al in 1972 (Kerr, Wyllie et al. 1972). Apoptosis comprises an orderly series of events resulting in the shut down of metabolism and digestion of cell contents, with a minimal leak of these contents. Unlike necrosis apoptosis does not elicit an inflammatory response (Gerschenson and Rotello 1992). It is an essential pathway for normally functioning organs, for example cells infected with a virus undergo apoptosis resulting in their death before the completion of the replication of the virus can occur thus preventing spread of infection. However, since its discovery its importance in the pathology of several diseases such as cancer, myocardial infarction, heart failure, autoimmune disease and neurodegenerative diseases has been increasingly recognised (Fadeel and Orrenius 2005). Mitochondria are now recognised to play a central role to the process of apoptosis (Fadeel and Orrenius 2005).

There are two main pathways that lead to the activation of apoptosis. The first is the extrinsic or death receptor-mediated pathway, which plays a major role in tissue homeostasis. The second is the intrinsic or mitochondrial receptor-mediated pathway, which is triggered by various forms of cellular stress, including DNA damage. In addition to the two major pathways several others have been described. One of these mechanisms is involved in viral defence whereby cytotoxic cells of the immune system release perforin and granzyme B from lytic granules, which in turn can activate procaspase-3 and the B-cell lymphoma 2 (Bcl-2) homology-3 (BH3) interacting domain death agonist (Bid) resulting in apoptosis. The Bcl-2 family of proteins are discussed later.

1.2.5.1.2 The extrinsic and intrinsic pathways of apoptosis

The extrinsic pathway can be triggered by one of two death receptors linked to a cytosolic “death domain”. Tumour necrosis factor (TNF)-related apoptosis-inducing ligand (TRAIL), otherwise known as APO-2 is associated with TNF receptor associated death domain (TRADD). The apoptosis-stimulating fragment (Fas), also known as CD95 or APO-1 is associated with Fas receptor associated death domain (FADD). FADD causes the formation of a death-induced signalling complex (DISC) which activates caspase 8, initiating a series of downstream caspases ultimately activating the ‘executioner’ caspases responsible for apoptosis, which include caspase-3 and caspase-7. In some cells Bid is released which then causes mitochondrial release of cytochrome *c.* TRADD causes the formation of a DISC, which causes apoptosis in the same way, it also causes Bid release (Fadeel and Orrenius 2005; Jeong and Seol 2008).

The intrinsic or mitochondrial pathway can be initiated by various forms of cellular stress. These lead to the opening of the mitochondrial permeability transition pore (MTP), which leads to the release of cytochrome *c* from the mitochondria into the cytosol and causes apoptosis as described below. Apoptosis-inducing factor (AIF) is a flavoprotein that has been shown to be one of the key activators of apoptosis via the intrinsic pathway and does this by directly activating caspase-3 and caspase -9. In addition AIF has also been shown to act directly on nuclei and cause their degradation by chromatin condensation as well as large-scale chromatin fragmentation (Susin, Lorenzo et al. 1999).

1.2.5.1.3 The role mitochondria play in apoptosis

Mitochondria play a fundamental role in apoptosis and the release of their cytochrome *c* to the cytosol is an integral and essential part of the process of apoptosis in both intrinsic and extrinsic pathways (Liu, Kim et al. 1996). Cytochrome *c* released into the cytoplasm binds with Apoptotic protease-activating factor-1 (Apaf-1), which recruits procaspase-9 leading to the formation of the apoptosome, a molecular complex that activates the 'executioner' caspases-3 and -7, the main effector caspases of apoptosis (Liu, Kim et al. 1996).

The Bcl-2 (named after the B-cell chronic lymphocytic leukaemia/lymphoma cells in which they were first discovered) family of proteins govern outer mitochondrial membrane permeabilisation and are key regulators of apoptosis that have been shown to act at the mitochondrial level and may be pro or anti-apoptotic. Bcl-2–associated X (Bax), Bcl-2/Bcl-X_L-associated death promoter (Bad) and Bid are

inert proteins in healthy cells but when cleaved by caspase-8 they act at the mitochondrial level, possibly by forming permeability pores allowing the release of cytochrome *c,* to propagate apoptosis (Fadeel and Orrenius 2005). However, it is important to recognise that the mitochondrial permeability transition pore is more heavily implicated in the mechanisms of necrosis (Rasola and Bernardi 2007; Azzolin, von Stockum et al. 2010). In contrast Bcl-2 and Bcl-x_L (similar to Bcl-2 but shows different lineage specificity) have been shown to have anti-apoptotic properties (Vaux, Cory et al. 1988; Yang and Korsmeyer 1996; Adams and Cory 1998).

Given that mitochondria play an essential role in apoptosis it is not surprising that cells lacking functional mitochondria have been shown to be resistant to apoptosis. Bax translocation is absent in these cells, which accounted for the failure of cytochrome *c* release and thus apoptosis (Lee, Kim et al. 2004). It has been shown that mitochondrial mutations occur with certain tumours and it has been postulated that these mutations could effect the resistance of cells to apoptosis and as a result the predisposition to cancer (Polyak, Li et al. 1998; Fliss, Usadel et al. 2000).

1.2.5.2 Production of reactive oxygen species by mitochondria

Given the vast number of electrons passing down the ETC it is not surprising that a proportion of these will leak and reduce O_2 to produce superoxide. It is estimated that 1-2 % of oxygen consumed by mitochondria is converted to superoxide and other ROS such as hydrogen peroxide and the hydroxyl radical (Boveris and Chance 1973). The rate of ROS production is strongly linked to the

mitochondrial membrane potential ($\Delta\psi_m$), which is generated by the protons in the intermembrane space. Mild uncoupling of mitochondria strongly reduces ROS production (Brand, Affourtit et al. 2004).

The passage of electrons from Complex I to QH2 and from QH2 to cytochrome bL at complex III both involve the production of the radical $\cdot Q^-$ as an intermediate. The $\cdot Q^-$ can pass an electron to oxygen leading to the formation of superoxide ($\cdot O_2^-$) in the following reaction:

$$O_2 + e^- \rightarrow \cdot O_2^-$$

Complexes I and III and are thus major sources of free radical production (Barja 1999). Conditions where downstream complexes of the ETC are reduced, such as complex IV in hypoxia, are associated with an increased production of ROS (Palacios-Callender, Quintero et al. 2004). It has been suggested that the ROS produced by mitochondria at complex III may be involved in hypoxia signalling (Chandel, McClintock et al. 2000; Wang, Fang et al. 2008), although more recent evidence has refuted this (Wang, Fang et al. 2008) and furthermore that mitochondria might be acting as signalling organelles in vascular endothelium (Quintero, Colombo et al. 2006).

Excess generation of superoxide can result in oxidative stress with ensuing damage to intracellular macromolecules (Davies 1995). To combat this cells have developed complex defence mechanisms that are discussed in the next section. Without these defences both H_2O_2 and $\cdot O_2^-$ can generate highly reactive radicals such as the hydroxyl radical ($OH^{\bullet}$) that can diffuse away and react in a non-specific way with almost any nearby molecule, such as DNA (Davies 1995).

One of the main theories of ageing, gaining an increasing weight of evidence, is that cumulative ROS-induced oxidative damage is responsible for many of the changes seen (Harman 1956; Passos, Zglinicki et al. 2006). This is discussed in greater detail in section 1.5.2.

1.3 Defence mechanisms of cells

Oxygen readily accepts unpaired electrons to give rise to reduced (or 'reactive') oxygen species, which can initiate and propagate a series of reactions that can be highly damaging to the cell. Cells have evolved a complex series of antioxidant defences and regulators of the cell cycle to counter these harmful effects and protect the cell (Riley 1994). When these mechanisms are either overwhelmed or do not function normally the cell either dies (by necrosis or apoptosis) or enters a state of senescence (discussed later in section 1.5). One of the key regulators of a cell's fate is the p53 gene and changes in the pathways involving p53 have been implicated in the pathogenesis of atherosclerosis (Bennett, Macdonald et al. 1998).

Cellular antioxidant defences are well described and include the superoxide dismutases, glutathione peroxidase, catalase, and a complete mitochondrial detoxification system comprised of manganese superoxide dismutase (MnSOD or SOD2), glutathione reductase, glutaredoxin, thioredoxin and the peroxiredoxins (Valle, Alvarez-Barrientos et al. 2005).

Manganese superoxide dismutase is a 96 kDa nuclear-encoded protein, found in the mitochondrial matrix. The cytosolic equivalent is copper-zinc superoxide

dismutase (CuZnSOD or SOD1). Superoxide dismutase catalyses the following reaction:

$$2 \cdot O_2^- + 2H^+ \rightarrow H_2O_2 + O_2$$

The hydrogen peroxide (H_2O_2) generated can form $\cdot OH$, which is an even more highly reactive free radical that can damage DNA, enzymes, membrane proteins and lipids.

However, H_2O_2 is rendered harmless and turned into H_2O by the enzyme glutathione peroxidase. In the reduction of H_2O_2 to H_2O, by glutathione peroxidase (GPx), reduced glutathione or γ-glutamylcysteinylglycine (GSH) is oxidised to the oxidised form of glutathione (GSSG). GSSG is then reduced to GSH by the enzyme glutathione reductase using electrons from nicotinamide adenine dinucleotide phosphate (NADPH). There are six reported isoforms of GPx with cytosolic GPX-1 being the most abundant and present in all cells. The GPx enzymes all have a selenocysteine residue with the exception of GPx-5 and GPx-6, which have cysteine residue and are known as Nonselenium GPx-like proteins (NS-GPxs). Evidence suggests the latter group (NS-GPxs) function more as active oxygen species sensors and less as scavengers (Herbette, Roeckel-Drevet et al. 2007).

Catalase is another antioxidant enzyme, which is present predominantly in the peroxisomes of all types of mammalian cells where H_2O_2 is generated, with the exception of erythrocytes. It catalyses the reduction of H_2O_2 to water and oxygen and its role in the defence of cells against oxidative stress has been extensively studied (Ho, Xiong et al. 2004). The glutaredoxins are small redox enzymes

which use glutathione as a cofactor and constitute part of the glutathione system (Holmgren 1989).

The thioredoxin (TRX) system has been shown to be both an important antioxidant and messenger system in all cells and has been implicated in cardiovascular disease. The TRX group reduces oxidised cysteine groups on protein and exerts most of its effects via TRX peroxidase (otherwise known as peroxiredoxin). TRX-1 is found throughout the cytosol, TRX-2 is confined to the mitochondria and little is known about its function. TRX-1 reduces the oxidised form of peroxiredoxin and in turn the reduced peroxiredoxin scavenges ROS. The TRX system is expressed in endothelial cells and has been shown to play an important role in protecting them from H_2O_2 induced damage (Yamawaki, Haendeler et al. 2003).

Finally both the heme-oxygenase and paraoxenase systems play a role in antioxidant defence in the cardiovascular system, although not directly in endothelial cells, and deserve a brief mention. Heme-oxygenase can indirectly reduce oxidative stress by reducing the pro-oxidative heme to biliverdin, which is converted to bilirubin (itself a ROS scavenger) (Jiang, Roberts et al. 2006). The paraoxenase family of enzymes are produced in the liver with HDL and account for HDLs ability to reduce lipid peroxidation (Aviram, Rosenblat et al. 1998).

1.4 Rho 0 cells

1.4.1 Definition and overview of Rho 0 cells

Cells lacking functional mitochondria are referred to as Rho 0 cells (otherwise termed ρ^0 cells) The concept of Rho 0 cells is not new and was first described in petite E5 mutants of *Saccharomyces cerevisiae* yeast in 1970 (Nagley and Linnane 1970). The term Rho (ρ) was used to describe the petite yeast mutant cells, with ρ^+ being cells with mitochondrial DNA and ρ^0 being cells that lack mitochondrial DNA (Nagley and Linnane 1970; Blanc, Dujon et al. 1978). Rho 0 cells contain mitochondria, however the morphology of the mitochondria is highly abnormal when studied using electron microscopy. The mitochondria have been shown to be enlarged, often vacuolated and have a distorted cristae pattern (Armand, Channon et al. 2004). The mitochondria of Rho 0 cells are non-functional and lack a functional respiratory chain.

The first description of Rho 0 human cells was by King and Attardi in 1989 in a transformed osteosarcoma cell line 143B.TK$^-$ (King and Attardi 1989). Subsequently a majority of the mammalian Rho 0 cells described have been transformed cells lines (King and Attardi 1996; Miller, Trimmer et al. 1996; Park, Nam et al. 2001). Prior to starting this project no published descriptions of primary endothelial Rho 0 cells could be found in the literature. To date the only published work with primary endothelial cells was from work by our group, using the cells from the work described in this thesis (Quintero, Colombo et al. 2006). All published Rho 0 cell work to date is otherwise in transformed cell lines.

1.4.2 Overview of method of producing Rho 0 cells

The method described by Attardi et al, and the most common way of depleting cells of functional mitochondria, involves growing cells in the presence of a low dose of ethidium bromide (50 ng / mL) in a glucose and pyruvate rich medium supplemented with uridine (King and Attardi 1996). Ethidium bromide is an intercalating agent that prevents the replication of mitochondrial but not genomic DNA at low doses, this is discussed in more detail below. Rho 0 cells are entirely dependent on glycolysis for their energetic demands (King and Attardi 1996; Miller, Trimmer et al. 1996) and thus require glucose rich medium, they are also auxotrophic for both uridine and pyruvate. The cells are auxotrophic for uridine because dihydrooratate dehydrogenase, an enzyme involved in the synthesis of uridine, is located on the inner mitochondrial membrane and requires mitochondrial electron transport for its normal function (Gregoire, Morais et al. 1984). The lack of a normally functioning ETC prevents the oxidation of NADH. However, NADH could be oxidised via the activity of NAD-linked dehydrogenase, thus allowing oxidisation of excess cytoplasmic NADH, which requires an excess of pyruvate as that cannot be met by glycolysis alone (DeFrancesco, Scheffler et al. 1976).

At a dose of 1 μg / mL ethidium bromide has been shown not to affect genomic DNA but to accumulate in mitochondria and intercalate with mitochondrial DNA, thereby preventing its replication leading to the cells Rho 0 status. Mitochondrial DNA is susceptible to damage as it is a simple structure with no introns and is neither supercoiled nor protected by histones. In addition it does not have the complex repair mechanisms of genomic nuclear DNA. As a result it is far more

susceptible to mutagens such as ethidium bromide (Zylber, Vesco et al. 1969; Nass 1970; Nass 1972).

The other described method of producing Rho 0 cells is to knockout the nuclear-encoded DNA polymerase gamma (DNA POLG, accession number: NM_002693.1), which is the sole DNA polymerase that is required for the replication of mitochondrial DNA. Such a method is attractive as it avoids the use of ethidium bromide, which is a toxic compound and may have other unmeasured effects on cell metabolism. The creation of single point mutation at codon 1135 (altering it from GAG to GCG) prevents DNA POLG from functioning and leads to mitochondrial depletion (Ropp and Copeland 1996; Jazayeri, Andreyev et al. 2003). In 2003 Jazayeri et al characterised a system for creating Rho 0 human embryonic kidney-293 (HEK-293) cells using an inducible dominant negative DNA Polymerase Gamma (dnDNA POLG) (Jazayeri, Andreyev et al. 2003). However beyond the work originally published by this group there is no subsequent published work on Rho 0 cells produced by this method.

1.4.3 Metabolism and oxygen consumption of Rho 0 cells

Rho 0 cells are entirely dependent on glycolysis for their metabolic demand and do not respire i.e. are unaffected by the classical inhibitors of the ETC (Herst, Tan et al. 2004). However, using Rho 0 cells, which do not consume oxygen via oxidative phosphorylation, it has been demonstrated that cells also consume oxygen via the plasma membrane oxidoreductase (PMOR) system and that this mechanism is often upregulated in Rho 0 cells (Shen, Khan et al. 2003; Herst and Berridge 2007). The PMOR system is a multienzyme complex that includes

NADPH-ferricyanide reductase and NADH-oxidase that is able to transfer electrons from the cytoplasmic NADH to extracellular electron acceptors such as ferricyanide (Larm, Vaillant et al. 1994). Highly glycolytic cells use this system to alleviate intracellular reductive stress. It has been suggested that upregulation of this system is essential to the survival of Rho 0 cells (Larm, Vaillant et al. 1994; Herst and Berridge 2007). Oxygen consumption by the PMOR system is often referred to as cell surface oxygen consumption, the other non-mitochondrial source of oxygen consumption in cells is known as basal oxygen consumption (Herst and Berridge 2007). There are over 60 described enzymes that utilise oxygen, for example xanthine oxidase, and the exact contribution of each of these to basal oxygen consumption is less well described (Vanderkooi, Erecinska et al. 1991). The interplay between mitochondrial respiratory chain function, the PMOR system and glycolysis allow the maintenance of an NAD^+/NADH ratio compatible with life (Larm, Vaillant et al. 1994). This has also been shown to be important in the maintenance of the metabolism of some glycolytic tumour cells (Herst and Berridge 2007).

1.4.4 Rho 0 cells and apoptosis

Given the central role mitochondria play in apoptosis, discussed in section 1.2.5.1.3, it is not surprising that Rho 0 cells have proven a very useful tool for the study of apoptosis. The evidence concerning the susceptibility of Rho 0 cells to apoptosis is conflicting, with some early evidence suggesting that Rho 0 cells could undergo apoptosis normally (Jacobson, Burne et al. 1993) but more recent evidence shows that Rho 0 cells are resistant to apoptosis (Lee, Kim et al. 2004; Park, Chang et al. 2004). However, the most recent work suggests other factors

including increased glutathione levels and multidrug resistance may also account for the resistance of Rho 0 cells to apoptosis (Ferraresi, Troiano et al. 2008). What is not in doubt is that mitochondria play a central role in apoptosis and that Rho 0 cells still posses all the nuclear encoded structures, such as cytochrome *c,* and it may be that a functioning ETC is not essential for cells to undergo apoptosis (Jiang, Cai et al. 1999; Cai, Wallace et al. 2000). One additional piece of work that can confuse the issue is that a majority of the Rho 0 work has been done with immortalised cell lines, which are derived from tumour cells, many of which will have a level of resistance to apoptosis (Vermeulen, Van Bockstaele et al. 2005).

1.4.5 ROS production and antioxidant defences of Rho 0 cells

It is now widely acknowledged that mitochondria are the main source of ROS production in cells (Boveris and Chance 1973; O'Malley, Fink et al. 2006). Rho 0 cells have been shown to produce less ROS compared with wild-type cells (Schauen, Spitkovsky et al. 2006; Le, Hailer et al. 2007). Other non-mitochondrial sources of ROS include NADPH oxidase of the PMOR system, xanthine oxidase and nitric oxide synthase (NOS), which have all been extensively studied in vascular (endothelial) cells (Cai and Harrison 2000). NADPH oxidases are discussed in more detail later in section 1.6.4.

The evidence looking at the effect of mtDNA depletion on cellular antioxidant levels is conflicting with some groups claiming levels are reduced (Vergani, Floreani et al. 2004) and others that they are increased (Park, Chang et al. 2004).

However all this work has been done on different types of transformed cells lines, many of which have different bioenergetic demands.

1.5 Senescence and aging

1.5.1 Definition and overview of senescence

Cellular senescence can best be described as “a stress response phenomenon resulting in the permanent withdrawal from the cell cycle and the appearance of distinct morphological and functional changes associated with an impairment of cellular homeostasis” (Erusalimsky and Kurz 2005). Senescent cells histologically have a distinct enlarged and flattened morphology. Senescent cells express a unique gene expression pattern including that of p53 and p16, both negative regulators of the cell cycle. The most commonly used marker of senescence is senescence-associated beta-galactosidase (SA βgal), which is a pH 4 β-galactosidase. SA βgal can be detected at the suboptimum pH of 6 in senescent cells because of the increased lysosomal content of these cells, but not in quiescent or terminally differentiated cells (Dimri, Lee et al. 1995; Kurz, Decary et al. 2000; Itahana, Campisi et al. 2007). Staining cells or tissue samples for SA βgal is a well-described, relatively straightforward technique that is fully described in section 2.9 of the methods.

There are two types of senescence: replicative or ‘intrinsic’ senescence and stress-induced senescence. Replicative senescence is the phenomenon first described by Hayflick et al in 1965 whereby cells in culture exhibit a limited capacity for subculture before they enter a senescent phase (Hayflick 1965).

Telomeres are the chromatin caps on the end of chromosomes that protect these regions from degradation and recombination during cell division. They are 10-15 kb long in humans and consist of TTAGGG repeats ending in a 150-200 nucleotide G-strand overhang. The whole structure is bound and stabilised by specific proteins called telomere repeat binding factor (TRF) proteins (Blasco 2005). Replicative senescence is thought to be due to the gradual erosion of telomeres until a critical length is reached that triggers the cell to become senescent i.e. the telomeres are sometimes considered to be functioning as a 'biological clock' (Hayflick 1997). Telomerase is a DNA polymerase that can elongate cells in which it is expressed. Telomerase levels are very low in normal cells but have been shown to be raised in cancer cells and immortalised cell lines, counteracting telomere shortening and maintaining cells viability (Blackburn 2000; Collins and Mitchell 2002). Low levels of telomerase have been shown to be associated with telomere shortening and senescence in cells from atherosclerotic plaques and this process has been shown to be accelerated by oxidative stress (Matthews, Gorenne et al. 2006). Furthermore antioxidants have been shown to prevent a reduction in telomerase levels suggesting a mechanism as to how antioxidants might counteract the effects of ageing (Haendeler, Hoffmann et al. 2004).

Stress-induced senescence is caused by a number of different types of sub-lethal cellular stress (an overview of these causes can be seen on the next page in figure 05), most commonly oxidative stress or persistent mitogenic stimulation. Other well-described causes include; DNA damage, oncogenic stress, loss of telomere integrity and metabolic stress (Toussaint, Medrano et al. 2000; Serrano and Blasco 2001).

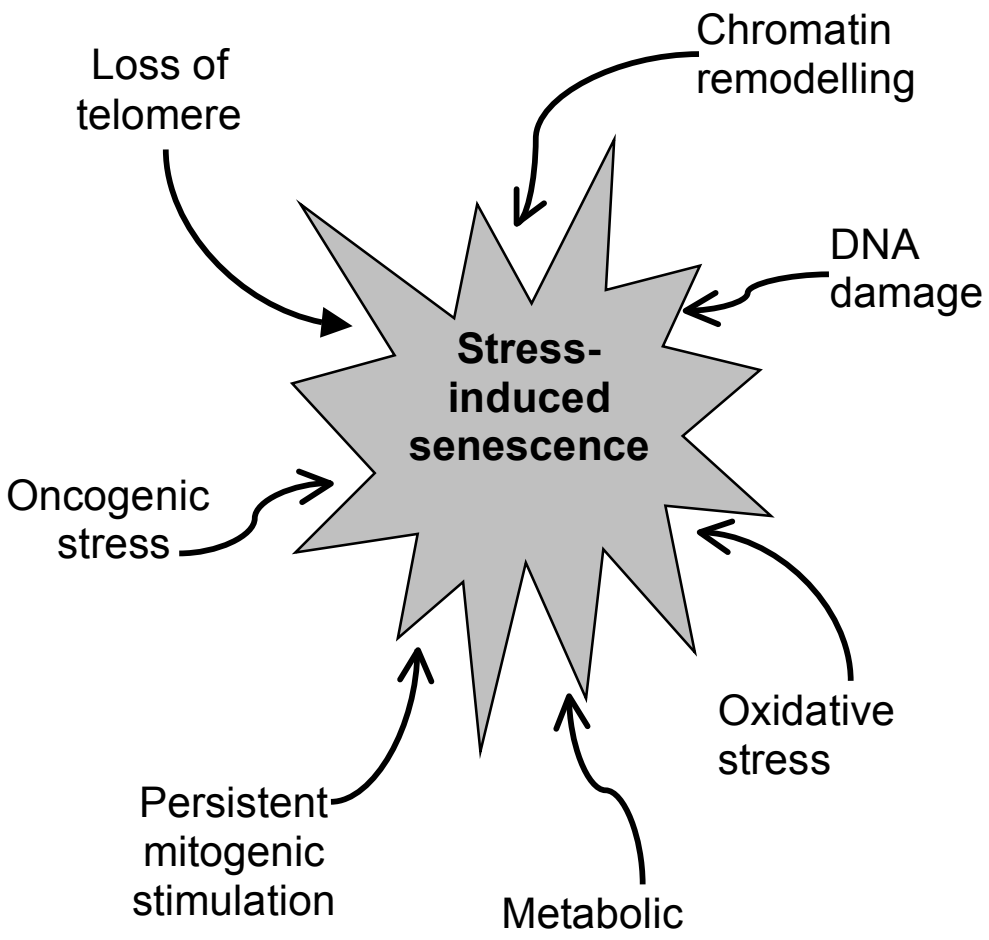

Figure 05 – An overview of the causes of stress-induced senescence

Stress-induced senescence is also sometimes referred to as 'stress-induced premature senescence' (SIPS) and 'stress or aberrant signalling-induced senescence' (STASIS), reviewed by Erusalimsky et al (Erusalimsky and Kurz 2005). There is a lot of work showing that oxidative stress, induced by treating cells directly with; H_20_2 (Chen and Ames 1994; von Zglinicki, Saretzki et al. 1995; Serrano and Blasco 2001), *tert*-butyl hydroperoxide (*t*BHP) (Dumont, Burton et al. 2000) or hyperoxia to cause increased ROS production (von Zglinicki, Saretzki et al. 1995) can induce stress-induced senescence.

1.5.2 Senescence and the theories of ageing

In 1956 Dennis Harman first proposed the free radical theory of ageing, whereby free radicals produced as a by product of aerobic respiration lead to cumulative oxidative stress, which ultimately leads to ageing and death (Harman 1956). Harman went on to make the link between mitochondria as a major source of free radical production and ageing (Harman 1972) and as a result the terms 'free radical theory of ageing' and 'mitochondrial theory of ageing' are often used interchangeably. Since then there has been a vast accumulation of evidence in support of this theory (Beckman and Ames 1998; Sanz, Pamplona et al. 2006). Although not all this work has supported this concept in higher vertebrates there is now increasing supportive evidence that this theory does indeed play an important role in aging and pathophysiology in *p53*$^{-/-}$ mice (Sablina, Budanov et al. 2005; Muller, Lustgarten et al. 2007).

However, it is possible that oxidative stress due to free radical production is a consequence of aging and not the cause. The main competing idea with the free radical theory of aging is that aging is genetically programmed and may be controlled by a single gene or pathway that is highly conserved across species (Sohal, Mockett et al. 2002). The concept of telomeres acting as a biological clock, determining when cells enter the irreversible state of senescence, was discussed in section 1.5.1. Another cause of aging is known as the "rate of living" theory described by Raymond Pearl in 1929 (Pearl 1929). According to this the life span of an organism is determined by its rate of energy utilisation (metabolic rate) and a genetically determined amount of energy consumed in adult life (metabolic potential). These parameters of metabolic rate and metabolic potential

are subject to a large amount of genetic control/pre-determination. This has been put forward as a source of life-span expansion in animals that hibernate (Lyman, O'Brien et al. 1981).

SA-β-gal staining of tissue specimens was first used to identify senescent fibroblasts and keratinocytes in ageing human skin (Dimri, Lee et al. 1995). There is now good evidence that senescence, observed in cell culture, is also associated with both physiological and pathological ageing in humans (Campisi 2001; Martin 2005). As described in section 1.5.1 the main cause of replicative senescence is telomere shortening. There is evidence that oxidative stress increases the rate of telomere shortening (von Zglinicki, Saretzki et al. 1995) and this may explain the link between the free radical theory of ageing and replicative senescence. The potential link between stress-induced senescence and the free radical theory of ageing is clear, from work described in section 1.5.1.

Mutations in mitochondrial DNA are seen in both physiological and pathological ageing (Barja and Herrero 2000). Such mutations lead to an increase in free radical generation by mitochondria. Whether these mutations are cause, effect or more likely both is still not clear (Passos and von Zglinicki 2005).

1.5.3 Senescence and cardiovascular disease

There is now a growing body of evidence suggesting that senescence may be associated with age related diseases such as atherosclerosis (Erusalimsky and Kurz 2005). In a rabbit model of vascular injury caused by a balloon denudation of the carotid endothelium, resulting in a proliferative response similar to that

seen in atherosclerosis, it has been shown that an increase in SA-β-gal a marker of senescence is seen in the area of injury but not in the sham operated contralateral artery (Fenton, Barker et al. 2001). When the senescence-accelerated mouse was fed a western-type diet accelerated ageing and premature atherosclerosis were observed (Fenton, Huang et al. 2004). In humans an increase in SA-β-gal staining was observed in diseased sections of coronary arteries but not in control non-diseased sections of left internal mammary arteries used for bypass grafts from the same patients (Minamino, Miyauchi et al. 2002). Similar work done in patients undergoing an emergency repair for a ruptured abdominal aortic aneurysm showed SA-β-gal staining in diseased sections of the aneurysmal artery resected but not from adjacent non-diseased sections of inferior mesenteric artery from the same patients used as controls (Liao, Curci et al. 2000). Therefore there is good evidence to suggest senescence is associated with vascular injury and atherosclerosis above and beyond that which would be expected as a result of physiological ageing (Minamino and Komuro 2007).

1.6 Endothelial cells

1.6.1 Endothelial cell overview

These are the cells lining the wall of blood vessels and are thus the interface between the blood and tissues. They were previously felt to be no more than a physical barrier, at most capable of facilitating the passage of substances from the blood to the tissues (Florey 1966). However it is now recognised that endothelial cells play an essential role on regulation of vascular tone and vascular homeostasis, interacting in a complex way with the blood and cells in the blood vessel wall, notably vascular smooth muscle cells (Michiels 2003).

1.6.2 Nitric oxide and endothelial cells

1.6.2.1 An overview of nitric oxide

Following the first publication proving that nitric oxide (NO), produced by endothelial cells, was endothelium-derived relaxing factor (EDRF) in 1987 (Palmer, Ferrige et al. 1987) there has been an explosion of research in to the role of NO in physiology and pathophysiology in endothelial cells. The enzymes known as NOS produce NO. Nitric oxide is synthesised from O_2 L-arginine and NADPH, which are reduced by NOS to NO, citrulline and NADP respectively. There are three well-established forms of NOS, each of which is coded for by a separate gene; type I NOS (neuronal or nNOS), type II NOS (inducible or iNOS) and type III (endothelial or eNOS) (Bredt 1999). Nitric Oxide is a gaseous free radical molecule that is soluble in water and lipids and has a half-life of seconds

(Palmer, Ferrige et al. 1987). The main action of NO is on a receptor known as soluble guanylate cyclase (sGC), which catalyses the conversion of GTP into cyclic guanosine 3',5'-monophosphate (cGMP) (Denninger and Marletta 1999). Cyclic GMP then exerts its downstream effects, which physiologically for NO include regulation of vascular tone, regulation of platelet aggregation and neurotransmission.

1.6.2.2 The role of nitric oxide in endothelial cells

In the endothelium NO plays an essential role in the maintenance of vascular tone, the maintenance of an anti-thrombogenic and anti-atherogenic surface. As well as its physiological roles NO has also been implicated in a number of pathophysiological processes including atherosclerosis (Moncada, Martin et al. 1993; Hobbs, Higgs et al. 1999; Minamino and Komuro 2007). Recent evidence has shown that NO may be involved in the regulation of respiration by its competitive effect with oxygen on complex IV of the electron transport chain (Palacios-Callender, Hollis et al. 2007) and that this mechanism plays a role in hypoxic vasodilatation (Palacios-Callender, Hollis et al. 2007).

In addition to the three well-described isoforms of NOS a mitochondrial isoform of NOS has recently been characterised and reported (Zemojtel, Kolanczyk et al. 2006). There is evidence that NO may be involved in modulation of respiration (Palacios-Callender, Hollis et al. 2007). Nitric Oxide has also shown to modulate telomerase and onset of senescence, although the results are conflicting with earlier studies suggesting NO upregulates telomerase and delays senescence (Vasa, Breitschopf et al. 2000; Hayashi, Matsui-Hirai et al. 2006) and later studies

that it neither effects telomerase nor the onset of senescence (Hong, Quintero et al. 2007). NO is also a modulator of apoptosis and has been shown to be both pro- and anti-apoptotic under different conditions (Brune 2003). Nitric Oxide has been shown to up-regulate sirtuin-1 (SIRT1), which has been shown to play an important role in cell survival and protect cells against apoptosis (Nisoli, Tonello et al. 2005; Cao, Lu et al. 2008; Pillarisetti 2008).

What now seems increasingly likely is that NO, acting on mitochondria, elicits complex intracellular signalling mechanisms that involve the orchestration of cellular defence mechanisms and the ultimate cellular response to stressors, including whether cells undergo apoptosis or senescence (Erusalimsky and Moncada 2007).

1.6.3 The role of mitochondria in endothelial cell metabolism

Human endothelial cells are known to be highly glycolytic and consume relatively low amounts of O_2 (Mann, Yudilevich et al. 2003; Quintero, Colombo et al. 2006). It has therefore been proposed that the primary role of mitochondria in endothelial cells may be to act as signalling organelles (Quintero, Colombo et al. 2006). Given that endothelial cells are highly dependent on glycolysis for their bioenergetic needs they lend themselves well to the development of a Rho 0 cell line. At the start of this research project there were no published reports of Rho 0 endothelial cells.

1.6.4 NADPH oxidase and endothelial cells

It is now widely recognised that NADPH oxidases are a major source of ROS production in endothelial cells and have been shown to be involved in the pathophysiology of numerous vascular pathologies such as atherosclerosis. NADPH oxidase was originally identified in phagocytes where it plays an essential role in defence against microbes. However five different isoforms of NADPH oxidase (Nox) have been subsequently identified: Nox 1-5 (Ray and Shah 2005). The isoforms Nox1, Nox2 and Nox4 are found in vascular cells. Although the relative roles of these have not been fully elucidated it has been shown that Nox4 is more common in arterial derived cells and is associated with atherosclerosis (Sorescu, Weiss et al. 2002; Guzik, Sadowski et al. 2004). Angiotensin II has been shown to activate NADPH oxidase via the regulatory subunit $p47^{phox}$ (associated with Nox2) and this is thought to be important in the pathogenesis of atherosclerosis (Li and Shah 2003).

1.6.5 Culture of endothelial cells as a research tool

Initial attempts to culture primary endothelial cells in the 1950s and 1960s proved difficult. Gimbrone first described a method for the isolation and culture of human umbilical vein endothelial cells (HUVEC), a readily available source of large vessel endothelial cells, in the early 1970s (Gimbrone, Cotran et al. 1974). However, despite this readily available source it usually proved difficult to grow HUVEC in culture for more than two to three passages until it was discovered that the addition of certain endothelial growth factors greatly facilitated the long term passage and culture of HUVEC (Maciag, Kadish et al. 1982). Culture of

primary endothelial cells, especially those of microvascular origin, remains difficult; HUVEC provide an easily available source of endothelial cells that behave in the same way as endothelial cells from blood vessels of the same size (Manconi, Markham et al. 2000).

A large proportion of the work published on endothelial cells is based on work on HUVEC. However, it must be borne in mind that there is heterogeneity within the endothelial cell population so results arising from work with HUVEC may not necessarily be applicable to all endothelial cells. (Cines, Pollak et al. 1998). For example endothelial cells grown from saphenous veins are able to synthesise less prostaglandin I_2 (PGI_2) than endothelial cells grown from internal mammary arteries and this difference may account for the reason saphenous vein grafts used in coronary artery bypass surgery have a much greater predisposition to develop atherosclerosis than internal mammary artery grafts (Subramanian, Hernandez et al. 1986).

A HUVEC model for stress-induced senescence has been developed whereby HUVEC treated with *tert*-Butyl hydroperoxide (*t*BHP) can be induced to undergo stress-induced senescence, as evidenced by the typical phenotypic changes of senescence, positive staining for SA-β-gal and cell cycle arrest. This model has been proposed as useful for analysing the mechanisms involved in senescence in endothelial cells (Unterluggauer, Hampel et al. 2003).

1.7 Atherosclerosis

1.7.1 Overview of atherosclerosis

Atherosclerosis is the pathophysiological process associated with the deposition of lipid-laden plaques in the arterial wall. The process starts as subendothelial accumulation of lipid laden, monocyte derived foam cells and associated T cells, which form fatty streaks. These eventually develop into fatty plaques (Weissberg 2000). This process starts in childhood and worsens with age and a high prevalence of atherosclerosis can be found in asymptomatic western teenagers (Tuzcu, Kapadia et al. 2001).

Atherosclerosis causes a number of disease processes such as ischaemic heart disease. The outcome of atherosclerosis is determined by the plaque composition. In ischaemic heart disease (IHD) the plaques can rupture leading to the local formation of a blood clot, which can block the coronary artery leading to a downstream death of the myocardium supplied by that artery, resulting in a myocardial infarction. The plaques can grow in size causing narrowing of the lumen and remodelling of the artery leading to increasing amounts of ischaemia in the downstream area supplied by that artery, which leads to increasing symptoms of chest pain (angina).

The leading cause of death in the United Kingdom is cardiovascular disease (CVD), which includes all diseases of the heart and circulation. About half of CVD deaths are from IHD. Ischaemic heart disease is the most common cause of

death in men under the age of 75 and the second most common cause of death in women under the age of 75 (The Office for National Statistics 2003).

1.7.2 Atherosclerosis, ageing and endothelial dysfunction

Whilst there are a number of treatable causes of atherosclerosis ageing is at present not one of them. Many physicians believe ageing is an independent risk factor for atherosclerosis. However, atherosclerosis is probably to some degree a characteristic feature of ageing. Furthermore, there is increasing evidence that senescence plays an important role in this process (Minamino and Komuro 2007) and understanding the signalling mechanisms involved may ultimately lead to better targeted treatments for atherosclerosis.

One of the earliest changes seen in vascular disease is endothelial dysfunction and is characterised by the failure of vessels to undergo endothelium dependent vasodilatation in response to known stimuli (Brandes, Fleming et al. 2005). Healthy human epicardial coronary arteries dilate when acetylcholine is infused, whereas atherosclerotic arteries constrict due to impaired release of NO. Endothelial dysfunction seen in the early stages of vascular disease is associated with a mild inflammatory state and the upregulation of intracellular adhesion molecules (CAM), such as Intercellular adhesion molecule-1 (ICAM-1) and Vascular-cell adhesion molecule-1 (VCAM-1) (Cines, Pollak et al. 1998). Clinically this can easily be measured non-invasively using vascular ultrasound, and has been shown to correlate with the development of atherosclerosis in man (Kasprzak, Klosinska et al. 2006).

1.8 Hypothesis

The hypothesis for this project is that the main role of mitochondria in endothelial cells is to act as defence signalling organelles, determining their fate when challenged with external stressors. Rho 0 endothelial cells will be used to investigate the role of mitochondria in stress-induced senescence, apoptosis and ROS production in endothelial cells.

1.9 Aims

- To investigate whether it is feasible to produce a model for generating human Rho 0 endothelial cells and to fully characterise these cells by:
    - Examining their growth rates and auxotrophy for uridine
    - Confirming that the mitochondrial genes encoding mitochondrial subunits are not expressed nor are the proteins
    - Confirming that their bioenergetic needs are from glycolysis and that they do not have a functional ETC
    - Confirming that they do not respire by studying the effects of the classical inhibitors of the ETC on oxygen consumption
    - Confirming that they do not have a mitochondrial membrane potential dependent on a functioning ETC by confocal microscopy
- To investigate these cells susceptibility to apoptosis and stress-induced senescence
- To see if ROS production and/or antioxidant defences of these cells account for the findings relating to their susceptibility to apoptosis and stress-induced senescence
- To investigate the possibility of generating Rho 0 endothelial cells by genetic means as a model for further studies

2 Materials and Methods

2.1 Reagents

Unless stated otherwise all reagents and drugs were purchased from Sigma®, Poole, UK. Whenever *t*BHP was used a fresh stock was always made. Appropriate safety precautions were taken when working with highly toxic reagents such as ethidium bromide or potassium cyanide. All basic laboratory disposable Falcon™ plasticware was purchased from BD Biosciences UK Ltd (Oxford, UK) or VWR International Ltd, (Lutterworth, UK). All water used in experiments was obtained from a Milli-Q integral system (Millipore UK Ltd, Watford, UK) in our laboratory, which produces deionised ultrapure Type II water (as described in ISO 3696) suitable for all laboratory needs up to and including genomics. Hereafter this ultrapure water is referred to as deionized water. For tissue culture GIBCO™ tissue culture grade deionized water (purchased from Invitrogen™, Paisley, UK) was used. Reusable laboratory glassware was cleaned and autoclaved by the central services (WIBR, Gower Street, London).

2.2 Cell culture

2.2.1 Human umbilical vein endothelial cells

Vials of human umbilical vein endothelial cells (HUVEC) were purchased from a commercial supplier (PromoCell®, Heidelberg, Germany). Each vial of cells was from a single donor and tested by the company for: bacteria, fungi, mycoplasma, Human immunodeficiency virus (HIV) 1 & 2 RNA, hepatitis B DNA and hepatitis C

RNA. In addition the company phenotypically characterised each vial. This was done by ensuring the cells were positive by immunofluorescence for: CD31 antigen, Von Willebrand Factor (VWF) / Factor VIII-related antigen and 1,1'-dioctadecyl-3,3,3',3'-tetramethyl-indocarbocyanine perchlorate labelled acetylated-low density lipoprotein (Dil-Ac-LDL) uptake and negative by immunofluorescence for smooth muscle alpha actin. (Voyta, Via et al. 1984; Galustian, Dye et al. 1995; Gifford, Grummer et al. 2004). The cells were grown in EGM-2 complete as recommended and supplied by PromoCell®. EGM-2 complete was made by adding the supplement pack to the EGM-2 basal medium. The supplement pack contained: foetal calf serum 10 mL; human recombinant endothelial growth factor (EGF) 5 μg/mL; Hydrocortisone 200 μg/mL; vascular endothelial growth factor 0.5 μg/mL; human recombinant Fibroblast growth factor (bFGF) 10 μg/mL; long R3 insulin growth factor (IGF-1) 20 μg/mL; Ascorbic acid, 1 mg/mL and Heparin 22.5 mg/mL. The company were not in a position to disclose the exact constituents of the EGM-2 basal medium. However, they did inform us, for the purposes of this project, that it contained glucose 5.5 mM and pyruvate 1 mM (personal communication). Where possible all experiments were conducted on cells from at least 2 different donors.

2.2.1.1 Growth and maintenance of cells

Cells were grown in sterile plasticware in humidified incubators in 5 % CO_2 in air at 37 °C. All tissue culture was carried out in a laminar flow tissue culture hood using aseptic technique, unless otherwise stated. The medium was changed every 2 – 3 days, 200 μL medium per cm^2 of effective growth area was used for all experiments. The effective growth area is the area of the plasticware on which

cells can grow. Cells were passaged before they were more than 90 % confluent. After washing cells in Phosphate Buffered Saline (PBS, purchased from Life Technologies, Paisley, UK) pre-warmed to 37 °C they were trypsinised with 0.05 % trypsin/ Ethylenediamine-tetraacetic acid (EDTA) pre-warmed to 37 °C, which was then neutralised with an equal volume of trypsin neutralising solution (TNS, purchased from PromoCell®, Heidelberg, Germany) pre-warmed to 37 °C. Cells were counted (as described in section 2.2.1.3) and seeded at 4000 cells per cm^2. The following day the medium was removed and replaced with fresh medium, pre-warmed to 37 °C. The number of dead cells in the medium removed was counted. From this the seeding or plating efficiency (percent of seeded cells alive) could be calculated. At each passage the number of cell population doublings (PD) was calculated for the cells using the formula: Log (N/N_o) x 3.33; where N = total number of viable cells in the growth vessel at the end of a period of growth. N_o = total number of viable cells plated in the growth vessel. The cumulative population doubling (CPD) is the cumulative sum of population doublings at each respective passage.

2.2.1.2 Freezing and thawing of cells

After trypsinisation cells were centrifuged at 200g for 3 minutes the supernatant was removed and the cell pellet re-suspended in 1 mL undiluted heat inactivated New Zealand foetal calf serum (FCS) (purchased from TCS Biologicals Ltd, Buckingham, UK) and counted with a Neubauer Haemocytometer. Foetal calf serum was then added to the cell suspension so that after adding the Dimethyl Sulfoxide (DMSO, purchased from Sigma®), to a final concentration of 10%, the cells were at a final concentration of 1 x 10^6 / mL. The DMSO was added to the

cells just prior to freezing them. Aliquots of 0.5 - 1 x 10^6 cells were placed in Nunc™ cryogenic vials (purchased from distributor VWR International Ltd, Lutterworth, UK). The cells were frozen at a rate of 1 °C per minute by placing the vials in a 'Nalgene™ Cryo 1C freezing container' (purchased from Fisher Scientific UK Ltd, Loughborough, UK), which was placed in a –80 °C freezer for 24 hours. After this the vials were transferred to a liquid nitrogen store.

Prior to thawing growth medium was placed in the appropriate tissue culture vessels and equilibrated in an incubator. Each cryogenic vial of cells was removed from the liquid nitrogen and the cap unscrewed, to reduce the pressure, then re-screwed. The vial was then held in a 37 °C water bath to thaw the contents. As soon as the last ice crystals could be seen the contents were transferred by pipette to the culture vessels. The medium was replaced after 24 hours at 200 μL / cm^2 of effective growth area,.

2.2.1.3 Cell counting

A small aliquot of cell suspension was mixed with an equivalent volume of 0.4 % Tryphan Blue (purchased from Life Technologies, Paisley, UK). The cells were then counted using a 'Neubauer Improved Haemocytometer' with an inverted microscope. Luminescent cells were counted as viable and blue stained cells counted as dead. A minimum of 400 cells was counted from each grid (i.e. upper and lower). If the count between the upper and lower quadrants varied by more than 10 % then the count was repeated. If less than 400 cells were present then the cells were spun down and re-suspended in a smaller volume, prior to re-counting. Cells were only used for an experiment if the viability was above 95 %.

Where smaller numbers of cells needed to be counted or greater precision was needed then a Z2™ Beckman Coulter® counter was used. The cells were diluted in 'Coulter® Isoton® II dilutent' (purchased from Beckman Coulter® UK Ltd, High Wycombe, UK) and the ratio of cell suspension to Isoton II dilutent was between 1:25 and 1:40 depending on the amount of cell suspension available. Counting was done as per the manufactures instruction and three counts from each sample were averaged.

2.2.1.4 Preparation of Rho 0 medium

Uridine (purchased from Sigma®) was added to deionized water to make up a final concentration of 10 mg/mL, this was filtered though a 0.45 μM Nalgene® syringe filter (purchased from Fisher Scientific UK Ltd) to make a sterile stock. Ethidium Bromide 10 mg/mL aqueous solution (purchased from Sigma®) was filtered though a 0.45 Nalgene® syringe filter (purchased from Fisher Scientific UK Ltd) then added to deionized water to make a 10 μg/mL sterile stock solution, which was kept at 4°C in a foil covered 15 mL BD Falcon™ tube (purchased from BD UK Ltd) to protect it from light.

EGM-2 is a pyruvate rich medium (1 mM) that contains 5.5 mM glucose. Prior to adding the bullet kit (as described in section 2.2.1) 40 mL of EGM-2 basic medium were removed and to this 1.75 g of D-(+)-Glucose (purchased from Sigma®, hereafter referred to as glucose) was added. This was then added back to the EGM-2 medium via a 0.45 μM Nalgene® syringe filter to give a total final glucose concentration of 25 mM. Uridine stock was added to the medium to give

a final concentration of 50 μg/mL. The bullet kit was then added in the usual manner.

2.2.1.5 Growth of Rho 0 and control (wild type) cells

Unless otherwise indicated all experiments were done with 2nd passage HUVEC. Fresh first passage cells were thawed, as described in section 2.2.1.2, and plated in the appropriate vessels. All cells were grown in Rho 0 medium (i.e. EGM-2 complete supplemented with glucose 25 mM and uridine 50 μg/mL). Rho 0 cells were generated by adding ethidium bromide stock to the Rho 0 medium, to reach a final concentration of 50 ng/mL. After 12 days in ethidium bromide the cells were confirmed as being Rho 0, as described in the results chapter. However, the cells were kept in ethidium bromide medium throughout cell culture in order to prevent the cells from reverting to wild type phenotype. Ethidium bromide is a toxic mutagenic compound and all work with this reagent was carried out with appropriate protective clothing in a ventilated hood. The respective medium was changed every 2 – 3 days. Control cells (wild type HUVEC) were grown under the same conditions, in the absence of ethidium bromide.

2.2.1.6 Preparation of Uridine-free medium

The FCS in EGM-2 complete contains uridine (personal communication from PromoCell®), uridine has a molecular weight of 244.2. In order to make Uridine-free medium the FCS was dialysed prior to use. 'SnakeSkin® pleated dialysis tubing' with a molecular weight cut-off of 3500 was used (made by Pierce Biotechnology and purchased from Fisher Scientific UK Ltd). The FCS (10 mL) was placed inside the dialysis tubing, which was sealed at both ends with purpose-supplied clips from the manufacturer. This was suspended in a large vessel containing 1 L of 1x PBS, which was the dialysis buffer. A continuous magnetic stirrer was used and the vessel kept in the cold room to maintain a temperature of 4 °C. The dialysate was changed 3 times a day and the dialysis continued for a total 3 days. The dialysed FCS was then filtered through a 0.45 μM Nalgene® syringe filter and added to the 25 mM glucose EGM-2 complete.

Medicinal chemistry (WIBR, Gower Street, London) kindly confirmed that the dialysed medium contained no uridine using a mass spectrometer.

2.3 Assessment of growth rate by BrdU incorporation

As cell proliferation requires the replication of cellular DNA the monitoring of DNA synthesis is an indirect parameter of cell proliferation. Traditionally this has been measured using the incorporation rate of radioactively labelled thymidine ([^{3}H]-thymidine). This method has been largely replaced by using 5-bromo-2'-deoxyuridine (BrdU), which is a non-radioactive measure of DNA synthesis. This technique is based on the incorporation of the pyrimidine analogue BrdU instead

of thymidine into the DNA of proliferating cells. BrdU incorporation was assessed using an Enzyme-Linked ImmunoSorbent Assay (ELISA) kit (Roche Diagnostics Ltd, Burgess Hill, UK).

The protocol used was as specified in the manufacturers instructions. In brief the cells were labelled with BrdU, the cells were then fixed with a reagent supplied with the kit. A monoclonal antibody from mouse-mouse hybrid cells conjugated with peroxidase (POD) was then added to the cells and binds to BrdU incorporated into newly dividing cells. A substrate is then added which reacts with the POD leading to a colorimetric reaction product. This reaction product is quantified by measuring the absorbance at 370nm (reference wavelength: 492nm) using a Spectra Max Plus Spectrophotometer (Molecular Devices Corporation, Sunnyvale, USA) and the data was processed in SOFTmax® Pro 3.0 software (Molecular Devices Corporation). The developed colour and thereby the absorbance values directly correlate to the amount of DNA synthesis and hereby to the number of proliferating cells in the respective microcultures (Roche 2004).

2.4 RNA Isolation and Reverse Transcriptase Polymerase Chain Reaction (RT-PCR)

2.4.1 General principles of PCR

The polymerase chain reaction (PCR) is a technique for amplifying DNA by several orders of magnitude. Kary Mullis invented PCR in 1984 and he was awarded the Nobel Prize for this work. It uses heat stable DNA polymerases such as Taq Polymerase, which was originally from the bacterium *Thermus aquaticus*

that is found in thermal vents in the ocean. The method involves thermal cycling to allow; denaturation or separation of the DNA into single strands, annealing of the primers and finally extension of the primers to replicate the region of interest. A reaction mix consisting of a deoxynucleotide phosphate (dNTP) mix, appropriate sense and antisense primers, an appropriate enzyme such as Taq polymerase, an appropriate enzyme buffer, Mg^{2+} and the template DNA is prepared. The dNTP mix contains: Deoxyadenosine triphosphate (dATP), Deoxyguanosine triphosphate (dGTP), Thymidine triphosphate (TTP) and Deoxycytidine triphosphate (dCTP).

This is then placed in a thermocycler, which is programmed to the conditions required. A standard programme would for example have an initial denaturation step of 5 minutes at 94 °C. This is followed by 30 cycles of: 20 seconds denaturation at 94 °C, 20 seconds annealing at a temperature appropriate for the primers and then 3 minutes extension at 68 °C. Finally, after the 30 cycles, it would be usual to have a final extension step of 30 minutes at 68 °C. Clearly these conditions need to be optimised for each individual reaction.

2.4.1.1 Primer design

Primers were designed from the sequences of the human genes of interest from the NCBI website Integrated DNA Technologies on-line software (IDT® SciTools) was used to ensure the primers had minimum annealing temperatures of 60 °C and did not have a strong tendency to form secondary structures. Primers were purchased from Sigma-Genosys Ltd (Haverhill, UK). The primers used are shown

in table 01, the accession number for the parent gene and gene number and position of the subunit gene (where relevant) are shown.

Table 01 – Human primers used for Real-Time qPCR

ATPase (Complex V) subunit-6 (Accession NC_001807.4, gene 4508, position 8528 bp- 9208 bp): Sense:5'-ACATTACTGCAGGCCACCTACTCA-3' Antisense: 5'-TGTCGCCTTAATCCAAGCCTACGT-3'
β-actin (Accession: NM_001101): Sense:5'- TGTGCCCATCTACGAGGGGTATGC -3' Antisense: 5'- GGTACATGGTGGTGCCGCCAGACA -3'
Catalase (Accession: NM_001752) Sense:5'- CAAAATGCTTCAGGGCCG -3' Antisense: 5'- TAATTGGGTCCCAGGCGA -3'
Cytochrome C oxidase (Complex IV) subunit-1 (Accession NC_001807.4, gene 4512, position 5905 bp- 7446 bp): Sense:5'-ATTTAGCTGACTCGCCACACTCCA-3' Antisense: 5'-TTCCCACAACACTTTCTCGGCCTA-3'
eNOS (Accession: NM_000603) Sense:5'- CGCAGCGCCGTGAAG -3' Antisense: 5'- ACCACGTCATACTCATCCATACAC -3'
γGCS (Accession: NM_001498) Sense:5'- GCACATCTACCACGCCGTC -3' Antisense: 5'- CCACCTCATCGCCCCAC -3'
MnSOD (Accession: NM_001024465) Sense:5'- GGTGGTGGTCATATCAATCATAGC -3' Antisense: 5'- GCTTCCAGCAACTCCCCTTT -3'

2.4.2 Isolation, extraction and quantification of RNA

All molecular biology work was done using Eppendorf® Biopur™ tubes (purchased from Eppendorf® UK Ltd, Cambridge, UK), which are individually wrapped and certified sterile. These tubes are pyrogen-free, RNase- free, DNA-free, ATP-free and supplied with a quality assurance card confirming this. Cell pellets were harvested and washed in PBS prior to re-suspending them in TRI Reagent™ (purchased from Sigma®) in Eppendorf® Biopur™ tubes at room temperature. A total of 1 mL of TRI Reagent™ was added per 1 x 106 cells and the solution mixed well by pipetting, prior to storage of the tubes at –80 °C.

To extract the RNA 200 μL of chloroform was added per 1 mL of TRI Reagent™, the mixture was vortexed for 15 seconds, then incubated for 2 minutes at room temperature before being centrifuged at 12000 g for 10 minutes at 4 °C. The aqueous (upper) phase was then carefully removed and transferred to a new Eppendorf® Biopur™ tube. 500 μL of isopropanol was added per 1 mL of TRI Reagent™, the mixture was vortexed for 15 seconds, then incubated for 10 minutes at room temperature before being centrifuged at 12000 g for 10 minutes at 4 °C. The supernatant was then removed and discarded. The RNA pellet was then washed once with 75 % ethanol, adding at least 1 mL of 75 % ethanol per 1 mL of TRI Reagent™ at room temperature, the mixture was vortexed for 15 seconds before being centrifuged at 7500 g for 5 minutes at 4 °C. The ethanol was then carefully removed before the RNA pellet was air dried for 4 – 5 minutes and finally re-suspended in 50 μL RNase-free polymerase chain reaction (PCR) grade water (purchased from Sigma®).

RNA concentration and purity was determined using the Nanodrop® ND-1000 Spectrophotometer (NanoDrop Technologies, Inc, USA) according to the manufacturer's guidelines. RNA concentration was measured by the absorbance at 260 nm (A260). RNA purity is determined by the ratio between 260 nm (A260) and 280 nm (A280) and the ratio between 260 nm (A260) and 230 nm (A230). For pure RNA the A260 / A280 ratio should be approximately 2.0 and the A260 / A230 ratio should be 1.8 – 2.2.

2.4.3 cDNA synthesis

For each sample of RNA to be analysed 4 wells were prepared (3 positive and 1 negative control) on a standard 96-well PCR plate. To each of the 4 wells the following were added: 1 μg of RNA, 1 μg of $OligoDT_{12-18}$ primer (purchased from Invitrogen™) and RNase-free PCR grade water to make a total reaction volume of 10 μL per well. The reaction was heated to 65 °C for 5 minutes in a Primus 96 *plus* Thermocycler (MWG Biotech, Milton Keynes, UK); the reaction mix was then placed on ice for 2 - 3 minutes. The following were added to all wells; 4 μL of 5x first-strand buffer, 1 μL of 0.1 M DL-Dithiothreitol (DTT), 2 μL of 10 mM deoxynucleotide phosphate (dNTP) mix and 1 μL of 40 units per μL RNase-out (all purchased from Invitrogen™). 1 μL of SuperScript™ II reverse transcriptase (purchased from Invitrogen™) was added to each of the 3 positive wells. 1 μL of PCR grade water was added to each negative control well. The reaction mix plate was then incubated at 42 °C for 60 minutes then 70 °C for 15 minutes in a Primus 96 *plus* Thermocycler. At the end 80 μL of PCR grade water was added to each well, giving a total volume of 100 μL. Using a multichannel pipette 10 μL from each column of 4 wells (3 positive and 1 negative) was transferred to a new

optical-grade 96-well PCR plate for each gene to be analysed by PCR. The cDNA was either used immediately for qPCR or stored at –80 °C for use at a later date.

2.4.4 Real-Time quantitative PCR (qPCR)

2.4.4.1 Real-Time qPCR set-up and analysis

To each well the following were added: 12.5 μL SYBR® Green Jumpstart™ *Taq* ReadyMix™ (purchased from Sigma®), 0.5 μL reference dye (supplied with SYBR® Green Jumpstart™ *Taq* ReadyMix™ mix kit), 0.5 μL forward primer, 0.5 μL reverse primer, 1 μL PCR grade water. This gave a total reaction volume of 25 μL. Primers for human β-actin were always used as the control.

The ABI Prism 7700 Sequence Detection System® was used to perform the PCR reaction. SYBR® was used as the internal control and after an initial step of 50 °C for 2 minutes followed by 96 °C for 2 minutes the programme ran for 45 cycles (96 °C for 15 seconds followed by 60 °C for 20 seconds). The data was acquired with the Applied Biosystems software and exported to Excel™ for analysis. The relative fluorescence for each well was calculated using the formula: 10^((CT-37.4)/-3.3), where CT = cycle threshold. Each value was corrected for background by subtracting the negative control value. Corrected values were then expressed as a % of the β-actin control. Final values for each condition were expressed as the mean of the 3 sample (positive) wells ± SEM.

2.5 Sodium dodecyl sulphate polyacrylamide gel electrophoresis (SDS-PAGE) and Western blotting

2.5.1 Basic principles of SDS-PAGE and western blotting

Proteins carry a charge that is directly proportional to their size and thus can be separated in a polyacrylamide gel by electrophoresis. The smallest, least charged proteins migrate the furthest and vice versa. Once proteins are separated by size in this way they can be transferred and fixed to a nitrocellulose membrane, again using electrophoresis, this is known as western blotting. Finally antibodies can be used to probe the membrane for the protein of interest.

2.5.2 Sample preparation for SDS-PAGE

2.5.2.1 Sample protein extraction

After trypsinisation cell pellets were harvested as described in section 2.2.1.2 and stored in eppendorf tubes at -20 °C. Fresh homogenisation buffer (pH 7.8) was prepared each time samples were processed. This consisted of: 62 mM Tris(hydroxymethyl)aminomethane hydrochloride (Tris-HCl), 2 % SDS and 1 Roche Complete Mini protease inhibitor tablet (Roche Diagnostics Ltd, Burgess Hill, UK) per 10 mL of buffer made. The protease inhibitors in the Roche preparation included inhibitors of: pancreas extract 0.015 mg/mL, Pronase 0.015 mg/mL, Thermolysin 0.0008 mg/mL, Chymotrypsin 0.015 mg/mL, Trypsin 0.0002 mg/mL and Papain 1.0 mg/mL. 150 μL of homogenisation buffer was added per 1 x 10^6 cells and mixed well by pipetting then vortexing them 3 times. The samples

were then left on ice for 30 minutes. The samples were finally sonicated on ice with 3 x 10 second bursts of sound, using a Soniprep 150 Ultrasonic Disintegrator (Sanyo Ltd, Moriguchi, Japan).

2.5.2.2 Protein determination

This was done using a bicinchoninic acid based BCA™ Protein Assay Kit (made by Pierce Biotechnology and purchased from Fisher Scientific UK Ltd). This method combines the biuret reaction, where Cu^{+2} is reduced to Cu^{+1} by protein in an alkaline medium, with the highly sensitive and selective colorimetric detection of the copper cation (Cu^{+1}) using a reagent containing bicinchoninic acid. Two molecules of BCA chelate with one copper ion forming a water-soluble purple-coloured reaction product that strongly absorbs light at 562 nm. The protein concentrations are determined from a standard curve of serial dilutions of bovine serum albumin (BSA) in the homogenisation buffer (standard concentrations 2, 1.5, 1, 0.75, 0.5, 0.25, 0.125, 0.0625 and 0 mg/mL). In a 96 well plate 25 µL of standard or sample were mixed with 200 µL of working reagent and then incubated at 37 ºC for 30 minutes. The working reagent was made by mixing 50 parts of 'Reagent A' with 1 part of 'Reagent B', the exact contents of Reagents 'A' and 'B' are not specified by the manufacturers. Absorbance was measured at 562 nm using a Spectra Max Plus Spectrophotometer and the data was processed in SOFTmax® Pro 3.0 software. If the correlation coefficient of the standard curve was less than 0.95 then the whole assay was repeated. Any sample with a coefficient of variation of greater than 10 % was re-measured. 30 µg of sample was used per well in the gel. Samples were prepared for SDS-PAGE immediately

and aliquots were made of any remaining sample for once-only use, to minimise protein degradation, and stored in a –20 ºC freezer.

Where protein content of wells, from tissue culture plates, needed to be measured the cells were washed in 1 x PBS then lysed by adding a set volume 2 % solution of SDS, mixing well with the pipette and then placing the plate on a shaker for 10 minutes at room temperature. 25 µL of this sample was then taken to measure the protein content, in triplicate. The total amount of protein per well could then be calculated.

2.5.2.3 Sample preparation

A stock of 5x loading buffer containing 250 mM Tris-HCl, pH 6.8, 50 % glycerol, 7.5 % SDS, 10 % 2-mercaptoethanol and 62.5 µg/mL bromophenol blue was made and stored in aliquots in a –20 ºC freezer. Eppendorfs with a single perforation in the lid were prepared. 9 µL of loading buffer was added to each tube, 30 µg of protein was added and the total volume then made up to 45 µL using whole cell homogenisation buffer. The samples were then heated to 96 ºC in a heating block (Grant Instruments, Cambridge, UK) for 10 minutes; the samples were then stored on ice for 5 minutes prior to centrifuging them at 6000 g for 3 minutes at 4 ºC.

2.5.3 SDS-PAGE

Two short glass plates were assembled in a casting frame in an upright position to make a 1.5 mm gel (Mini-PROTEAN 3 Cell and System purchased from

Biorad, Hertfordshire, UK). A 12 % acrylamide separating gel was prepared by mixing 30 % Acrylamide/Bis Solution (37.5:1, purchased from Bio-Rad), separating gel buffer (0.375 M Tris, 0.1 % SDS, deionized water, pH 8.8), 0.1 % Ammonium Persulphate (APS, purchased from Sigma®), 0.001 % N,N,N',N'-Tetramethylenediamine (TEMED, purchased from Sigma®). The TEMED was added just prior to pouring the gel into the glass plates. The gel was overlaid with isopropanol to remove any bubbles and smooth out the surface. After the separating gel had set and polymerised a 4% acrylamide stacking gel was prepared by mixing 30 % Acrylamide/Bis Solution, stacking gel buffer (0.125 M Tris, 0.1 % SDS, deionized water, pH 6.6), 0.1 % APS and 0.001 % TEMED. The stacking gel mix was then poured on top of the separating gel, plastic combs inserted and the gel allowed to set and polymerise. Fresh running buffer was prepared with deionized water (25 mM Tris base, 0.19 M Glycine and 0.1 % SDS -all purchased from Sigma®). Combs were removed from the gel and the gel was assembled in a mini-PROTEAN 3 gel tank system and the running buffer added. 10 µL of rainbow high-range molecular weight markers (purchased from Amersham Pharmacia, Chalfont St. Giles, UK) were loaded in the left lane then 45 µL of each respective sample into the other lanes. The gel was run at a constant voltage of 125 volts for approximately 2 hours, until the dye front reached the bottom of the gel.

2.5.4 Wet transfer

Fresh transfer buffer consisting of 25 mM Tris base, 0.19 M Glycine and 0.1 % SDS, 20 % methanol (BDH®, purchased from VWR International, Poole, UK) was prepared with deionized water and stored in the cold room at 4 ºC until used. A

piece of Hybond™-ECL™ nitrocellulose membrane (purchased from Amersham Biosciences, Bucks, UK) was cut to size. A mini transblot electrophoresis transfer cell (Biorad) was used and a sandwich of filter paper, nitrocellulose membrane, SDS-PAGE gel and fibre pads, which had all been pre-soaked in cold transfer buffer at 4 ºC for 10 minutes, was built up in the Biorad gel holder cassette carefully avoiding air bubbles as shown in figure 06. For ease of use the cassette is colour coded with one cassette being black and the other clear, to ensure the gels were always loaded in the correct orientation. Failure to load the gel in the correct orientation would lead to the loss of proteins into the buffer as opposed to transfer to the membrane.

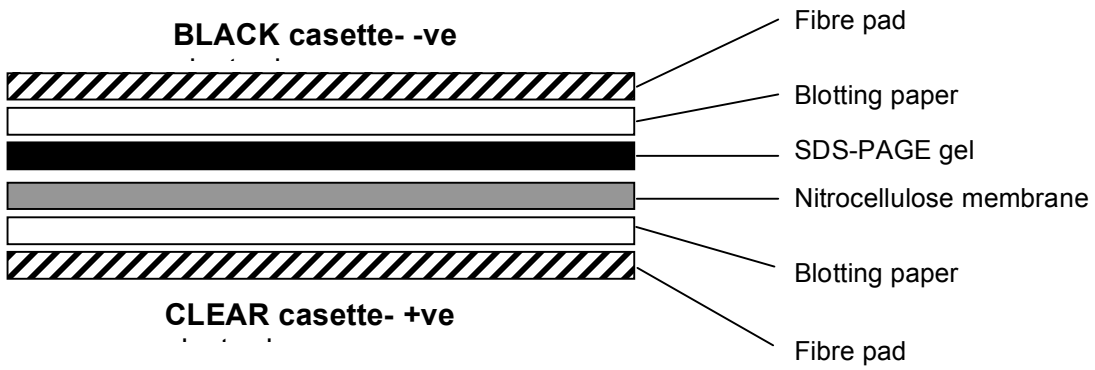

Figure 06 – Blotting setup for protein transfer

The gel holder cassette was closed once the sandwich was complete and placed into the electric module in the tank with an ice block and magnetic stirrer and the apparatus topped up with transfer buffer. The transfer was either carried out at 100 volts for 75 minutes on a magnetic stirrer plate or at 25 volts overnight in the cold room on a magnetic stirrer plate.

2.5.5 Immunoblotting

A 1 L stock of 10 x tris-buffered saline tween-20 (TBS-T) was prepared (1.5 M NaCl, 25 mM Tris base, 0.01 % polyoxyethylene-sorbitan monolaurate (Tween) - all purchased from Sigma®) using deionized water. Finally the pH was adjusted to 7.5. This stock was kept at room temperature and 1 x TBS-T was made up with deionized water each time it was needed. The nitrocellulose membrane was washed in TBS-T and the top right corner cut for the purposes of orientation. The membrane was then incubated in 5% dried skimmed milk (Marvel, Premier International Foods Ltd, Lincs, UK) in 1 x TBS-T on a shaker for 60 minutes at room temperature. The membrane was the washed for 15 minutes and 4 x 5 minutes washes in 1 x TBS-T with continuous shaking at room temperature. The membrane was incubated with primary antibody in 1 % dried skimmed milk in TBS-T overnight on a shaker in the cold room (4ºC). A list of primary antibodies used is shown in table 02.

Antibody	Working dilution	Catalog. number	Supplier/distributor
Mouse monoclonal anti-human mitochondrial complex IV subunit 1	1:1400	Ab14705	Abcam®, Cambridge, UK
Mouse monoclonal anti-human complex II 30 kDa subunit	1:200	Ab14714	Abcam®, Cambridge, UK
Mouse monoclonal anti-human alpha tubulin	1:5000	Ab7291	Abcam®, Cambridge, UK
Rabbit polyclonal anti-gamma-GCS	1:200	Sc-22755	Santa-Cruz Biotechnology/ Insight Biotechnology Ltd, Wembley, UK
Rabbit polyclonal anti-MnSOD	1:5000	Ab13533	Abcam®, Cambridge, UK
Rabbit polyclonal anti-eNOS	1:200	Sc-654	Santa-Cruz Biotechnology/ Insight Biotechnology Ltd, Wembley, UK

Table 02 – Primary antibodies used in Western blots

Following this the membrane was then washed in 1 x TBS-T with continuous shaking at room temperature, initially for 15 minutes and then subsequently washed four times, for 5 minutes on each occasion. The membrane was then incubated for 60 minutes in the appropriate secondary antibody (either Peroxidase-Conjugated Goat Anti-Mouse Immunoglobulins (catalogue number P

0447)- purchased from DAKO UK Ltd, Ely, UK or Peroxidase-Conjugated Goat Anti-Rabbit Immunoglobulins (catalogue number PI-1000)- purchased from Vector laboratories UK Ltd, Peterborough, UK) at a dilution of 1 in 2000 in 1 % dried skimmed milk in TBS-T on a shaker at room temperature. The membrane was then washed in 1 x TBS-T with continuous shaking at room temperature, initially for 15 minutes and then 4 x 5 minutes washes. The proteins were then visualised using enhanced chemiluminescence (ECL Western Blotting detection reagents) by mixing equal volumes of reagents 1 and 2 then covering the membrane and gently stirring for 2 minutes. The membrane was then exposed to Hyperfilm™ ECL, a high performance chemiluminescence film, in an autoradiography hypercassette (purchased from Amersham Biosciences) and developed using an automated developer (Compact X4, X-ograph, Wilts, UK). The images were scanned and analysed quantitatively by densitometry (Image J software, version 1.3x; National Institutes of Health, USA).

2.6 ATP determination

ATP concentration was determined using the ATPlite™ luminescence ATP detection assay system (purchased from PerkinElmer® UK, Beaconsfield, UK). This assay is based on firefly (*Photinus pyralis*) luciferase, which in the presence of D-Luciferin and ATP reacts to form light. The amount of light is proportional to the ATP concentration. ATPlite™ is a proprietary mixture of substances that extends the half-life of ATP to over 5 hours. 5000 cells were seeded per well onto a COSTAR® black 96 well assay plate with a clear bottom (made by Corning Incorporated, purchased from Fisher Scientific UK Ltd) the day before experimentation. A custom preparation of phenol-free EGM-2 was purchased

from PromoCell® and used for these experiments. The cells were treated with a total volume of medium and reagent of 100 µL per well, in triplicate for each experimental condition. Using an ATP 10 mM standard, supplied with the kit, standards of 100 µM, 10 µM, 1 µM, 0.1 µM, 0.01 µM, 0.001 µM and 0 µM were made using phenol-free EGM-2 in Eppendorf® Biopur™ tubes. 100 µL of each standard was added in triplicate to the plate. 50 µL of mammalian cell lysis solution (contents not specified by manufacturer) was added to each well and the plate was placed on a shaker for 5 minutes. One vial of the substrate solution was then reconstituted, as per the manufacturers instructions, and 50 µL added to each well. The plate was then covered in tin foil and placed on a shaker for 5 minutes. A TopSeal™ -A 96-Well microplate press-on adhesive sealing film (purchased from PerkinElmer® UK) was then used to seal the plate. Finally the luminescence was measured, at room temperature, after a 10 minute count delay on a TopCount-NXT™ microplate scintillation & luminescence counter (Packard BioScience, now PerkinElmer® Life and Analytical Sciences) and analysed in TopCount-NXT™ version 1.05 software. The raw data was then exported into a text file and imported into Excel where background luminescence from wells not treated with the ATPlite™ reagent was subtract from all wells to give the final values. A standard curve was then calculated and the final ATP values of the samples calculated.

2.7 Lactate assay

A lactate reagent and standards from Trinity Biotech was used (Trinity Biotech, Co. Wicklow, Ireland). This is based on the principle that lactic acid is converted to pyruvate and H_2O_2 by lactate oxidase. In the presence of the H_2O_2 formed,

peroxidase catalyzes the oxidative condensation of chromogen precursors to produce a coloured dye with a maximum absorption at 540 nm. The increase in absorbance at 540 nm is directly proportional to lactate concentration in the medium sample. Serial dilutions of the standard provided (8.8 mM) were made in EGM-2 medium to give the following standards; 8.8 mM, 4.4 mM, 2.2 mM, 1.1 mM, 0.55 mM and 0 mM. 2 µL of sample or standard was added to each well, all measurements were done in triplicate, and 98 µL of lactate reagent was added to each well. After 10 minutes absorbance was measured at 540 nm using a Spectra Max Plus Spectrophotometer (Molecular Devices Corporation); the data was processed in SOFTmax® Pro 3.0 software (Molecular Devices Corporation). If the correlation coefficient was less than 0.95 then the whole assay was repeated. Any sample with a coefficient of variation of greater than 10 % was re-measured. The raw data was then exported into a text file and imported into Excel where background readings were subtracted from all wells to give the final values. A standard curve was then calculated and the final lactate values of the media samples calculated. Results were then adjusted to represent concentration of lactate in the media produced per mg of protein.

2.8 Respirometry using a Clark-type electrode

Oxygen consumption (respirometry) of cells was measured using a Clark-type O_2 electrode (shown in figure 07, purchased from Rank Brothers, Bottisham, UK). The Clark electrode was first described by Leland Clark in 1953 (Clark, Wolf et al. 1953) and measures the partial pressure of oxygen in solution or gas phase.

2.8.1 Principle of operation of Clark electrode

When the platinum electrode is polarised at -0.6 V with respect to the silver electrode, every oxygen molecule that reaches its surface from the test medium, via the gas permeable membrane, is reduced to water through the following reaction:

$$O_2 + 2H_2O + 4e^- \rightarrow 4OH^-$$

For every reduction reaction there must be an oxidation and this occurs at the silver electrode as follows:

$$4Ag + 4Cl^- - 4e^- \rightarrow 4AgCl$$

Thus the overall electrochemical process that occurs in an oxygen electrode is as follows:

$$4Ag + O_2 + 2H_2O + 4Cl^- \rightarrow 4AgCl + 4OH^-$$

As the oxygen electrode is repeatedly used the bright silver ring electrode rapidly becomes ‘tarnished’. Eventually an even coat of brown silver chloride forms on the silver electrode. The presence of this silver chloride layer is desirable (it stabilises the overall behavior of the electrode) and should not be removed except if it grows very thick (after many months of use).

The polarising voltage at the platinum electrode is so negative that the current, id is related to the $P(O_2)$, via the following expression:

$id = 4 \cdot F \cdot P_m \cdot A \cdot P(O_2) / b$ (4)

Where F = Faraday's constant (9.64 x 104 $C.mol^{-1}$), P_m = O_2 permeability of the Teflon membrane (typically 1.05 x 10-12 $mol.atm^{-1}.s^{-1}$), A = surface area of the Pt working electrode (typically 0.031 cm^2) and b = thickness of the Teflon membrane (typically 12.5 x 10^{-4} cm). Thus in air-saturated water, a test medium, $P(O_2)$ = 0.2 atm, the oxygen electrode would have a value for id of 2 μA approximately.

2.8.2 The Rank Brothers oxygen electrode

The Rank Brothers oxygen electrode system (shown in figures 07 and 08) was used for all experiments in this project. It comprises of a gas-tight incubation chamber, which has a surrounding jacket of water that is kept at 37°C. Cells suspended in medium are placed in the incubation chamber and the chamber sealed with a plastic plunger. The suspension is stirred with a small magnetic stirrer to keep the solution homogenous. A concentration of 1 x 10^6 cells per ml of medium was used. The decrease in O_2 (O_2 consumption) was recorded using the DUO18 recording system (purchased from World Precision Instruments, Stevenage, UK). Treatments were administered via a port in the plunger with a microsyringe. The system had two respirometry chambers so simultaneous experiments could be carried out on two different sets of cells.

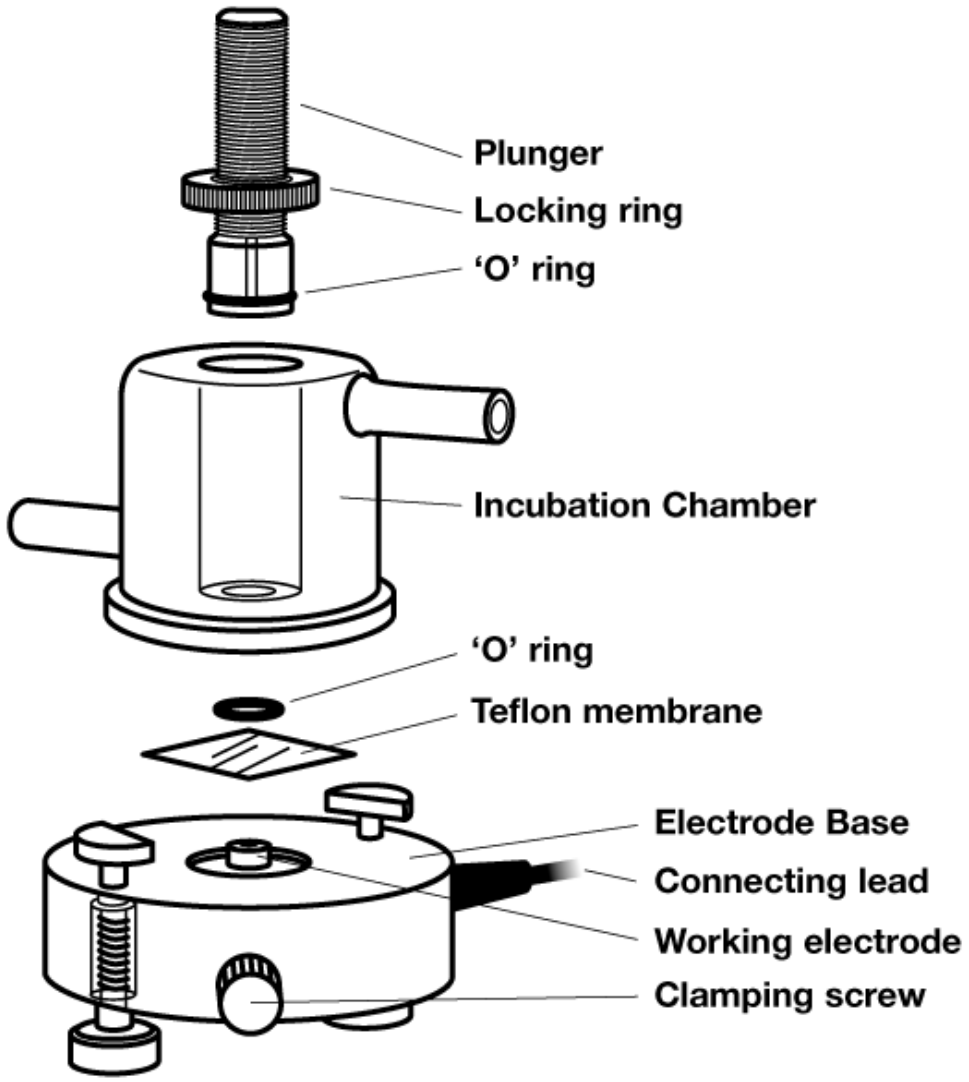

Figure 07 – Diagrammatic representation of Clark-type electrode used (*adapted from* Rank Brothers Oxygen Electrode manual)

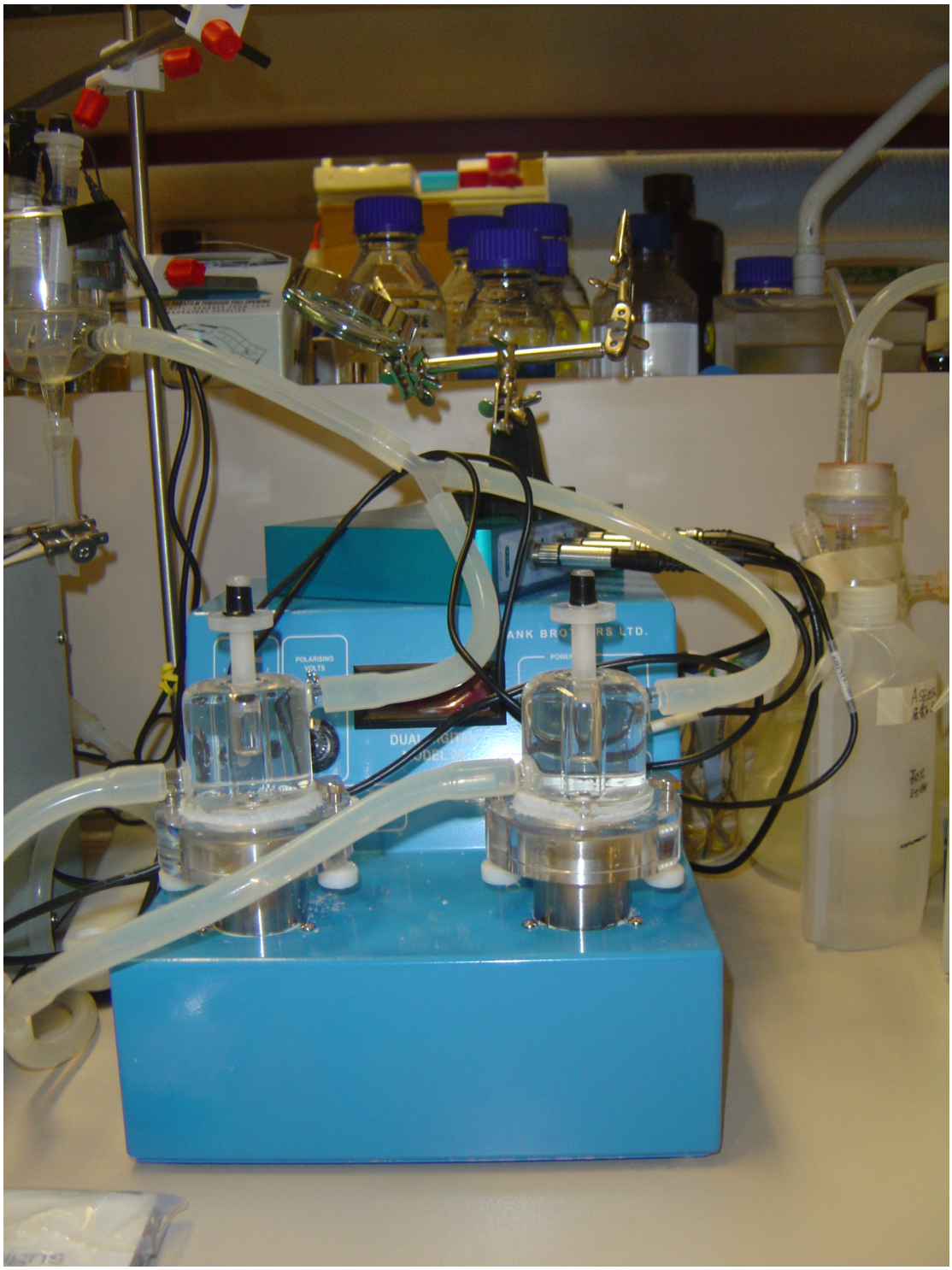

Figure 08 – Photograph of Rank Brothers oxygen electrode set-up in the laboratory. It consists of two chambers, allowing two samples to be run in parallel

The oxygen electrode consists of two electrodes set in a well, with a small central platinum disc working electrode in the centre (the cathode at which the O_2

diffusing through the membrane is reduced) and a silver ring reference electrode surrounding the working electrode. Conduction between the two electrodes was achieved using a 3 M potassium chloride solution to saturate the paper tissue covering the two electrodes. On top of this a gas-permeable membrane of 12.7 μm thick Teflon was placed and sealed from the test sample in the incubation chamber by a silicone rubber 'O' ring. Prior to use the oxygen electrode was calibrated with air saturated medium, assuming an O_2 concentration of 200 μM.

The controller was used to apply a voltage to the central platinum electrode that was sufficiently negative, with respect to the silver electrode, so that all the oxygen diffusing through the membrane and reaching this electrode was reduced. The resultant current, which flowed between the two electrodes, was proportional to the oxygen partial pressure in the test system and thus oxygen consumption by the cells could be measured.

2.8.3 Measurement of NO with an NO electrode

NO was measured using an ISO-NOP NO electrode (World Precision Instruments, Stevenage, UK). This is a Clark-type electrode that is a nitric oxide sensor with a replaceable stainless steel membrane sleeve filled with an electrolyte solution. The current generated is proportional to the amount of NO present. The current is generated from the following reaction, which occurs at the platinum anode:

$2NO + 4\ H_2O \rightarrow 2HNO_3 + 6e^- + 6H^+$

In order to calibrate the electrode known amounts of NO were generated by the following reaction:

$2KNO_2 + 2KI + 2H_2SO_4 \rightarrow 2NO + I_2 + H_2O + K_2 SO_4$

The amount of NO is proportional to the amount of $2KNO_2$ added. So, in the presence of excess KI and H_2SO_4, addition of known amounts of $2KNO_2$ generates known amounts of NO.

The NO electrode is positioned via a port in the plunger into the chamber allowing simultaneous measurement of NO during the experiment in addition to oxygen. The system set-up is otherwise identical to the one used to measure oxygen.

2.9 Cell staining for senescence-associated beta-galactosidase

Acid β-D-galactosidase is a hydrolase found in eukaryotic lysosomes, whose activity can be detected in situ with a cytochemical assay, carried out at pH 4, using the chromogenic substrate 5-bromo-4-chloro-3-indolyl b-D-galactopyranoside (X-Gal, purchased from Sigma®) (Dimri, Lee et al. 1995). In senescent cells SA βgal can be detected at pH 6.0, for reasons explained in section 1.5.1.

The protocol for SA βgal staining was carried out as previously described by the group (van der Loo, Fenton et al. 1998), all steps were undertaken at room temperature, unless specified otherwise. In brief, cells were washed twice in fresh PBS then fixed for exactly 3 minutes in 3% paraformaldehyde in PBS before being washed twice in fresh PBS. Cells were then incubated for 24 h at 37°C in freshly prepared SA-β-gal staining solution containing 1 mg/ml X-gal, 5 mM

potassium ferrocyanide, 5 mM potassium ferricyanide, 150 mM NaCl, 2 mM $MgCl_2$ and 40 mM citric acid, titrated with NaH_2PO_4 to pH 6.0. At the end of the culture the cells were washed twice with PBS then passed through increasing grades of ethanol to 99.9% and left to air dry. The cells were then viewed under a phase contrast using an Axiovert 25 CFL inverted microscope (Carl Zeiss, Germany). β-galactosidase stains blue and the number of positive staining cells were counted and compared to the number of non-staining cells.

2.10 Flow cytometry

The concept of flow cytometry, first described by Wolfgang Göhde, is a method of counting, examining and sorting particles suspended in fluid, this was rapidly adopted as a method for counting, characterising and sorting cells (Dittrich and Gohde 1969; Buchner, Dittrich et al. 1971; Schumann, Ehring et al. 1971). A series of lasers measures the scatter, forward scatter is related to cell size and side scatter is related to the cell granularity/internal complexity. In addition relative fluorescence intensity can be measured, which is proportional to the number of flurometric groups (i.e. conjugated antibodies) present on each cell.

The work was carried out using a Becton-Dickinson FACSCalibur™ flow cytometer and analysed using the associated BD Cellquest software. Wherever possible for fluorescence-activated cell sorting (FACS) analysis a minimum of 10 000 cell events were counted and the appropriate non-staining controls used. The FACS machine was calibrated on a daily basis using Becton-Dickinson CaliBRITE™ Beads.

2.11 Caspase assay for apoptosis

Apoptosis was quantified using a Caspase-Glo® 3/7 Assay kit (purchased from Promega UK, Ltd, Southampton, UK), which measures the activation of caspase-3 and caspase-7, both of which play key effector roles in apoptosis of mammalian cells (Garcia-Calvo, Peterson et al. 1999). Adding a Caspase-Glo® 3/7 reagent causes cell lysis and a luminogenic caspase 3/7 substrate is then cleaved by caspases 3 and 7 resulting in a luciferase produced luminescence, which is directly proportional to the amount of caspases 3/7 present (Liu, Li et al. 2004). This method has been shown to be an accurate measure of apoptosis in HUVEC (Olofsson, Vestberg et al. 1999).

Cells were seeded into a white walled, clear-bottomed COSTAR® 96 well plate (purchased from Fisher Scientific UK Ltd) at 7000 cells per cm^2 24-48 hours prior to the experiment. Each condition was done in triplicate. After the treatment the cells were washed in PBS and 50 μL of their normal respective medium was then added to each well. The two kit reagents were mixed in equal quantities to make the necessary volume to add 50 μL of the reagent mix to each well. The plate was then put in tin foil on continuous shaking for 30 seconds. Finally the luminescence was measured using a Victor^{2}™ 1420 Multilabel counter (PerkinElmer Life Sciences, Boston, USA). Background luminescence from wells not treated with the Caspase-Glo® 3/7 reagent was subtracted from all wells to give the final values.

2.12 Measurement of Reactive Oxygen Species

The compound 2′,7′-dichlorodihydrofluorescein diacetate (H_2DCFDA) (Brandt and Keston 1965) is a probe that when oxidised by ROS emits fluorescence, it is non-ionic and nonpolar so crosses cell membranes readily. Once inside the cell H_2DCFDA is hydrolyzed enzymatically by intracellular esterases to nonfluorescent dichlorofluorescein (DCFH). Reactive oxygen species produced from any source within the cell are then able to oxidase DCFH to highly fluorescent dichlorofluorescein (DCF). DCF it not specific for ROS generated from mitochondria. DCF can be measured in a spectrofluorimeter using excitation and emission wavelengths of 488 and 520 nm, respectively (Rosenkranz, Schmaldienst et al. 1992; Wang and Joseph 1999). This reaction can be used to measure the pro-oxidant capacity within cells using a microplate reader as described by Wang et al (Wang and Joseph 1999), an in-house protocol based on this paper was developed.

Passage 3 cells were washed, trypsinised, counted and seeded onto a COSTAR® black 96-well plate at 5000 cells per well. Four wells were used for each experimental condition. The following day cells were washed twice in warm PBS then phenol-free medium containing 100 μM H_2DCFDA probe (Invitrogen™ Molecular Probes, Paisley, UK) was added and the cells incubated for 30 minutes. The probe was then removed and the cells washed twice in warm medium before adding medium containing defined treatments, every treatment was done in quadruplicate. Cells without probe were used as negative controls, to correct for background fluorescence. The plate was then placed in a Victor$^{2\,™}$ 1420 Multilabel counter, in a pre-warmed reading chamber (kept at 37°C

throughout the experiment). The plate was then read using the filters: Fluorescein excitation: F485 centre wavelength =485 nm, bandwidth 15 nm; Fluorescein emission: F535 centre wavelength =535 nm, bandwidth 25 nm. Sequential readings were taken every 10 minutes. At the end of the experiment protein analysis was carried out on the plates to ensure equal loading of cells and if there was a significant difference in protein levels this was corrected for. Background fluorescence from cells not treated with H_2DCFDA was subtracted from all values to give the final values.

2.13 Live confocal microscopy

Confocal microscopy was invented and patented by Michael Minsky in 1961 (Minsky 1961). The process uses an optical imaging technique to increase micrograph contrast and/or to reconstruct three-dimensional images by using a spatial pinhole to eliminate out-of-focus light or flare in specimens that are thicker than the focal plane. The use of spinning disks and lasers greatly improves the resolution and allows sectioning and three-dimensional reconstruction of images taken of samples. Cells can be labelled with fluorochromes or fluorophores, which are compounds that can be excited at one specific wavelength and emit light at a different specific wavelength. More than one fluorochrome can be used to label cells provided that their excitation and emission spectra do not significantly overlap.

For this work H_2DCFDA, a fluorochrome, which is a carboxy derivative of fluorescein, and Tetramethylrhodamine (TMRM), which is an red-orange fluorophore, were used. The fluorochrome DCF was used at a final working

concentration of 10 μM and is excited at a wavelength of 488 nm and emits at a wavelength of 520 nm. The fluorophore TMRM was used at a final working concentration of 50 nM and is excited at a wavelength of 548 nm and emits at a wavelength of 573 nm.

Confocal microscopy was carried out using a PerkinElmer Ultra*VIEW* ERS spinning disk confocal microscope (PerkinElmer Life Sciences, Boston, USA) with a live cell system, which consisted of an incubation chamber around the microscope stage allowing samples to be kept at 37°C. Images were processed using the Ultra*VIEW* ERS software. All the fluorochromes used were purchased from Invitrogen™ Molecular Probes. Phenol-free EGM-2 medium was used for all experiments. Cells were cultured on Lab-TeK™ II chambered coverglass chambers (purchased from Fisher Scientific UK Ltd), which are designed for confocal image analysis. All images were collected using identical gain, black settings and time frame.

2.14 Glutathione assay

Reduced glutathione (GSH) is a major antioxidant in human tissues. During the reaction whereby H_2O_2 and lipid hydroperoxides are reduced to water and the respective alcohol, GSH becomes oxidized glutathione (GSSG). When cells are exposed to increased oxidative stress, the ratio of GSH/GSSG will decrease as a consequence of GSSG accumulation (Vergani, Floreani et al. 2004). GSH can be measured using Ellman's reagent (5,5'-dithiobis-2-nitrobenzoic acid or DTNB), which reacts with GSH to form a spectrophotometrically detectable product at

412 nm. GSSG is quantified by reducing it to GSH and then measuring GSH with Ellman's reagent (Tietze 1969).

BIOXYTECH® GSH/GSSG-412™ a commercially produced kit (purchased from *Oxis*Research™, Portland, USA) was used to measure the ratio of GSH/GSSG in cells. The kit contains 1-methyl-2-vinylpyridiniumtrifluoromethanesulfonate (M2VP), which rapidly scavenges GSH but does not interfere with the assay. The kit has been fully validated in whole blood but not other samples. Whole human blood contains 6.01 x 10^6 cells per μL and the manufacturers recommend adding 10 μL scavenger per 100 μL blood i.e. 1 μL scavenger per 6.01 x 10^7 cells. Therefore based on this 5 μL of scavenger was empirically added per cell pellet. The assay was performed as described in the manufacturer's instruction handbook. The absorbance of the spectrophotometrically detectable product, from the reaction of GSH with Ellman's reagent, was read at 412 nm for 3 minutes using a Spectra Max Plus Spectrophotometer. The reaction rate of this product is proportional to the amount of GSH present. The data was processed in SOFTmax® Pro 3.0 software then exported to a text file which was imported into Excel and analysed according to the manufacturer's instructions.

2.15 Basic molecular biology techniques

All DNA and RNA was processed in Eppendorf® Biopur™ tubes. All Gilson pipettes were serviced, calibrated and certified on an annual basis. A Primus 96 *plus* Thermocycler was used for all PCR reactions. DNA and RNA concentration and purity were determined using the Nanodrop® ND-1000 Spectrophotometer as described in section 2.4.2.

2.15.1 Working with restriction enzymes and agarose gels

Restriction enzymes are enzymes that cut double stranded DNA following their recognition of specific sequences of DNA known as restriction sites. Werner Arber, Daniel Nathans and Hamilton Smith were awarded the Nobel Prize in physiology or medicine for their discovery and application to problems of medical genetics in 1978. All restriction enzymes were stored at -80°C and kept on ice during use. All restriction enzymes were purchased from New England Biolabs (UK) Ltd, Hertfordshire, UK. All restriction enzymes were used with the appropriate supplied buffers according to the manufacturers instructions. A list of the restriction enzymes used is shown in table 03.

Agarose gel electrophoresis is a method used to separate DNA, or RNA molecules by size and is achieved by moving negatively charged nucleic acid molecules through an agarose matrix with an electric field (electrophoresis). Shorter molecules move faster and migrate farther than longer ones. This is used for restriction analysis following digestion with restriction enzymes. Fresh 1 % agarose gels were made on each occasion using 1 x TAE (0.04 M Tris-Acetate

0.002M Sodium EDTA in deionized water) buffer, which was also used as the running buffer. On parafilm 10 μL of each sample was added to 2 μL of loading buffer and this mix loaded into respective wells. In the first lane on the left of the gel 10 μL of 1 kb ladder (purchased from New England Biolabs (UK) Ltd) was added as a marker. A constant current of 50 mA was then applied to the gel until adequate separation of the bands was achieved. Bands were visualised and analysed using GeneGenius automated gel documentation and analysis system, GeneSnap and GeneTools image capture and analysis software (Syngene, Cambridge, UK).

Table 03 – Restriction enzymes used.

Note: N = C or G or T or A. A is a methylated base

Enzyme	Origin	Recognition sequence	Cut
*Age*I	*Ruegeria gelatinovora*	5'ACCGGT 3'TGGCCA	5'---A CCGGT---3' 3'---TGGCC A---5'
*BamH*I	*Bacillus amyloliquefaciens*	5'GGATCC 3'CCTAGG	5'---G GATCC---3' 3'---CCTAG G---5'
*Dpn*I	*Diplococcus pneumoniae*	5'GATC 3'CTAG	5'---GA TC---3' 3'---CT AG---5'
*EcoR*I	*Escherichia coli*	5'GAATTC 3'CTTAAG	5'---G AATTC---3' 3'---CTTAA G---5'
*Hind*III	*Haemophilus influenzae*	5'AAGCTT 3'TTCGAA	5'---A AGCTT---3' 3'---TTCGA A---5'
*Not*I	*Nocardia otitidis*	5'GCGGCCGC 3'CGCCGGCG	5'---GC GGCCGC---3' 3'---CGCCGG CG---5'
*Nde*I	*Neisseria denitrificans*	5'CATATG 3'GTATAC	5'---CA TATG---3' 3'---GTAT AC---5'
*Spe*I	*Sphaerotilus natans*	5'ACTAGT 3'TGATCA	5'---A CTAGT---3' 3'---TGATC A---5'
*Xho*I	*Xanthomonas holcicola*	5'CTCGAG 3'GAGCTC	5'---C TCGAG---3' 3'---GAGCT C---5'
*Xmn*I	*Xanthomonas manihotis*	5'GAANNNNTTC 3'CTTNNNNAAG	5'---GAANN NNTTC---3' 3'---CTTNN NNAAG---5'

2.15.2 Preparation of agar plates

Agar plates with *E.Coli* selection medium were made using pre-made Fast-Media® Agar (InvivoGen, San Diego, USA purchased from Autogen Biolclear™, Wiltshire, UK). This contained a Luria broth (LB) based agar medium containing the appropriate concentration of selection antibiotic Ampicillin at a concentration of around 100 μg / mL (exact concentration not specified by manufacturer). Agar plates were made according to the manufacturers instructions and were stored at 4 °C for up to two weeks until use.

2.15.3 Transformation of competent cells

Competent cells are cells that can take up exogenous DNA from the environment, bacteria can be made competent by exposing them to conditions to which they are not normally exposed. This normally involves the addition of Ca2+ and the presence of low temperatures. Commercially produced One Shot® TOP10 chemically competent *E. coli* (purchased from Invitrogen™) were used. Other commercially available competent cells were also used, as described in the relevant results sections in chapter 5. The manufacturer's exact instructions were followed.

In brief the general principles are as follows. A small amount of plasmid was added to competent cells on ice and the tube gently tapped (not repeated pipeting, as this can damage cells) to mix the contents in a BD Falcon™ round bottomed tube. The tube was then placed in a water bath pre-heated to 42°C for the specified time. The tube was then placed on ice before adding its contents to

LB medium pre-warmed to 37°C and then placing the tube in an incubator at 37°C on continuous agitation for 45 minutes to an hour. The contents of the tube were then plated onto pre-prepared LB-Ampicillin agar plates, nothing being plated onto one plate as the negative control. The plates were then covered in tin foil and placed in an incubator at 37°C, after 10 to 15 minutes the plates were inverted and left overnight. The following day the plates were checked for colonies. There should be none seen on the negative control plate. Discrete colonies from the transformed cells could then be picked and used to set up mini-preps, as described in section 2.15.5.

2.15.4 Direct colony PCR

This was a useful way to quickly check if the colonies contained the DNA sequence required. A master mix of PCR enzyme, appropriate buffer, forward and reverse primers and PCR grade water was made to give a total volume of 24.5 μL of this mix per PCR tube (one per colony to be analysed). After setting up the mini-prep the pipette tip from each colony was placed in a PCR tube, containing the 24.5 μL of master mix, and thoroughly mixed. The samples were then subject to the appropriate PCR conditions, according to the specific DNA sequence required. The samples were then run in a 1% agarose gel and analysed in the GeneGenius automated gel documentation and analysis system to see if the appropriate size bands are present.

2.15.5 Minipreps

2.15.5.1 Preparation of minipreps

For high yield growth of *E.Coli* a commercial Terrific Broth (TB) liquid medium called Fast-Media® TB (InvivoGen, San Diego, USA purchased from Autogen Biolclear™, Wiltshire, UK) was pre-prepared according to the manufacturers instructions. This was then sterilized in an autoclave and just prior to use Ampicillin was added, to achieve a final working concentration of 100 μg / mL.

For each colony picked a BD Falcon™ round bottomed tube was prepared containing 5 mL of Fast-Media® TB and ampicillin pre-warmed to 37°C. A fresh sterile pipette tip was used to pick a discrete colony and this was mixed with the contents of the BD Falcon™ tube. The minipreps were then placed in a rack, covered in foil and put in an incubator at 37°C on continuous agitation overnight.

The following day the cloudy suspension was aliquoted into Eppendorf ® Biopur™ tubes, the tubes were then spun down at 5400 g for 10 minutes at 4 °C. The supernatant was carefully removed and the pellet either stored at -20°C or processed immediately as outlined in the following section.

2.15.5.2 Extraction of miniprep DNA using QIAprep® Miniprep

A commercially made QIAprep® Miniprep kit (purchased from QIAGEN® Ltd, West Sussex, UK) was used to extract DNA from the cell pellets produced from the minipreps. The exact protocol specified by the manufacturers was followed, this will now be outlined in principle (QIAGEN 2005).

In principle extraction of miniprep DNA using QIAprep® Miniprep involves three steps:

1) Preparation and clearing of bacterial lysate

In this step bacteria were lysed under alkaline conditions. A buffer was then added to neutralise this and provide the high salt conditions necessary. The tube was then centrifuged at 17900 g for 10 minutes at 4°C and the supernatant, containing the DNA, was placed into QIAprep® spin columns for the next step.

2) Adsorption of DNA onto the QIAprep® membrane

The columns contain a silica membrane so when they were centrifuged at 17900 g for 30-60 seconds in high-salt buffer it caused adsorption of the plasmid DNA to the column.

3) Washing and elution of plasmid DNA

The columns were washed with the appropriate buffers. Finally a low-salt elution buffer was added, prior to centrifuging the columns at 17900 g for 30-60 seconds at 4°C to elute the DNA. The DNA concentration and purity was then measured using the Nanodrop® ND-1000 Spectrophotometer.

When DNA needed to be purified in steps of experiments then the high-salt buffer was added to the sample, which was then passed through stages 2 and 3 as described above.

2.15.6 Maxi-preps

2.15.6.1 Preparation of maxi-preps

These are identical in principle to minipreps but simply involve plasmid production on a larger scale. 200 mL of Fast-Media® TB and ampicillin (100 μg / mL) pre-warmed to 37°C were placed in a large autoclaved 500 mL conical flask. 1 mL of *E.Coli* suspension from the miniprep was then added to the flask, the top was covered with foil in an incubator at 37°C on continuous agitation overnight. The following day the resultant cloudy suspension of *E.Coli* was aliquoted into 50 mL BD Falcon™ tubes. The tubes were then centrifuged at 6000 x g for 15 minutes at 4°C to harvest the cell pellets.

A QIAGEN® HiSpeed® Plasmid Maxi Purification kit (purchased from QIAGEN® Ltd, West Sussex, UK) was then used to purify and elute the plasmid DNA according to the manufacturer's instructions. This is identical in principle to the QIAprep® Miniprep kit, except that it is on a larger scale. The DNA concentration and purity was then measured using the Nanodrop® ND-1000 Spectrophotometer.

2.16 DNA sequencing

DNA sequencing was done at our institute (Wolfson Institute for Biomedical Research, University College London) by an independent commercial company known as 'scientific services'. These sequences were analysed and corrected using a free chromatogram reader programme called FinchTV (Geospiza, Seattle, USA).

2.17 Site-Directed Mutagenesis

The principle of Site-Directed Mutagenesis (SDM) involves designing primers specific for the single point mutation required. A plasmid containing the gene of interest is then subjected to standard PCR with the SDM primers to generate copies of the plasmid with the required single point mutation. The resulting product is then treated with *Dpn*1 under the appropriate conditions to digest all parental (bacterial) DNA, which is methylated whereas the non-parental (plasmid) DNA is not and therefore left unaffected. This remaining plasmid DNA, containing the required SDM is then used to transform competent cells as described in section 2.15.3. The resulting plasmid DNA can then be amplified, harvested and purified as described in sections 2.15.5 and 2.15.6. Figure 09 shows the process schematically (*adapted from* (Stratagene 2004).

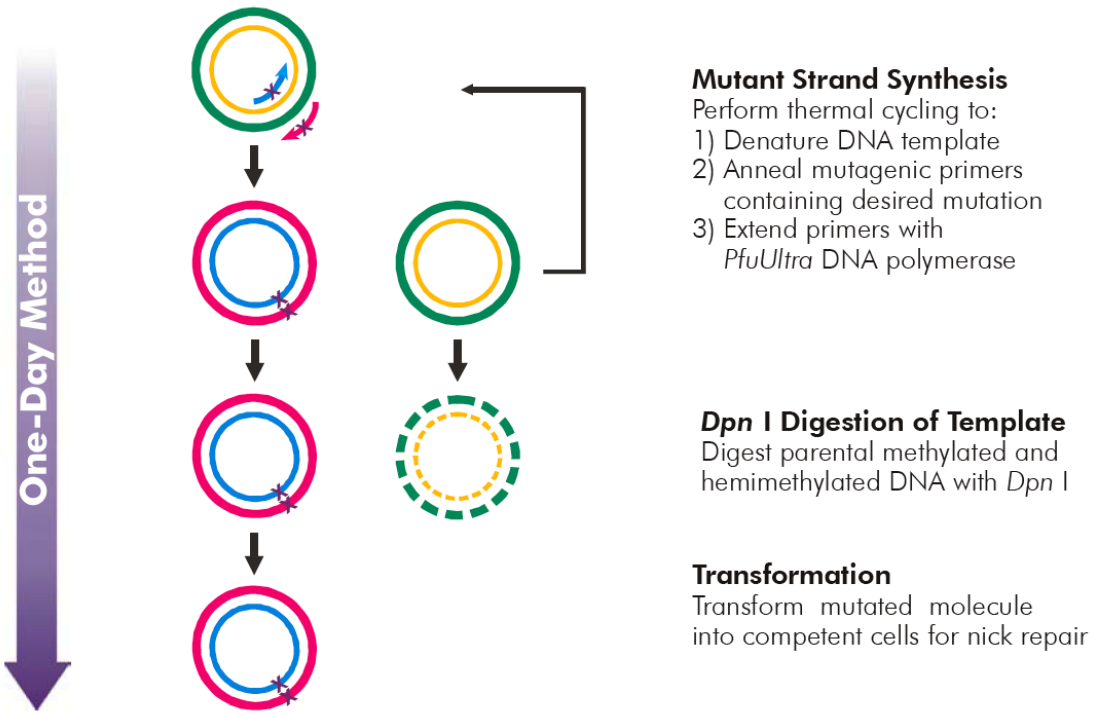

Figure 09 shows the process of plasmid SDM schematically.

(*adapted from* (Stratagene 2004).

A QuikChange® II XL Site-Directed Mutagenesis Kit (Stratagene, an Agilent Technologies company purchased from Agilent Technologies UK Ltd, Stockport, UK) was used for some of the work, according to the manufacturers instructions, as described in section 5.3.1.

2.18 Transfection techniques

Transfection is the delivery of foreign molecules, such as DNA into eukaryotic cells. Classical methods include use of Diethylaminoethyl (DEAE)-dextran and calcium-phosphate. However, DEAE-dextran has cytotoxic side effects and only causes transient transfection (Vaheri and Pagano 1965); calcium-phosphate has low reproducibility and poor efficacy in primary cells (Graham and van der Eb 1973). Electroporation uses high-voltage pulses to introduce DNA into cells, however it is associated with a high cell mortality and repeated experiments are needed to optimise the process to avoid this (Wong and Neumann 1982).

Liposomes contain a mixture of cationic and neutral lipids organised into lipid bilayer structures, a complex forms from the interaction of the negatively charged DNA and the positively charged liposome. Liposomes have a much higher transfection efficiency and reproducibility, however one of their disadvantages is that the presence of serum during transfection can significantly reduce the efficacy so serum-free medium must be used (Felgner, Gadek et al. 1987).

Virus-mediated gene transfer involves the modification of infectious viruses to transfer non-viral genes into cells. Retroviral vectors are useful for stable gene transfer into primary cells but successful infection requires dividing cells

(Grandgenett and Mumm 1990). However, construction of replication-incompetent retroviruses is complex and often liposomes are needed to initially get the plasmids into the packaging cell line to produce the required virus.

2.18.1 Direct transfection with liposome

Lipofectamine™ 2000 Transfection Reagent (purchased from Invitrogen™) is a cationic liposome based reagent that provides high transfection efficiency (Dalby, Cates et al. 2004) was used. OPTI-MEM® (GIBCO™, purchased from Invitrogen™), a versatile chemically defined medium formulated to reduce significantly the amount of serum required for cultivating mammalian cells in vitro, was also used.

All work was done in a sterile tissue culture cabinet. Cells to be transfected were grown in the usual manner on six well plates to be about 70% confluent for the transfection. Transfection involved creation of two mixtures:

Mixture A: This consists of 250 μL of OPTI-MEM® medium and 10 μL of Lipofectamine™ 2000
Mixture B: This consists of 250 μL of OPTI-MEM® medium and 4 μg of DNA

Mixtures A and B were allowed to stand for 5 minutes at room temperature before adding them together and allowing them to stand for 30 minutes at room temperature. The cells were then washed with PBS and the medium replaced with medium containing 2% FCS. Finally 500 μL of transfection mix was added per well. After 48 hours the medium was changed, the cells washed with PBS

and new medium containing selection antibiotic at the appropriate concentration added. Exact details of the plasmids used are described in the relevant results sections.

2.18.2 Transfection with replication-incompetent retroviruses

To create a replication incompetent retrovirus a viral envelope plasmid and the plasmid of interest are introduced into a packaging cell line, which then produces replication incompetent viral particles containing the plasmid of interest. This virus is then harvested from the supernatant and used to infect dividing cells. All viral work was conducted in a dedicated level 2 tissue culture room.

The plasmid pBABE-puromycin is a transfer system for the transfer of exogenous genes and was chosen for this project. It is based on Moloney murine leukemia virus that was first described in 1990 (Morgenstern and Land 1990). Puromycin is a potent inhibitor of protein synthesis in mammalian cells; it does this by inhibiting synthesis of ribosomal RNA. (Holland 1963). Puromycin is toxic to mammalian cells and insertion of a puromycin resistance gene in a plasmid therefore allows selection of cells containing the plasmid (Vara, Portela et al. 1986). This retroviral expression vector was selected because members of the group had successfully used it to transfect HUVEC with other genes being studied and it was readily available. The system used in this work utilised a HEK-293 gp packaging cells supplied by another member of this group.

The first step was to transfect the packaging cell line with the p-BABE-puromycin plasmid containing the mutated gene of interest and a plasmid expressing the

viral envelope protein (pVSVG), as described in section 2.18.2. This was done using a ratio of pVSVG to expression vector of 1:3. After 60 hours the supernatant containing the replication-incompetent retrovirus was harvested and filtered through a 0.45 Nalgene® syringe filter.

Cells to be transfected were grown in six well plates in the appropriate conditions, as described earlier, until they were approximately 70% confluent. The medium was changed and 4 μg / mL of Polybrene (purchased from Sigma®) was added to each well prior to adding the virus. Polybrene (hexadimethrine bromide) is a cationic polymer used to increase the efficiency of infection of cells with a retrovirus (Davis, Rosinski et al. 2004), it acts by neutralizing the charge repulsion between the virons and cell surface. Then 500 μL of virus-containing supernatant was added to each well. After 6 hours the medium was changed and the cells infected a second time in exactly the same way. After 48 hours the medium was changed, the cells washed with PBS and new medium containing selection antibiotic at the appropriate dose added.

2.19 Statistical analysis

All data are expressed as the mean ± SEM (Standard error of mean). All experiments were repeated on a minimum of three independent occasions, unless otherwise stated. Student's t-test was used when comparing significant differences of two means. One-way Analysis of Variance (ANOVA) was used to compare significant differences between three or more samples categorised in one way. Two-way ANOVA was used to compare significant differences between three or more samples categorised in two ways. Where posthoc testing was needed Bonferroni's post test was used. Statistical analysis was done in GraphPad Prism version 4 (GraphPad Software Inc, La Jolla, USA). For all statistical analyses a probability (P) value of <0.05 (denoted as *) was considered significant. Unless indicated by bars comparing columns all significance levels are compared to the control.

3 Results chapter 1: characterisation of the system

3.1 Effects of ethidium bromide on HUVEC growth rate

Ethidium bromide (EB) is an intercalating agent known to inhibit the reproduction of mitochondrial DNA as discussed in section 1.4.2. To determine whether HUVEC could be grown in Rho 0 growth medium in the presence of 50 ng/mL EB, and what effects EB has on cells growth rate compared to wild type (WT) cells growth rate, HUVEC in their first passage were thawed and grown in T-75 flasks in conditions as described in section 2.2.1.5. Thus all experiments start from passage 2. At each passage the number of cell population doublings (PD) was calculated for the cells, as described in section 2.2.1.1. The cumulative population doubling (CPD) is the cumulative sum of population doublings at each respective passage. For single representative cultures the CPD is plotted against the days in culture. However, when plotting combined growth data for more than one experiment the CPD is plotted against passage because the number of days between each passage varies between cultures. The plating efficiency for all cultures used was greater than 90%.

It has been reported that once Rho 0 cells have been created that if the cells are not kept in the continuous presence of EB they can recover their mitochondria and as little as a single mitochondrion is enough to repopulate all cells in a culture (Desjardins, Frost et al. 1985; King and Attardi 1989). Therefore it was decided to look at the effects of removing EB after 21 days versus its continuous presence. In the presence of EB it was observed that the growth rate (measured as population doublings per 24 hours) of HUVEC after 7 days was significantly

reduced compared to WT cells (shown in figure 10). However, 7 days after removing the EB from the medium the growth rate of the cells had recovered and was not significantly different from the WT cells.

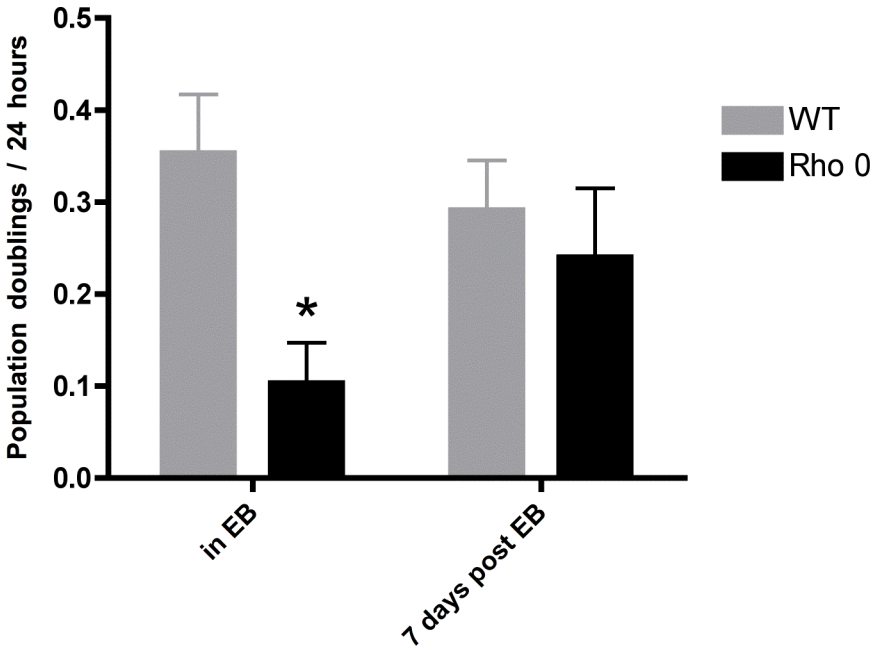

Figure 10 shows the effect of 50 ng/mL EB on HUVEC growth rate, after 7 days. There is a significant reduction in population doublings per 24 hours in EB treated compared to WT cells. 7 days after removing the EB from the medium the population doubling is not significantly different between the groups. Data are represented as mean ± SEM, n = 3. * $p < 0.05$.

To substantiate these findings, the effect of EB treatment on cell growth was also investigated by BrdU incorporation. This method revealed that EB reduces BrdU incorporation in HUVEC (shown in figure 11).

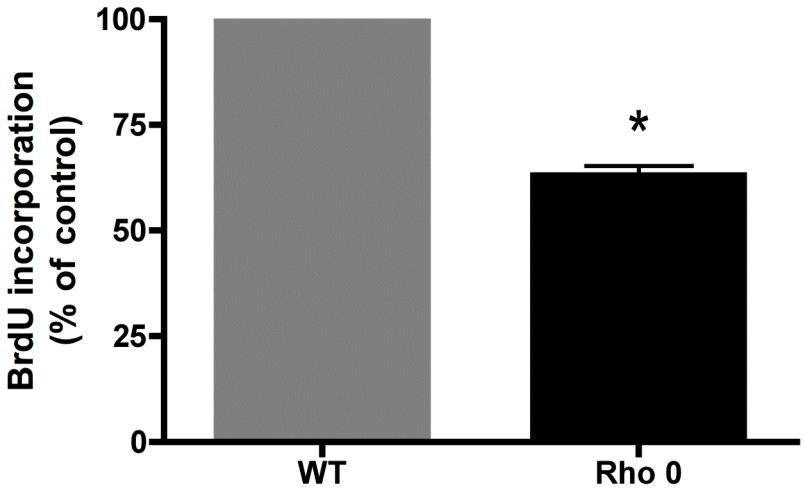

Figure 11 shows the effect of 50 ng/mL EB on HUVEC growth rate. There is a significant reduction in BrdU incorporation in EB treated cells compared to control (WT) cells. Data are represented as mean ± SEM, n = 3. * $p < 0.05$.

In the presence of continuous EB the long-term growth rate of Rho 0 HUVEC remains significantly reduced compared to the WT cells (shown in figure 12).

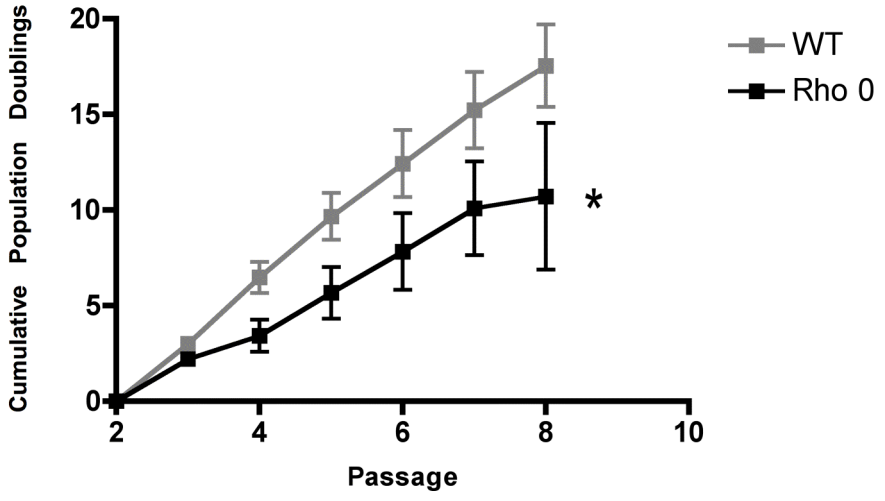

Figure 12 shows that continuous culture of HUVEC in the presence of 50 ng/mL EB significantly reduces their growth rate. Data are represented as mean ± SEM, n = 3. * $p < 0.05$.

In a cultures grown to replicative senescence the growth rate of the cells grown in EB remained reduced throughout the entire length of the culture, compared to WT cells, in 3 independent long-term growth experiments (1 such representative long term growth curve is shown in figure 13). It was interesting to observe that the cells seem to stop growing at the same point irrespective of their Rho 0 status. On more than one occasion the growth rate of the cells grown in EB accelerated after 50 days, compared to the WT cells, and showed no signs of reaching replicative senescence (data not shown). This suggested that either the EB was having undesirable effects on the HUVEC long term, which could include transformation into an immortal cell line; or that there was a problem with that specific batch of WT cells. It was therefore decided, to minimise other potential deleterious effects of EB, to not grow the cells for longer than 50 days in the continuous presence of EB.

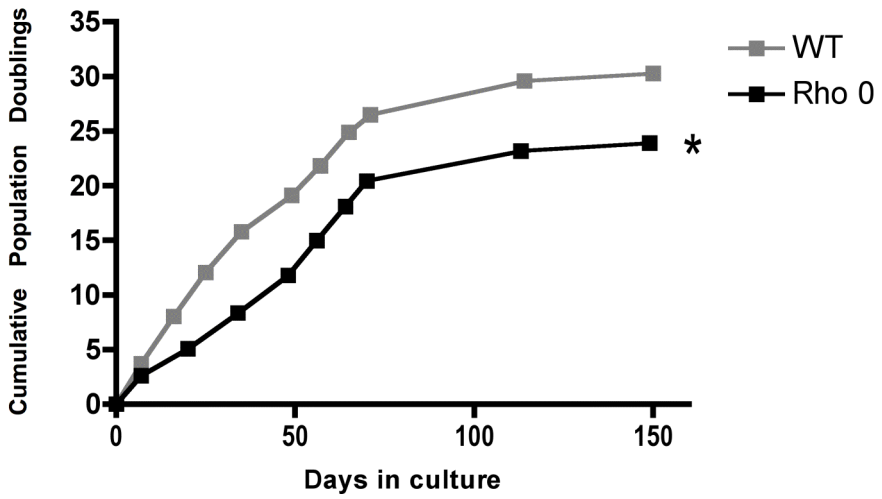

Figure 13 shows the effect of 50 ng/mL EB on HUVEC growth rate in long-term cultures grown to senescence, there is a reduction in population doubling of EB treated cells compared to control (WT) cells. Data are from a single representative culture (one of three experiments).

3.2 Effects of glucose concentration on HUVEC growth rate

It has been reported that high glucose causes oxidative stress and oxidative stress-induced senescence (Piconi, Quagliaro et al. 2006; Tsuneki, Sekizaki et al. 2007). Therefore it was confirmed that the growth rate of WT HUVEC grown in Rho 0 medium was not affected by the continuous presence of a high level of glucose (25 mM) compared to the normal level of glucose in EGM-2 (5 mM). In two independent cultures no significant difference in growth rate was observed between WT cells grown in 25 mM and WT cells grown in 5 mM glucose (shown in figure 14A) for each passage, which was the same point in time for this experiment. The CPD of cells grown in 25 mM correlated highly with the CPD of cells grown in 5 mM glucose ($r = 0.997$, shown in figure 14B).

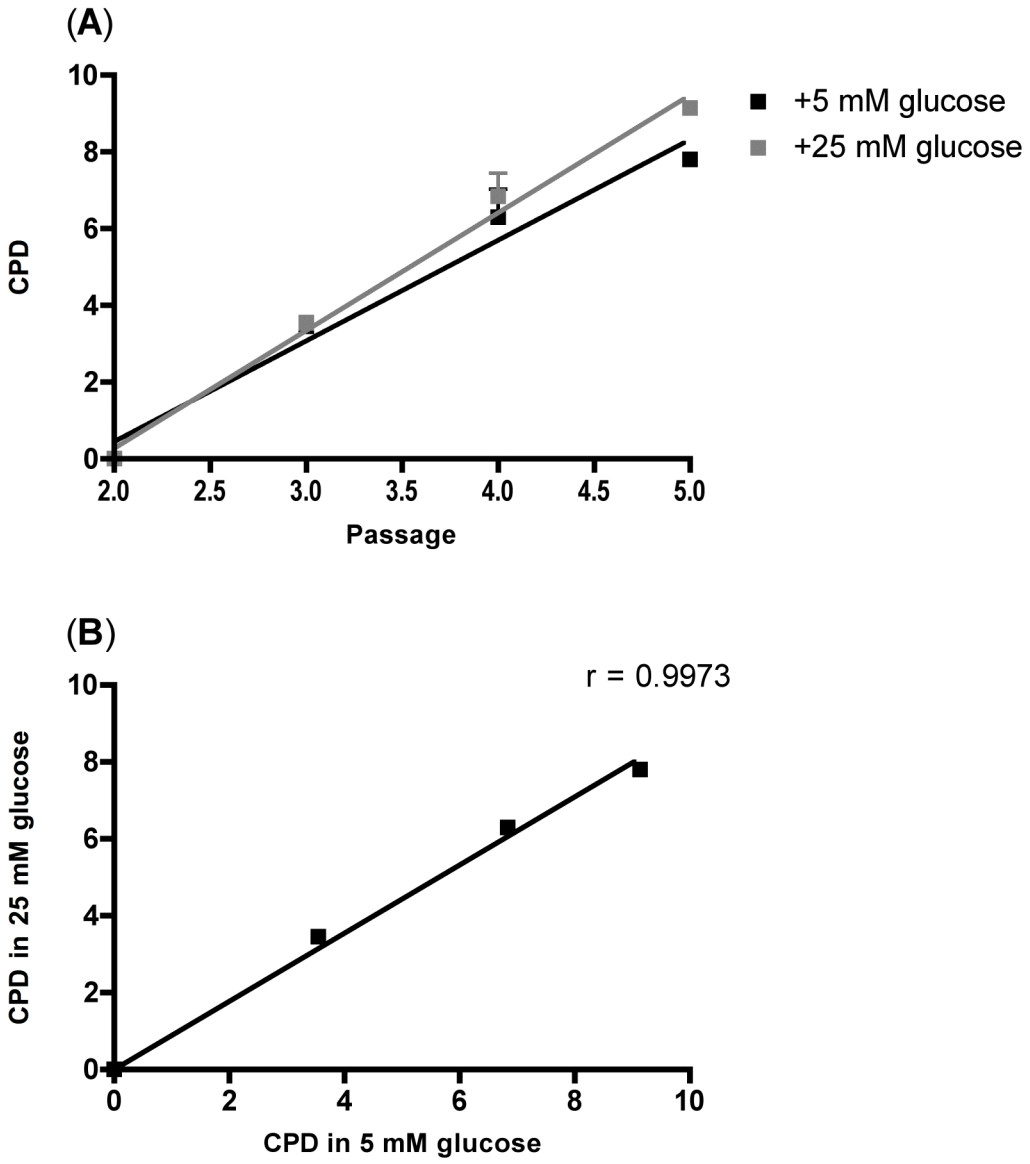

Figure 14 shows the effect of culturing HUVEC in different concentrations of glucose on growth rate. **14A** shows the cumulative population doublings (CPD) in cells grown in 5 mM vs. 25 mM glucose for each passage. **14B** shows the correlation between the CPD of HUVEC grown in 5 mM vs. 25 mM glucose. Data are represented as mean ± SEM, n = 2.

3.3 Effects of uridine on HUVEC growth

Rho 0 cells are auxotrophic for uridine because the enzyme responsible for uridine synthesis (dihydrooratate dehydrogenase) is situated on the inner mitochondrial membrane and requires a functional ETC for its activity. Rho 0 cells need medium supplemented with uridine in order to proliferate and survive (King and Attardi 1996).

Rho 0 medium lacking uridine was produced by dialysis as described in section 2.2.1.6. After a minimum of 12 days in culture Rho 0 and WT cells were trypsinised and seeded into 6 well plates. For each condition 3 wells were placed in Rho 0 medium (+ uridine) or Rho 0 uridine-free medium (- uridine). The Rho 0 HUVEC were maintained in EB. 1 well per condition was trypsinised and counted using the Coulter™ counter at 24 hours, 48 hours and 144 hours. The number of cells is expressed as a % of the number of cells in Rho 0 medium (+ uridine) at first count (24 hours).

WT cells continue to proliferate in both types of medium (shown in figure 15A) although they proliferate significantly more slowly in uridine-free medium. Rho 0 HUVEC do not proliferate in uridine-free medium. Furthermore after 24 hours the number of cells in the culture is reduced in a time-dependent manner (shown in figure 15B) indicating that the cells are auxotrophic for uridine.

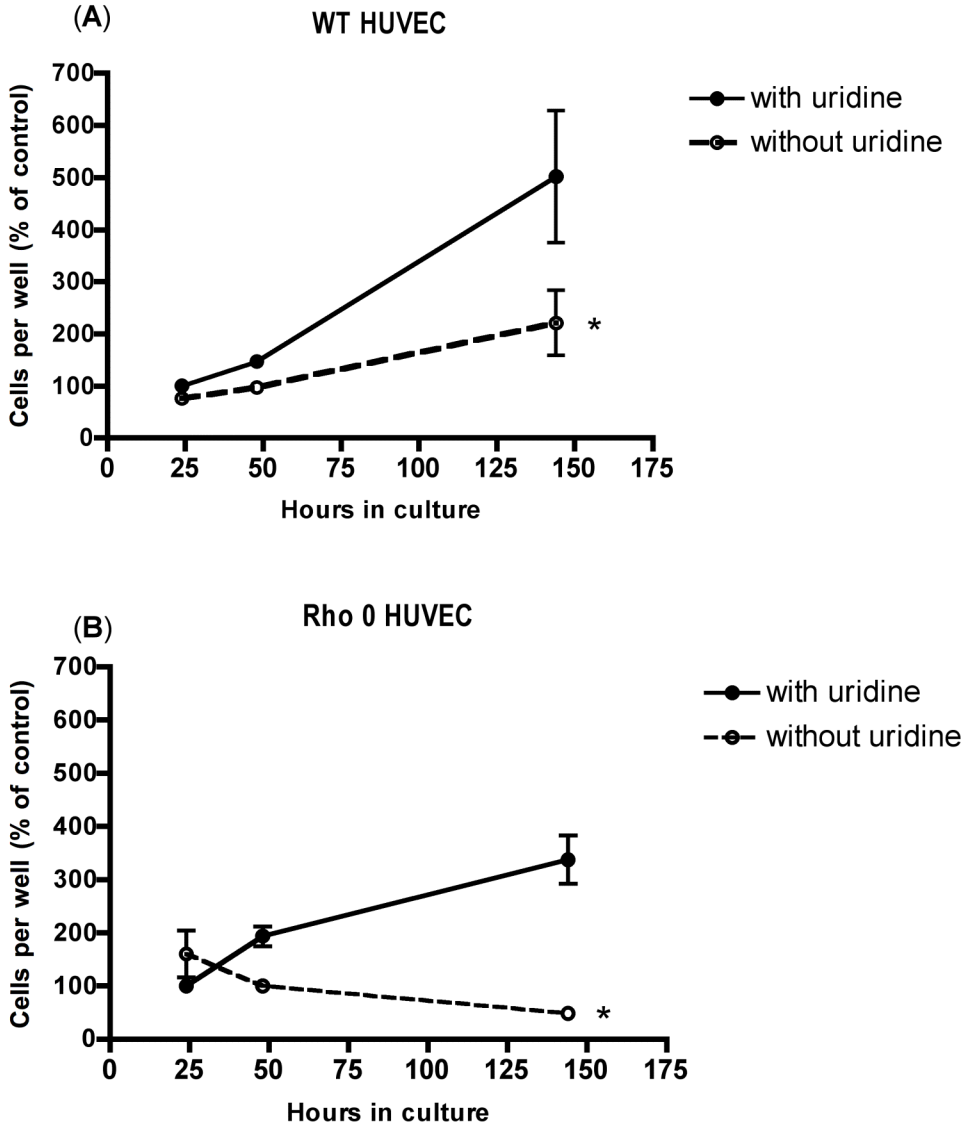

Figure 15 shows the effect of culturing HUVEC with (+uridine) and without (-uridine). Cells per well are expressed as a % of the number of cells with uridine at 24 hours. **15A** shows growth of WT cells in both conditions **15B** shows that EB cells only grow in the presence of Uridine. Data are represented as mean ± SEM, n = 9, from 3 independent experiments. * $p < 0.05$.

3.4 Effects of Ethidium Bromide on expression of mitochondrial encoded genes

Primers were designed for cytochrome C oxidase (Complex IV of the ETC) subunit-1 and ATPase (Complex V) subunit-6 genes, both of which are coded for by mitochondrial DNA. β-actin, which is a housekeeping gene encoded by nuclear DNA, was used as the control. After 7 days treatment with EB RNA from Rho 0 and WT cells was harvested and processed by quantitative RT-PCR, as described in section 2.4.4.1. Gene expression is shown relative to ß actin in figure 16.

Looking at the expression of cytochrome C oxidase (CcO) subunit-1 it can be seen that mRNA is undetectable after 7 days of EB treatment compared to WT cells (shown in figure 16A). It has been reported that the continuous presence of low dose EB is needed to maintain the Rho 0 phenotype (Desjardins, Frost et al. 1985; King and Attardi 1989). As shown in Figures 16A this was also confirmed in HUVEC since removal of EB restored mRNA of the mitochondrial genes to the original levels. Levels of WT mRNA did not significantly change over time so are not shown beyond 7 days. The pattern of expression for ATPase subunit-6 was found to be identical to that of cytochrome C oxidase subunit-1 (shown in figure 16B).

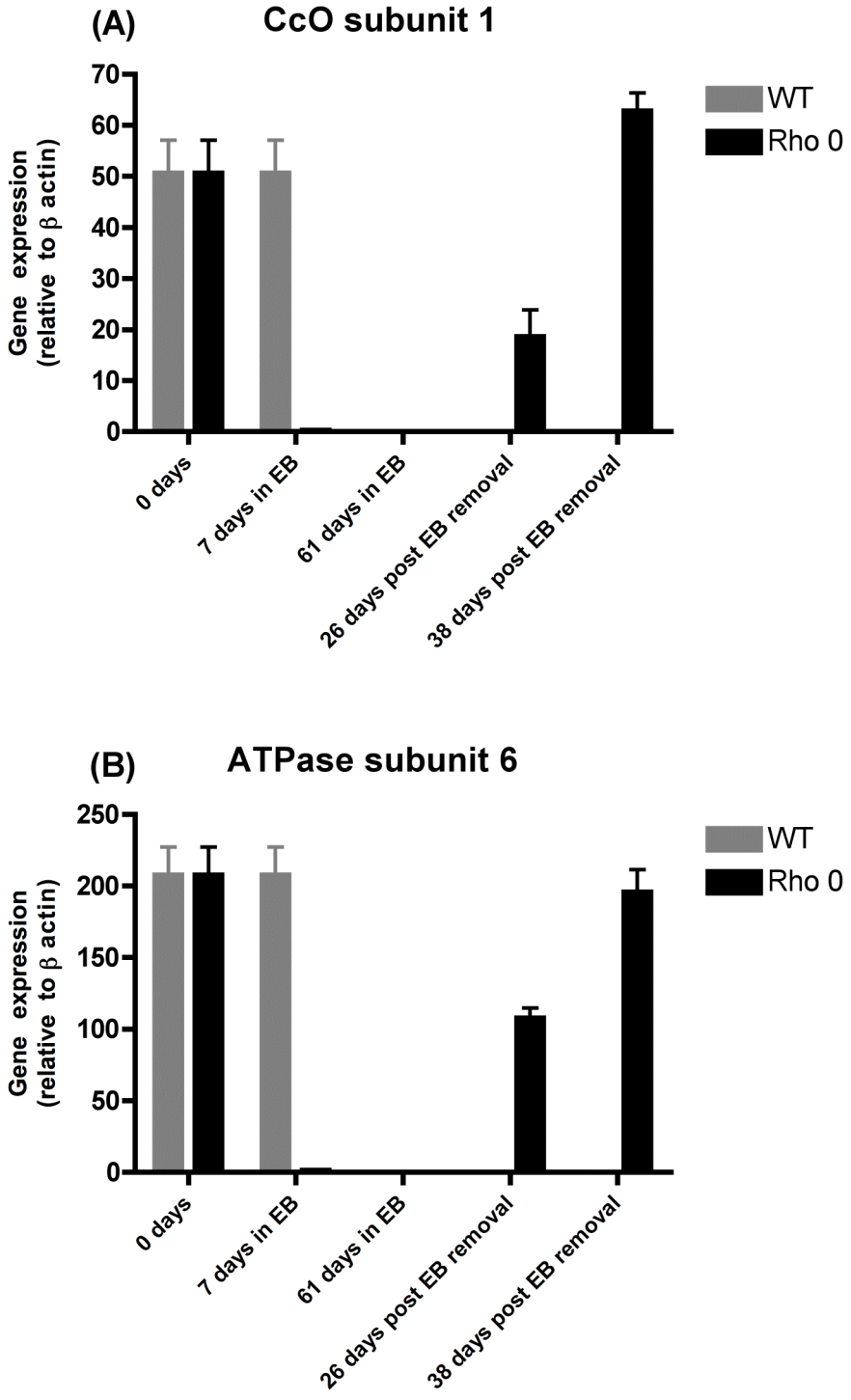

Figure 16 shows expression of mitochondrial-encoded genes by quantitative RT-PCR relative to β-actin. **16A** shows cytochrome C oxidase subunit-1 and **16B** shows ATPase subunit-6. The effects after 7 days in respective medium (Data from 4 independent experiments represented as mean ± SEM, n = 12) and of removal of EB, after long-term culture in EB, (Data from 1 experiment represented as mean ± SEM, n = 3) on gene expression are shown.

3.5 Effects of Ethidium Bromide on expression of electron transport chain proteins

After 12 days treatment protein from Rho 0 and WT cells was harvested and processed by SDS-PAGE and western blot analysis, as described in section 2.5.

The mitochondrial-encoded protein, 57 kDa cytochrome C oxidase subunit-1, was completely absent in the EB treated cells, whereas the nuclear-encoded protein, 30 kDa subunit of succinate-ubiquinol oxidoreductase (Complex II), was present in equal amounts in both Rho 0 and WT cells. The 50 kDa α-tubulin subunit, used as a loading control, was found to be expressed equally in all cells. This was shown in 4 independent experiments (a representative experiment is shown on the next page, with the quantitative densitometry from all 4 independent experiments in figure 17).

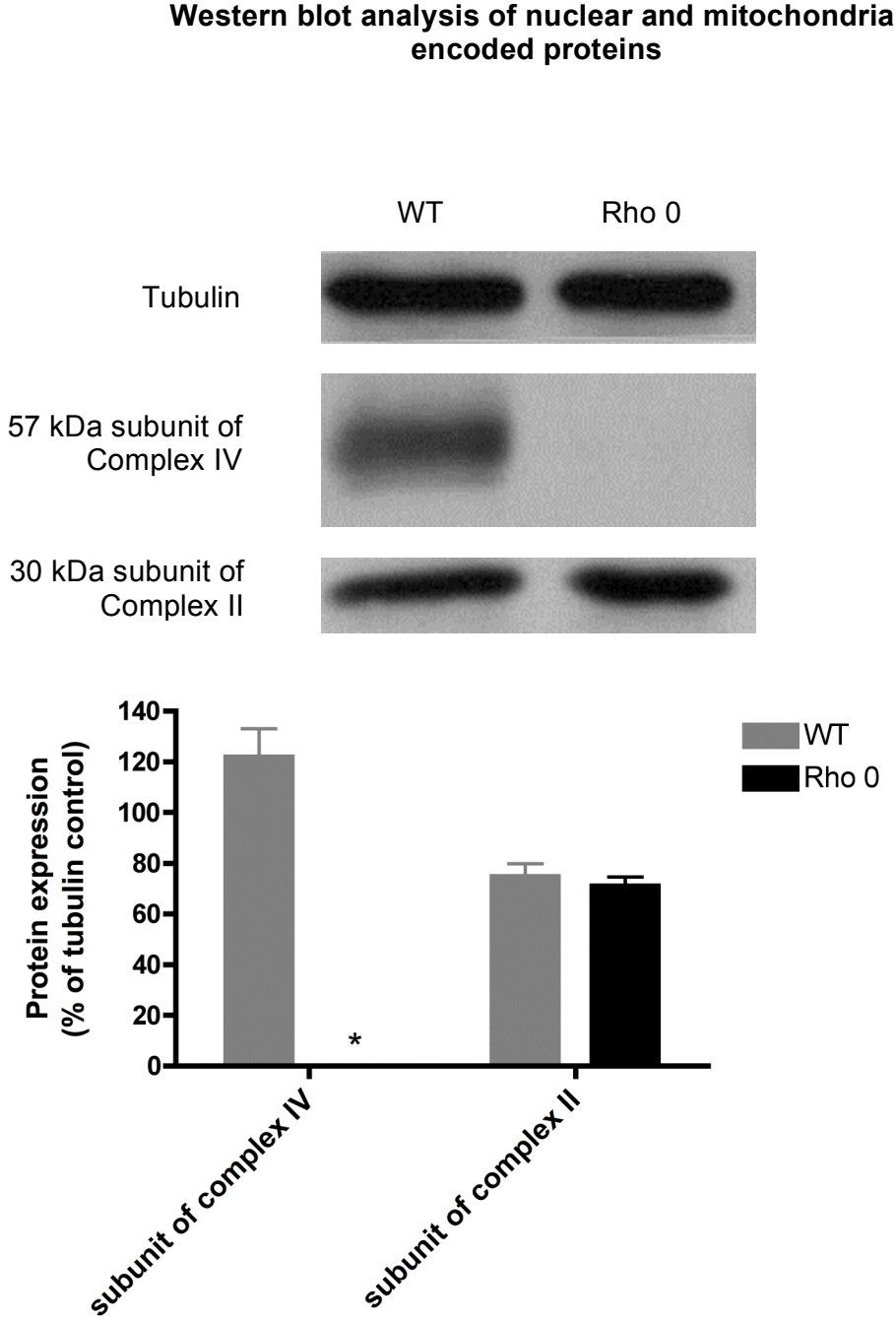

Figure 17 shows western blot analysis of HUVEC for the mitochondrial-encoded 57 kDa subunit-1 of complex IV (cytochrome c oxidase) and the nuclear-encoded 30 kDa subunit of complex II (Succinate-ubiquinol oxidoreductase). The 50 kDa α-Tubulin subunit is shown as a loading control. A representative gel is shown. The graph shows quantitative analysis, from which it can clearly be seen that the mitochondrial-encoded protein is absent in the Rho 0 HUVEC, whereas the nuclear-encoded proteins are unaffected. Data are represented as mean ± SEM, n = 4, from 4 independent experiments. * $p < 0.05$.

3.6 ATP and lactate production by HUVEC

After 12 days treatment EB and WT cells were trypsinised and plated onto 96-well plates for ATP production measurements using the ATPLite™ kit, as described in section 2.6. Protein content of the wells was measured using the BCA™ Protein Assay Kit, as described in section 2.5.2.2. ATP levels were expressed per mg of protein. Aliqouts of medium from EB and WT cells were taken at 48 hours, just prior to the medium change, and the lactate content measured as described in section 2.7. Average ATP levels for 9 independent cultures showed that Rho 0 HUVEC produce significantly less ATP than WT cells (shown in Table 04). Lactate measurement, from 3 independent cultures showed that Rho 0 HUVEC produce significantly more lactate than WT cells (shown in Table 04).

	ATP **pmol/mg protein** Mean ± SEM, n = 9 ‡	**Lactate** **mM** Mean ± SEM, n = 3 ‡‡
WT cells	913 ± 48	7.49 ± 0.69
EB cells	580 ± 64 *	17.76 ± 2.26 *

Table 04 – Metabolic profile of HUVEC

‡ Results represent mean of 9 independent experiments. * $p < 0.05$

‡‡ Results represent mean of 3 independent experiments. * $p < 0.05$

3.7 Source of ATP production in HUVEC

In order to determine the source of ATP production in HUVEC a series of experiments were conducted using different inhibitors of respiration. After 12 days treatment Rho 0 and WT cells were trypsinised, plated onto 96-well plates and their ATP production measured using the ATPLite™ kit, as described in section 2.6. Protein content of the wells was measured using the BCA™ Protein Assay Kit, as described in section 2.5.2.2. To compare treatments all values are shown as a % of the control WT cells ATP levels.

All treatments for each experiment were done in triplicate. In each independent experiment cells in 96-well plates were treated for two hours before performing the ATPLite™ assay as described in section 2.6. Each well was washed with 1 x PBS prior to adding the inhibitors to phenol-free EGM-2, after which the cells were placed in a standard incubator at 37 °C.

2-Deoxy-D-glucose (2-DOG) is a competitive inhibitor of hexokinase and thus glycolysis (Nirenberg and Hogg 1958). Oligomycin is a macrolide antibiotic made from *Streptomyces diastochromogenes* and contains a mix of oligomycins A, B and C, of which approximately 65 % is oligomycin A. Oligomycin is known to inhibit mitochondrial ATPase (complex V) at a dose of 20 µg/mL (Drobinskaya, Kozlov et al. 1978).

As shown in figure 18A Rho 0 HUVEC produce significantly less ATP than WT HUVEC (also shown in table 04). Throughout all the experiments the Rho 0 HUVEC always produce significantly less ATP than the WT cells. However, the

amount of reduction in basal ATP production in Rho 0 cell varied from 60 to 20 %. Addition of 20 mM 2-DOG reduced ATP production of WT HUVEC from (100 ± 4.3) % to (30.9 ± 2.7) % i.e. by 69 % ($p < 0.05$). Addition of 20 µg/mL oligomycin reduced ATP production of WT HUVEC from (100 ± 4.3) % to (84.2 ± 3.3) % i.e. by 16 % ($p < 0.05$). The combination of 20 mM 2-DOG and 20 µg/mL oligomycin reduced ATP production of WT HUVEC from (100 ± 4.3) % to (7.2 ± 0.9) % i.e. by 92.8 % ($p < 0.05$). In contrast addition of 20 mM 2-DOG reduced ATP production of Rho 0 HUVEC from (37.4 ± 6.1) % to (1.9 ± 0.3) % i.e. by 95 % ($p < 0.05$). Addition of 20 µg/mL oligomycin reduced ATP production of Rho 0 HUVEC from (37.4 ± 6.1) % to (26.5 ± 5.0) % i.e. by 29 % (p = ns). The combination of 20 mM 2-DOG and 20 µg/mL oligomycin reduced ATP production of Rho 0 HUVEC from (37.4 ± 6.1) % to (1.1 ± 0.2) % i.e. by 97 % ($p < 0.05$).

When ATP production is directly measured it can be seen that WT HUVEC depend on glycolysis for a majority of their ATP production, however mitochondria make a significant contribution to the cells' ATP production. The addition of oligomycin to 2-DOG leads to a significant further reduction in ATP production in WT HUVEC compared to WT HUVEC treated with 2-DOG alone ($p < 0.05$). In contrast no significant further reduction in ATP production is seen in Rho 0 HUVEC treated in the same way (shown in figure 18B, which is data from figure 18A drawn on a different scale to clearly illustrate this point). Taken together these results demonstrate that Rho 0 HUVEC are entirely dependent on glycolysis for their metabolic demands.

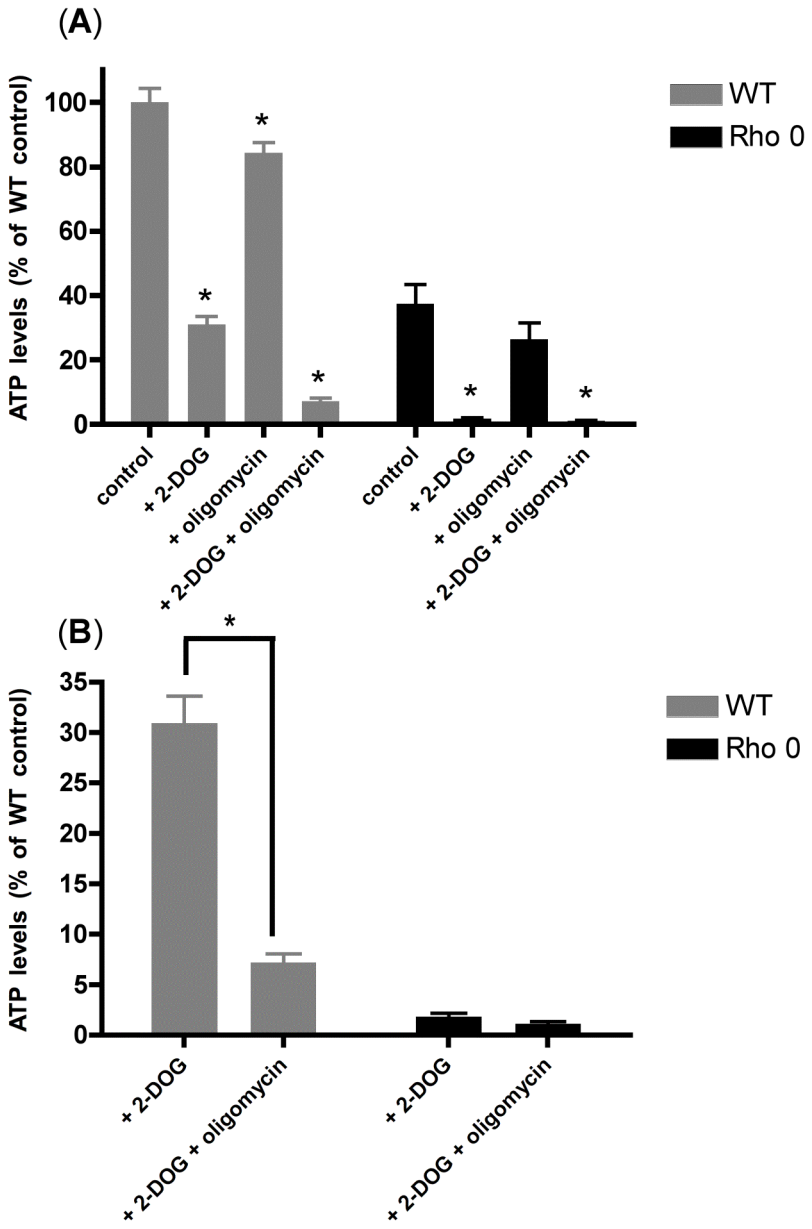

Figure 18 shows the effects of different metabolic inhibitors on HUVEC ATP production. **18A** shows that 20 mM 2-DOG significantly reduces ATP production to a greater extent in Rho 0 HUVEC than in WT HUVEC. 20 μg/mL oligomycin causes a small reduction in WT HUVEC but has no significant effect on Rho 0 HUVEC. Addition of 20 μg/mL oligomycin to 20 mM 2-DOG further reduces ATP production in WT HUVEC but has no significant effect on Rho 0 HUVEC ATP, shown more clearly when data in 18A is plotted on a larger scale in **18B**, indicating that Rho 0 HUVEC derive all their ATP from glycolysis. Data are represented as mean ± SEM, n = 9, from 3 independent experiments. * $p < 0.05$.

3.8 Effects of inhibitors of ETC on ATP production in HUVEC

Finally whether inhibitors of components of the ETC had any effect on HUVEC ATP production was investigated. The same experimental setup was used as described in section 3.7.

Addition of 0.5 μM rotenone, an inhibitor of complex I of the ETC (Lambert and Brand 2004), on its own did not significantly effect ATP production in either WT or Rho 0 HUVEC. However, in WT HUVEC, when added in addition to 20 mM 2-DOG it led to a significant further reduction in ATP levels, from (43.0 ± 3.0) % in cells treated with 20 mM 2-DOG alone to (12.6 ± 1.5) % in treated with both 20 mM 2-DOG and 0.5 μM rotenone ($p < 0.05$). There was no significant change in the EB HUVEC (shown in figure 19A). A similar pattern was seen with the addition of 0.5 μM myxothiazole, an inhibitor of complex III of the ETC (Thierbach and Reichenbach 1981; Thierbach and Reichenbach 1981), shown on the next page in figure 19B. These results confirm that the ATP production of WT cells, which have a functioning ETC, is not effected by inhibitors of the ETC and that these cells can rely entirely on glycolysis for their metabolic demands. So without 2-DOG present inhibitors of the ETC have little or no effect on the ATP levels of HUVEC because they can meet their metabolic demands via glycolysis.

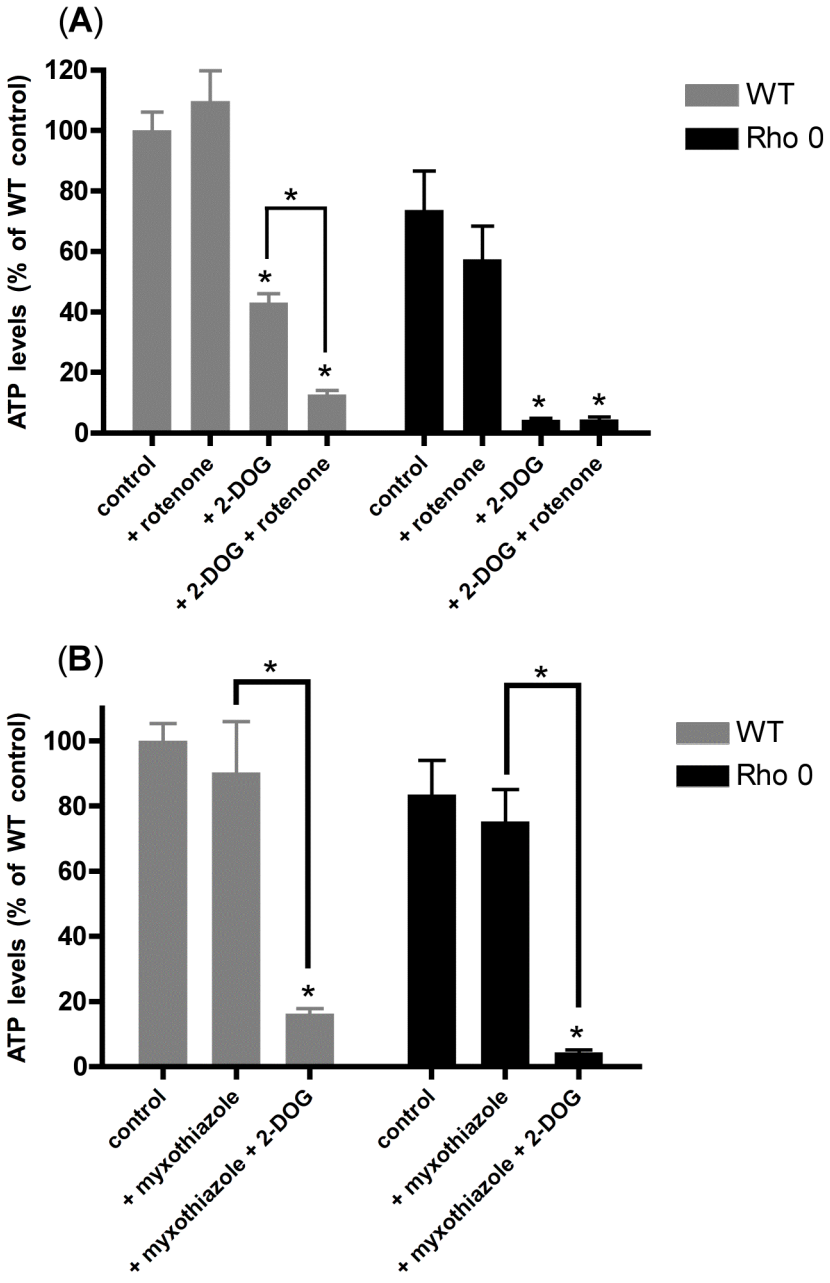

Figure 19 shows the effects of different inhibitors of the electron transport chain on ATP production in HUVEC, compared to control cells. **19A** shows that 0.5 μM rotenone alone has no significant effect, however, in addition to 20 mM 2-DOG, 0.5 μM rotenone significantly reduces ATP production in WT HUVEC but not Rho 0 HUVEC. **19B** shows that 0.5 μM myxothiazole has the same effect as rotenone. Data are represented as mean ± SEM, n = 8, from 3 independent experiments. * $p < 0.05$.

3.9 Cellular Oxygen Consumption and NO production in HUVEC

Cellular oxygen consumption was measured using a Clark-type O_2 electrode, as described in section 2.8.2. Routine steady-state oxygen consumption was significantly less in Rho 0 HUVEC at (19.27 ± 0.69) pmol $O_2.s^{-1}.10^{-6}$ cells compared to WT cells at (35.04 ± 2.21) pmol $O_2.s^{-1}.10^{-6}$, as shown in figure 20 (n = 7, $p < 0.05$).

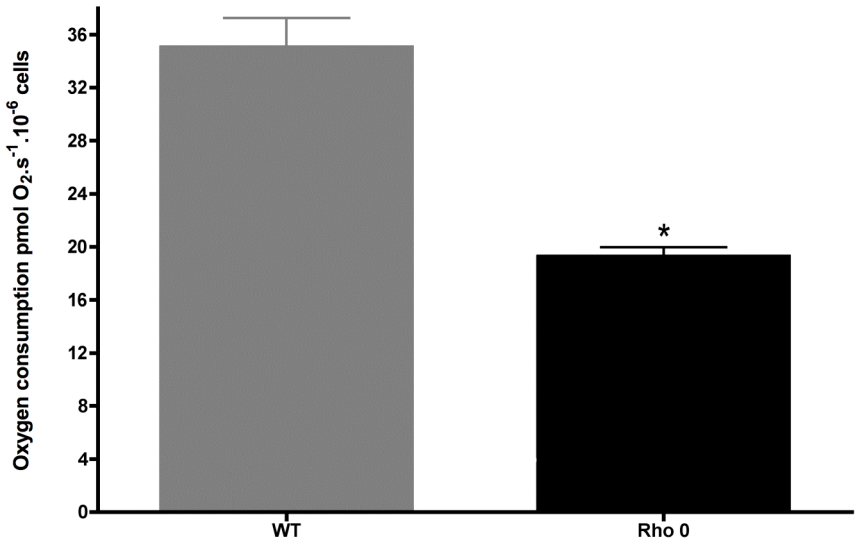

Figure 20 Routine steady-state oxygen consumption in WT and Rho 0 HUVEC. Data are represented as mean ± SEM, n = 7, from 7 independent experiments. * $p < 0.05$.

In figure 21A it can be seen that addition of 2 μg/mL oligomycin caused oxygen consumption to decrease from (100 ± 0) % to (53.0 ± 6.6) % in WT HUVEC. For the ATP experiments 20 μg/mL oligomycin was used, as per the protocol developed. However when cellular oxygen consumption was studied it was demonstrated by the person who developed this protocol that 2 μg/mL oligomycin was enough to produce the maximal effect on oxygen consumption of cells and that addition of doses up to a dose of 20 μg/mL had no further additional effect. Sequential addition of carbonyl cyanide 4-trifluoromethoxyphenylhydrazone

(FCCP) an uncoupler of the ETC (Sokal and Bartosz 1998) in 1 μM aliquots up to a total dose of 3 μM leads to a maximum oxygen consumption of (267.7 ± 39.8) %. Finally sequential addition of 2 μM myxothiazole reduced oxygen consumption to a minimum level of (24.4 ± 8.5) %. This demonstrates that cellular oxygen consumption is predominantly from respiration using the ETC. In contrast, none of these reagents significantly changes the routine oxygen consumption of Rho 0 HUVEC (55.0 ± 8.1 %) demonstrating that they do not have a functional ETC. This data is shown as a time course figures 21B.

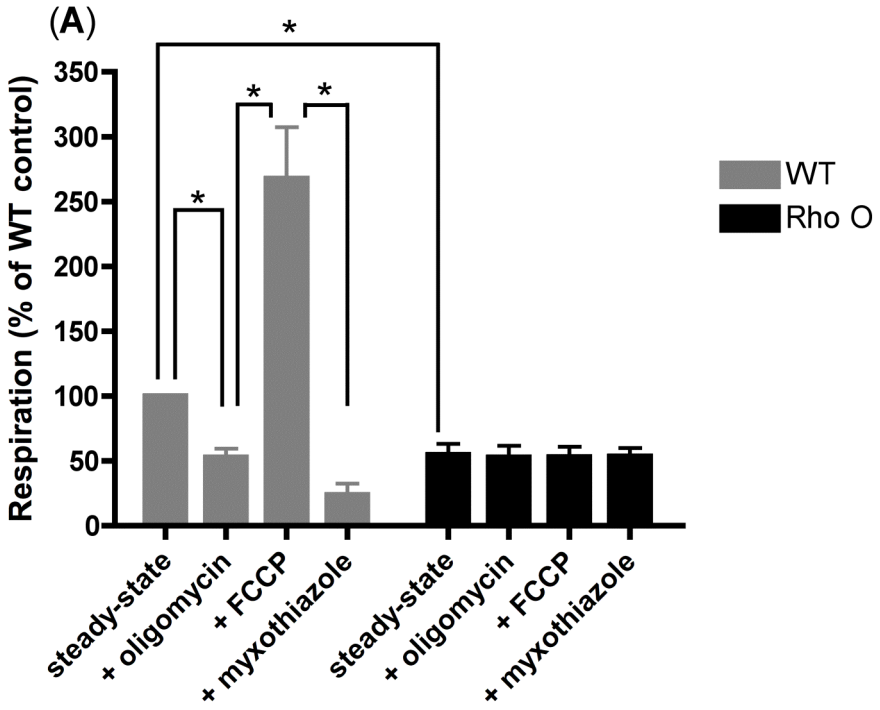

Figure 21A shows oxygen consumption in WT versus Rho 0 HUVEC. The baseline oxygen consumption in WT HUVEC is predominantly from oxidative phosphorylation. Drugs were added sequentially to the same sample of cells. Addition of 2 μg/mL oligomycin reduces this by 47 % i.e. from (100 ± 0) % to (53.0 ± 6.6) %, FCCP increases it to a maximum at (267 ± 39.8) % and finally 0.5 μM myxothiazole reduces this to a minimum of (24.0 ± 8.5) %. In contrast none of these reagents significantly altered oxygen consumption in Rho 0 HUVEC. Data are represented as mean ± SEM, n = 3, from 3 independent experiments. * $p < 0.05$.

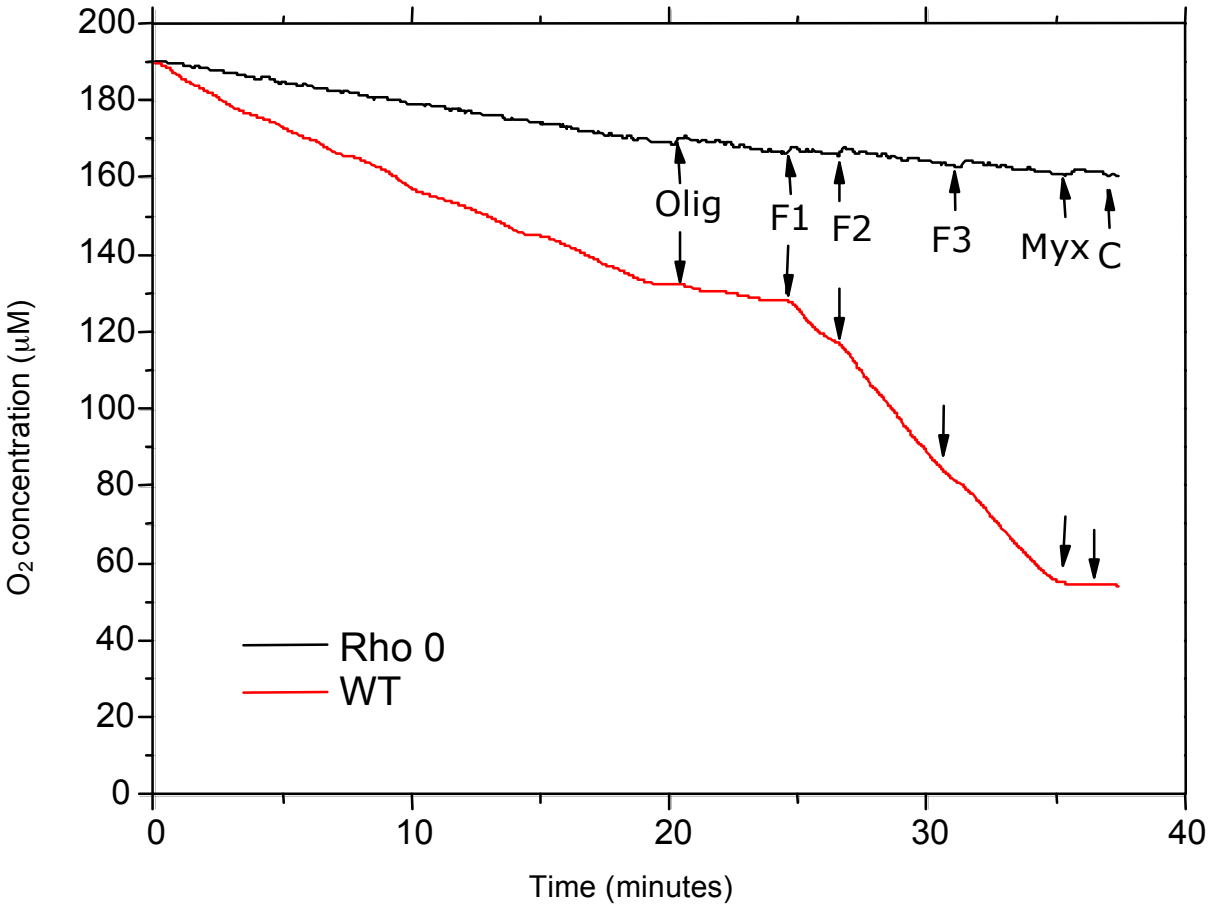

Figure 21B shows a trace of oxygen consumption over time from a representative experiment. Where Olig = 2 μg/mL oligomycin, F1 = 1 μM FCCP total, F2 = 2 μM FCCP total, F3 = 3μM FCCP total, Myx = 0.5 μM myxothiazole, KCN = 0.5 μM potassium cyanide.

NO production was measured in HUVEC and is shown as a time course in figure 22A and quantitatively for all three experiments in figure 22B. Baseline NO production was significantly less in WT HUVEC at (30.59 ± 1.69) pM compared to Rho 0 HUVEC at (62.43 ± 0.52) pM. Addition of 0.5 μM KCN caused a significant increase in WT HUVEC to (37.39 ± 2.08) pM, compared to base line (30.59 ± 1.69) pM ($p < 0.05$) but no significant change in Rho 0 HUVEC (62.48 ± 0.54) pM compared to base line (62.43 ± 0.52) pM.

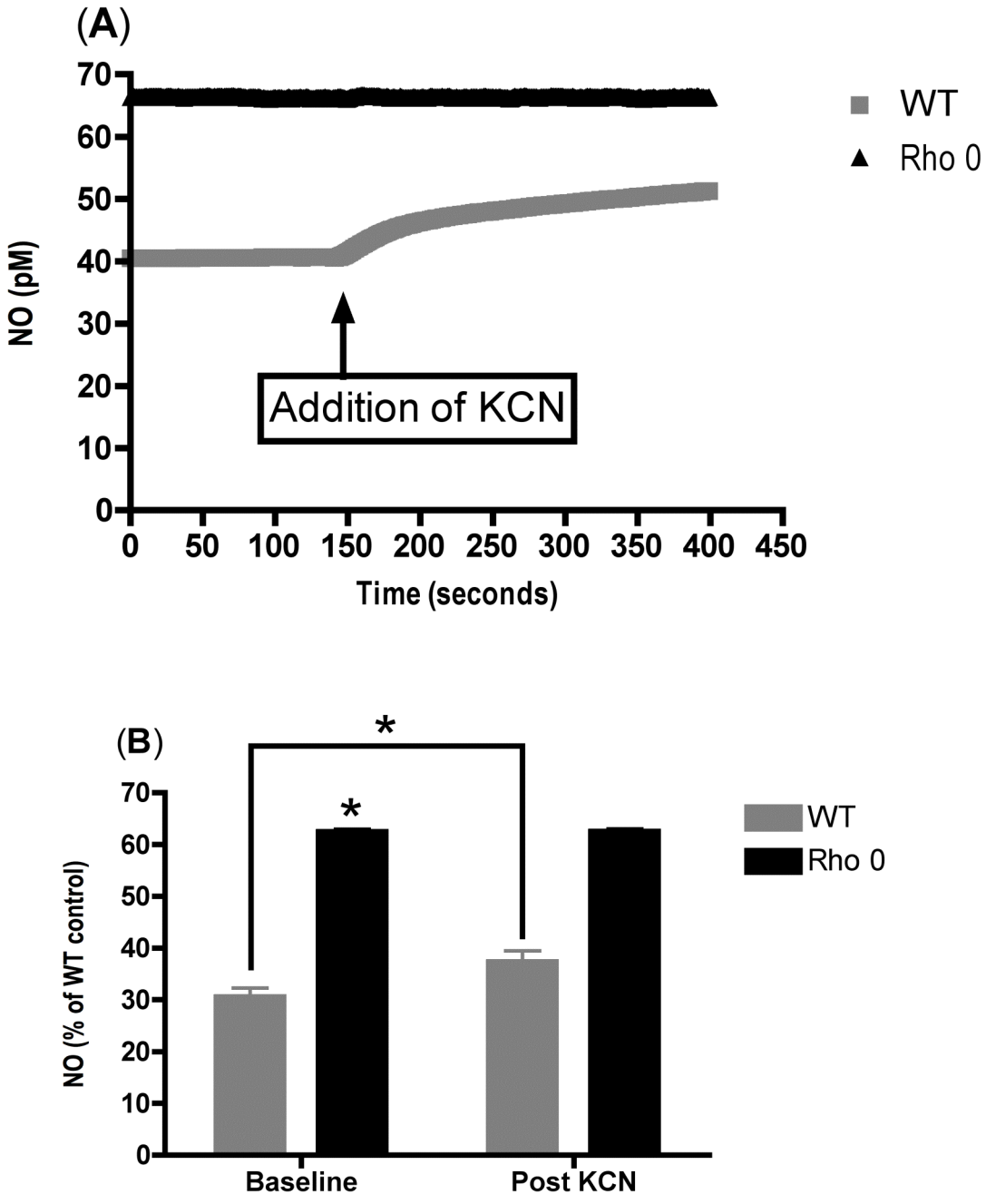

Figure 22 shows NO production in WT versus Rho 0 HUVEC. **22A** shows NO over a time course and the point at which 0.5 μM KCN was added. From **22B** it can be seen that the baseline NO levels in WT HUVEC are significantly less than in Rho 0 HUVEC. Addition of KCN causes a significant increase in NO in WT HUVEC (30.59 pM ± 1.69 pM to 37.39 pM ± 2.08 pM) but no significant change in Rho 0 cells (62.43 pM ± 0.52 pM to 62.48 pM ± 0.54 pM). Data are represented as mean ± SEM, n = 10, from 3 independent experiments. * $p < 0.05$.

Sequential addition of 0.5 μM potassium cyanide, an inhibitor of complex IV (Wilson, Greenwood et al. 1975), after the addition of 0.5 μM myxothiazole had no additional effect on oxygen consumption in either WT or Rho 0 HUVEC (shown in figure 23). Clearly non-mitochondrial sources of oxygen consumption must account for the oxygen consumption seen in the Rho 0 HUVEC. Intracellular NADPH oxidases are one potential candidate source to explain this finding in Rho 0 cells (Li and Shah 2002), therefore it was determined whether these were a significant source of oxygen consumption in HUVEC. The isoforms of Nox in endothelial cells are thought to be Nox1, Nox2 and Nox 4, as discussed in section 1.6.4. After complete inhibition of oxidative phosphorylation 10 μM apocynin, an inhibitor of NADPH oxidases was added (Simons, Hart et al. 1990; Weber, Erl et al. 1994). As shown in figure 23 in Rho 0 cells there was a reduction in oxygen consumption from baseline at (61.7 ± 13.3) % to (28.0 ± 7.1) % ($p < 0.05$) following the addition of apocynin, in contrast there was no significant effect in WT cells.

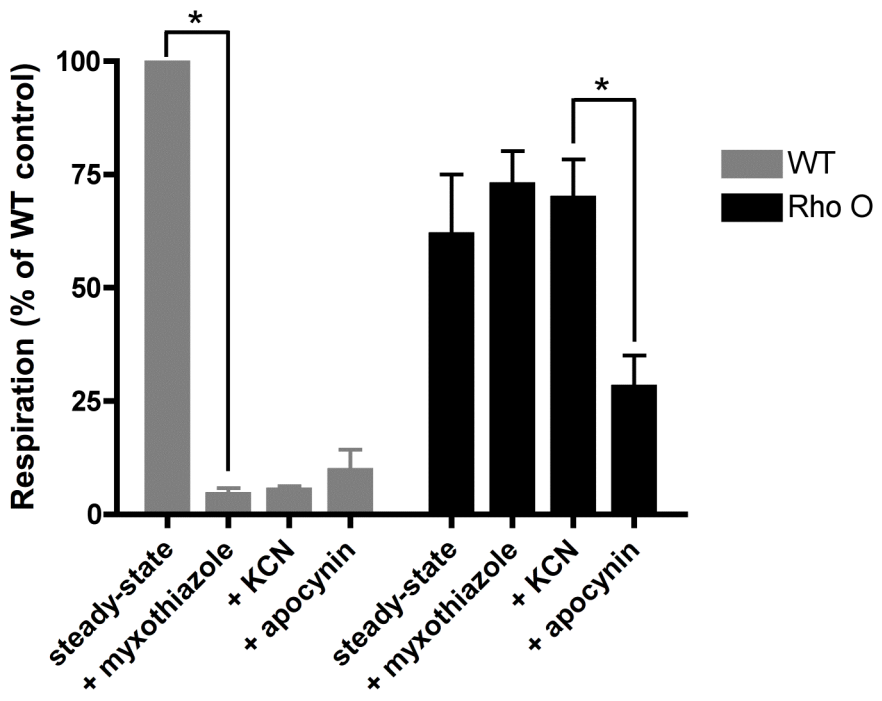

Figure 23 shows the source of baseline oxygen consumption in WT versus Rho 0 HUVEC. Drugs were added sequentially to the same sample of cells. The baseline oxygen consumption in WT HUVEC is predominantly from oxidative phosphorylation and that addition of 0.5 μM myxothiazole reduces this to a minimum of (4.3 ± 0.8) %, addition of 0.5 μM KCN does not significantly reduce this further. In contrast none of these reagents significantly alters oxygen consumption in Rho 0 HUVEC. In contrast 10 μM apocynin reduces oxygen consumption from (61.7 ± 13.3) % to (28.0 ± 7.1) % in Rho 0 HUVEC but has no effect on WT cells. Data are represented as mean ± SEM, n = 3, from 3 independent experiments. * $p < 0.05$.

There is some controversy in the literature about the mechanism of action of apocynin and although the majority of literature suggests it inhibits NADPH oxidases more recently there has been some evidence to suggest it may act as an antioxidant and not a specific inhibitor of NADPH oxidases (Heumuller, Wind et al. 2008). Therefore the oxygen consumption experiments were repeated with

diphenyleneiodonium chloride (DPI), which is known to inhibit NADPH oxidases (O'Donnell, Tew et al. 1993). Figure 24 shows that addition of 33 μM DPI to Rho 0 HUVEC caused a reduction in oxygen consumption from baseline at (54.0 ± 3.0) % to (26.8 ± 1.8) % ($p < 0.05$), in contrast there was no significant effect on WT cells, indicating that NADPH oxidase is a significant source of oxygen consumption in Rho 0 endothelial cells.

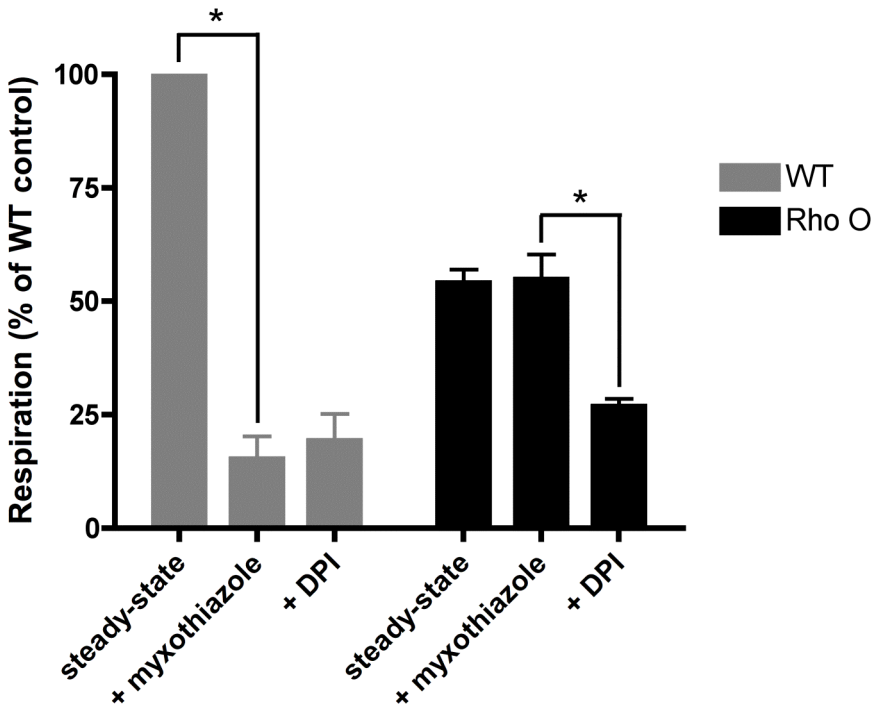

Figure 24 shows the effect of DPI on oxygen consumption in HUVEC. Drugs were added sequentially to the same sample of cells. 33 μM DPI reduces oxygen consumption from (54.0 ± 3.0) % to (26.8 ± 1.8) % in Rho 0 HUVEC but has no effect on WT cells. Data are represented as mean ± SEM, n = 4, from 4 independent experiments. * $p < 0.05$.

3.10 Mitochondrial membrane potential by live confocal microscopy

This was studied using live cells in culture medium, as described in section 2.13. Tetramethylrhodamine (TMRM) is a potentiometric fluorophore, which is readily sequestered by functioning mitochondria and its uptake by mitochondria is proportional to the mitochondrial membrane potential (Poot, Zhang et al. 1996; Bkaily, Pothier et al. 1997). The cells were labelled with 50 nM TMRM for 30 minutes prior to placing them in the live chamber to record their membrane potential in real-time using live confocal microscopy and study the effect of the addition of drugs to this (shown in figures 25 and 26). Average signal intensity was quantified using specialist software (kindly done by Dr Sean Davidson, UCL, London) and plotted over time as a percentage of the starting value of 100 % (shown in figure 25). Representative still images are shown in figure 26 and the full movies can be viewed in the supplementary material disk attached to the back cover of this thesis. TMRM labelling of the cells showed that mitochondria maintain a membrane potential in Rho 0 cells, although to a lesser degree than WT cells (see figures 26A and 26B). It has previously been shown that Rho 0 cells maintain a mitochondrial membrane potential via the adenine nucleotide translocator (ANT) and a functional F1 component of ATPase (Buchet and Godinot 1998).

It can clearly be seen from this confocal work that the mitochondria from Rho 0 cells are morphologically different from WT cells. The Rho 0 HUVEC mitochondria are less filamentous in shape and appear more rounded and swollen than the WT mitochondria. This is entirely in keeping with previously published work on Rho 0 cells as explained earlier in section 1.4.1.

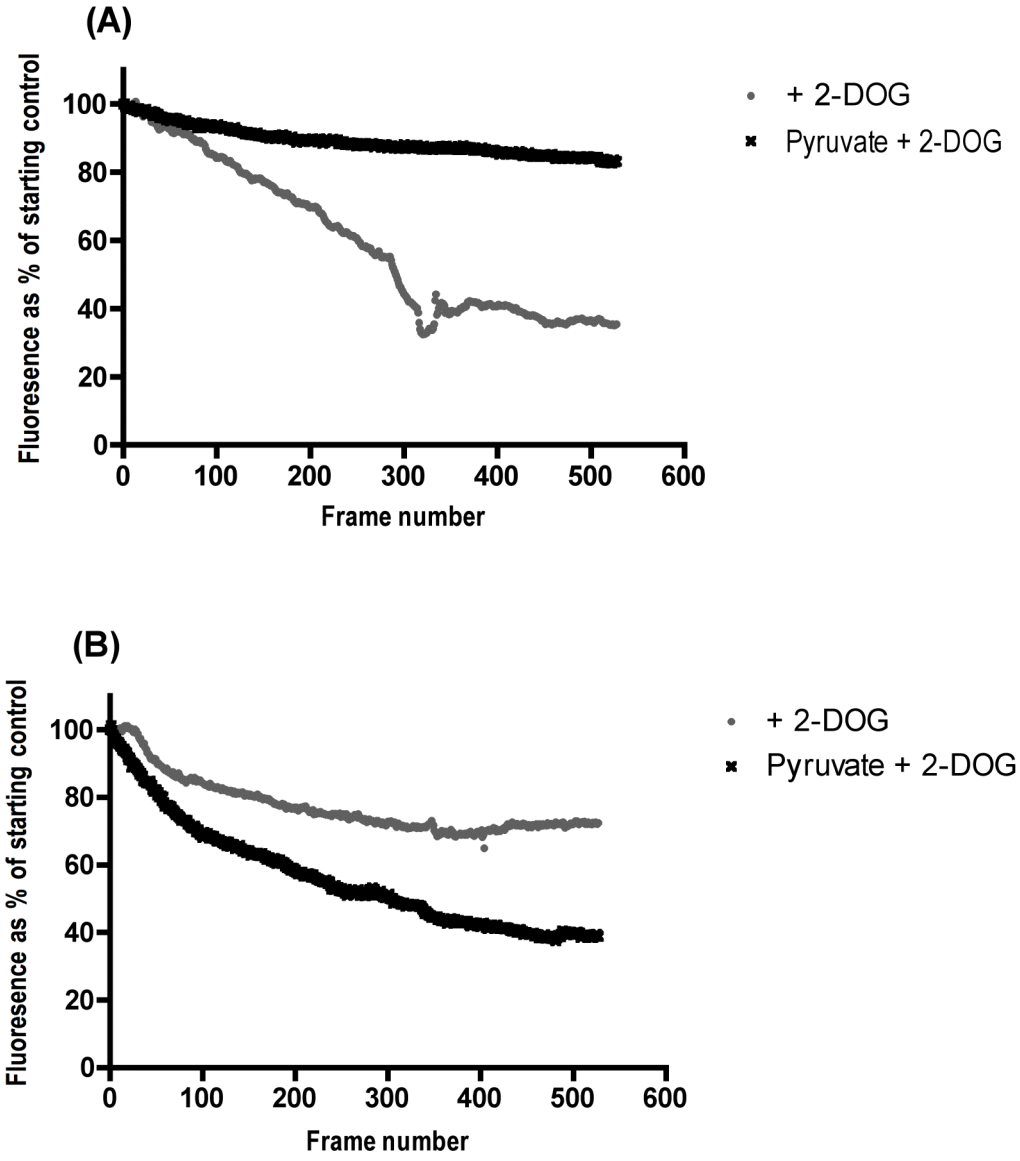

Figure 25 shows the effect of drugs added at the start of the graphs (frame 0) on mitochondrial membrane potential **25A** shows WT cells and **25B** shows Rho 0 cells. The addition of 20 mM 2-DOG causes the collapse of membrane potential in both WT and Rho 0 cells, shown as grey lines. When the media contains 20 mM pyruvate the WT cells are able to maintain their membrane potential after the addition of 20 mM 2-DOG, in contrast the Rho 0 cells do not, shown as black lines. Data are represented as mean ± SEM, n = 2, from 2 independent experiments.

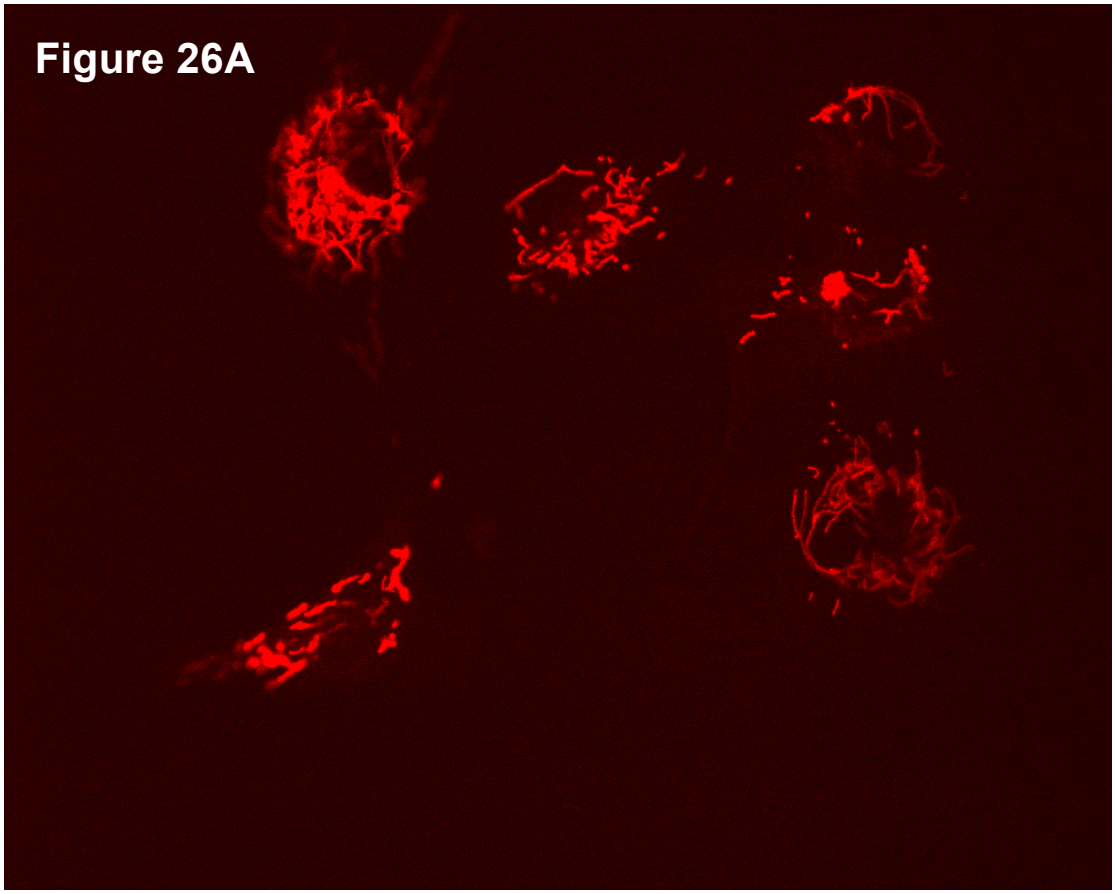

Figure 26A shows TMRM staining of mitochondrial membrane potential of WT HUVEC, which is red and the intensity of which is proportional to the membrane potential. This is from one representative experiment.

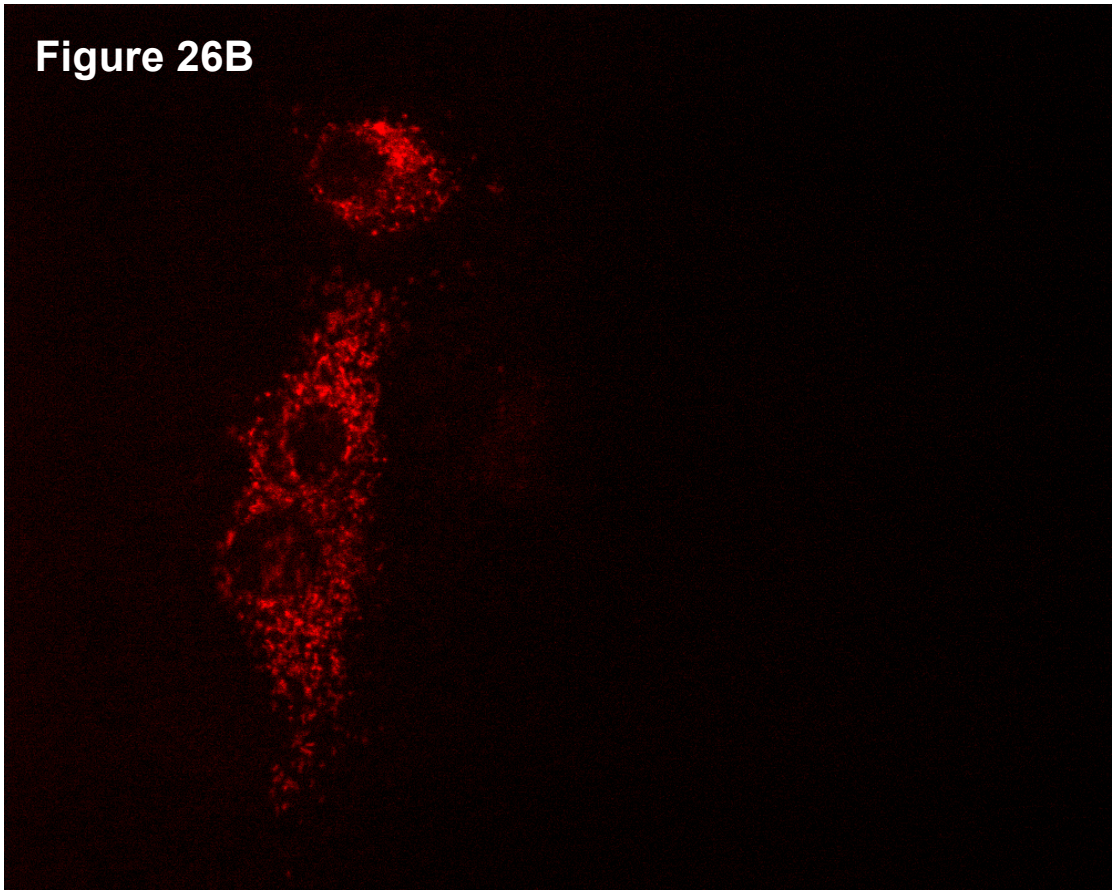

Figure 26B shows TMRM staining of mitochondrial membrane potential of Rho 0 HUVEC, which is red and the intensity of which is proportional to the membrane potential. The Rho 0 HUVEC showing less fluorescence than the WT cells, indicating that Rho 0 HUVEC have a weaker mitochondrial membrane potential. This is from one representative experiment.

The addition of 20 mM 2-DOG to the medium causes complete collapse of the mitochondrial membrane potential in both WT and Rho 0 HUVEC (see figures 25, 26C to 26F and movies A and B on supplementary material disk). When the cells were placed in a 20 mM pyruvate rich medium then addition of 20 mM 2-DOG did not lead to the collapse of the mitochondrial membrane potential in the WT cells but did in the Rho 0 HUVEC (see figures 25, 26G to 26J and movies C and D on supplementary material disk). This demonstrates the Rho 0 HUVEC complete dependence on glycolysis to maintain their mitochondrial membrane potential.

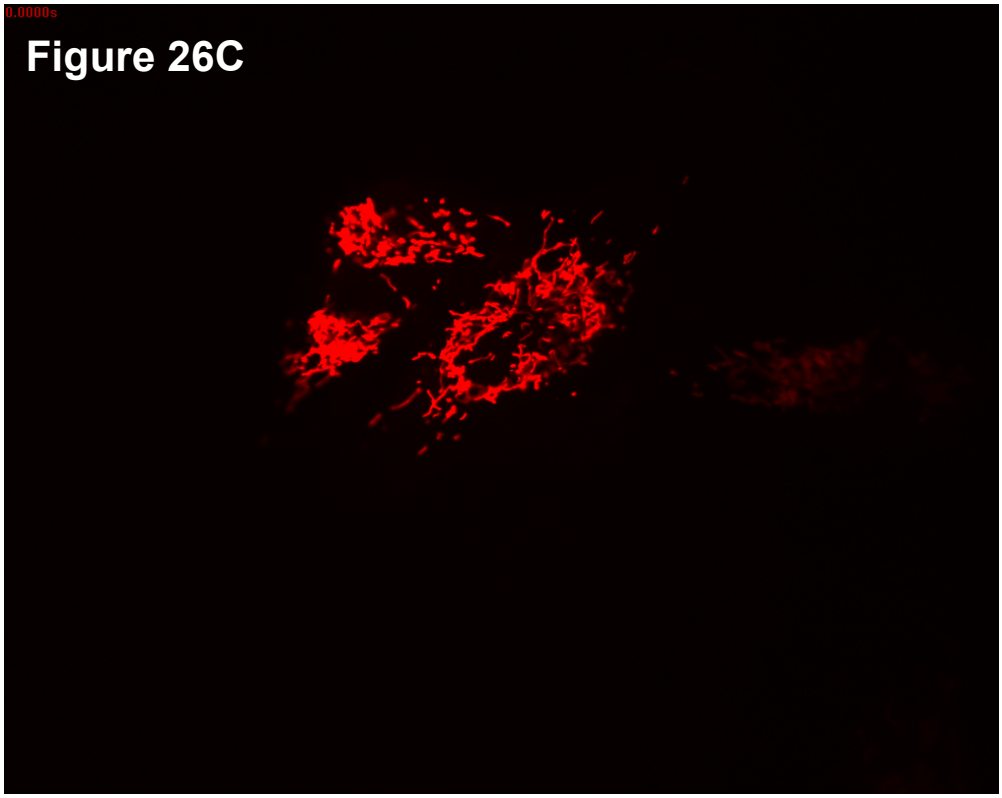

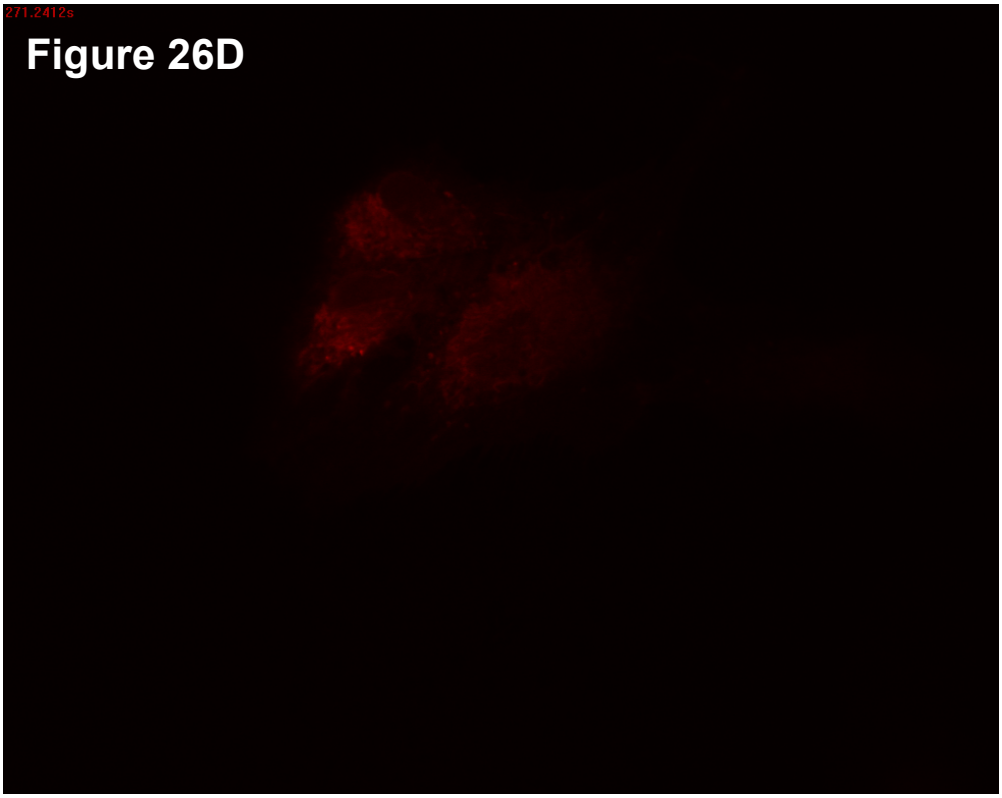

Figures 26C and **26D** show the effect of addition of 2-DOG on TMRM staining of mitochondrial membrane potential of WT cells. Mitochondrial membrane potential is lost after the addition of 2-DOG (**26D**)**.** This is from one representative experiment.

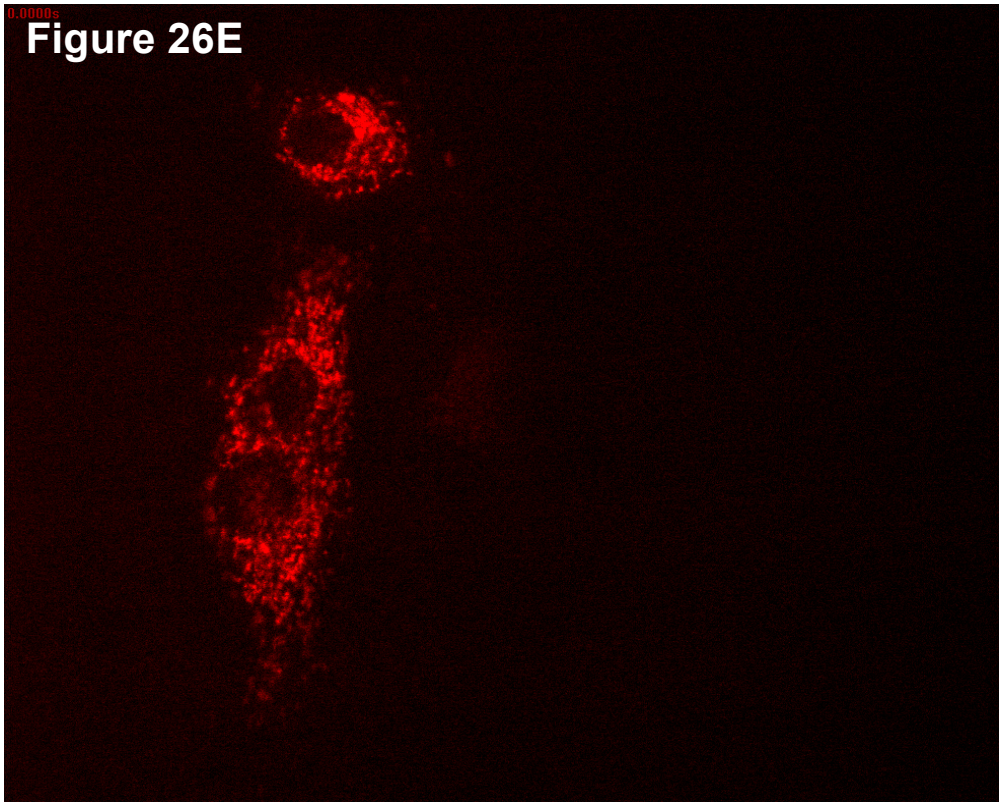

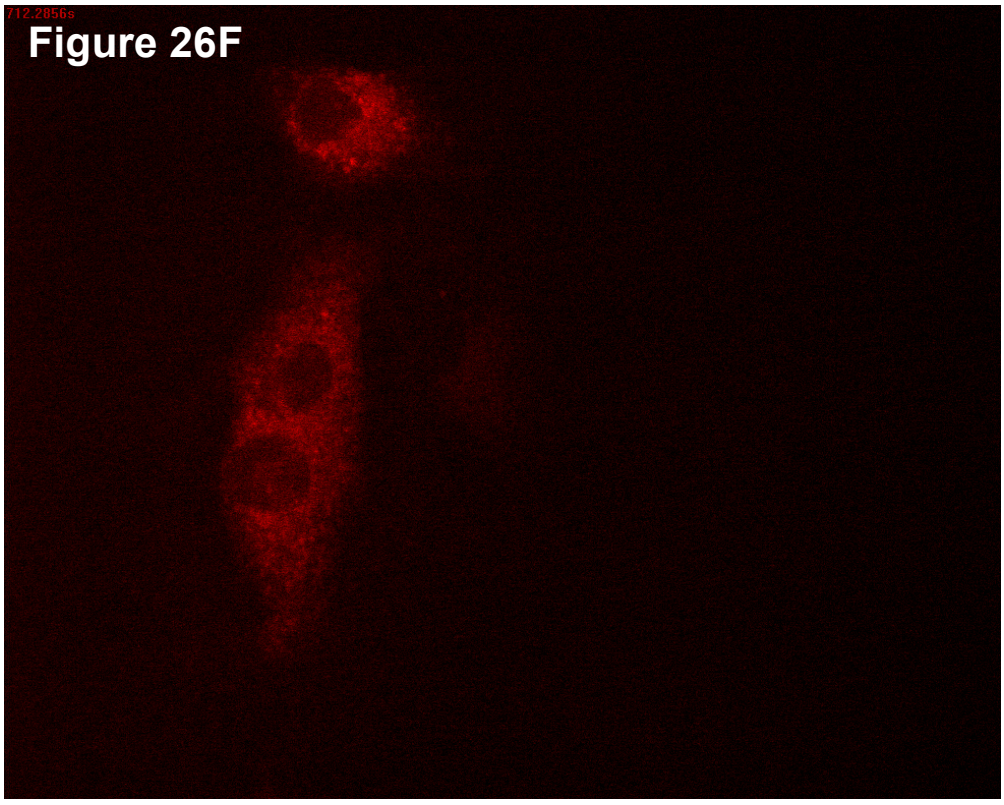

Figures 26E and **26F** show the effect of addition of 2-DOG on TMRM staining of mitochondrial membrane potential of Rho 0 cells. Mitochondrial membrane potential is lost after the addition of 2-DOG (**26F**)**.** This is from one representative experiment

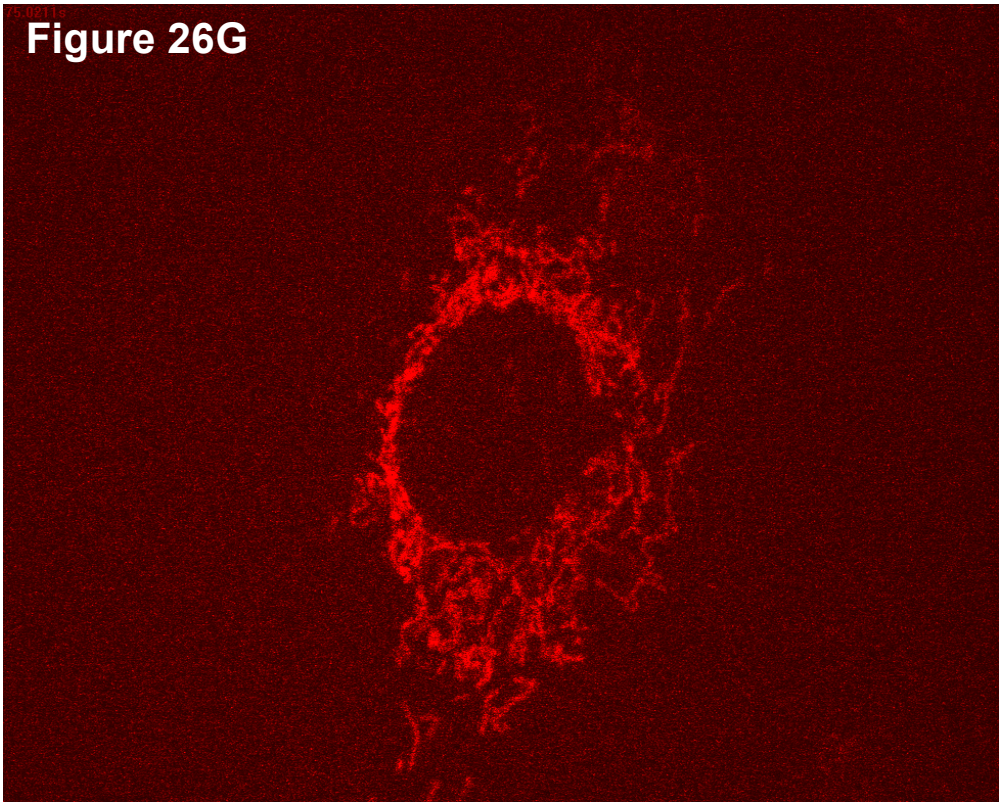

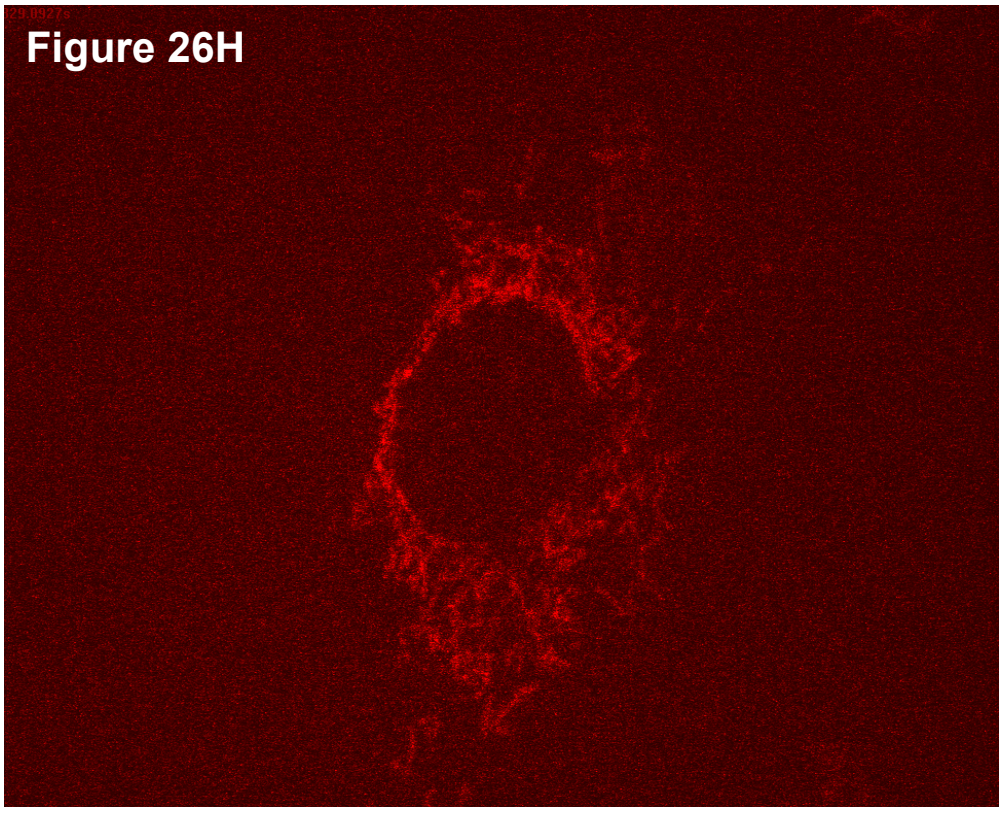

Figures 26G and **26H** show the effect of addition of 2-DOG on TMRM staining of mitochondrial membrane potential of WT cells pre-treated with pyruvate. Membrane potential is maintained after the addition of 2-DOG (**26H**)**.** This is from one representative experiment.

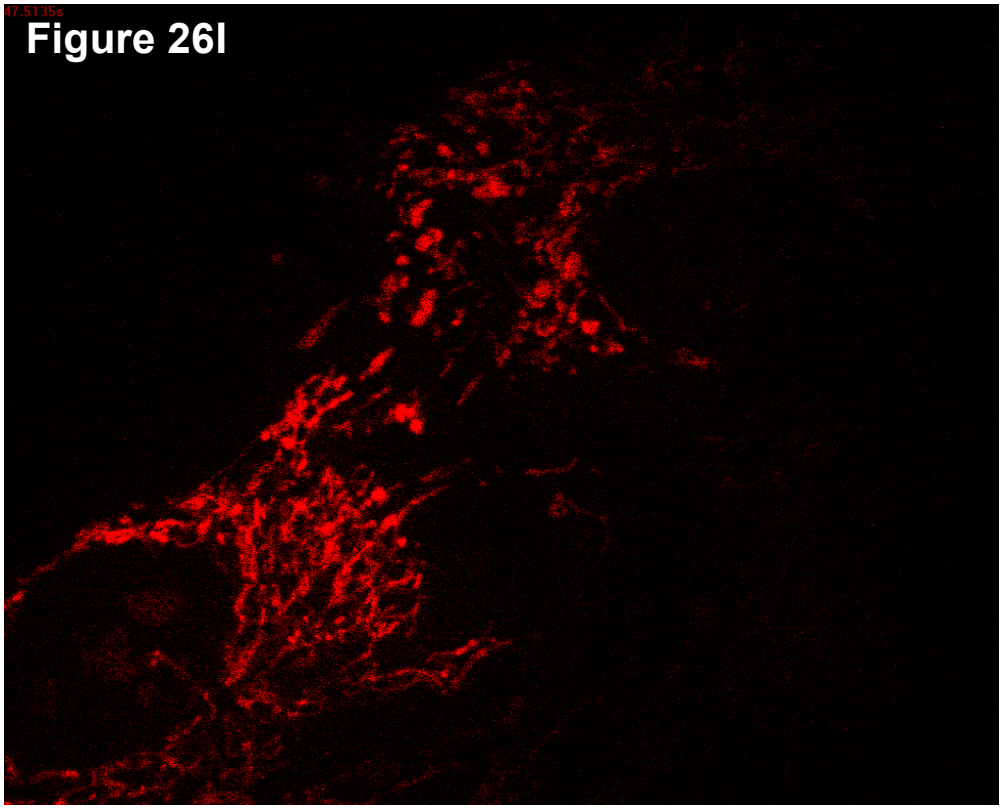

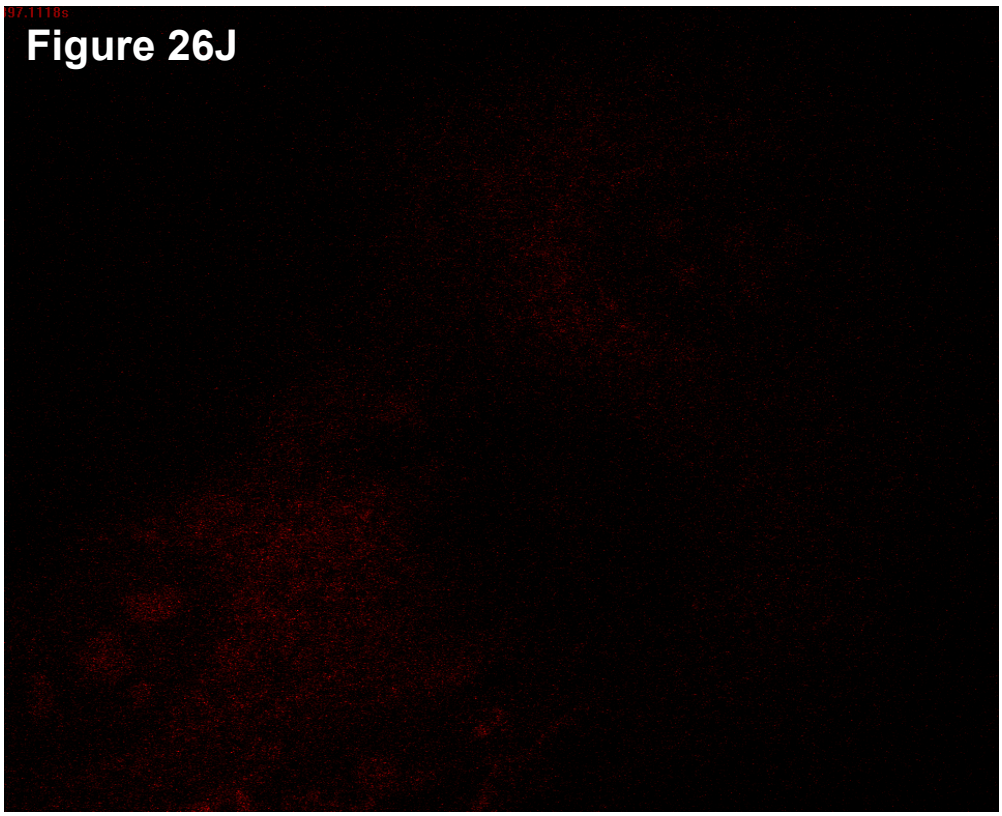

Figures 26I and **26J** show the effect of addition of 2-DOG on TMRM staining of mitochondrial membrane potential of Rho 0 cells pre-treated with pyruvate. Membrane potential is lost after the addition of 2-DOG (**26J**)**.** This is from one representative experiment.

4 Results chapter 2: endothelial cell defence

4.1 Stress-induced senescence in endothelial cells

4.1.1 Stress-induced senescence in HUVEC by SA-β-gal staining

A daily pulse of *t*BHP has been shown to induce stress-induced senescence in HUVEC (Unterluggauer, Hampel et al. 2003). It was therefore investigated whether Rho 0 HUVEC were more or less prone to stress induced senescence, using this method. Passage 3 cells were plated into 6 well plates and treated daily with a pulse of 25 μM tBHP, 50 μM *t*BHP or an equivalent amount of vehicle for 1 hour. After this the medium was removed and replaced with fresh medium. Fresh stock of *t*BHP was made every day. After 5 days treatment the cells were left overnight then stained for SA-β-gal, as described in section 2.9.

From the results shown in figure 27 it can be seen that there is no significant difference between the rates of senescence in the control groups. Treatment of the WT cells with 25 μM *t*BHP led to a significant increase in the percentage of senescent cells from (3.4 ± 0.9) % in the control cells to (29.9 ± 2.4) % ($p < 0.05$, n=3). Treatment of the WT cells with 50 μM *t*BHP led to a significant increase in the percentage of senescent cells from (3.4 ± 0.9) % in the control cells to (50.7 ± 4.6) % ($p < 0.05$, n=3), which is a significant increase compared to the percentage of senescent cells seen with 25 μM *t*BHP treatment ($p < 0.05$, n=3). Treatment of the Rho 0 HUVEC with 25 μM *t*BHP led to an increase in the percentage of senescent cells from (1.8 ± 0.9) % in the control cells to (7.7 ± 1.4) % but this was not statistically significant (p = ns, n=3). Treatment of the Rho 0

HUVEC with 50 μM *t*BHP led to an increase in the percentage of senescent cells from (1.8 ± 0.9) % in the control cells to (11.0 ± 2.7) % but this was not statistically significant (p = ns, n=3).

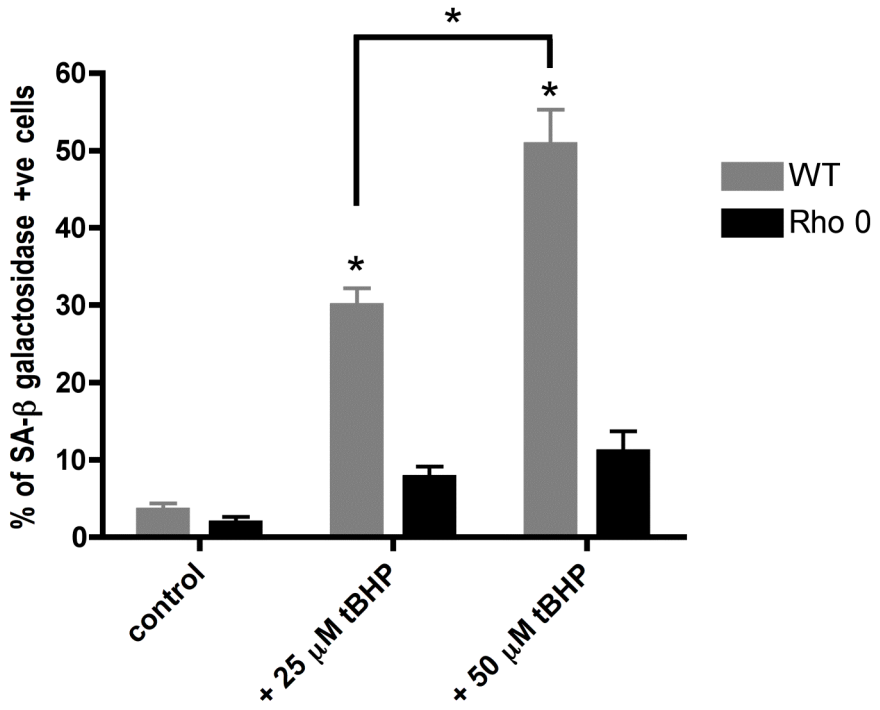

Figure 27 shows the effect of *t*BHP, which is known to induce stress-induced senescence, on HUVEC. Clearly WT cells undergo stress-induced senescence in a dose responsive manner. In contrast Rho 0 HUVEC are resistant to stress-induced senescence. Data are represented as mean ± SEM, n = 3, from 3 independent experiments. * $p < 0.05$.

This experiment clearly demonstrates that Rho 0 HUVEC are resistant to stress-induced senescence compared to WT cells, as shown by the marker SA-β-gal. In cells under routine culture conditions (not treated with *t*BHP) more large cells, consistent with a senescent phenotype, were noted in the WT cultures. These can be seen in figure 28A (a phase contrast photomicrograph), as large morphologically highly abnormal cells. In contrast these cells are not seen in Rho 0 HUVEC (under the same passage and conditions), shown in figure 28B.

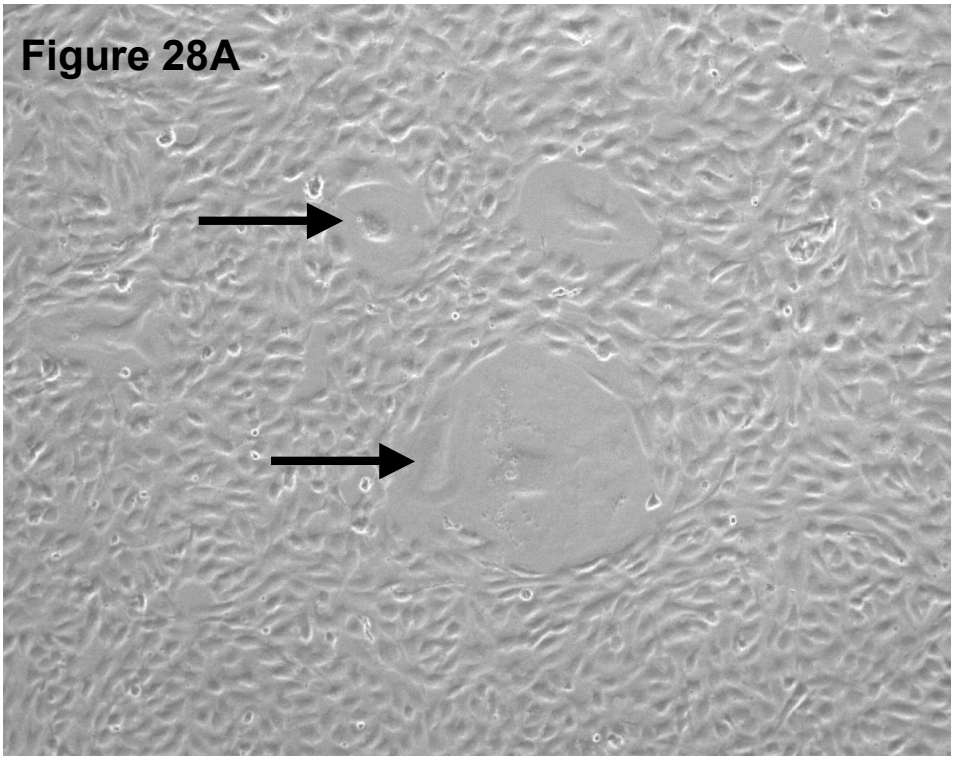

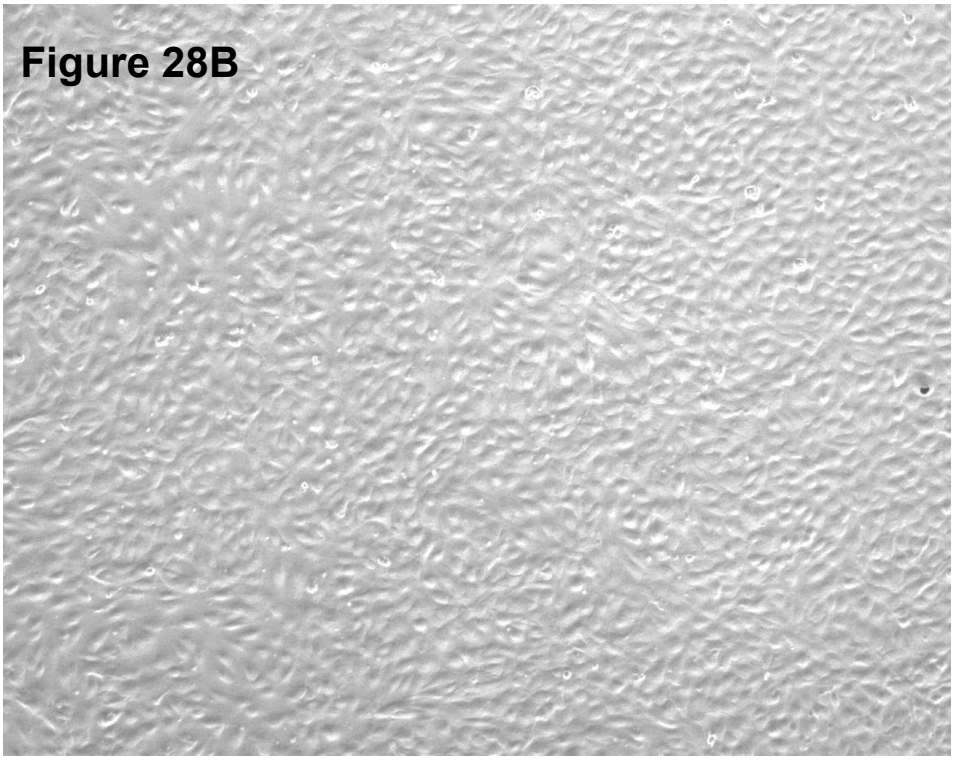

Figure 28 shows photomicrographs of WT and Rho 0 HUVEC cells (magnification x50). Large morphologically highly abnormal cells, consistent with a senescent phenotype, can be seen in the WT (marked with arrows) but not the Rho 0 HUVEC.

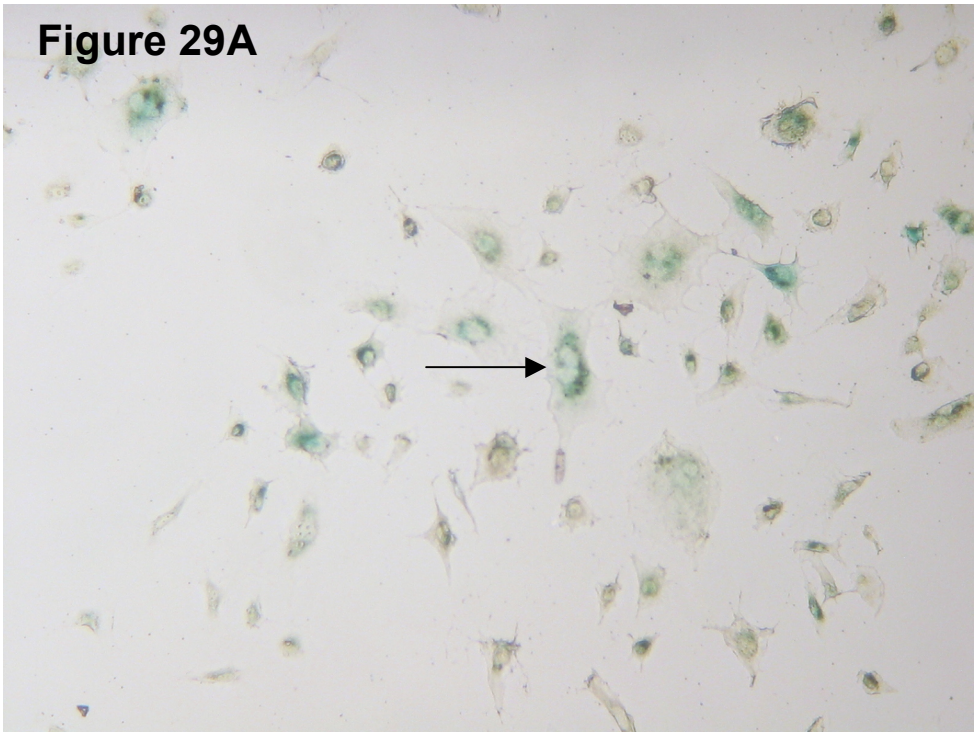

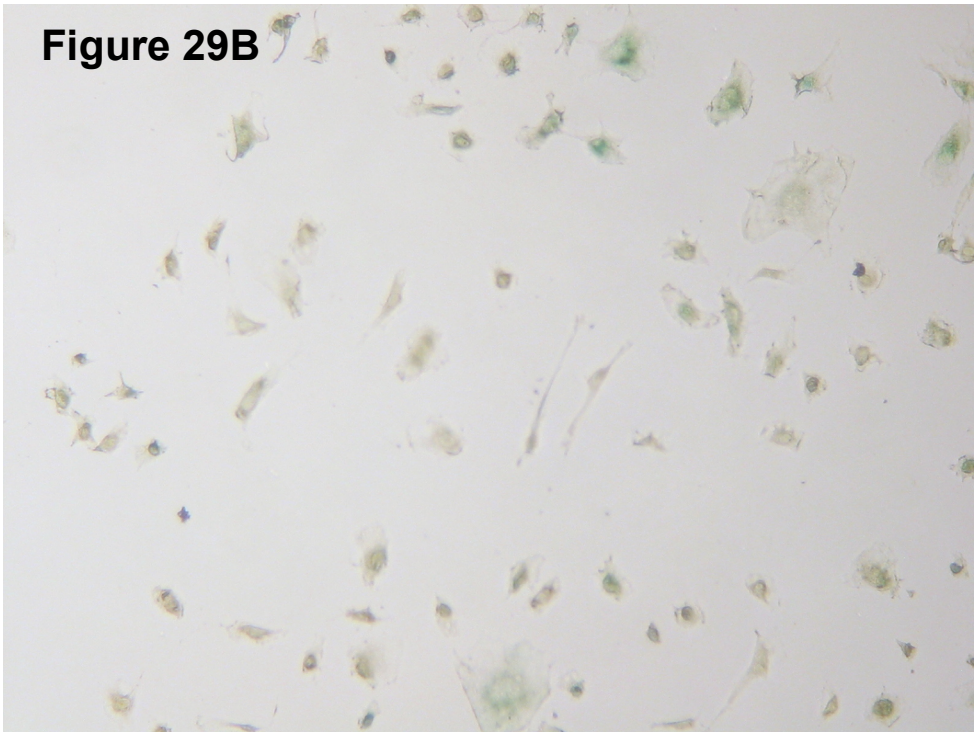

Figure 29 shows a photomicrograph (magnification x75) of cells stained for SA-β-gal after treatment with 25 μM *t*BHP, **29A** shows WT cells with senescent cells staining blue clearly seen (an example is indicated with the arrow), **29B** shows there is less SA-β–gal-staining in the Rho 0 HUVEC.

Representative photomicrographs of WT and Rho 0 cells stained for SA-β-gal after treatment with 25 μM *t*BHP are shown in figure 29. SA-β-gal is a lysosomal enzyme that stains at pH 6 in senescent cells due to their increased lysosomal mass. Lysosomal β galactosidase, a eukaryotic hydrolase localised in the lysosome, can be detected in most cells at pH 4 using X-gal, as described in section 2.9 (Kurz, Decary et al. 2000). In order to determine whether the reduced SA-β-gal staining in Rho 0 HUVEC was truly due to their resistance to senescence and not a reduction in lysosome numbers the cells were stained with X-gal at pH 4, as described in section 2.9. All the Rho 0 and WT cells stained positive for this marker, indicating that the reduction in SA-β-gal staining in Rho 0 HUVEC was not merely a reflection of them having less lysosomes (data not shown).

4.1.2 Stress-induced senescence in endothelial cells by ICAM-1 analysis with FACS

Having demonstrated that Rho 0 HUVEC are resistant to stress-induced senescence both morphologically and using a cytochemical assay, a functional marker was used to further demonstrate the resistance of Rho 0 cells to senescence. It has previously been demonstrated that the expression of intracellular adhesion molecule-1 (ICAM-1), which is known to be associated with vascular disease, is associated with endothelial cell senescence (Xu, Neville et al. 2000).

Three T-25 flasks of cells were grown for each cell type and treated for 60 minutes every day for 5 days. Two flasks were treated as controls with an equal

volume of vehicle (deionized water) and one flask with 50 μM *t*BHP. After each treatment the medium was changed. On the final day one control flask of cells was treated for 90 minutes with 200 ng/mL of human interleukin 1 beta (IL-1β), which is known to activate HUVEC and up-regulate ICAM-1 expression (Ahluwalia, Foster et al. 2004). The remaining two flasks were treated with an equal volume of deionized water for 90 minutes. The cells were then washed in PBS, trypsinised and counted, as described in section 2.2.1.3, to provide three samples: control, IL-1β-treated and *t*BHP-treated. Each of these 3 samples was then spit into 3 aliquots. The first was labelled with 1:10 R-phycoerythrin (RPE)-anti human CD54 (clone 58, BD Pharm) for ICAM. The second was labelled with 1:20 Negative control RPE non-conjugated mouse IgG1 (Dako) as a negative control. The third was the non-staining control. The samples were then processed in a Becton Dickinson FACSCalibur machine and analysed with CellQuest software.

The fluorescence histograms of ICAM-1 expression following the various treatments are shown in figures 30A and 30B for WT and Rho 0 HUVEC respectively. In the WT cells there is a clear right shift with IL-1β treatment (green curve) and a further right shift in the tBHP treated cells (red curve), indicating increasing ICAM-1 expression. This is not seen to the same extent in the Rho 0 HUVEC.

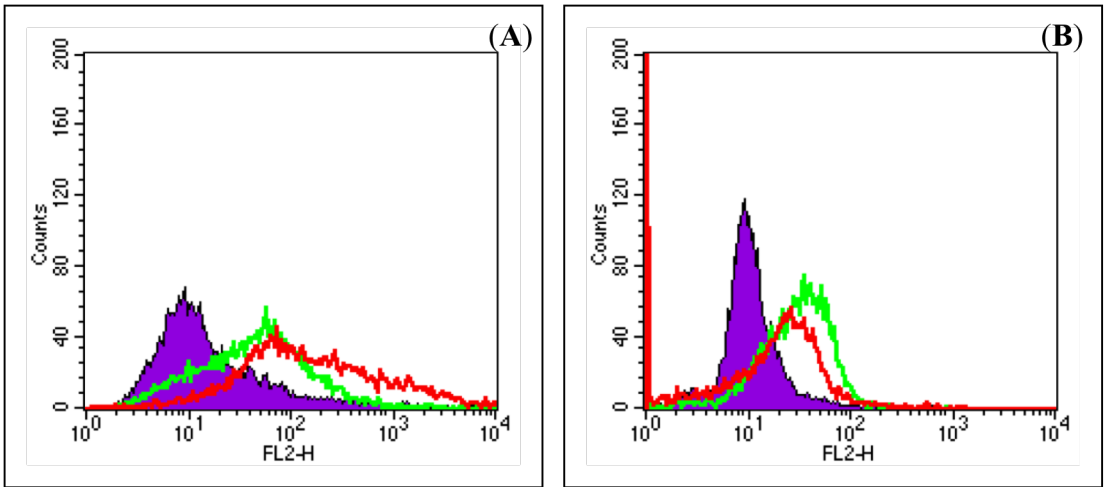

Figure 30 shows the effect of tBHP, which is known to induce stress-induced senescence in HUVEC, on ICAM-1 expression by FACs analysis, from one representative experiment, of three. The purple curve represents control cells, the green curve represents IL-1β treated cells and the red curve represents *t*BHP treated cells. **30A** shows WT cells, which undergo a significant up-regulation of ICAM-1 expression in response to both IL-1β and 50 μM *t*BHP. In contrast Rho 0 HUVEC, shown in **30B**, are resistant to this effect.

The expression of ICAM-1 was measured using the geometric mean and expressed as a % of the WT control in each experiment. The baseline expression of ICAM-1 in Rho 0 HUVEC was (94.7 ± 38.3) %, which was not significantly different from the WT control (p = ns, n=3). In figure 31 it can be seen that in WT cells the addition of IL-1β causes an increase in ICAM-1 expression from (100 ± 0) % in the control cells to (373.4 ± 68.5) % ($p < 0.05$, n=2). After treatment with 50 μM *t*BHP there was an increase in ICAM-1 expression from (100 ± 0) % in the control cells to (1280.6 ± 221.4) % ($p < 0.05$, n=3). In the Rho 0 HUVEC the addition of IL-1β did not significantly change ICAM-1 expression, it was (94.7 ± 38.3) % in the control cells versus (148.2 ± 65.0) % in the treated cells (p = ns, n=3). After treatment with 50 μM *t*BHP there no significant change in ICAM-1

expression, it was (94.7 ± 38.3) % in the control cells versus (168.9 ± 45.7) % in the treated cells (p = ns, n=3).

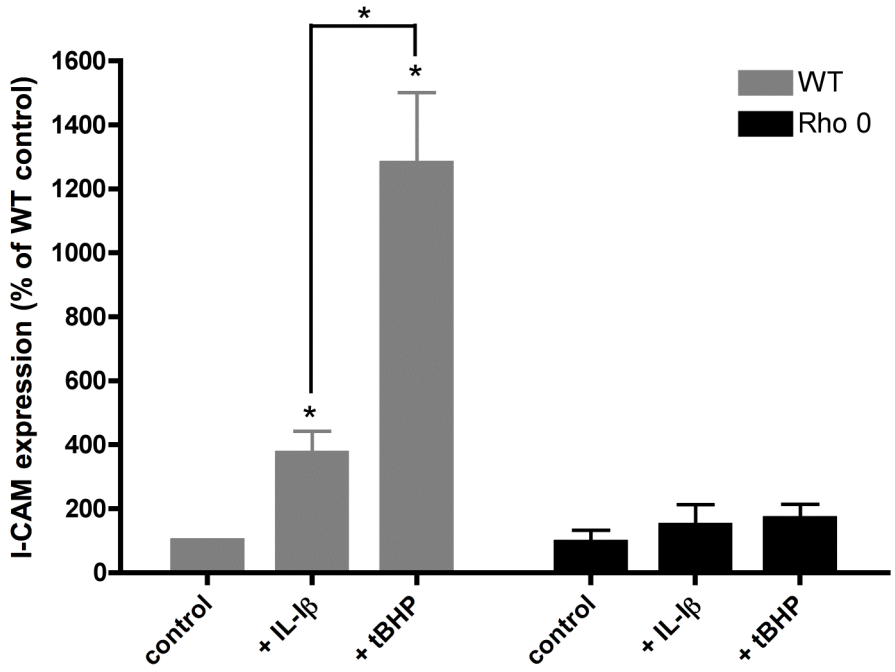

Figure 31 shows the effect of *t*BHP, which is known to induce stress-induced senescence in HUVEC, on ICAM-1 expression by FACs analysis. WT cells undergo a significant up-regulation of ICAM-1 expression in response to both 200 ng/mL IL-1β and 50 μM tBHP. In contrast Rho 0 HUVEC are resistant to this effect. Data are represented as mean ± SEM, n = 3, from 3 independent experiments (apart from WT cells treated with IL-1β, where n = 2). * $p < 0.05$, * $p < 0.05$.

4.2 Apoptosis in endothelial cells

As explained in section 1.2.5.1 it is well established that mitochondria play a central role in apoptosis. Furthermore it has been demonstrated that cells lacking functional mitochondria have been shown to be resistant to apoptosis (Lee, Kim et al. 2004). However all this work has been done on immortalised cell lines. It was therefore felt important for this thesis to demonstrate that Rho 0 HUVEC behave in the same way.

4.2.1 Apoptosis measured by caspase assay

Cells in passage 2 were washed, trypsinised and counted in the usual manner. 7000 cells per well were seeded into a 96 well plate. The following day the cells were washed twice with PBS and 50 μL of medium and treatment added to each well. For each experiment every treatment was done in triplicate and repeated twice on the same plate, i.e. there was one set of wells for caspase analysis and one set for protein analysis. The treatments were: deionized water (control), 50 μM *t*BHP and 100 μM *t*BHP. The treated 96 well plates were placed in the incubator for 4 hours prior to removal of the plates for caspase analysis using the kit as described in section 2.11. Preliminary experiments showed the time course of generation of luminescence curves to be identical in shape at 4, 6 and 8 hours. In addition they showed the assay to be sensitive enough to detect clear differences in activity at 4 hours, with different doses of *t*BHP. Therefore caspase measurements were made after 4 hours treatment for all experiments. The duplicate of each experiment on the same plate was kept and assayed for protein to ensure equal cell seeding. If there was found to be a significant difference in

protein levels the luminescence values could be corrected accordingly. However, protein levels were not significantly different in any of the experiments, so correction was not necessary.

Figure 32 shows apoptosis as measured by the caspase assay in cells treated with *t*BHP. In WT cells treatment with 50 μM *t*BHP led to an increase in apoptotic cells from (100 ± 5.6) % to (146 ± 18.9) % ($p < 0.05$, n = 9, from 3 independent experiments), although treatment with 100 μM *t*BHP led to an increase in apoptotic cells from (100 ± 5.6) % to (169 ± 14.2) % ($p < 0.05$, n = 9, from 3 independent experiments) this was not a significant further increase from the values obtained at 50 μM *t*BHP. The level of apoptosis was lower in the Rho 0 control cells at (40.3 ± 2.38) % compared to the WT control cells at (100 ± 5.6) % ($p < 0.05$, n = 9, from 3 independent experiments). Treatment of Rho 0 HUVEC with 50 μM and 100 μM *t*BHP led to apoptosis levels of (59.9 ± 6.63) % and (66.2 ± 6.51) % respectively, neither of which were statistically significantly different from control Rho0 cells (p = ns, n = 9, from 3 independent experiments).

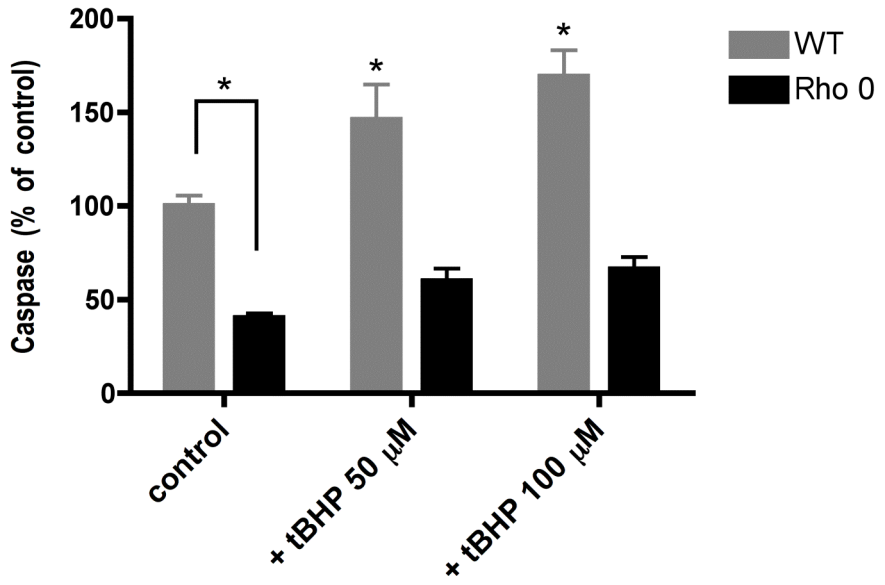

Figure 32 shows the effect of *t*BHP on apoptosis in HUVEC, measured by the caspase assay. WT cells undergo increased apoptosis in response to *t*BHP. In contrast Rho 0 HUVEC are resistant to this effect. The level of apoptosis is significantly less in Rho 0 control cells compared to the WT cells. Data are represented as mean ± SEM, n = 9, from 3 independent experiments. * $p < 0.05$.

These experiments were repeated with 4 μM staurosporine, a known protein kinase inhibitor and potent inducer of apoptosis (Belmokhtar, Hillion et al. 2001; Tesauro, Thompson et al. 2005). The cells were treated with staurosporine for 4 hours. Figure 33 shows that in WT cells staurosporine induces a marked increase in apoptosis from (100 ± 5) % to (1698 ± 343) % ($p < 0.05$, n = 9, from 3 independent experiments). In Rho 0 HUVEC although there is an increase in apoptosis from (39 ± 11) % to (421 ± 81) % it is not statistically significant (p = ns, n = 9, from 3 independent experiments).

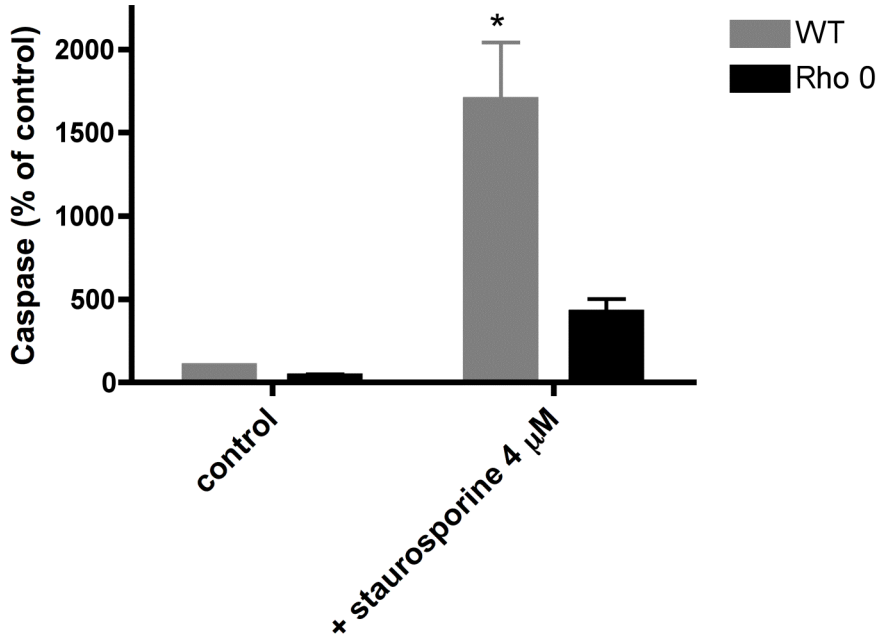

Figure 33 shows the effect of 4 μM staurosporine on apoptosis in HUVEC, measured by the caspase assay. WT cells undergo a marked increased apoptosis in response to tBHP. In contrast Rho 0 HUVEC are resistant to this effect. Data are represented as mean ± SEM, n = 9, from 3 independent experiments. * $p < 0.05$.

4.2.2 Apoptosis measured by FACS analysis

Apoptosis was also measured using FACS analysis. During the early stages of apoptosis phosphatidylserine (PS) is translocated from the inner side of the plasma membrane to the outer side (Vermes, Haanen et al. 1995), thus exposing PS to the external surface of apoptotic cells. Annexin-V is a Ca^{2+} dependent phospholipid-binding protein that possesses high affinity for PS. Propidium iodide (PI) is a DNA intercalating agent that can enter and stain dead cells (Hudson, Upholt et al. 1969). Cells expressing Annexin-V but not uptaking PI are in the early stages of apoptosis (Vermes, Haanen et al. 1995). There is some overlap between apoptosis and necrosis in that both sets of cells will express both

Annexin-V and PI (Blankenberg, Katsikis et al. 1998). I used the Roche Annexin-V-FLUOS staining kit (Roche Diagnostics), which contained Annexin-V-Fluorescein and Propidium iodide. In brief passage 4 cells were plated in four T-25 flasks for each cell type. The flasks were treated overnight in the following way: two with deionized water (one as a control and one for staurosporine treatment), one with 25 μM *t*BHP and one with 50 μM *t*BHP, freshly made *t*BHP stock was always used. The following day one control flask per cell type was treated with 4 μM staurosporine for 4 hours. All cells were then washed and split before staining as per the manufacturers instructions. The samples were then processed in a Becton Dickinson FACSCalibur instrument and analysed with CellQuest software.

Figure 34 shows a dot-plot from one representative experiment. FL-1 height represents Annexin-V (AV) fluorescence with cells on the right quadrants being positive and those on the left negative. FL-3 height represents Propidium Iodide (PI) fluorescence with cells at the top quadrants being positive and those at the bottom negative. It can be seen that there is a difference in the FL-3 scale between WT and Rho 0 HUVEC, this is due to the ethidium bromide (itself a fluorogenic substance) present in these cells. The plot can therefore be divided into four quadrants with bottom left representing normal cells (AV-/PI-), bottom right representing apoptotic cells (AV+/PI-), top right representing necrotic and apoptotic cells (AV+/PI+). Apoptotic cells were taken as the percentage of those in the bottom right quadrant (AV+/PI-). In the WT cells (shown on the left) it can be seen that there is a clear shift to the bottom right quadrant i.e. apoptotic cells with 4 μM staurosporine. In contrast the Rho 0 HUVEC shown on the right are resistant to this effect.

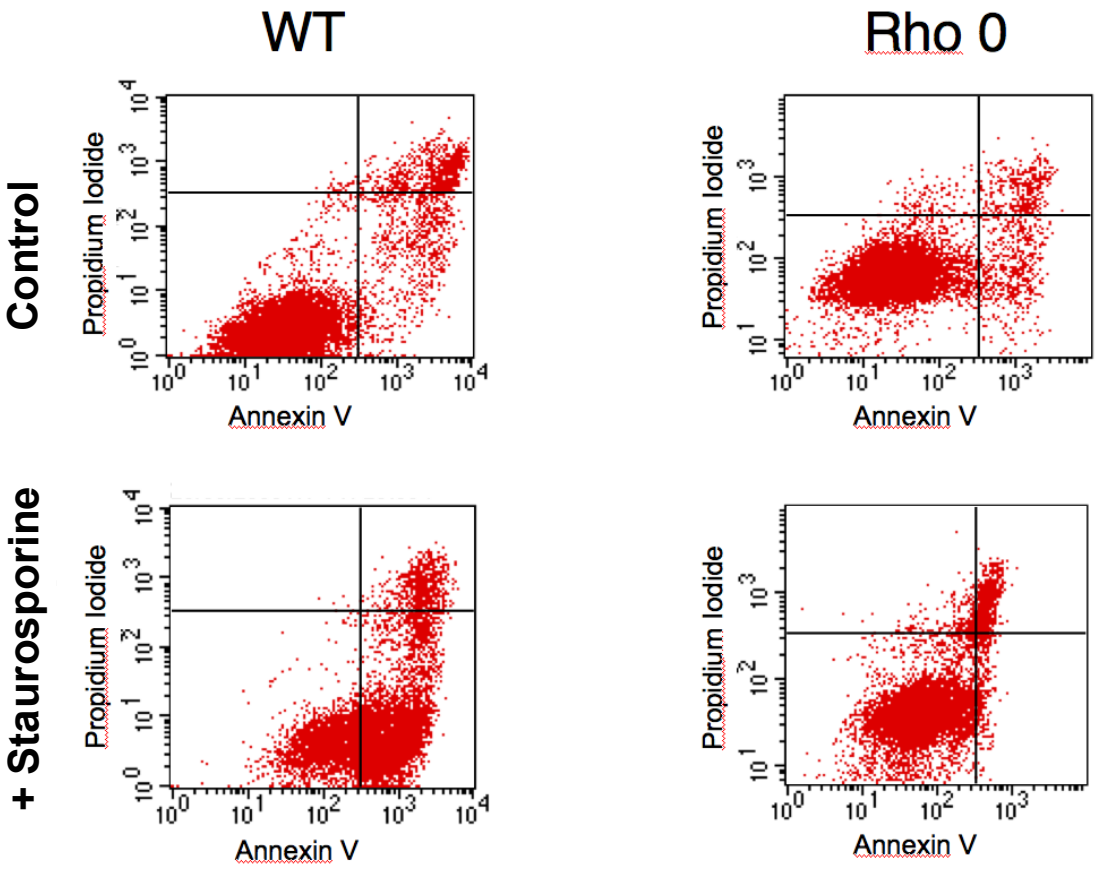

Figure 34 shows the effect of 4 μM staurosporine on apoptosis in HUVEC, using FACS analysis with Annexin-V and Propidium Iodide. Apoptotic cells are represented by the cell population in the lower right quadrant of each plot (AV+/PI-). Normal cells are represented by the cell population in the lower left quadrant of each plot (AV-/PI-). WT cells (shown in the left upper and lower plots) undergo a marked increased apoptosis in response to staurosporine, as shown by the cells shift to the lower right quadrant. In contrast Rho 0 HUVEC (shown in the right upper and lower plots) are resistant to this effect.

Figure 35 shows apoptosis as measured by FACS analysis. In WT cells treatment with 25 μM *t*BHP and 50 μM *t*BHP led to a non-significant increase in apoptotic cells from (3.40 ± 0.35) % to (6.70 ± 1.20) % and (6.90 ± 2.80) % respectively (p = ns, n = 4, from 4 independent experiments). Treatment of WT cells with 4 μM staurosporine led to a significant increase in apoptotic cells (3.40

± 0.35) % to (33.10 ± 7.10) % ($p < 0.05$, n = 4, from 4 independent experiments). In the Rho 0 HUVEC treatment with 25 μM *t*BHP, 50 μM *t*BHP and 4 μM staurosporine led to non-significant increases from baseline at (11.00 ± 2.20) % to (12.00 ± 3.20) %, (14.00 ± 2.30) % and (22.00 ± 9.90) % respectively (p = ns, n = 4, from 4 independent experiments). This demonstrates that the Rho 0 HUVEC are resistant to apoptosis compared to the WT cells.

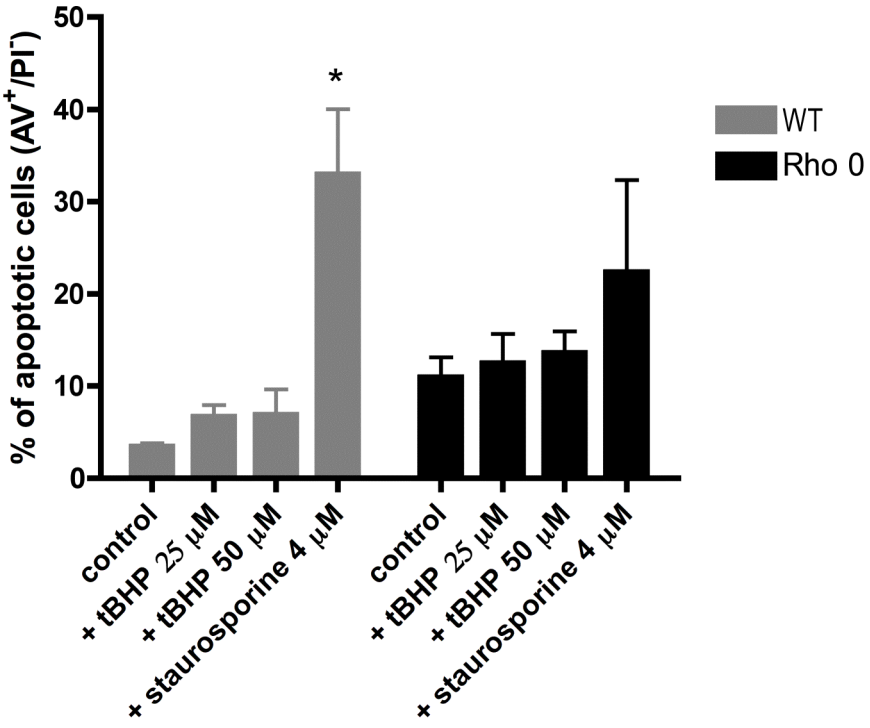

Figure 35 shows the effect of *t*BHP and staurosporine on apoptosis in HUVEC, using FACS analysis with Annexin-V and propidium iodide. Only WT cells undergo a statistically significant increase in apoptosis in response to 4 μM staurosporine. In contrast Rho 0 HUVEC are resistant to this effect. Data are represented as mean ± SEM, n = 4, from 4 independent experiments. * $p < 0.05$.

4.3 Reactive Oxygen Species production in endothelial cells

4.3.1 Quantification of ROS production in WT versus Rho 0 HUVEC and the effects of glutathione depletion and NADPH oxidase inhibition on ROS production

Mitochondria are thought to be a major source of intracellular ROS production (Jensen 1966; Boveris and Chance 1973). It was postulated that Rho 0 HUVEC might produce less ROS than WT cells and this may in part account for them being more resistant to stress-induced senescence and apoptosis. In order to study real-time ROS production the probe H_2DCFDA was used as described in section 2.12.

Baseline production of ROS in WT versus Rho 0 HUVEC is shown in figure 36, which is a representative one of three identical experiments performed. It can be seen that at 60 minutes WT cells generate significantly more ROS at (59572 ± 130) relative fluorescence units (RFU) than Rho 0 HUVEC at (51935 ± 142) RFU ($p < 0.05$, $n = 3$). N-Acetyl Cysteine (NAC) protects cells against oxidative damage by both scavenging free radicals and raising intracellular GSH levels (Aruoma, Halliwell et al. 1989). Addition of 10 mM NAC reduces H_2DCFDA oxidation in WT and Rho 0 HUVEC leading to levels of (44413 ± 912) RFU and (43730 ± 655) RFU respectively (p = ns, $n = 3$).

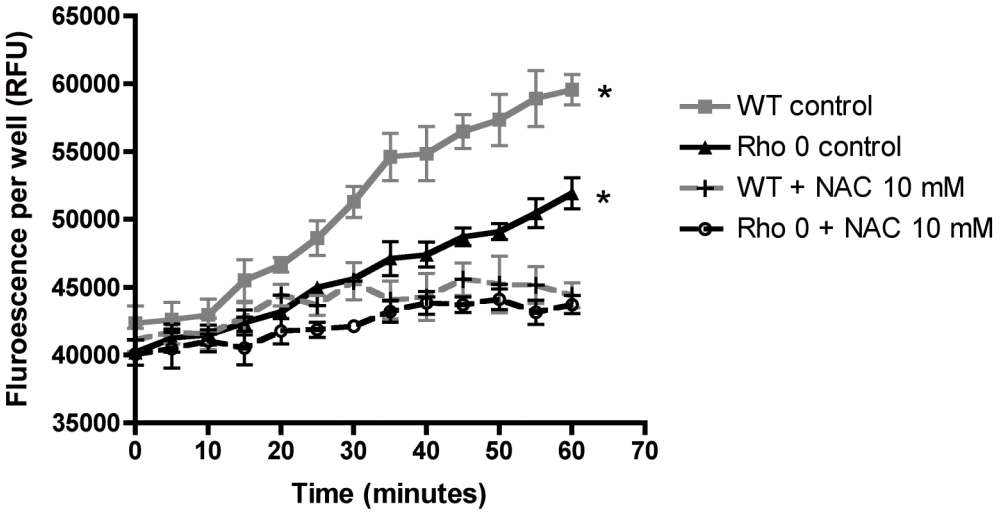

Figure 36 shows the ROS production measured by DCF fluorescence in a spectrofluorimeter. Addition of 10 mM NAC inhibits ROS production in both WT and Rho 0 HUVEC. Over the time course of the experiment it can be seen that WT cells generate significantly more ROS than Rho 0 HUVEC compared to baseline (cells + NAC). Data are represented as mean ± SEM, n = 4, from 1 representative experiment out of three. * $p < 0.05$.

The cells were then treated with *t*BHP, which is reported to deplete glutathione (a major intracellular antioxidant) and cause oxidative-stress induced senescence (Unterluggauer, Hampel et al. 2003; Kurz, Decary et al. 2004). Cells were either treated with 50 μM *t*BHP or 10 mM NAC. Figure 37 shows that ROS production at 60 minutes was significantly greater in WT cells, at (171208 ± 9146) RFU compared to Rho 0 HUVEC at (104050 ± 2833) RFU ($p < 0.05$, n=3).

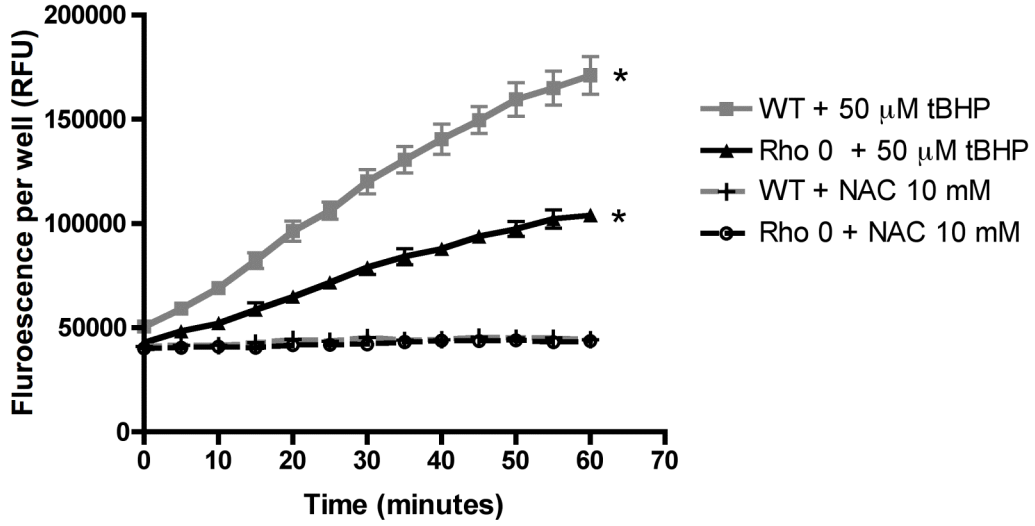

Figure 37 shows the ROS production measured by DCF fluorescence in a spectrofluorimeter. Over the time course of the experiment it can be seen that with treatment of 50 μM *t*BHP WT cells generate significantly more ROS than Rho 0 HUVEC. Addition of 10 mM NAC inhibits ROS production in both WT and Rho 0 HUVEC. Data are represented as mean ± SEM, n = 4, from 1 representative experiment out of three. * $p < 0.05$.

It has already been shown that DPI, an NADPH oxidase inhibitor, has a significant effect on oxygen consumption in Rho 0 but not WT cells, indicating that NADPH oxidase might be upregulated in Rho 0 HUVEC (figure 25). Therefore the effect of NADPH oxidase inhibition on ROS production in these cells was studied. Figure 38 shows these data, which is a representative one of three identical experiments performed. Again it can be seen that after 60 minutes Rho 0 HUVEC generate significantly less ROS (50553 ± 566) RFU than WT cells (58882 ± 259) RFU ($p < 0.001$, n = 3). Importantly treatment with 33 μM DPI leads to a significant reduction in ROS production in Rho 0 HUVEC compared to the control cells (45685 ± 262) RFU vs (50553 ± 566) RFU at 60 minutes, respectively) ($p < 0.001$, n = 3). In contrast there is no significant change in the

WT cells (58977 ± 697) RFU vs (58882 ± 259) RFU, with DPI and vehicle, respectively (p = ns, n = 3).

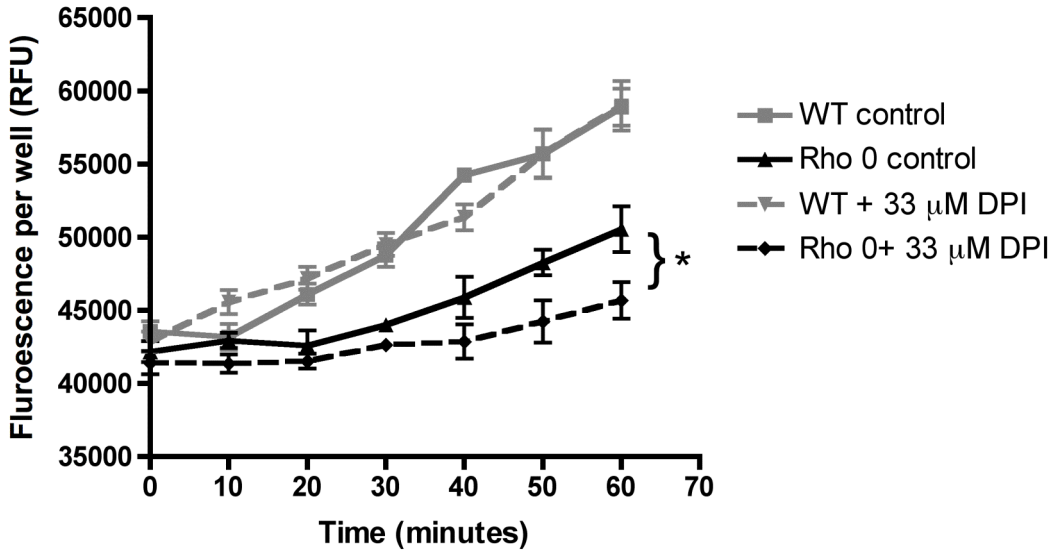

Figure 38 shows the ROS production measured by DCF fluorescence in a spectrofluorimeter. Over the time course of the experiment it can be seen that with treatment of 33 μM DPI there is a significant reduction in ROS production in Rho 0 but not WT cells. Data are represented as mean ± SEM, n = 4, from 1 representative experiment out of three. * $p < 0.05$

Finally the effect of buthionine sulfoximine (BSO), which is known to deplete the intracellular pool of glutathione (Rouzer, Scott et al. 1981), was examined. As shown in Figure 39 when treated with 1 mM BSO WT cells oxidise significantly more DCFDH (60390 ± 3228) RFU compared to control (41377 ± 339) RFU ($p < 0.001$, n = 3). The Rho 0 HUVEC treated with BSO also oxidise significantly more DCFDH (51222 ± 224) RFU compared to control (38246 ± 318) RFU ($p < 0.001$, n = 3). However, maximal DCFDH oxidation is significantly less in Rho 0 HUVEC at (51222 ± 224) RFU compared to WT cells (60390 ± 3228) RFU ($p < 0.001$, n = 3). Taken together these results indicate that Rho 0 HUVEC are able to generate less ROS than WT cells.

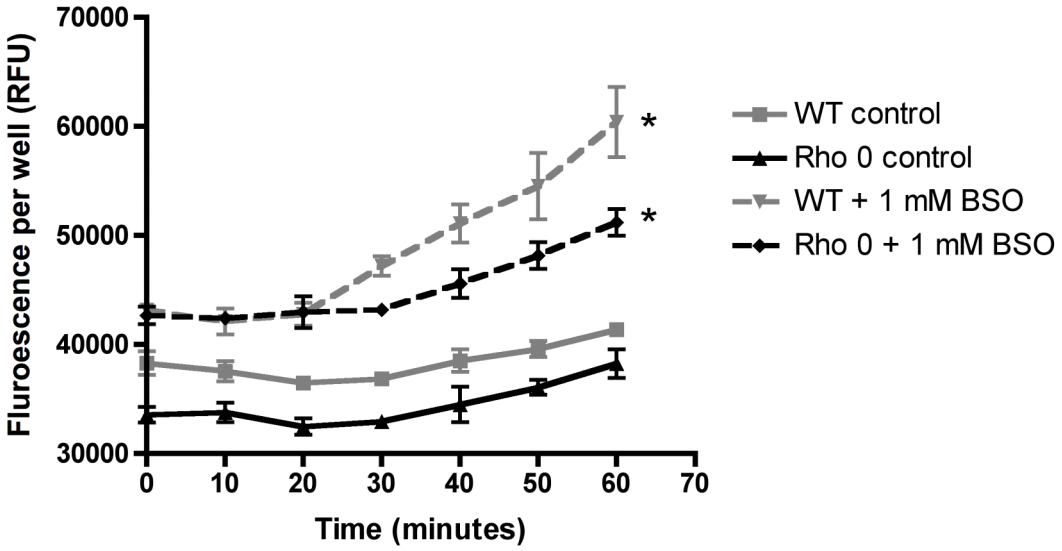

Figure 39 shows the ROS production measured by DCF fluorescence in a spectrofluorimeter from a representative experiment, of three. Over the time course of the experiment it can be seen that with treatment of 1 mM BSO that Rho 0 HUVEC are able to generate significantly less ROS than WT cells. Data are represented as mean ± SEM, n = 4, from 1 representative experiment. * $p < 0.05$

4.3.2 Site of ROS production by live confocal microscopy

Finally live cells were labelled with H_2DCFDA for 30 minutes and ROS production studied by live confocal microscopy, as described in section 2.13. DCF production (from H_2DCFDA by ROS) shows as green fluorescence. Figure 40A shows WT cells with DCF being concentrated in filamentous mitochondria (shown as bright green), reflecting the generation of ROS by these organelles. Figure 40B shows Rho 0 HUVEC in which the concentration of DCF in mitochondria has been lost, suggesting lack of ROS production by the organelles.

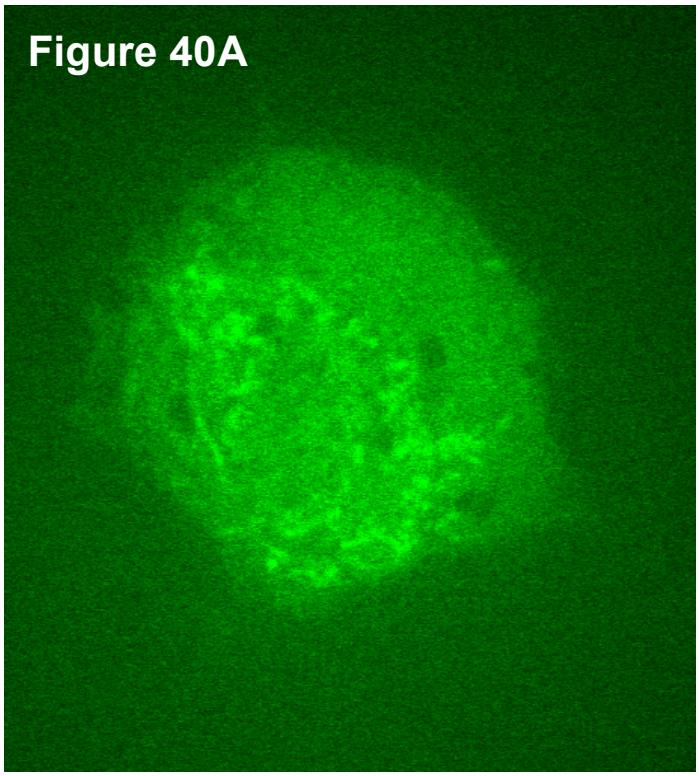

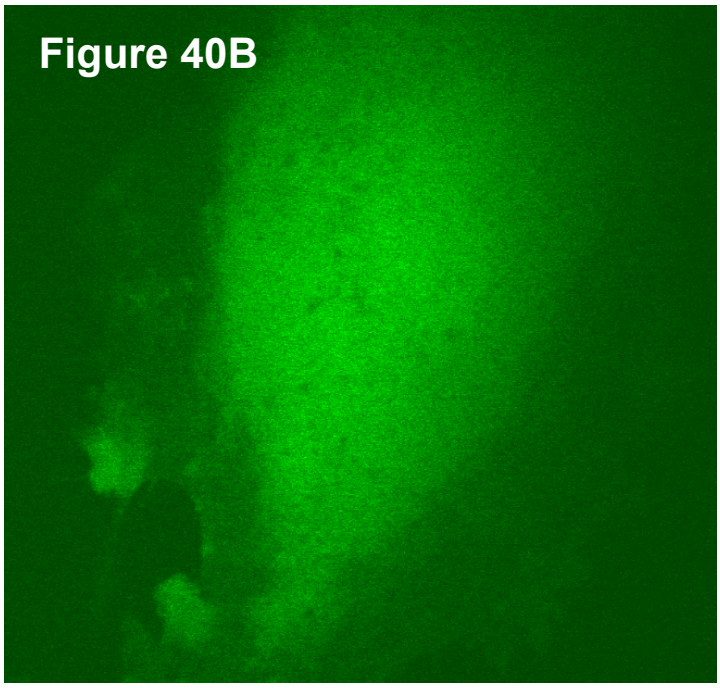

Figure 40 shows H2DCFDA staining of cells for ROS, which produce DCF. DCF emits a green fluorescence, the intensity of which is proportional to ROS production. **40A** shows WT cells, which produce ROS from the mitochondria. **40B** shows Rho 0 HUVEC, which show far less fluorescence and hence ROS production, which is not localised to the mitochondria in these cells. This is from one representative experiment of two.

4.4 Antioxidant defence levels in endothelial cells

4.4.1 Antioxidant gene expression

Primers were designed for three antioxidant genes: Gamma-glutamylcysteine synthase (γ-GCS), the rate-limiting step enzyme for the synthesis of glutathione (Orlowski and Meister 1970), catalase and manganese superoxide dismutase (MnSOD) (Riley 1994). ß actin, a housekeeping gene encoded by nuclear DNA, was used as a control. RNA from Rho 0 and WT cells was harvested and processed by quantitative RT-PCR, as described in section 2.4.4. Gene expression is shown relative to ß actin.

Figure 41 shows expression of γ-GCS, catalase and MnSOD. There was no significant difference in gene expression of γ-GCS between WT cells at (0.036 ± 0.008) and Rho 0 HUVEC at (0.035 ± 0.009) AU (p = ns, n = 12, from 4 independent experiments). The expression of catalase and MnSOD were significantly higher in Rho 0 HUVEC at (0.628 ± 0.099) and (0.240 ± 0.098) AU respectively than in WT cells at (0.448 ± 0.045) and (0.015 ± 0.032) AU respectively ($p < 0.05$, n = 12, from 4 independent experiments).

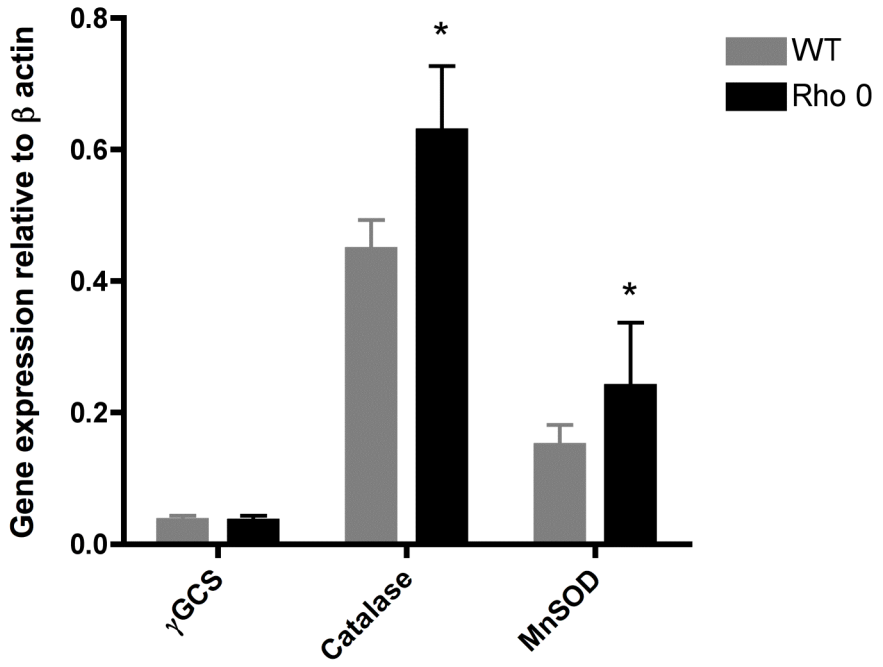

Figure 41 shows the expression of antioxidant genes in WT and Rho 0 HUVEC. There is a statistically significant increase in catalase and MnSOD expression in Rho 0 HUVEC. However, there is no statistically significant change in γ-GCS expression in Rho 0 HUVEC. Data are represented as mean ± SEM, n = 12, from 3 independent experiments. * $p < 0.05$

These data suggests that Rho 0 HUVEC may have higher levels of antioxidant defences.

4.4.2 Antioxidant protein levels

Protein levels of γ-GCS and MnSOD were investigated. Protein from Rho 0 and WT cells was harvested and processed by SDS-PAGE and western blot analysis, as described in section 2.5.

Figure 42 shows the western blot for γ-GCS, a 73 kDa protein. There was no significant difference in γ-GCS between Rho 0 and WT cells. The 50 kDa α tubulin subunit, used as a loading control, was found to be expressed equally in all cells. This was shown in 3 independent experiments, all of which are all shown in figure 42.

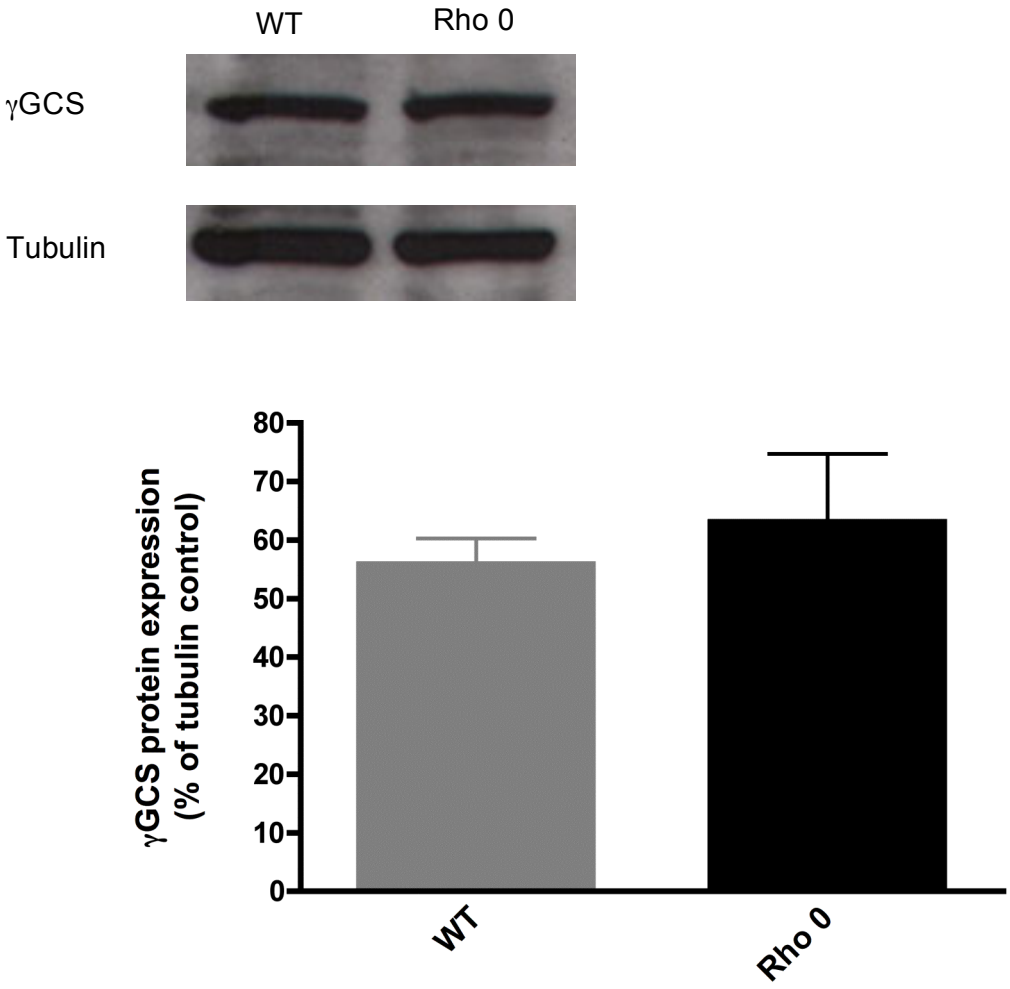

Figure 42 shows western blot analysis of HUVEC for γ-GCS, a 73 kDa protein, whose levels were not significantly different in Rho 0 and WT cells. The 50 kDa α tubulin subunit is shown as a loading control. A representative gel is shown. The graph shows quantitative analysis, from which it can clearly be seen that there is no difference in expression between Rho 0 and WT cells. Data are represented as mean ± SEM, n = 3, from 3 independent experiments. p = ns.

Figure 43 shows the western blot for MnSOD, a 25 kDa protein. There is a increase in MnSOD in Rho 0 HUVEC compared to WT cells. The 50 kDa α tubulin subunit, used as a loading control, was found to be expressed equally in all cells. This was shown in 4 independent experiments, which are all shown in figure 43.

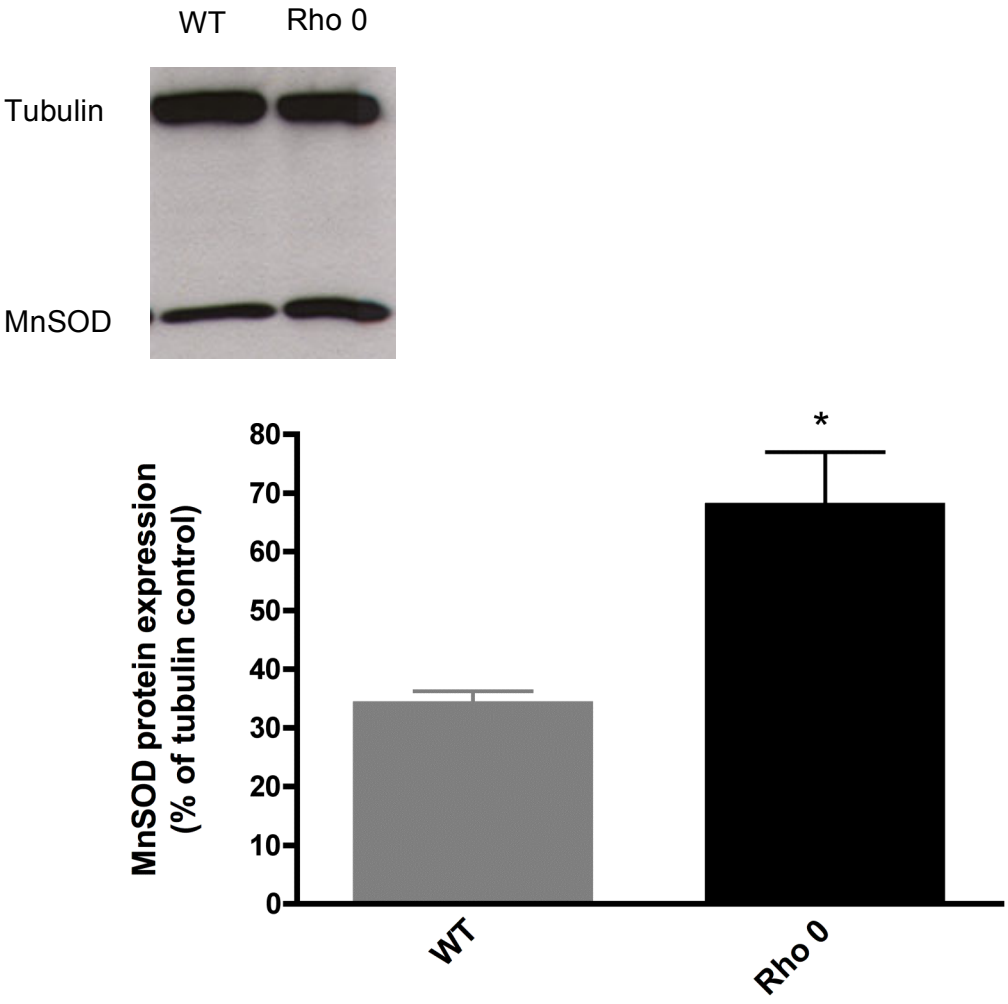

Figure 43 shows western blot analysis of HUVEC for MnSOD, a 25 kDa protein, which is significantly upregulated in Rho 0 HUVEC, compared to WT cells. The 50 kDa α tubulin subunit is shown as a loading control. A representative gel is shown. The graph shows quantitative analysis, from which it can clearly be seen that MnSOD is upregulated in the Rho 0 HUVEC compared to WT cells. Data are represented as mean ± SEM, n = 4, from 4 independent experiments. * $p < 0.05$.

4.4.3 Glutathione levels

Cell extracts were prepared and analysed for GSH/GSSG, as described in section 2.14. Figure 44 shows GSH/GSSG ratio in WT versus Rho 0 HUVEC. Values are expressed as a % of WT control. It can be seen that the ratio is significantly less in Rho 0 HUVEC at (48.2 ± 9.6) % compared to WT cells at (100.0 ± 27.8), this is statistically significant ($p < 0.05$, $n = 8$, from 3 independent experiments).

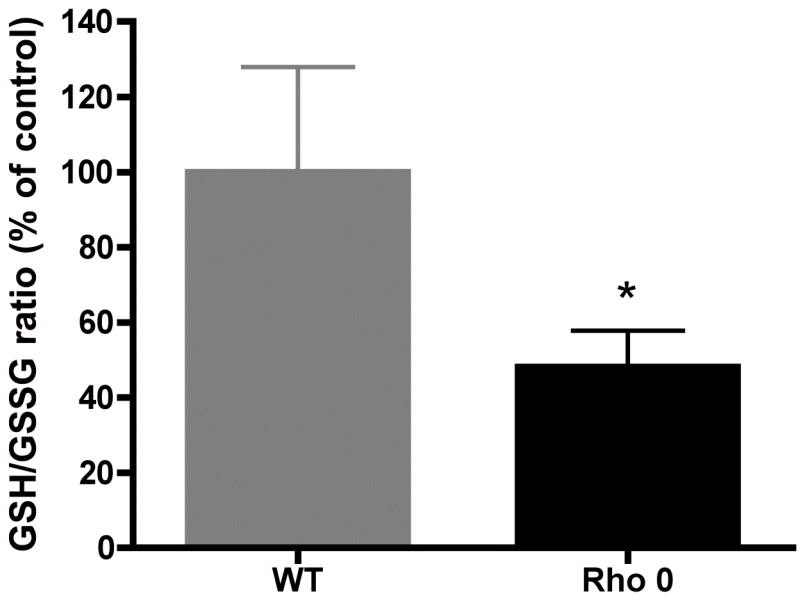

Figure 44 shows GSH/GSSG ratio (as a % of WT control) in WT and Rho 0 HUVEC. The ratio is significantly less in the Rho 0 HUVEC than WT cells. Data are represented as mean ± SEM, $n = 8$, from 3 independent experiments. * $p < 0.05$

4.5 eNOS production in endothelial cells

Lower eNOS levels in endothelial cells are known to be associated with senescence and atherosclerosis (Minamino, Miyauchi et al. 2002; Hayashi, Matsui-Hirai et al. 2006). Therefore whether a discrepancy in eNOS levels was

responsible for difference in stress-induced senescence seen between WT and Rho 0 HUVEC was investigated.

Primers for eNOS were designed and its mRNA expression levels examined by quantitative RT-PCR, as described in section 2.4.4. Gene expression is shown relative to ß actin. As shown in figure 45 there was no significant difference in gene expression of eNOS at (0.107 ± 0.009) AU in WT cells and (0.092 ± 0.006) AU in Rho 0 HUVEC (p = ns, n = 12, from 4 independent experiments).

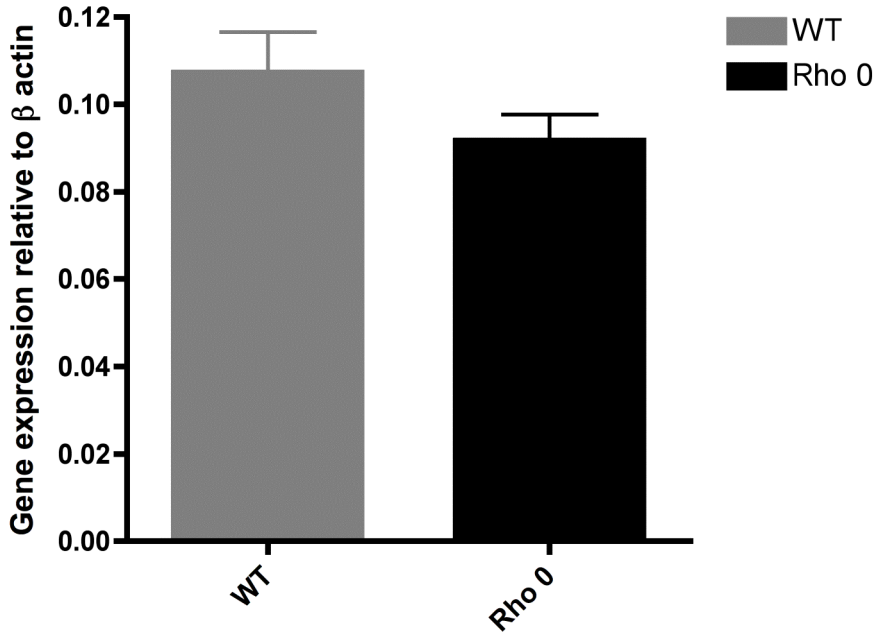

Figure 45 shows the expression of the eNOS gene in WT and Rho 0 HUVEC. There is no significant difference in gene expression between the two cell types. Data are represented as mean ± SEM, n = 12, from 4 independent experiments.

Following this eNOS levels in Rho 0 and WT cells was studied using protein, which was harvested and processed by SDS-PAGE and western blot analysis, as described in section 2.5.

Figure 46 shows the western blot for eNOS, a 140 kDa protein. There was no significant difference in eNOS levels between WT and Rho 0 HUVEC. The 50 kDa α tubulin subunit was used as a loading control. This was shown in 4 independent experiments, 2 of which are all shown in figure 46.

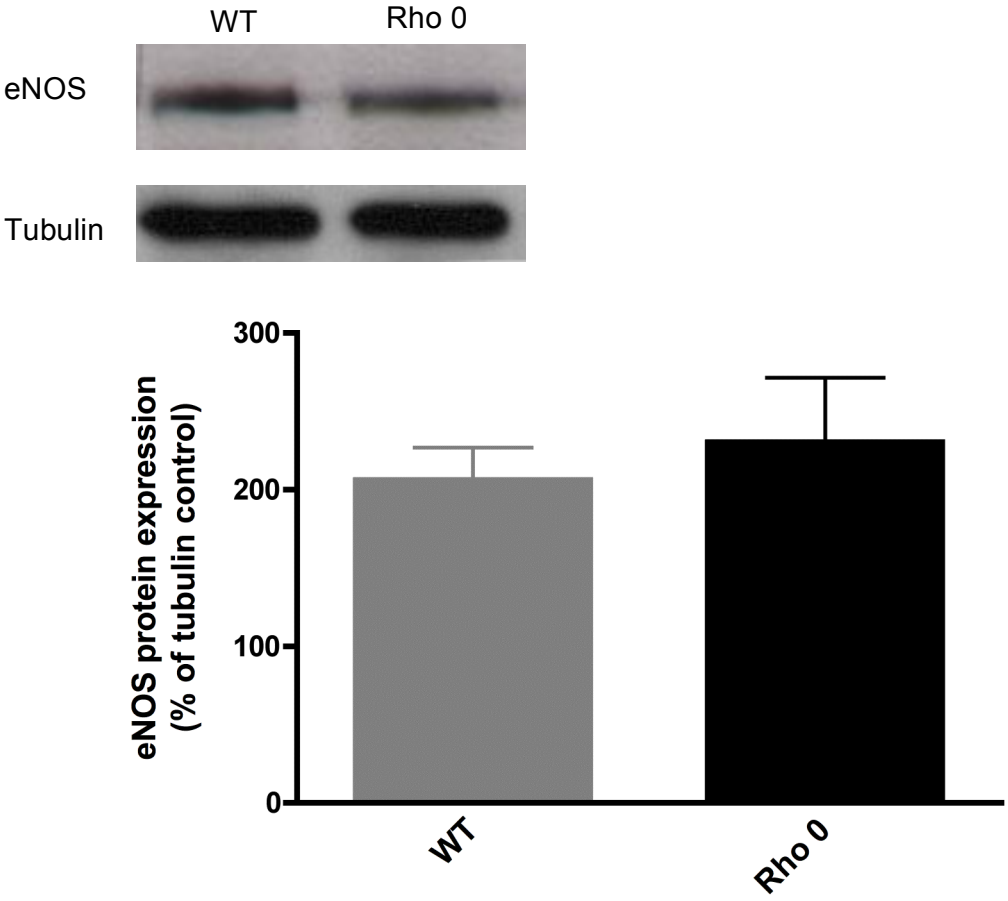

Figure 46 shows western blot analysis of HUVEC for eNOS, a 140 kDa protein, whose levels were not significantly different in WT and Rho 0 HUVEC. The 50 kDa α tubulin subunit is shown as a loading control. A representative gel is shown. The graph shows quantitative analysis, from which it can clearly be seen that there is no difference in expression between Rho 0 and WT cells. Data are represented as mean ± SEM, n = 3, from 3 independent experiments. p = ns

5 Results chapter 3: a molecular approach to creating Rho 0 HUVEC

5.1 Strategy overview and primer design

The main criticism of our model is that some or all of our observations could be due to other effects of ethidium bromide such as mutations of genomic DNA. For this reason it was felt important to investigate alternative methods of creating Rho 0 HUVEC using a genetic strategy, which would not be associated with these problems. As discussed in section 1.4.2 the creation of a single point mutation at codon 1135 (altering it from GAG to GCG) prevents DNA POLG (accession number: NM_002693.1) from functioning and leads to mitochondrial depletion (Ropp and Copeland 1996; Jazayeri, Andreyev et al. 2003). In 2003 Jazayeri et al characterised a system for creating Rho 0 HEK-293 cells using an inducible dominant negative DNA Polymerase Gamma (dnDNA POLG) (Jazayeri, Andreyev et al. 2003). This strategy was used to attempt to create Rho 0 HUVEC. Attempts to obtain the plasmid directly from the senior authors on Jazayeri's paper were unsuccessful.

The initial strategy was to isolate and clone DNA POLG, then use a site-directed mutagenesis (SDM) kit with primers specific for the single point mutation at codon 1135 (altering it from GAG to GCG) to create dnDNA POLG as reported in Jazayeri's paper. The aim was to then insert the dnDNA POLG into the vector pBABE-puro and use this to create a replication-incompetent retrovirus with which to infect the HUVEC. As a vector pBABE-puro was chosen because it was already being successfully used in HUVEC by another member of our group, to

create cells in which telomerase was knocked down (Dr Hong, personal communication).

The primers designed and used for this work are shown below in table 05

DNA POLG, used to isolate POLG gene Sense: 5'-TCTCCACGTCTTCCAGCCAGTAAA-3' Antisense: 5'-AAGCTCCACGGGAGCAAATACAGA-3'
DNA nested POLG, used to isolate section of DNA which includes POLG gene Sense: 5'-CACCATGAGCCGCCTGCTCTGGAGG-3' Antisense: 5'-CTATGGTCCAGGCTGGCTTCGTTTTTC-3'
DNA POLG SDM1, used to create GAG to GCG mutation Sense: 5'-CCATAGATGGGCGCTTCTGCATCAGCATCCATG CGGAGGTTCGCTACCTGGTGCGGGAGGAGGACCG-3' Antisense: 5'-CGGTCCTCCTCCCGCACCAGGTAGCGAACCTC CGCATGGATGCTGATGCAGAAGCGCCCATCTATGG-3'
DNA POLG SDM2, alternative primers used to create GAG to GCG mutation Sense: 5'-CTGCATCAGCATCCATGCGGAGGTTCGCTACCTGG-3' Antisense: 5'-CCAGGTAGCGAACCTCCGCATGGATGCTGATGCAG-3'
DNA POLG SDM sequencing primers, used to sequence POLG gene Sense: 5'- ATCTGCGCAAGGTCCAGAGAGAAA-3' Antisense: 5'- TGCCTACAAGCTGGGTCTGAATGA-3'
Table 05 – Human primers used for POLG molecular biology work

5.2 Isolation of DNA polymerase gamma gene

5.2.1 Attempt to isolate DNA POLG from cDNA libraries

Attempts to isolate the POLG gene were made initially from cDNA from two sources: HEK-293 (kindly provided by Dr Colombo in our lab) and WT HUVEC. cDNA was prepared and isolated from mRNA, which was extracted from the cells as described in section 2.4.3.

Standard reaction conditions were used in each well: 0.5 mM dNTP, 1x buffer, 2 mM Mg^{2+}, 0.4 μM DNA POLG sense primer, 0.4 μM DNA POLG antisense primer, 2.5 units of Taq polymerase and 100 ng template cDNA. The reaction conditions were the same as those described in section 2.4.1. An Eppendorf gradient PCR machine was then used to optimise the annealing reaction temperature by setting it to have an evenly distributed gradient from 52 °C to 65 °C across 10 wells.

An aliquot of each of the 10 samples was then run on a 1% agarose gel, as described in section 2.15.1. A fragment around the 4 kb marker was expected, as the sequence between the primers is 3.8 kb. Products were seen, however no products were visible around 4 kb. This process was then repeated unsuccessfully using cDNA synthesised from different sources of RNA, from both HEK-293 and WT HUVEC.

Other projects being run in the same laboratory to isolate genes from the same sources of cDNA (from both HEK-293 and WT HUVEC) were successful and it

was not clear why the process was not working. In the interests of time and resources it was therefore decided to search on the internet to see if an affordable commercial clone of DNA POLG was available.

5.2.2 Isolation of DNA POLG from commercial vector

OriGene Technologies, Inc (Rockville, USA) produce a human cDNA clone of DNA POLG (Accession number NM_002693.1) inserted in their pCMV6-XL4 vector, which was purchased. The plasmid contains an ampicillin resistance gene, a cytomegalovirus (CMV) promoter and the POLG gene. A physical map of the sequence of the plasmid is shown in figure 47. The map shows restriction enzyme sites, which produce three or less cutting sites, for enzymes held in our lab.

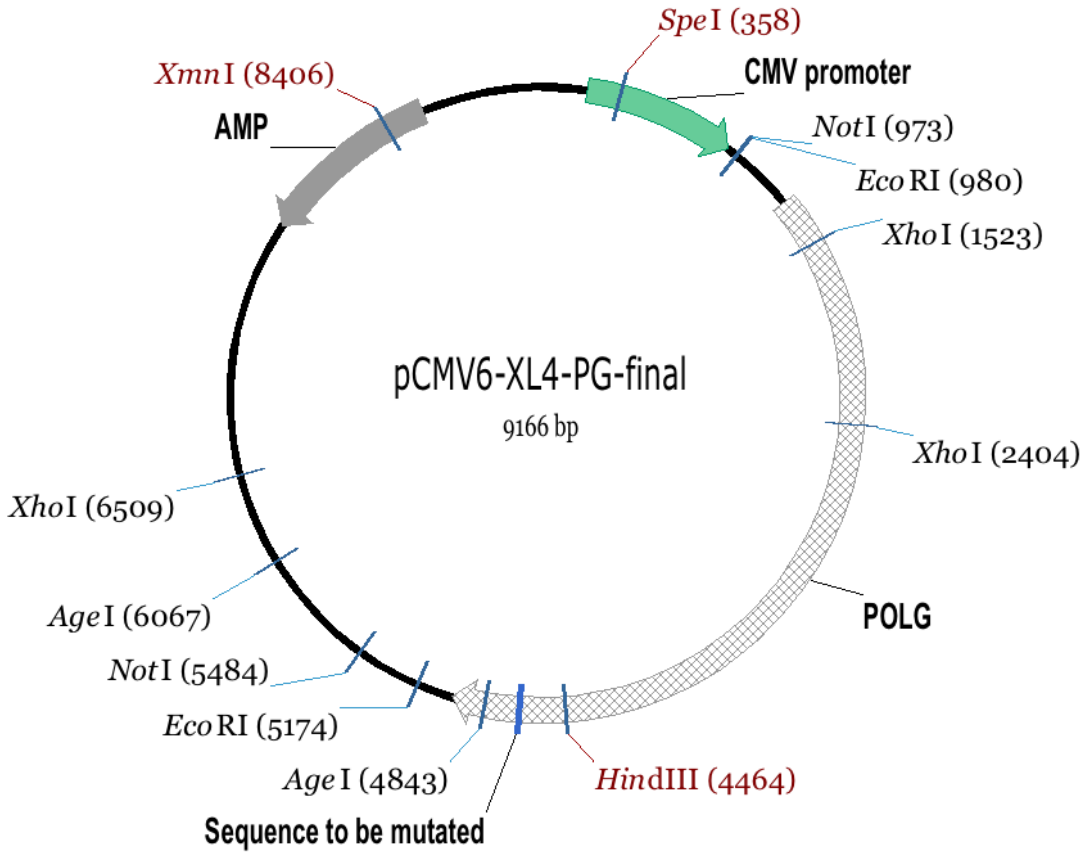

Figure 47 shows a map of pCMV-XL4 DNA POLG plasmid purchased from OriGene.

The plasmid was reconstituted in deionized water according to the manufacturers instructions. One Shot® TOP10 competent cells (Invitrogen™) were transformed, plated onto pre-prepared LB-amp agar plates and incubated overnight according to the protocol as described in section 2.15.3. Three plates were used: negative control, 150 μL of transformed cells and 75 μL of transformed cells, which respectively produced: no cells, very heavy growth and numerous discrete colonies.

The following day 5 separate colonies were picked and used to create 5 mini-preps, as described in section 2.15.5.1. From these one of the mini-preps was

used to create a maxi-prep as described in section 2.15.6.1. One mL of this mini-prep was used for this and 1 mL of glycerol was added to the remainder, which was stored in the - 80 °C freezer as stock. The remaining 4 mini-preps were spun down at 3500 rpm and kept in the - 20 °C freezer for future use. The following day the maxi-prep was processed using a QIAGEN® HiSpeed® Plasmid Purification kit (QIAGEN® Ltd, West Sussex, UK), as describer earlier in the methods section. The plasmid DNA yield from this maxi-prep was 1064.8 ngμL, this was stored in an Eppendorf ® Biopur™ tube in the - 20 °C freezer.

125 ng of the plasmid DNA was then subjected to PCR in order to amplify and thus confirm the presence of the POLG gene. This was done using both the DNA POLG and DNA POLG nested sense and antisense primers and enzyme/reagent conditions as described above. An initial denaturation step was set for 90 seconds at 98 °C. This was followed by 30 cycles of: 15 seconds at 98 °C (denaturation), 30 seconds at 58 °C (annealing) and 3 minutes at 72 °C (extension). A final extension step was set for 10 minutes at 72 °C. The PCR products were then run on an agarose gel with a 1 kb markers, which yielded a single band at 3.8 kb as expected for POLG (this is shown in figure 48). To confirm this was the correct gene the plasmid DNA was sequenced.

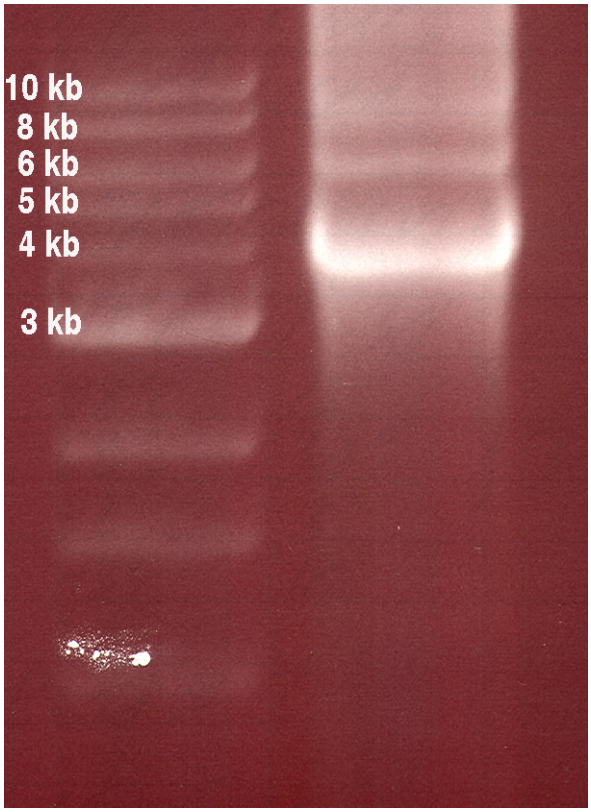

Figure 48 shows an agarose gel of PCR products confirming the presence of a 3.8 kb band consistent with POLG gene as expected.

DNA sequencing was performed using forward sequencing primers supplied by OriGene Technologies with the plasmid. The forward primer was called Vector Primer 1.5 and its priming site is located approximately 120-bp upstream of the polylinker. The reverse primer was called XL39 vector primer and its priming site is approximately 70 bp downstream of the polylinker sequence. Sequencing confirmed that the correct DNA POLG sequence was present in the plasmid DNA obtained from the maxi-prep.

5.3 Creation of dominant negative DNA POLG

5.3.1 Site directed mutagenesis of DNA POLG

The principle and methods used to create the dominant negative DNA POLG (dnDNA POLG) using site directed mutagenesis (SDM) PCR are fully described in the methods section 2.17. Preliminary work was conducted in order to optimise the SDM PCR and this step. Throughout all the steps described below different PCR cycle set-ups (i.e. annealing temperatures and times) were tried.

Initially the POLG SDM1 sense and antisense primers as listed above were used. The appropriate buffer for each enzyme was used, no additional Mg^{2+}, and 1.25 μL dNTP for the first 3 SDM PCR attempts. For each SDM PCR reaction varying loads of plasmid DNA from 5 to 250 ng were used. Initially Deep Vent® DNA Polymerase (New England Biolabs (UK) Ltd, Hertfordshire, UK) was used, which has a high fidelity 3' →5' proofreading exonuclease (Jannasch, Wirsen et al. 1992), however this yielded no colonies. Next the enzyme was switched to Phusion™ High-Fidelity DNA Polymerase (Finnzymes, Finland), which has 5′→3′ DNA polymerase activity and 3′→5′ exonuclease activity and is suitable also for amplification of long amplicons. (Lundberg, Shoemaker et al. 1991) After running an agarose gel of the PCR products smearing was noticed, suggesting the possibility of RNA contamination (see figure 49).

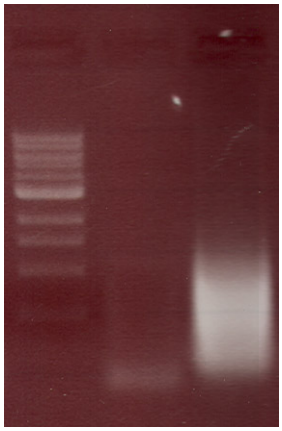

Figure 49 shows an agarose gel with smearing of the products consistent with RNA contamination.

To remove any possible contaminating RNA the plasmid DNA was processed through QIAprep® Miniprep columns. Repeating the SDM PCR with clean DNA and the Phusion™ HF again yielded no colonies.

There was a concern that the DNA POLG SDM1 primers were too long (67 bases) so shorter DNA POLG SDM2 primers (24 bases) were designed. The initial SDM PCR reaction with the DNA POLG SDM2 primers and Phusion™ HF again yielded no colonies. It was then decided to use a combination of Phusion™ HF and *Taq* DNA polymerase (Invitrogen™) in the hope that the latter would improve the yield of the reaction. The transformed cells from this reaction yielded colonies, which were isolated and made into mini-preps from which DNA was extracted using Miniprep columns. DNA POLG SDM sequencing primers were designed in order to be able to screen for the mutation required in the POLG gene (GAG to GCG at codon 1135). DNA samples were sent for sequencing. None of the colonies contained the dnDNA POLG mutation and they were all wild type POLG.

It was then decided to try a combination of Deep Vent®, Phusion™ HF and *Taq* DNA polymerase enzymes, however this produced no colonies. Other strategies that were tried and failed included: altering the concentration of Mg^{2+} and use of Accuprime *Taq* DNA polymerase (Invitrogen™). A combination of Accuprime *Taq* DNA polymerase and Accuprime *Taq* DNA polymerase HF (Invitrogen™) did produce colonies but sequencing their DNA showed none to contain the required mutation.

Finally a QuikChange® II XL Site-Directed Mutagenesis Kit was purchased, as described in section 2.17. This contains a PfuUltra™ high-fidelity (HF) DNA polymerase for mutagenic primer directed replication of both plasmid strands with the highest fidelity. (Hogrefe, Hansen et al. 2002) The reagents were used to set up the PCR with DNA POLG SDM2 primers exactly as specified in the manufacturer's kit. Both the XL-10 Gold® ultracompetent cells (provided in the kit) and One Shot® TOP10 competent cells were transformed. All the plates produced colonies, 14 of which were selected and made into mini-preps from which DNA was extracted using Miniprep columns. Only 6 of the 14 DNA samples were of sufficient quality (concentration and purity) to be sent for sequencing, all of which were from the XL-10 cells.

DNA sequencing using DNA POLG SDM sequencing primers showed 4 out of the 6 samples contained the dnDNA POLG mutation (GAG to GCG at codon 1135). A maxi-prep was prepared from one of these dnDNA POLG samples, from this the DNA was harvested the following day using the QIAGEN® HiSpeed® Plasmid Purification kit, as described earlier in the methods section. The DNA from this maxi-prep was sent with primers for sequencing, which confirmed that

the correct pCMV6-XL4 dnDNA POLG plasmid was present (a map of this plasmid is shown in figure 50).

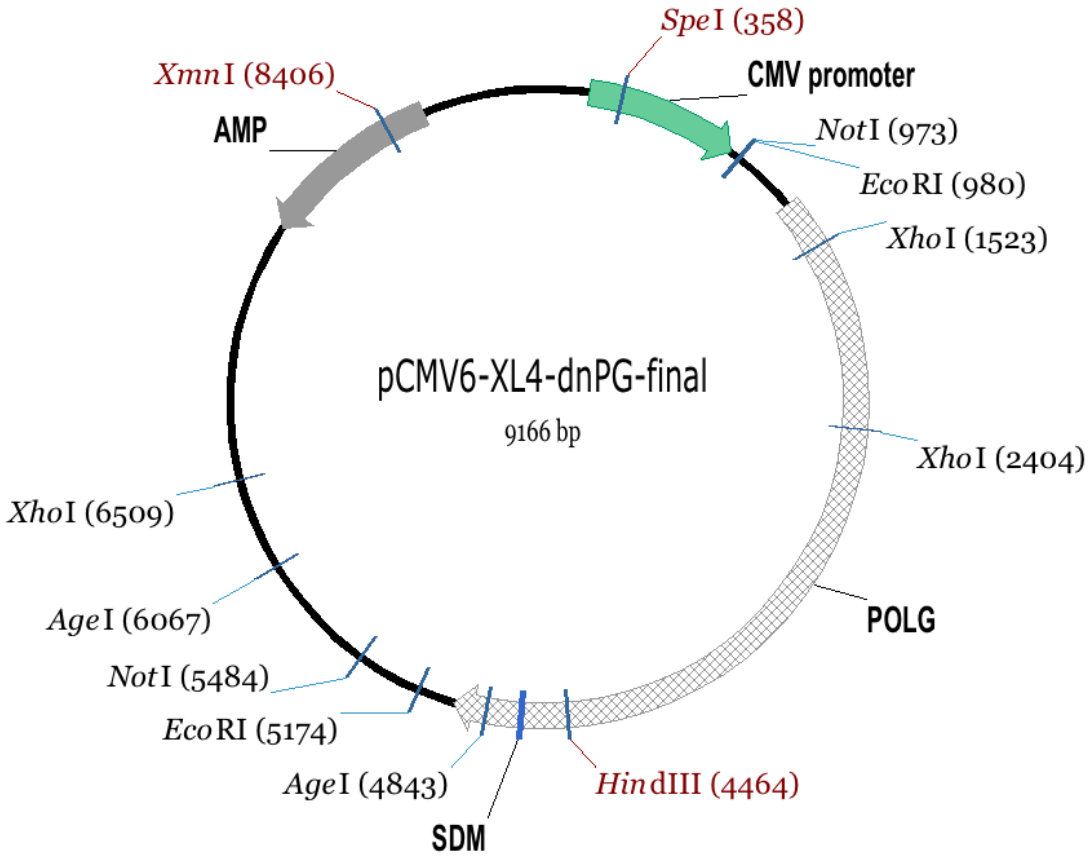

Figure 50 shows a map of the final pCMV-XL4 dnDNA POLG plasmid

5.4 Creation of pBABE-dnPOLG plasmid

A map of the pBABE plasmid described in section 2.18.2, which was provided by Dr Hong, is shown in figure 51. It is a 5.1 kb plasmid that contains a cloning site, an ampicillin resistance gene and a puromycin resistance gene. This plasmid can then be used with a packaging cell line to create a replication incompetent retrovirus.

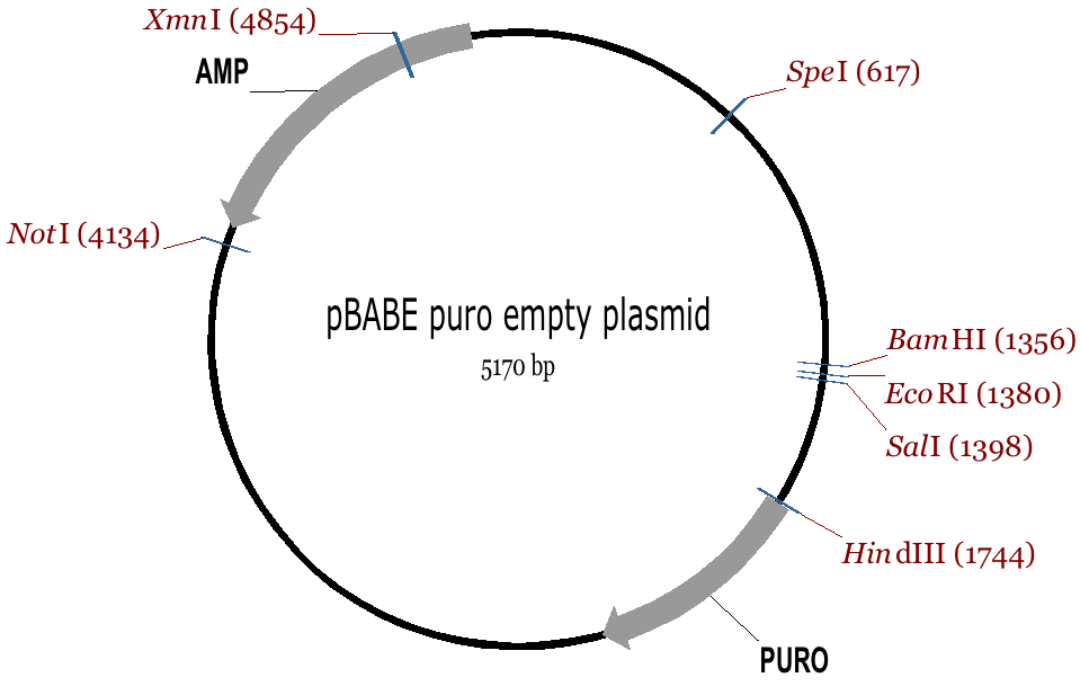

Figure 51 shows a map of pBABE vector plasmid.

5.4.1 Optimisation of ligation strategy

A number of strategies were tried and failed in order to reach the final successful ligation strategy. For reference the details of the four optimisation strategies that failed are described in detail below in sections 5.4.1.1 – 5.4.1.4. However, the reader may wish to skip directly to the final successful ligation strategy described in section 5.4.2.

5.4.1.1 Strategy 1: *EcoR*1 cut of both insert and vector and sticky end cloning

The pBABE vector was cut with *Eco*R1 by incubating it with the appropriate buffer at 37 °C for 2 hours. The reaction mixture was then treated with Antarctic

phosphatase with the appropriate buffer at 37 °C for 1 hour. Antarctic phosphatase catalyses the removal of 5' phosphate groups from DNA thus preventing re-ligation of the vector. The enzyme was then completely denatured by heating to 65 °C for 5 minutes (Rina, Pozidis et al. 2000). Passing it through Miniprep columns purified the end vector product DNA. The dnDNA POLG insert was prepared from the pCMV6-XL4 dnDNA POLG plasmid by digesting it with *Eco*R1 by incubating it with the appropriate buffer at 37 °C for 2 hours. Passing it through Miniprep columns purified the resulting DNA. To remove any remaining plasmids, to leave only the dnDNA POLG insert, this DNA was digested with *Spe*1 by incubating it with the appropriate buffer at 37 °C for 2 hours. Passing it through Miniprep columns purified the resulting DNA. An agarose gel confirmed the insert expected was present. The final concentration of insert and vector DNA was then measured and a ligation reaction. This was set up with a ratio of 3 molecules insert: 1 molecule vector using T4 DNA ligase, which catalyses the formation of phosphodiester bonds between 5' and 3' DNA ends (Weiss, Jacquemin-Sablon et al. 1968), with the appropriate buffer at room temperature overnight.

One Shot® TOP10 competent cells (Invitrogen™) were then transformed with the ligation mixture, plated onto LB-amp agar plates and incubated overnight according to the protocol, as described earlier in the methods section. A few discrete colonies were seen the following day, there were none on the negative control plate, and 12 of these were picked and put into mini-preps. Direct PCR of these colonies showed 10 of the 12 contained the dnDNA POLG mutation. DNA was then extracted from the mini-preps using Miniprep columns. Aliquots of the samples were then each digested with *Spe*1 and *Xho*1 in the appropriate buffer

at 37 °C for 1 hour and run on an agarose gel. This restriction analysis suggested two of the samples possibly contained the correct plasmid. These samples were then subjected to a further restriction analysis with *Bam*H1 and *Xho*1 in the appropriate buffer at 37 °C for 2 hours and run on an agarose gel. The theoretical gel shown on the next page in 52 shows the restriction maps expected for: 1) empty pBABE plasmid, 2) pCMV6-XL4 dnDNA POLG plasmid 3) expected pBABE- dnDNA POLG plasmid and 4) expected pBABE- dnDNA POLG plasmid with dnDNA POLG inserted in reverse.

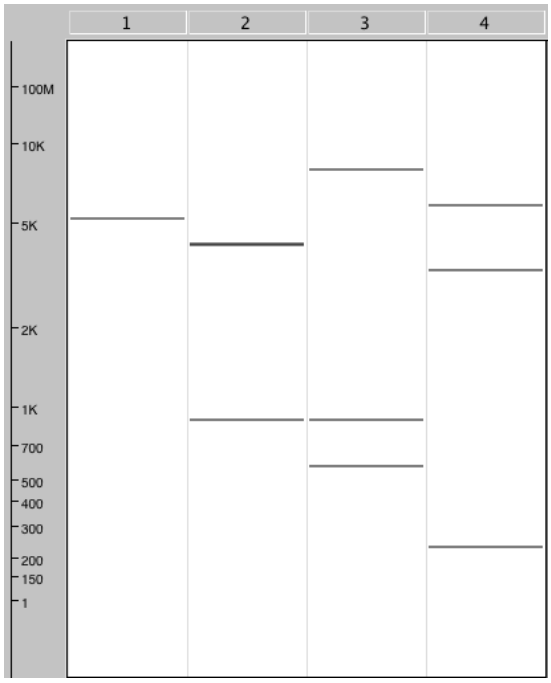

Figure 52 shows the expected BamH1 and Xho1 restriction map for 1) empty pBABE plasmid, 2) of pCMV-XL4 dnDNA POLG plasmid, 3) expected pBABE- dnDNA POLG plasmid and 4) expected pBABE- dnDNA POLG plasmid with dnDNA POLG inserted in reverse.

From the actual gel (figure 53) it can be seen that the ligation had failed and that two samples contained the pCMV6-XL4 dnDNA POLG plasmid (double bands) and one the empty pBABE plasmid (single band).

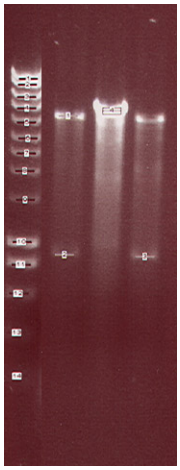

Figure 53 shows the agarose gel from the BamH1 and Xho1 digest of the final product showing the expected ligation has failed and two samples contain pCMV-XL4 dnDNA POLG plasmid (1st and 3rd column) and the third empty pBABE plasmid (middle column).

5.4.1.2 Strategy 2: *Not*1 and *Xmn1* cut of insert and *EcoR*1 cut of vector and blunt end cloning

It was decided to try a new strategy to prepare the insert that would minimise the chances of the pCMV6-XL4 dnDNA POLG plasmid simply re-annealing and ending up in the final ligation reaction.

The dnDNA POLG insert was prepared from the pCMV6-XL4 dnDNA POLG plasmid by digesting it with *Not*1 by incubating it with the appropriate buffer at 37 °C for 1 hour. Passing it through Miniprep columns purified the resulting DNA. To remove any remaining plasmids, to leave only the dnDNA POLG insert, this DNA was digested with *Xmn*1 by incubating it with the appropriate buffer at 37 °C for 1 hour. Passing it through Miniprep columns purified the resulting DNA. An agarose gel of the sample split into 2 lanes was then run (shown in figure 54). From this it can be seen there were 3 distinct bands: the insert at 4.5 kb and the two remaining fragments of the plasmid at 2.9 kb and 1.8 kb respectively.

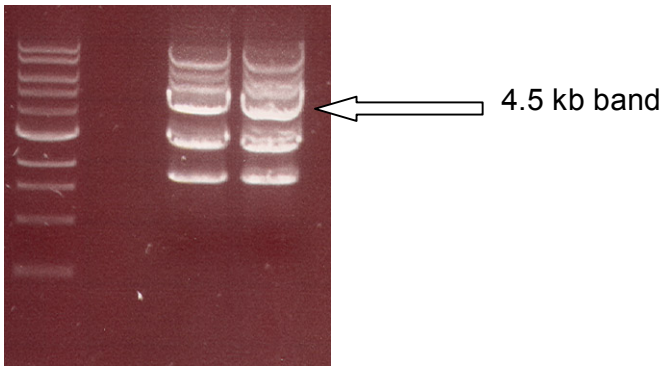

Figure 54 shows the agarose gel from the Not1 and Xmn1 digest of the pCMV-XL4 dnDNA POLG plasmid. There are 3 distinct bands, the insert is the 4.5 kb band.

Under UV light the two 4.5 kb bands were cut out with a scalpel. These samples were then added to 4 M potassium iodide (KI) and heated to 55 °C for 5 minutes to dissolve the agarose. The resulting solution was then passed through Miniprep columns to purify the resulting insert DNA.

The pBABE vector was cut with *Eco*R1 by incubating it with the appropriate buffer at 37 °C for 1 hour. Passing it through Miniprep columns purified the end vector product DNA.

Blunt ends had to be created on both the insert and vector as the *Not*1 and *Eco*R1 on the respective DNA fragments are not directly compatible. This was done using DNA Polymerase 1, Large (Klenow) Fragment (New England Biolabs (UK) Ltd, Hertfordshire, UK), which fills in 5' and 3' overhangs to form blunt ends. Both the insert and vector were each treated with Klenow, the appropriate buffer and dNTP at 25 °C for exactly 15 minutes, as per protocol. The resulting DNA was purified with Miniprep columns. A ligation reaction was then set up with a ratio of 3 molecules insert: 1 molecule vector using T4 DNA ligase, with the appropriate buffer at room temperature overnight.

XL-10 Gold® ultracompetent cells from the Stratagene kit were used (as described in section 2.17) as there was a concern that the yield of plasmid from the blunt ligation would be very low and these cells would maximize the chances of transforming the cells. The XL-10 Gold® ultracompetent cells transformed with the ligation mixture were plated onto LB-amp agar plates and incubated overnight. Numerous colonies were seen the following day, there were none on the negative control plate, and 8 of these were picked and put into mini-preps. Direct PCR of these colonies showed 4 of the 8 contained the dnDNA POLG mutation. DNA was then extracted from the mini-preps using Miniprep columns. Aliquots from 6 of the samples (4 positive from PCR and 2 others) were then each digested with *Hind*III and *Xho*1 in the appropriate buffer at 37 °C for 1 hour and run on an agarose gel. This restriction analysis showed only a single 5.1 kb band, consistent with empty pBABE vector.

5.4.1.3 Strategy 3: *Not*1 and *Xmn1* cut of insert and *EcoR*1 cut of vector with Alkaline Phosphatase treatment of vector and blunt end cloning

Treating the prepared pBABE with Antarctic phosphatase was then tried with the appropriate buffer at 37 °C for 1 hour to reduce the chances of re-ligation of pBABE during the ligation reaction. The ligation reaction and transformation were then repeated, as described in section 5.4.1.2 above. Few colonies were visible the following day and direct PCR showed no evidence of the dnDNA POLG mutation in any of the samples, so this approach was no longer pursued.

5.4.1.4 Strategy 4: *Not*1 and *Xmn1* cut of insert and *EcoR1* and *BamH1* cut of vector and blunt end cloning

The pBABE was then prepared by cutting it with the restriction enzymes *Eco*R1 and *Bam*H1 incubated with the appropriate buffer at 37 °C for 1 hour. The resulting DNA was purified with Miniprep columns. The DNA was then treated with Klenow, the appropriate buffer and dNTP at 25 °C for exactly 15 minutes, as per protocol, to create blunt ends. The resulting DNA was purified with Miniprep columns. Finally the DNA was treated with Antarctic phosphatase with the appropriate buffer at 37 °C for 1 hour to reduce the chances of re-ligation of pBABE during the ligation reaction. The insert was prepared exactly as in section 5.4.1.2 except that after isolation of the 4.5 kb band DNA the digestion with *Not*1 and *Xmn*1 was repeated and the gel run again to ensure only the 4.5 kb band (i.e. insert) was present (shown in figure 55).

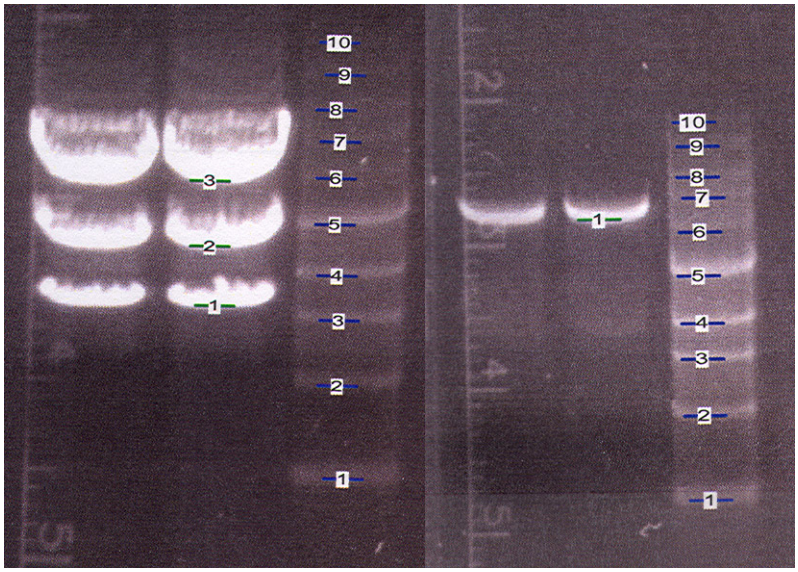

Figure 55 shows the agarose gel from the second Not1 and Xmn1 digest of the pCMV-XL4 dnDNA POLG plasmid, showing the 4.5 kb insert band. The first digest is shown on the left and the second digest (of the cut 4.5 kb band from the first) on the right.

The band was then cut out and dissolved in KI and prepared with Klenow as described in section 5.4.1.2. The ligation reaction and transformation were then done, as described in section 5.4.1.2. The following day a few colonies were observed and 12 mini-preps were set up from 12 discrete colonies. DNA was then extracted from the mini-preps using Miniprep columns. Aliquots from each of the samples were then each digested with *Hind*III and *Xho*1 in the appropriate buffer at 37 °C for 1 hour and run on an agarose gel. This restriction analysis showed only a single 5.1 kb band, consistent with empty pBABE vector. This whole strategy was repeated again with a ligation ratio of 10 insert molecules: 1 vector molecule to try and improve the chances of a successful reaction but restriction analysis of the end products showed only a single 5.1 kb band, consistent with empty pBABE vector.

5.4.2 Final successful ligation strategy

Finally phosphorylating the insert ends with T4 polynucleotide kinase, which increases the phosphorylation of the 5' and 3' ends of the insert, was tried to see if it would improve the efficacy of the ligation reaction.

The insert prepared from section 5.4.1.4 was re-treated with Klenow, as described earlier, to ensure the ends were blunt. The resulting DNA was purified with Miniprep columns. The DNA was then treated with T4 polynucleotide kinase with the appropriate buffer at 37 °C for 30 minutes. The resulting DNA was purified with Miniprep columns. The ligation reaction was set up using pBABE vector prepared exactly as described in section 5.4.1.4 with a ratio of 10 molecules insert: 1 molecule of vector. XL-10 cells were transformed and plated

onto LB-amp agar plates. The following day discrete colonies were visible, with none on the negative controls, 6 discrete colonies were set up as mini-preps. DNA was then extracted from the mini-preps using Miniprep columns. Aliquots from each of the samples were then each digested with *Hind*III and *Xho*1 in the appropriate buffer at 37 °C for 1 hour and run on an agarose gel. The theoretical gel in 56 shows the restriction maps expected for: 1) empty pBABE plasmid, 2) pCMV6-XL4 dnDNA POLG plasmid 3) expected pBABE- dnDNA POLG plasmid and 4) expected pBABE- dnDNA POLG plasmid with dnDNA POLG inserted in reverse.

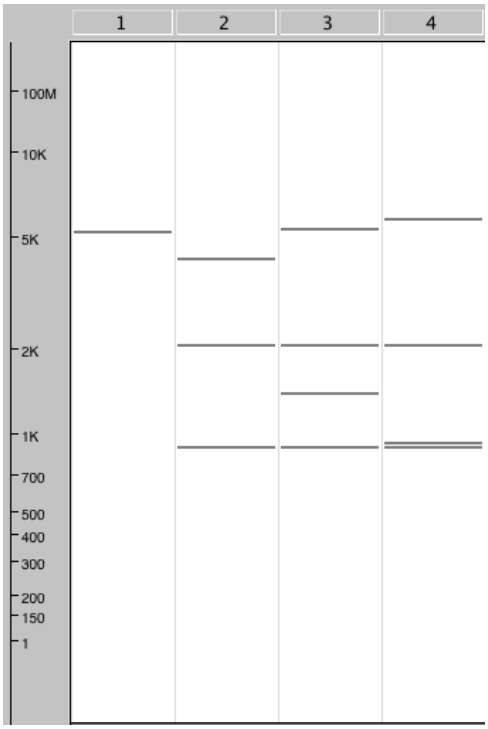

Figure 56 shows the expected HindIII and Xho1 restriction map for 1) empty pBABE plasmid, 2) of pCMV-XL4 dnDNA POLG plasmid, 3) expected pBABE- dnDNA POLG plasmid and 4) expected pBABE- dnDNA POLG plasmid with dnDNA POLG inserted in reverse.

From the actual gel in figure 57 it can be seen that the ligation was successful in column 2 but had failed in the lanes, which contained the empty pBABE plasmid.

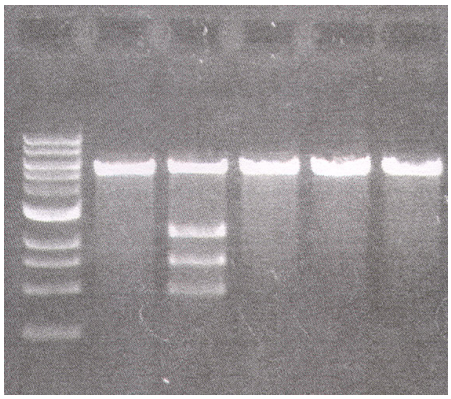

Figure 57 shows the agarose gel from the HindIII and Xho1 digest confirming the expected product (4 bands) in lane 2 but empty pBABE vector (single band only) in the other lanes.

From the mini-prep of the successful ligation a maxi-prep was set up from which the DNA was harvested the following day using the QIAGEN® HiSpeed® Plasmid Purification kit. The DNA from this sample was sent with primers and the whole plasmid was sequenced, confirming the correct pBABE-dnDNA POLG plasmid was present (a map of this is shown in figure 58).

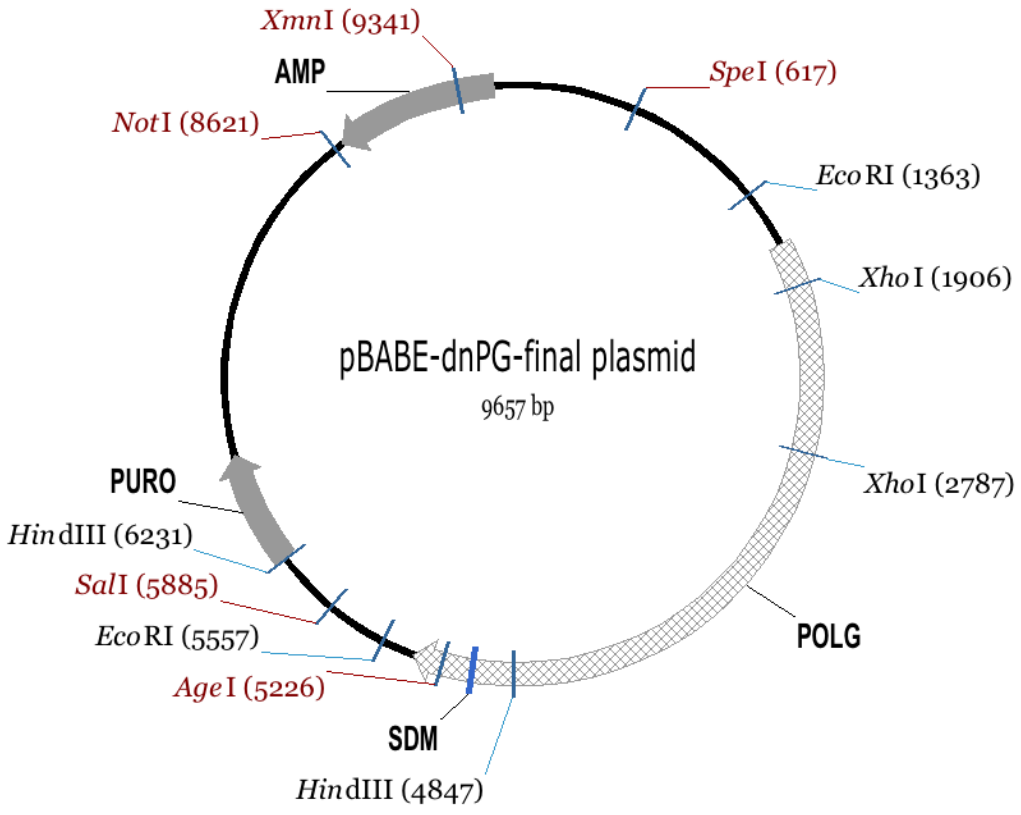

Figure 58 shows a map of the final pBABE-dnDNA POLG plasmid.

5.5 Transfection of HUVEC with plasmid

5.5.1 Transfection of HUVEC with plasmid using retrovirus

Three days before retrovirus production a fresh vial of HEK-293 gp packaging cells (kindly supplied by Dr Hong, from our group) were thawed and plated onto a 6 well plate. The following day mixtures A and B were prepared, as described in section 2.18.1, using a ratio of pVSVG (kindly supplied by Dr Hong, from our group) to pBABE-dnDNA POLG of 1:3. Mixtures A and B were then mixed and 0.5 mL of the resulting mixture added to each of the wells. Supernatant containing the retrovirus, produced from the packaging cells, was removed after 60 hours and filtered using a 0.45 Nalgene® syringe filter. The supernatant was then used to infect WT HUVEC as described in section 2.18.2.

0.5 mL of supernatant containing the retrovirus was added to 4 of the wells and 2 were left as controls. A second 6 well plate containing fresh HUVEC was kept as a WT control. After 48 hours the medium was changed to selection medium, which contained Puromycin at a final concentration of 1 μg / ml. The following day all control cells were dead and 85% of the infected HUVEC were dead. The selection medium was changed. After 8 days there were enough infected HUVEC to split and transfer to T25 flasks, 7 days later these cells were split and transferred to T75 flasks. After 21 days in selection medium enough infected cells were available to do respirometry to test for the Rho 0 phenotype, as described in section 2.8.2. The results of the respirometry are shown in figure 59 and confirm that the infected cells respired normally and thus did not have the Rho 0

phenotype. Two further attempts at producing Rho 0 HUVEC in this manner also failed to work.

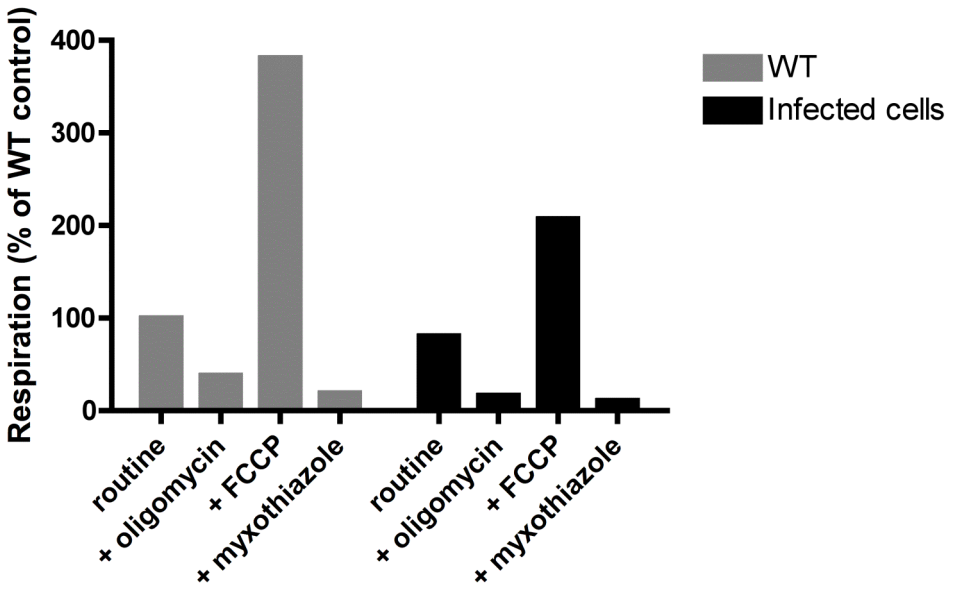

Figure 59 shows oxygen consumption in WT HUVEC versus HUVEC transfected with the plasmid. Baseline oxygen consumption in WT HUVEC is predominantly from oxidative phosphorylation and that addition of 2 μg/mL oligomycin reduces this by 47 % (from 100 % ± 0 % to 53.0 % ± 6.6 %), FCCP increases it to a maximum at (267 ± 39.8) % and finally 0.5 μM myxothiazole reduces this to a minimum of (24.0 ± 8.5) %. Cells transfected with the plasmid respire in the same manner as WT cells, confirming they do not have a Rho 0 phenotype. Data are represented as mean ± SEM, n = 3. * $p < 0.05$, * $p < 0.05$.

In an attempt to improve the virus yield the protocol was repeated increasing the ratio of pBABE-dnDNA POLG to pVSVG. A Rho 0 phenotype in the cells was still not obtained.

5.6 Transfection of HEK-293 with plasmid

5.6.1 Transfection of HEK-293 with plasmid using retrovirus

HEK-293 cells were infected using the protocols as described above but all respirometry measurements of the puromycin selected cells confirmed that they did not contain the Rho 0 phenotype.

5.6.2 Transfection of HEK-293 with plasmid using liposome

Finally HEK293 cells were directly transfected with the pBABE-dnDNA POLG plasmid using a liposome as described in Jazayeri's original paper, as described in the methods section 2.18.1 using a ratio of plasmid DNA to Lipofectamine of 3:1. (Jazayeri, Andreyev et al. 2003). Although the plasmid was taken up by the cells, as evidenced by their survival in the puromycin selection medium, respirometry confirmed they did not have the Rho 0 phenotype.

5.7 Alternative pBABE-dnPOLG strategy

Although the plasmid was being taken up by the cells, as evidenced by their survival in puromycin selection medium, the dnDNA POLG was not being expressed at a level sufficient enough to create the Rho 0 phenotype. There was concern that this was because the original strategy cut out a substantial proportion of the CMV promoter and this was the reason that the dnDNA POLG was not being expressed in sufficient quantities. It was therefore decided to develop a strategy to alter the final plasmid so that it contained the complete CMV promoter that was present in the original pCMV-XL4 dnDNA POLG plasmid, in the hope this would increase expression of the dnDNA POLG to sufficient levels to create the Rho 0 phenotype.

A segment of DNA was cut containing most of the CMV promoter and the dnDNA POLG insert from the pCMV6-XL4 dnDNA POLG plasmid (shown in figure 50). First the pCMV6-XL4 dnDNA POLG plasmid was cut with the restriction enzymes *Spe*1 and *Xmn*1 and incubated with the appropriate buffer at 37 °C for 1 hour. The resulting DNA was purified with Miniprep columns. The resulting DNA was then cut with the restriction enzymes *Age*1 and incubated with the appropriate buffer at 37 °C for 1 hour. The resulting insert DNA was purified with Miniprep columns.

The dnDNA POLG insert was then removed from the pBABE dnDNA POLG vector plasmid (shown in figure 58). First the pBABE dnDNA POLG plasmid was cut with the restriction enzymes *Spe*1 and *Xho*1 and incubated with the appropriate buffer at 37 °C for 1 hour. The resulting DNA was purified with

Miniprep columns. The resulting DNA was then cut with the restriction enzymes *Age*1 and incubated with the appropriate buffer at 37 °C for 1 hour. The resulting vector DNA was purified with Miniprep columns.

The insert and vector DNA samples were then run on a standard agarose gel (shown in figure 60), which confirmed the presence of a 4.48 kb insert band and 5.05 kb vector band.

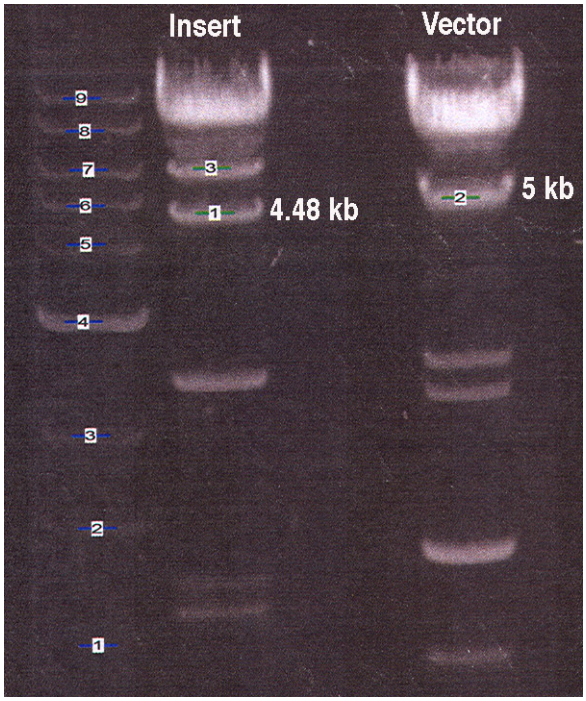

Figure 60 shows the agarose gel from the Spe1, Xmn1, Age1 digest of the pCMV6-XL4 dnDNA POLG plasmid and Spe1, Xho1, Age1 digest of pBABE dnDNA POLG plasmid, with the insert band at 4.48 kb and vector band at 5.05 kb.

These bands were then cut out and dissolved in KI and prepared as described earlier in section 5.4.1.2. A ligation reaction was then set up with a ratio of 3 molecules insert: 1 molecule vector using T4 DNA ligase, with the appropriate buffer at room temperature overnight.

XL-10 Gold® ultracompetent cells were transformed with the ligation mixture, plated onto LB-amp agar plates and incubated overnight. Numerous colonies were seen on all treatment plates the following day, there were none on the negative control plate. Two of these colonies were picked and put into mini-preps.

DNA was then extracted from the mini-preps using Miniprep columns. Aliquots from 2 of the samples were then each digested with *Hind*III and *Xho*1 in the appropriate buffer at 37 °C for 1 hour and run on an agarose gel. The restriction analysis, shown in figure 61, confirmed both samples contained the correct bands as expected with the plasmid being made (a map of which is shown in figure 62).

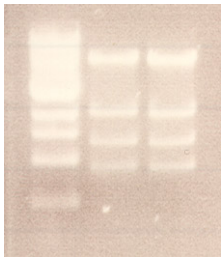

Figure 61 shows the agarose gel from the HindIII and Xho1 digest of the final ligation product confirming three bands.

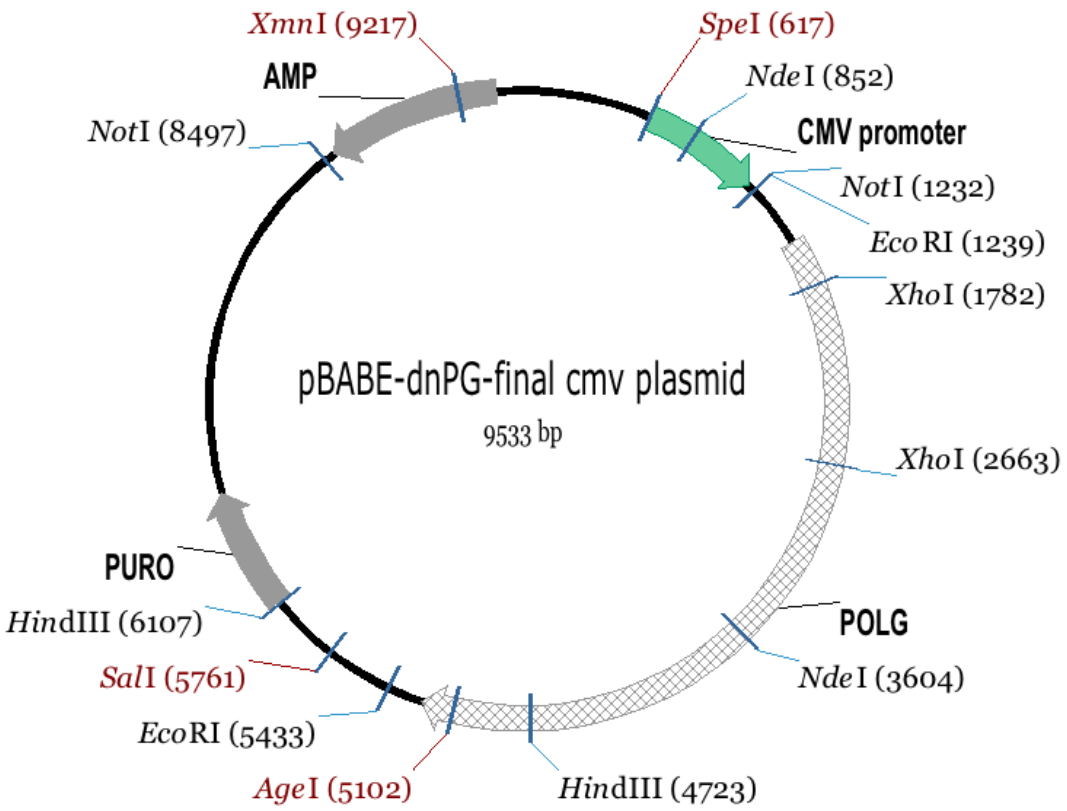

Figure 62 shows a map of final pBABE dnDNA POLG plasmid with CMV promoter.

Finally to ensure that these results were not simply due to the original plasmid, which had an identical *Hind*III and *Xho*1 restriction map, one of the pBABE dnDNA POLG samples and new samples were digested with *Nde*1 in the appropriate buffer at 37 °C for 1 hour. The pBABE dnDNA POLG plasmid contains only 1 *Nde*1 restriction site, whereas the new plasmid with the CMV promoter contains a second *Nde*1 restriction site in the CMV promoter and would be expected to produce two DNA bands. The agarose gel shown in figure 63 confirms the new plasmid contained the CMV promoter.

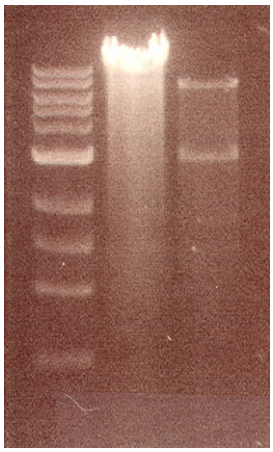

Figure 63 shows the agarose gel from the Nde1 digest of final ligation product confirming a single band in the original pBABE dnDNA POLG plasmid and two bands in the final pBABE dnDNA POLG plasmid product, due the presence of a CMV promoter.

From this sample a maxi-prep was set up, from which the DNA was harvested the following day using the QIAGEN® HiSpeed® Plasmid Purification kit,.

5.8 Transfection of HEK with alternative plasmid using liposome

Using the alternative pBABE dnDNA POLG plasmid, which contained the CMV promoter, HEK-293 cells were transfected. Freshly plated HEK 293 cells in a 6 well plate were treated as described in section 2.18.1 using a ratio of plasmid DNA to Lipofectamine of 3:1. After 48 hours the cells were put in puromycin selection medium and expanded over time. All the control cells died as expected. After 6 weeks enough infected cells were available to subject them to respirometry studies (shown in figure 64), which confirmed the cells were not actively respiring, the cells had the Rho 0 phenotype and the plasmid containing the CMV promoter was working.

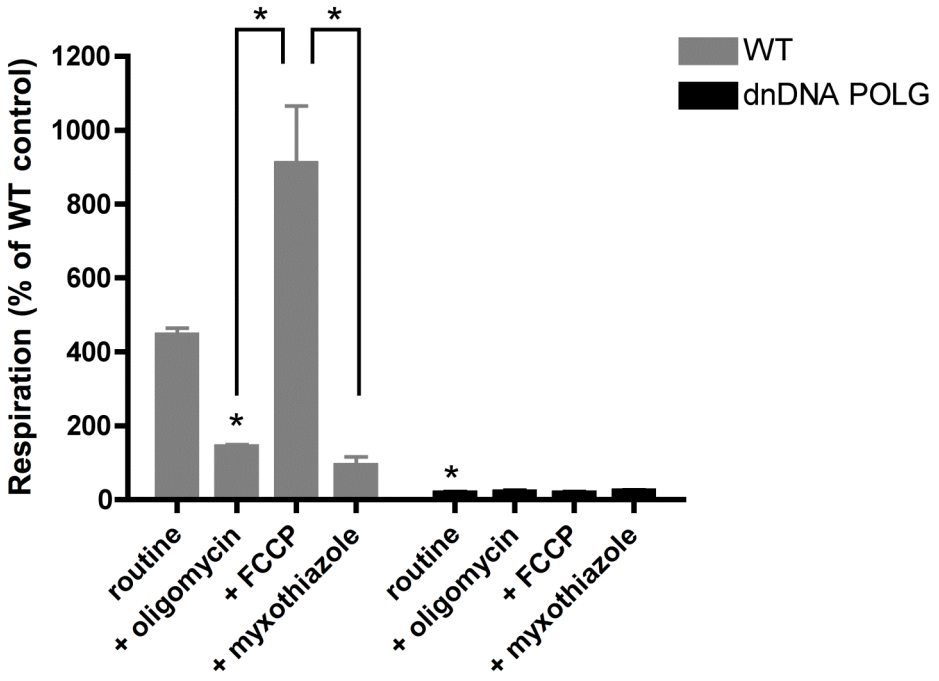

Figure 64 shows the oxygen consumption in WT HEK versus Rho 0 HEK. It shows that baseline oxygen consumption in WT HEK is predominantly from oxidative phosphorylation and that addition of 2 μg/mL oligomycin reduces this from 100.0 % ± 4.4 % to 32.0 % ± 1.2 %, FCCP increases it to a maximum at (204.0 ± 35.0) % and finally 0.5 μM myxothiazole reduces this to a minimum of (20.8 ± 5.4) %. In contrast none of these reagents significantly alters oxygen consumption in Rho 0 HEK cells. Data are represented as mean ± SEM, n = 3. * $p < 0.05$.

Samples were then harvested in order to carry out quantitative PCR and western blots to characterise the cells as described in sections 3.4 and 3.5. However, these studies were unable to be completed due to technical reasons. More importantly further work to optimise this system in HUVEC was not possible due to time and resource constraints.

6 Conclusions and Discussion

6.1 The ethidium bromide model for the production of Rho 0 HUVEC

This is the first reported successful attempt to grow a primary Rho 0 cell culture of endothelial cells. This work has demonstrated that it is feasible to generate Rho 0 HUVEC by growing them in the presence of low-dose ethidium bromide for 12 days. The cells need to be continuously subcultured in ethidium bromide to maintain their Rho 0 status, otherwise they are able to regain functional mitochondria (as shown in figure 16). This phenomenon is well described (King and Attardi 1989) and it is known that the injection of as little as a single mitochondrion can repopulate a whole cell culture although the exact mechanisms for this are not fully understood (King and Attardi 1988).

In cells grown for more than 50 days in the continuous presence of EB unwanted changes in growth rate are sometimes seen, such as those discussed in section 3.1 of the results. Given that EB is a known mutagen the possibility that these cells may have been transformed as a result of a mutation in nuclear DNA cannot be entirely discounted. Assessment of this phenomenon was beyond the realms of this work.

All HUVEC were grown in 25 mM glucose for this work. It is generally accepted that high glucose levels have a number of deleterious effects on endothelial cells including: increased ROS, apoptosis and senescence (Hayashi, Matsui-Hirai et al. 2006; Piconi, Quagliaro et al. 2006; Berge, Behrens et al. 2007). However, initial experiments comparing growth of WT HUVEC in physiological (5 mM

glucose) vs 25 mM did not show any difference in proliferative capacity up to passage 5. However, had the experiments been done on stress-induced senescence and apoptosis using HUVEC grown in 5 mM glucose the differences in effects observed in the Rho 0 HUVEC, compared to WT, may have been more pronounced. However there is some recent evidence to suggest that the deleterious effects seen in diabetes, a condition associated with hyperglycaemia, may be due to glucose enhancing a pre-existing inflammatory condition as opposed to a direct harmful effect of hyperglycaemia in human vascular smooth muscle cells (Lafuente, Matesanz et al. 2008).

The Rho 0 HUVEC grew more slowly than WT cells and had a reduced proliferative capacity, as confirmed by both growth curves and BrdU incorporation. It is well recognised that Rho 0 cells grow more slowly than their WT parent cells (Morais, Desjardins et al. 1988; Miller, Trimmer et al. 1996; Park, Nam et al. 2001). One group have shown that levels of glucose 6-phosphate dehydrogenase (G6PDH) are significantly reduced in Rho O cells (Park, Nam et al. 2001) and suggest that in addition to low ATP levels this is the cause of slow growth in these cells. G6PDH is an enzyme in the pentose phosphate pathway, which is the main producer of NADPH. NADPH is the main intracellular determinant of a cells redox potential, which has been shown to be a key determinant of cell growth. In support of the findings of Park et al it has been demonstrated that changes in G6PDH levels have a direct effect on cells growth (Tian, Braunstein et al. 1998).

As expected the Rho 0 HUVEC are auxotrophic for uridine. Although there was a reduction of the growth rate of WT cells grown in uridine free medium, unlike the

Rho 0 HUVEC the WT cells did not die (as shown in figure 15). It is likely that this reduction in growth rate observed in the WT cells was due to a reduction in essential growth factors by the dialysis process. This phenomenon is well recognised (Chen and Chen 1982; Clemmons, Isley et al. 1983), especially when a dialysis membrane with a molecular weight of 3500 is used, as in this work (Clemmons, Isley et al. 1983).

The Rho 0 status of the cells was confirmed by a lack of expression of mitochondrial-encoded genes and proteins (as shown in figures 16 and 17). As expected nuclear-encoded mitochondrial proteins were unaffected (as shown in figure 18).

6.2 The bioenergetic consequences of Rho 0 status

This work showed that Rho 0 HUVEC produce less ATP than WT cells. Furthermore, it also demonstrated that Rho 0 HUVEC were entirely dependent on glycolysis for their energetic demands. The ATP production of Rho 0 HUVEC was unaffected by inhibitors of ATPase or the ETC (as shown in figures 18 and 19) therefore confirming their lack of a functional ETC. The main source of ATP production in WT HUVEC has previously been shown to be glycolysis and it is has been suggested that the main role of mitochondria in these cells could be to act as signalling organelles (Quintero, Colombo et al. 2006). This is discussed in more detail in section 1.6.3 of the introduction.

All the published work on Rho 0 cells to date has been done predominantly on either immortalised or cancer cell lines and confirms that Rho 0 cells produce

significantly less ATP than the counterpart WT cells (Appleby, Porteous et al. 1999; Park, Nam et al. 2001; Park, Choi et al. 2005; Chiaratti and Meirelles 2006). Only one group has published data on ATP production in Rho 0 cells using the same units (nMol / mg protein), they studied SK-Hep1 cells (derived from hepatoma cells). They showed that Rho 0 cells produced 0.5 nMol / mg protein i.e. 500 pmol / mg protein, about a quarter of the amount of ATP produced in the WT cells (2 nMol / mg protein) (Park, Nam et al. 2001). This is very similar to the ATP produced by Rho 0 HUVEC in this thesis (580 pmol / mg protein). The fact that the WT SK-Hep1 cells produce proportionally much more ATP than the Rho 0 SK-Hep1 cells would suggest that these WT cells rely less in glycolysis as their main source of ATP.

Respirometry studies shown in figure 21 demonstrated that Rho 0 cells consume significantly less oxygen than WT cells, as has been shown in previous work on other Rho 0 cell lines (Herst, Tan et al. 2004). As expected from previous work the Rho 0 HUVEC did not consume O_2 via aerobic respiration as demonstrated by the respirometry experiments with classical inhibitors of the ETC and ATPase (shown in section 3.9).

Nitric oxide is known to competitively compete with complex IV for oxygen and mitochondria are believed to act as signalling organelles in endothelial cells by this mechanism, as discussed in detail in section 1.6.2.2. The results presented in figure 22 demonstrate that Rho 0 HUVEC have higher levels of NO than WT cells and this may in its own right have a protective effect on the cells, as discussed in section 6.2.2.2. The fact that KCN, a competitive inhibitor of complex IV, causes a rise in NO when added to WT cells but has no effect on

Conclusions and Discussion

Rho 0 HUVEC suggests that NO is indeed bound to complex IV in WT cells but not Rho 0 cells. It therefore seems plausible that NO binding to complex IV plays an important role in mitochondria signalling and the coordination and regulation of endothelial cells defence mechanisms.

The experiments shown in figures 23 and 24 suggest that approximately half of the non-mitochondrial oxygen consumption seen in Rho 0 HUVEC was due to NADPH oxidase. Identification of which isoforms of NOX were responsible for these observations in the Rho 0 HUVEC was beyond the scope of this work. After inhibition of NADPH oxidase with DPI the oxygen consumption of Rho 0 HUVEC (and WT HUVEC) did not come down to zero. Clearly this means that other unmeasured sources of non-mitochondrial oxygen consumption were responsible.

One of the main sources of non-mitochondrial cellular oxygen consumption is NADH oxidase (DeFrancesco, Scheffler et al. 1976), which forms part of the PMOR (otherwise known as the transplasma membrane electron transport – tPMET), which is described in section 1.4.3 (Larm, Vaillant et al. 1994; Shen, Khan et al. 2003; Herst and Berridge 2007). It is also well recognised that the PMOR system is upregulated in Rho 0 cells (Larm, Vaillant et al. 1994). Cell surface oxygen consumption was shown to be a major source of oxygen consumption in glycolytic cells, explaining its importance in Rho 0 cells. It has been suggested that as Rho 0 cells develop there is a gradual upregulation of the PMOR system, which is essential for their metabolism. It has been suggested that attempts to produce a Rho 0 cells acutely with inhibitors of the ETC, for example rotenone, fail resulting in cell death because the PMOR system cannot

be upregulated acutely (Larm, Vaillant et al. 1994). Studies of the PMOR system's role in non-mitochondrial oxygen consumption and attempts to identify other sources of non-mitochondrial oxygen consumption were beyond the scope of this work. One other final possibility is that some of this non-mitochondrial oxygen consumption was due to unmeasured effect of the equipment and/or system.

It has been shown that Rho 0 cells can maintain a mitochondrial membrane potential, otherwise maintained by a functional ETC. The adenine nucleotide translocase (ANT) is responsible for carrying ADP and P_i into the matrix in exchange for ATP into the cytosol. It has been shown that Rho 0 cells maintain a mitochondrial membrane potential by a combination of ANT and an incomplete F_0F_1-ATPase both working in the reverse direction to normal (Buchet and Godinot 1998; Appleby, Porteous et al. 1999). So in Rho 0 cells ANT transports ATP from the cytoplasm into the mitochondrial matrix and the F_0F_1-ATPase hydrolyses this ATP and thus pump protons in the reverse direction, thereby maintaining a proton gradient. This work confirmed that the Rho HUVEC had a mitochondrial membrane potential and that the maintenance of the membrane potential was entirely dependent on glycolysis in Rho 0 HUVEC. Treatment of both types of cells with 2-DOG lead to the inhibition of glycolysis and collapse of the membrane potential. However, pre-treating the cells with pyruvate, before adding 2-DOG, mitigated this effect in the WT cells, which were able to produce ATP using the pyruvate via aerobic respiration, but not the Rho 0 HUVEC. Inhibition of the membrane potential, which is reliant on glycolysis, by inhibitors of glycolysis has been directly demonstrated before (Scott and Nicholls 1980).

6.3 Resistance of Rho 0 HUVEC to stress-induced senescence

It was observed that HUVEC continuously subcultured in the presence of ethidium bromide, for more than 50 days, occasionally showed an erratic proliferative behaviour. Therefore it was not possible to reliably study replicative senescence in WT versus Rho 0 HUVEC. As a result of this observation replicative senescence with SA-β-gal staining in Rho 0 HUVEC was not studied, in order to avoid working with cells beyond the fifth passage. However, the growth curves in some of the initial cultures suggested that the cells have a reduced replicative capacity. Furthermore, under direct observation with light microscopy it was noticed that the Rho 0 HUVEC developed a senescent morphology at an earlier stage compared to WT cells of the same passage (as shown in figure 28). These observations suggest that Rho 0 HUVEC are more prone to replicative senescence. The only published work on senescence in Rho 0 cells has shown that SK-Hep1 Rho 0 cells (derived from a hepatoma cell line) are more prone to replicative senescence compared to WT cells (Park, Choi et al. 2004). In addition they noted the SK-Hep1 Rho 0 cells to have lower levels of telomerase. However, it must be borne in mind that the cells used in Park et al's work were SK-HEP-1 cells. SK-HEP-1 is an immortal human cell line derived from the ascitic fluid of a patient with adenocarcinoma of the liver (Heffelfinger, Hawkins et al. 1992). Immortalised cell lines usually have high levels of telomerase in order to maintain telomere length, a pre-requisite for immortalisation, and are highly resistant to senescence (Duncan, Wadhwa et al. 2000). Results from studies using immortal cells may not therefore always necessarily apply to normal cells. No work has been published looking at replicative senescence in primary, non-tumour derived, Rho 0 cells.

Conclusions and Discussion

An established model using *t*BHP to induce stress-induced senescence in HUVEC (Unterluggauer, Hampel et al. 2003) was used to study the propensity of Rho 0 HUVEC to undergo stress-induced senescence. This work demonstrated that Rho 0 HUVEC are significantly more resistant to stress-induced senescence compared to WT cells, as revealed by SA-β-gal staining (as shown in figures 27 and 29). These results were substantiated by FACS analysis looking for expression of ICAM, a marker associated with both senescence and endothelial dysfunction, as discussed in section 4.1.2. The IL-1β, which was used as the positive control, is known to induce both necrosis and apoptosis and had no effect on the Rho 0 cells in the experiments described in this work (Wang, Wang et al. 2005). No evidence was found in the literature to suggest that mitochondria are involved in IL-1β signalling, however this is a possibility. One possible explanation for the lack of effect of IL-1β on the Rho 0 cells is that they are resistant to apoptosis and that IL-1β is exerting most of its effects on WT HUVEC by inducing apoptosis. This phenomenon warrants further investigation in the future. The ICAM results presented in this work may provide a pathological link between stress-induced senescence observed in Rho 0 HUVEC culture and the endothelial dysfunction that occurs with atherosclerosis, which has also been shown to be associated with senescence. Whilst the finding of increased ICAM expression being associated with senescence is not new it is an important link if one is trying to establish a link between mitochondrial signalling as a potential cause of stress-induced senescence and ultimately atherosclerosis.

There are numerous ways by which *t*BHP has been shown to affect cells. The metabolism of *t*BHP directly leads to the formation of ROS (Ochi and Miyaura 1989), which can directly damage intracellular contents. It is known that *t*BHP

depletes intracellular glutathione levels (Bellomo, Jewell et al. 1982) and increases cytosolic Ca^{2+} levels (Bellomo, Thor et al. 1984). It has also been shown that *t*BHP causes collapse of the mitochondrial membrane potential leading to depletion of ATP and acidification of the cytosol (Masaki, Kyle et al. 1989). However, more recent research has shown that *t*BHP does not affect mitochondrial viability (Spector, Ma et al. 2002). It seems the most likely mechanism by which *t*BHP exerts its adverse affects on cells is by directly increasing ROS production and depleting glutathione levels, which can lead to either senescence or apoptosis.

From this work it can be seen that Rho 0 cells generate less ROS than WT cells and that the addition of *t*BHP generates far less of an increase in ROS production in Rho 0 than WT cells (as shown in figures 36 and 37). The most obvious explanation for the reduced ROS production in Rho 0 cells is that they can't generate mitochondrial ROS (mtROS) and are therefore able to mount less of an increase in ROS production in response to stimuli, such as *t*BHP. It may be that this inability to generate mtROS accounts for their resistance to stress-induced senescence.

Another explanation for the resistance Rho 0 cells to stress-induced senescence, following exposure to a stressor, is that the source or type of ROS produced and not the total burden of ROS *per se* that determine the cell's response and whether it enters a state of stress-induced senescence. It is therefore possible that mitochondrially-produced ROS play an essential role in defence-signalling, orchestrating a cells defensive response to stressors. There is now evidence accumulating that ROS produced by mitochondria play an essential role in

signalling in endothelial cells response to stressors (Quintero, Colombo et al. 2006). There is also evidence to suggest that acute insults lead to mitochondrial production of ROS which signal the upregulation of vascular NADPH oxidase and it is this activation of vascular NADPH oxidase that produces the ROS necessary for cell death (Lee, Bae et al. 2006). It seems that the role of mitochondrially-produced ROS in senescence signalling provides a highly plausible explanation for the Rho 0 HUVEC resistance to stress-induced senescence.

The experiments presented in this work suggest that the main source of non-mitochondrial ROS production in Rho 0 HUVEC is NADPH oxidase. This is demonstrated by the fact that DPI (an NADPH oxidase inhibitor) significantly reduces ROS generation in Rho 0 cells but does not significantly change it in WT cells (as shown in figure 38). NADPH oxidase is an important source of ROS in endothelial cells and has been implicated in endothelial dysfunction and a number of pathological processes (Ray and Shah 2005; Guzik and Harrison 2006). ROS are known to be a major cause of stress-induced senescence. This work supports the theory that it is the type of ROS, i.e. the mitochondrially produced ROS, which play a fundamental role in the signalling pathways leading to stress-induced senescence and not the total amount of ROS *per se*.

A final possible explanation or contributory mechanism for the Rho 0 cells reduced ROS production in response to *t*BHP is their increased anti-oxidant defence levels as shown in this work (this is discussed in section 6.5). This may also account for their resistance to stress-induced senescence. However, this does not explain why Rho 0 cells may be more prone to replicative senescence

(Park, Choi et al. 2004). It was not possible to study replicative senescence with EB generated Rho 0 HUVEC for reasons discussed earlier.

6.4 Resistance of Rho 0 HUVEC to apoptosis

The Rho 0 HUVEC were resistant to apoptosis induced by both staurosporine and *t*BHP, as measured by both caspase assay and FACS analysis (as shown in figures 32, 33 and 35). As alluded to in section 1.2.5.1.2 of the introduction there are two apoptotic pathways; the extrinsic or death receptor pathway and the intrinsic or stress-induced pathway. Mitochondria and cytochrome c are central to the functioning of the intrinsic pathway and as would be expected previous work has shown that Rho 0 cells are resistant to apoptosis caused by this pathway (discussed in section 1.4.4). Staurosporine, the treatment used to induce apoptosis in the work presented in this thesis, induces apoptosis by the intrinsic pathway (Feng and Kaplowitz 2002; Tesauro, Thompson et al. 2005). The mechanisms by which *t*BHP induces apoptosis are less well defined, however there is a strong weight of evidence to suggest it does so predominantly by the intrinsic pathway (Unterluggauer, Hampel et al. 2003). The work presented in this thesis showing Rho 0 HUVEC to be resistant to apoptosis supports the existing literature, demonstrating the central role of mitochondria in the intrinsic pathway of apoptosis. Studies using specific activators of the extrinsic pathway (e.g. agonistic anti-Fas monoclonal antibodies, which are known to induce apoptosis via the extrinsic pathway) were not felt to be directly relevant to this work. This is due to the fact that the extrinsic pathway can be activated and lead to apoptosis without any involvement of mitochondria in many cell types (Scaffidi, Fulda et al. 1998).

One of the technical problems with FACS analysis of the Rho 0 HUVEC is that the baseline fluorescence was higher than that of the WT cells as a result of the ethidium bromide in the cells. This is because both propidium iodide and ethidium bromide have similar excitation wavelengths and virtually identical emission wavelengths, both are usually measured with the same compensation channels (FL3 in this case). Non-staining Rho 0 cells therefore had a higher level of fluorescence in this channel than their WT controls. It was impossible to control for this and a successful genetic strategy for creating Rho 0 HUVEC would resolve this issue. In retrospect perhaps a choice of a different dye for DNA could have avoided these issues. However despite these limitations it was clear that the Rho 0 HUVEC were more resistant to apoptosis.

Although most of the evidence suggests Rho 0 cells are resistant to apoptosis there is some evidence that Rho 0 cells are able to undergo H_2O_2 induced apoptosis (Cardoso, Rego et al. 2004). More recent research investigating the resistance of Rho 0 cells to apoptosis has suggested that drug resistance may play a role (Ferraresi, Troiano et al. 2008). There is a possibility that cells may undergo caspase-independent apoptosis, although the physiological role of this is not fully understood (Adams and Cory 1998). Hence the importance of also studying apoptosis by FACS as the caspase assay would not be of any use in detecting caspase-independent apoptosis. It is interesting to note that a clear albeit non-significant rise in apoptosis was seen in Rho 0 HUVEC treated with staurosporine (as shown in figure 35), which is also known to cause caspase-independent apoptosis in addition to causing apoptosis by the intrinsic pathway (Belmokhtar, Hillion et al. 2001). This raises the possibility that the Rho 0 cells

were undergoing caspase-independent apoptosis, although further experimental investigation of this was beyond the scope of this work.

6.5 Antioxidant defences in Rho 0 HUVEC

It was found that the expression of MnSOD and catalase genes were both upregulated in Rho 0 HUVEC, whereas the expression of the γ-GCS was no different in Rho 0 compared to WT HUVEC (as shown in figure 41). These results were confirmed by corresponding changes in the expression of the relevant proteins (as shown in figures 42 and 43). For technical reasons it was not possible to do a western blot for catalase. Measurement of the ratio of GSH/GSSG showed this to be reduced in Rho 0 HUVEC suggesting the cells were under more oxidative stress in their basal state (as shown in figure 44), which could explain on the one hand the upregulation of some of the antioxidant defences and on the other why in the long term Rho 0 status leads to an increase in replicative senescence.

Another possible explanation for the reduced GSH/GSSG ratio in Rho 0 HUVEC could be that they are not able to produce sufficient NADPH to reduce GSSG back to GSH. The pentose phosphate pathway is the main source of NADPH from glucose 6-phosphate in normal cells. However in Rho 0 cells all glucose 6-phosphate is needed for glycolysis, which is their only source of ATP. It may be that Rho 0 cells either have a defect of the pentose phosphate pathway or that the Rho 0 cells cannot produce enough ‘spare’ glucose 6-phophate to allow this pathway to function. No evidence of work looking directly at the function of the pentose phosphate pathway in Rho 0 cells could be found in the literature.

Conclusions and Discussion

Upregulation of the antioxidant defences of Rho 0 HUVEC would provide an explanation for their resistance to stress-induced senescence. Upregulation of antioxidant defences has been previously been demonstrated in Rho 0 cells and is thought to contribute to their resistance to apoptosis (Park, Chang et al. 2004; Ferraresi, Troiano et al. 2008). One possible explanation for the resistance of Rho 0 HUVEC to stress-induced senescence (shown in section 4.1) could be that the cells have increased antioxidant defences, which directly counteract and reduce the damage from the oxidant stress by reducing ROS levels, as mentioned in section 6.3.

What is less clear is why Rho 0 cells, which are not able to produce ROS from aerobic respiration, would have upregulated antioxidant defences? Given that Rho 0 HUVEC produce less ROS than WT cells it would be expected that they have lower levels of antioxidant defences. The work presented in this thesis shows that NADPH oxidases appear to be the major source of ROS in Rho 0 compared to WT HUVEC. Furthermore, NADPH oxidases are a major source of oxygen consumption in Rho 0 HUVEC. These results suggest that NADPH oxidases are upregulated in Rho 0 HUVEC. This upregulation of NADPH oxidases, the major source of non-mitochondrial ROS, could be the cause of the upregulation of antioxidant defences shown in this work.

There is evidence to show that upregulation of MnSOD affords protection to cells against *t*BHP-induced apoptosis and that the levels of MnSOD proportionally afford this level of protection irrespective of the levels of other antioxidants and the redox status of the cell (Pias, Ekshyyan et al. 2003). The work presented in

this thesis would support this finding. This finding of increased MnSOD mRNA and protein expression in Rho 0 cells is well described (Park, Chang et al. 2004).

Heme-oxygenase-1 (HO-1) is well known to reduce oxidative stress; classically this involves the breakdown of heme to carbon monoxide (CO), biliverdin and free ferrous iron. Biliverdin is broken down to bilirubin, which is a ROS scavenger and can also directly downregulate NADPH oxidase (Forstermann 2008). This is supported by work showing that HO-$1^{-/-}$ mice have significantly decreased ability to withstand oxidative stress-induced injury compared to WT cells (Yet, Layne et al. 2003). The mechanisms signalling the upregulation of HO-1 by ROS are complex, not fully understood and detailed discussion of these is beyond the scope of this work. However, thiol redox–mediated modification of the cytoplasmic factor Keap1 and related alterations in the nuclear translocation of nuclear factor-erythroid 2-related factor-2 (Nrf2) could provide a general underlying mechanism for HO-1 regulation (Stocker and Perrella 2006).

In brief Nrf2 is a transcription factor that binds to the antioxidant responsive element (ARE), which in turn leads to the upregulation of antioxidant defences that include HO-1 (Yu, Chen et al. 2000). Keap1 is a protein that suppresses transcription of Nrf-2 and it has been suggested that it acts as a cellular sensor for oxidative stress. Oxidative stress causes Keap1 to release Nrf-2 allowing binding to the ARE and appropriate upregulation of antioxidant defences (Itoh, Wakabayashi et al. 1999). It may be that it is ROS produced specifically from NADPH oxidase, i.e. non-mitochondrially produced ROS, that signal upregulation of antioxidant defences in this way. This would explain why Rho 0 cells, which

have reduced overall levels of ROS but increased ROS from NADPH oxidase, have upregulated antioxidant defences.

Induction of HO-1 has been shown to protect cells from ROS-induced injury (Clark, Foresti et al. 2000). However, in addition to these classical effects Park et al's work (2004) suggested HO-1 is responsible for the upregulation of MnSOD in Rho 0 cells and that nuclear factor kappa-light-chain-enhancer of activated B cells (NF-κB) is not responsible for this effect. ARE are known to be present in the promoter of the MnSOD gene (Scandalios 2005), so it seems possible that the alternate mechanism is that activation of ARE induces both HO-1 and MnSOD upregulation at the same time. Various pro-oxidants have been shown to induce a rise in HO-1, which in addition to its classical antioxidant effects can cause the upregulation of various antioxidants including MnSOD and catalase (Applegate, Luscher et al. 1991; Frankel, Mehindate et al. 2000; Turkseven, Kruger et al. 2005). Upregulation of HO-1 in endothelial cells has been shown to confer them resistance against oxidative stress-induced injury (Yang, Quan et al. 1999).

It is also not clear why γ-GCS is not upregulated but other antioxidant defences are in Rho 0 HUVEC. Park et al showed that glutathione peroxidases (GPx), the enzymes responsible for the reduction of peroxide to water (as discussed in section 1.3), were upregulated in Rho 0 cells (Park, Chang et al. 2004). It does not necessarily follow that the γ-GCS levels were upregulated in these cells and it may be that γ-GCS levels are not regulated by HO-1, unlike GPx levels. One of the reasons why the GSH/GSSG ratio drops in Rho 0 HUVEC (shown in figure 44) could be that the pool of glutathione is static and an increase in ROS and/or

GPx levels leads to more reduced glutathione being oxidised dropping the ratio. Why the cells should fail to respond to this and not upregulate γ-GCS levels is not clear.

Finally the thioredoxin system (outlined in section 1.3) have been shown to play an important role in limiting oxidative stress by both direct antioxidant effects and protein signalling with key regulators of processes such as apoptosis in endothelial cells. In particular they have been shown to be important in the signalling of the extrinsic pathway of apoptosis. They have also been shown to play an important role in the regulation of GPx and MnSOD (Yamawaki, Haendeler et al. 2003). Study of this system was beyond the scope of this work but such studies may help further elucidate the findings in Rho 0 HUVEC.

Work by Quintero et al has demonstrated that HUVEC cultured in 3% oxygen have an increase in adenosine 5'-monophosphate (AMP)-dependent protein kinase (AMPK) activity levels that is due to ROS produced by mitochondria and independent of the cellular ATP:AMP ratio (Quintero, Colombo et al. 2006). AMPK is a key regulator of cellular energy and its activation causes increased glucose transport and activates glycolysis and fatty acid oxidation, while suppressing energy requiring processes such as the synthesis of fatty acids, cholesterol and protein. However, in addition to this well described role of AMPK recent work by Colombo et al suggests that AMPK also plays a key role in regulating the antioxidant status of HUVEC (Colombo and Moncada 2009). Colombo et al showed that there is a marked downregulation in the expression of the antioxidant levels (both mRNA and protein expression) of MnSOD, catalase, γ-GCS and thioredoxin in AMPK-silenced HUVEC cells cultured in 3% oxygen.

However, expression of other genes and their respective proteins, which are part of the cellular antioxidant defences, including glutathione transferase P1 (GSTP1), aldehyde dehydorgenase 1 (ALDHA1) and HO-1 were unaffected. Forkhead transcription factor 3a (Foxo3a), a transcription factor associated with expression of antioxidant genes was down regulated in AMPK-silenced HUVEC cells cultured in 3% oxygen. However, the expression of Nrf2 and NF-κB, both transcription factors implicated in the oxidative stress response, were unaffected. AMPK-silenced HUVEC cells cultured in 3% oxygen were able to generate more ROS than WT HUVEC and were more susceptible to *t*BHP-induced apoptosis.

The AMPK-silenced HUVEC cells cultured in 3% oxygen expressed less peroxisome-proliferator-activated receptor γ co-activator 1α (PGC1α), a major regulator of mitochondrial biosynthesis, and the cells correspondingly had less mitochondrial content (Colombo and Moncada 2009). It has been shown by another group that in neural cells activation of PGC1α, in addition to upregulating mitochondrial biosynthesis, also upregulates antioxidant defence levels (St-Pierre, Drori et al. 2006). PGC1α could be upregulated in Rho 0 cells, because they lack functional mitochondria and the cells are trying to compensate by producing more mitochondria, and as a result the antioxidant levels of the cells are upregulated.

In Rho 0 HUVEC it is possible that a bioenergetic crisis caused by lower levels of ATP activates AMPK, which in turn may cause upregulation of PGC1α, which would increase antioxidant defences. In their work Colombo et al have shown that AMPK, activated by mitochondrial ROS (mtROS) is a major regulator of antioxidant defences in HUVEC cultured in 3% oxygen. What role mtROS play in

regulation of AMPK and thus antioxidant levels in cells cultured in 21% oxygen has not yet been elucidated. Rho 0 HUVEC are unable to produce mtROS so will not be able to activate AMPK and therefore may not be able to regulate antioxidant defences in the usual manner. This inability of Rho 0 HUVEC to activate AMPK in cells cultured in 3% oxygen has been demonstrated by other members of our group (Quintero, Colombo et al. 2006). The inability of Rho 0 cells to activate AMPK via mtROS may explain why they do not have downregulated antioxidant defences in cells cultured at 3% oxygen and it may well be that the same system regulates antioxidant defences in Rho 0 cells cultured in 21% oxygen. So the higher antioxidant defences seen in Rho 0 HUVEC may be as a result of upregulation of PGC1α. Three mechanisms either alone or in combination could account for this effect: the classical pathway of PGC1α activation due to bioenergetic crisis, the activation of PGC1α by mtROS and/or the stimulus for mitochondriogenesis causing activation of PGC1α as a compensatory mechanism for the lack of functional mitochondria. The regulation of PGC1α activity is complex and beyond the scope of this discussion (Lin, Handschin et al. 2005).

The regulation of cellular antioxidant defences is complex and it may be that changes in the Nrf2-ARE pathway are responsible for the changes seen in the Rho 0 cells. This pathway is upregulated by ROS and leads to the upregulation of antioxidant defences (Nguyen, Nioi et al. 2009). It may well be that non-mitochondrial ROS are the main species responsible for activation of this pathway and thus antioxidant defences. There is good evidence that NADPH oxidase is responsible for the upregulation of the Nrf2-ARE pathway and thus antioxidant defences in cells (Sekhar, Crooks et al. 2003; Papaiahgari,

Kleeberger et al. 2004; Gao and Mann 2009). The work presented in this thesis supports the notion that NADPH oxidase is upregulated in Rho 0 cells. This could provide another plausible mechanism to explain the upregulation of antioxidant defences in Rho 0 HUVEC.

6.6 Potential implications of these findings with respect to ageing, cardiovascular disease and developing treatment for cardiovascular disease

In man mitochondrial DNA mutations are implicated in both ageing (Cortopassi and Arnheim 1990; Michikawa, Mazzucchelli et al. 1999) and resistance of cancer cells to apoptosis and senescence (Polyak, Li et al. 1998; Fliss, Usadel et al. 2000). From work with Rho 0 cells it has been suggested that changes in antioxidant defence mechanisms are responsible for some of these effects (Park, Chang et al. 2004).

As discussed in section 1.5.2 there is good evidence to support the association of mitochondrial dysfunction with ageing. Prior to starting this work there was no good animal model for the study of the role of mitochondrial dysfunction in ageing. However, in 2004 Trifunovic et al published the details of homozygous knock-in mice that express a proof-reading-deficient version of PolgA, the nucleus-encoded catalytic subunit of mtDNA polymerase. The knock-in mice were shown to have a reduced lifespan and all the phenotypic features of premature ageing (Trifunovic, Wredenberg et al. 2004).

Conclusions and Discussion

NADPH oxidase is an important source of ROS production in endothelial cells. A number of studies have shown that NADPH oxidase is upregulated in vascular disease and is a major source of ROS production (Cai and Harrison 2000; Ray and Shah 2005). Many risk factors for atherosclerosis have been shown to increase NADPH oxidase activity and thus ROS production (Cai and Harrison 2000; Ray and Shah 2005).

It has been shown that Angiotensin II (ATII) mediates endothelial dysfunction and promotes vascular inflammation and atherogenesis associated with vascular disease. More recently ATII has been shown to induce mitochondrial dysfunction and production of ROS by a mechanism that is dependent on NADPH oxidase. The mitochondrial ROS sets up a positive feedback loop leading to further NADPH oxidase produced ROS leading to worsening endothelial dysfunction (Doughan, Harrison et al. 2008). Rho 0 HUVEC would be a useful tool for the further elucidation of these mechanisms.

Two classes of drugs, which are used extensively in the treatment of cardiovascular disease and have been shown to reduce morbidity and mortality: angiotensin converting enzyme inhibitors (ACE inhibitors) (Yusuf, Sleight et al. 2000; Fox 2003) and hydroxy methylglutaryl coenzyme A (HMG-CoA) reductase inhibitors, commonly referred to as statins (4S-investigators 1994; Shepherd, Cobbe et al. 1995). The primary mechanism of action of ACE inhibitors is reduction of blood pressure by blocking ACE thus counteracting the effects of angiotensin. However, ACE inhibitors have been shown to be beneficial in improving endothelial function due to effects not attributable to blood pressure lowering (Klingbeil, John et al. 2003). It is thought one of the main mechanisms

for this additional effect of ACE inhibitors is their prevention of the activation of NADPH oxidase (Warnholtz, Nickenig et al. 1999). Antiotensin receptor blockers (ARBs), which work on the same pathway as ACE inhibitors by blocking the angiotensin receptor, have been shown in clinical trials to have the same clinical benefits as ACE inhibitors in terms of reduction of cardiovascular morbidity and mortality. There is evidence that both ACE inhibitors and antiotensin receptor blockers (ARBs) reduce age and vascular disease-related mitochondrial dysfunction (de Cavanagh, Piotrkowski et al. 2003; Monteiro, Duarte et al. 2005; de Cavanagh, Toblli et al. 2006). Likewise statins have also been shown to have pleiotropic beneficial effects beyond those attributable to lipid lowering, one of which is downregulation of NADPH oxidase (Liao 2002). Therefore it is plausible that inhibition of NADPH oxidase by these drugs could be partly responsible for the reduction in the burden of vascular disease. This outlines the importance of NADPH oxidase as a mediator of damage in endothelial cells and potential therapeutic target. Rho 0 HUVEC cannot produce mitochondrial ROS, therefore will be a useful tool for the further elucidation of the role of non-mitochondrial ROS production in apoptosis, senescence and cell death of endothelial cells. This may lead to the identification of other new drug targets for the treatment of cardiovascular disease.

Given the protective effects of the drugs described above and the knowledge that ROS are involved in senescence, apoptosis, ageing and cardiovascular disease, antioxidant therapy would seem to be a promising avenue for treatment in cardiovascular disease. There is evidence that vitamin C is protective at a cellular level (Heller, Unbehaun et al. 2001), restores endothelial dysfunction in a mouse model of endothelial dysfunction (Matsumoto, D'Uscio L et al. 2003) and is

beneficial in small studies of patients (Heitzer, Schlinzig et al. 2001). Similar evidence for the protective effects of vitamin E against endothelial dysfunction also exists (Verlangieri and Bush 1992; Skyrme-Jones, O'Brien et al. 2000). It is therefore surprising that large-scale trials of the antioxidants vitamin C and vitamin E have not shown them to reduce cardiovascular morbidity or mortality (Heart-Protection-Study-Collaborative-Group 2002; Paolini, Sapone et al. 2003; Lonn, Bosch et al. 2005). However, these trials were poorly conducted using surrogate endpoints with no measure of the antioxidants efficacy in these patients. This is analogous to running a trial looking at a new blood pressure lowering agent, not measuring the blood pressure of subjects and drawing conclusions on the ability of the drug to reduce cardiovascular mortality and morbidity without knowing whether it reduced blood pressure and if so by how much. It is therefore likely that further carefully planned trials of antioxidant strategies in patients with cardiovascular disease are a promising avenue for therapy.

One such agent that merits further investigation is NAC. This work clearly demonstrated that treatment of HUVEC with NAC almost abolishes ROS production in both WT and Rho 0 HUVEC (as shown in figures 36 and 37). This implies that it is a highly effective scavenger of both mitochondrially-produced and non-mitochondrially-produced ROS. As well as its direct antioxidant properties and ability to increase intracellular GSH levels it has been shown to have a number of other effects in vascular endothelial cells including the reduction of intracellular adhesion molecules associated with inflammation, such as ICAM-1 (Zafarullah, Li et al. 2003). It has been shown in a HUVEC model of oxidative-stress that pre-treatment with NAC ameliorates these effects and is

associated with a decrease in ICAM-1 expression (Wagener, da Silva et al. 1999). There is a growing amount of evidence that NAC reduces endothelial cell dysfunction caused by risk factors for atherosclerosis, improves endothelial function and may attenuate vascular inflammatory disease (atherosclerosis) by antagonizing the effects of intracellular ROS generation (Zafarullah, Li et al. 2003). NAC has been shown to be beneficial in animal models of vascular disease (Mass, Pirazzi et al. 1995; Cabassi, Dumont et al. 2001). Finally there are small trials of NAC in humans suggesting it may improve endothelial function in patients with vascular disease (De Mattia, Bravi et al. 1998; Andrews, Prasad et al. 2001). Thus NAC is potentially a promising agent for the treatment of vascular disease.

6.7 Use of dnDNA POLG to create Rho 0 cells

The problem of this work with the ethidium bromide model is that it is a known mutagen. Although it is said not to affect genomic DNA at the doses used in this work (as discussed in section 1.4.2) occasional erratic proliferative behaviour was noted in long term culture with low dose ethidium bromide, which could be due to genomic DNA mutations as discussed in section 6.1.

Therefore dnDNA POLG, with exactly the same mutation as reported in Jazayeri's paper (Jazayeri, Andreyev et al. 2003), was made. One of the most time consuming stages of this work was the optimisation of the subcloning strategy to create the pBABE-dnDNA POLG plasmid. This process involved designing a ligation strategy and refining the various steps until the correct product was obtained. Ultimately a 'blunt end' ligation strategy proved the best for

our needs. However, we initially opted for a 'sticky end' ligation strategy because it is technically far easier to do resulting in a higher ligation rate. Treatment of the vector with Antarctic phosphatase proved essential to stop it self-ligating before addition of the insert. Double digestion of the insert to minimise contamination and use of T4 polynucleotide kinase to phosphorylate both end of the insert proved to be essential steps in the treatment of the insert to ensure the final ligation reaction was successful.

The initial attempts to transfect both HUVEC and HEK-293 (as reported in their original paper) using both replication incompetent retroviral plasmids and liposomes did not work. The plasmid was clearly taken up by the cells as evidenced by their puromycin resistance. The strategy did not even work when trying to transfect HEK-293 (i.e. confirm Jazayeri's findings), although the plasmid was clearly taken up and expressed by the cells as evidenced by their puromycin resistance. The simplest and first explanation addressed in this thesis was that the plasmid did not have a sufficiently powerful promoter to allow expression of the dnDNA POLG to a high enough level to produce the Rho 0 phenotype. The other possible explanation could be that the cells are developing resistance to the puromycin. The pcDNA™4/TO commercial vector used by Jazayeri et al contained a 726 bp CMV promoter (Invitrogen 2008). The final alternative plasmid produced, described in section 5.7 of the results, contained a 615 bp CMV promoter and was slightly smaller in size than the first plasmid used, described in section 5.4.2 of the results.

Using this alternative plasmid it was possible to successfully transfect HEK-293 cells with the plasmid and respirometry confirmed that they had a Rho 0

phenotype. This confirmed that the dnDNA POLG was expressed sufficiently using the CMV promoter, which significantly enhances gene expression in plasmids (Foecking and Hofstetter 1986).

Due to time constraints it was not possible to go on and produce a retrovirus and transfect HUVEC with the plasmid. Given time one would have wanted to produce a retrovirus, in the same way described in section 5.5 of the results, and to have optimized the protocol for infecting HUVEC with this virus to see if a Rho 0 phenotype was produced using respirometry to confirm this.

6.8 General conclusions

As discussed in section 1.6.5 it must be borne in mind that endothelial cells are a heterogeneous population of cells and that not all work done with HUVEC can necessarily be generalised to all endothelial cells. Bearing this in mind, the use of HUVEC seems to be the best practical method for studying the biology of endothelial cells in a cell culture system.

The findings presented in this thesis are consistent with the published literature that there is a spectrum of mitochondrial function ranging from no mitochondrial function to normal mitochondrial function through to dysfunctional mitochondria. At one end of the spectrum cells lacking functional mitochondria (Rho 0 cells) produce less ROS and are resistant to stress-induced senescence and at the other end of the spectrum dysfunctional mitochondria produce more ROS and cells are more prone to stress-induced senescence.

One possible explanation for these findings is that the main role of ROS produced by mitochondria (mtROS) is signalling and that mtROS orchestrate the endothelial cell's defence mechanisms, both in terms of deciding a cell's fate when exposed to stressors and regulation of antioxidant defences. It may be that a basal production of ROS is necessary to maintain the endothelial cells redox state. In the absence of mtROS then NADPH oxidase is upregulated, which in turn leads to the upregulation of certain antioxidant defences. However, although the Rho 0 cells have an increased amount of NADPH oxidase it is the ROS produced by mitochondria that determine the cells defence response to external stressors. Therefore Rho 0 cells are resistant to stress-induced senescence

because the signalling pathways, involving mtROS that orchestrate a cell's response to external stressors are unable to function in the usual manner. Thus cells produce mtROS, which are produced by mitochondria and are important in maintaining cells basal redox state and signalling the cell's response to external stressors. In contrast the cell also produces non-mtROS, which are those produced by non-mitochondrial mechanisms such as NADPH oxidase in response to external stressors. Non-mtROS also play a role in control of antioxidant defences, by mechanisms including the Nrf2-ARE pathway, but can damage the cell irreversibly if not opposed.

Thus a possible model to explain these findings is that in WT endothelial cells external stressors lead to an increase in non-mtROS, which in turn increases antioxidant defence mechanisms via the Nrf2-ARE pathway, and that these non-mtROS have a positive feedback effect on mtROS production by the mitochondria. This positive feedback leads to an increase in mtROS production. Antioxidant defences are also upregulated in response to activation of AMPK by mtROS and PGC1α activated by either AMPK or by other means discussed earlier. External stressors may also directly increase mtROS production by the mitochondria. When the levels of mtROS reach a critical point, at which the cells upregulated antioxidant defences are unable to cope, the cell is triggered to enter either a state of senescence or apoptosis to protect it from further damage.

Removal of mtROS production by creating Rho 0 cells means that potential damage by external stressors is now unchecked as the cells can no longer utilise their normal defence mechanisms. So whilst they are resistant to stress-induced senescence and apoptosis in the short term they are not protected from the long

term cumulative potentially harmful effects of stressors. This would explain the observations in this thesis that Rho 0 cells have a reduced replicative capacity and on occasions proliferate in an abnormal way. This proposed model for the orchestration of endothelial cell defences in WT cells is shown as a diagram in the next figure.

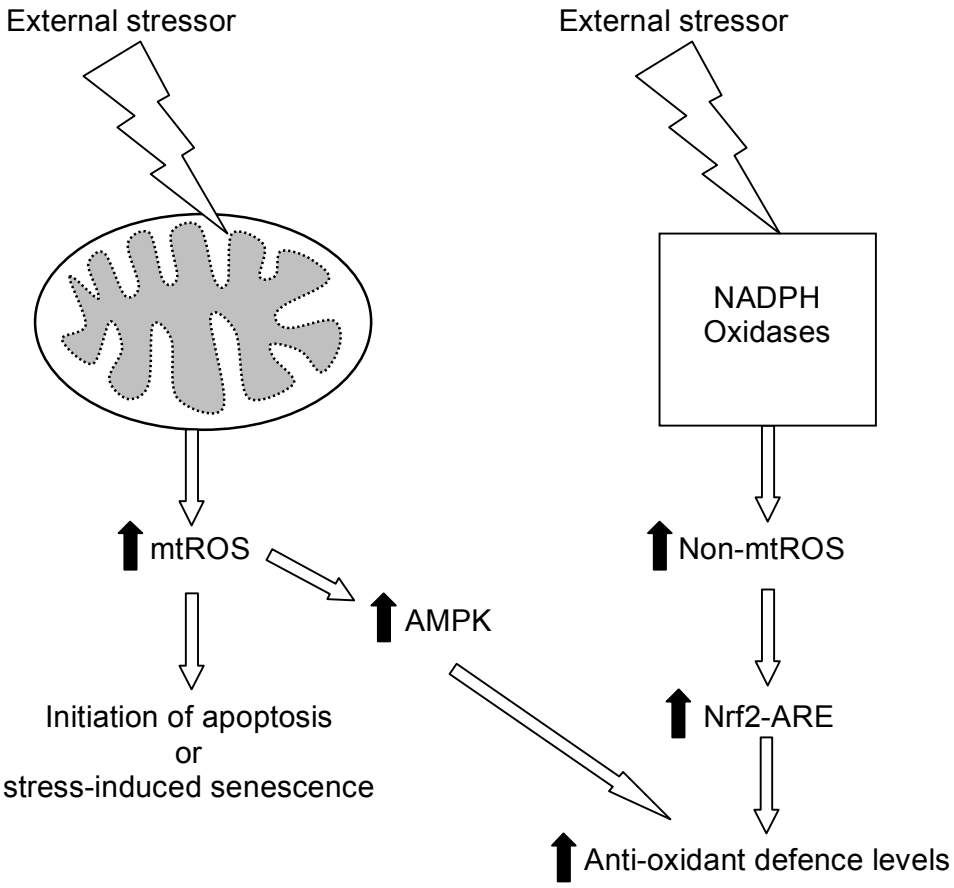

Figure 65 shows the model for the potential role of mtROS in endothelial cell defence to external stressors.

This model explains the experimental findings, as presented in this thesis, that Rho 0 HUVEC: produce less ROS but have increased antioxidant defences, have upregulated NADPH oxidase and are resistant to stress-induced senescence.

Conclusions and Discussion

Rho 0 HUVEC are a powerful tool for the further elucidation and understanding of the complex mechanisms involved in cell defence systems and their responses to stressors. Further elucidation of these mechanisms may reveal more specific targets for the treatment and prevention of cardiovascular disease.

7 Future investigations

7.1 Generation of Rho 0 cells using dnDNA POLG plasmid

It will be important to develop a successful method for transfecting HUVEC with the pBABE dnDNA POLG plasmid that was created. The first approaches would be to try the methods originally used with the first plasmid in HUVEC, as described in section 5.5 of the results. This system could then be characterised in the same way that the Rho 0 status of HUVEC created using the ethidium bromide model was done, by repeating the experiments described in chapter 3 of this thesis. Once a successful model for generating Rho 0 HUVEC using the dnDNA POLG method has been established it would provide a powerful tool for further study of the role of mitochondria in senescence in these cells and the role they play in endothelial cell defence mechanisms.

In the unlikely event that this strategy was not successful then alternative mutations could be investigated. Alternatively a strategy using small interfering RNA (siRNA), which are small 20-25 bp molecules of double stranded RNA that interfere with a specific gene could be tried. These were first described in animals by Andrew Fire and Craig Melloe in 1998 (Fire, Xu et al. 1998). They can be synthesised and artificially introduced into cells to knockdown the expression of genes of interest.

7.2 Further studies on Rho 0 HUVEC

Ideally all this work should be done using Rho 0 HUVEC created using the dnDNA POLG model but in the interim studies could be done using the ethidium bromide model, allowing for the shortcomings of this model.

All the experiments described in chapter 4 could be repeated using a successful genetic model for producing Rho 0 HUVEC. An attempt should then be made to finish characterisation of all antioxidant defences in the Rho 0 cells. In particular catalase protein levels would be studied with the appropriate antibody. It would be important to study HO-1 gene expression and protein levels in light of previous findings as discussed in section 6.5. Furthermore the study of Nrf2, Keap1 and the ARE system would help elucidate the mechanisms in light of these findings. Both gene and protein expression of antioxidant defences in response to treatment with *t*BHP would be studied. In view of the putative role of AMPK in the orchestration of antioxidant defences in endothelial cells, as discussed in section 6.5, it would be important to fully study AMPK activation in Rho 0 cells. It would be interesting to look at the role of mtROS in the activation of AMPK in cells grown in 21% oxygen to see if they act in the same way as they have shown to in 3% oxygen. Studies looking at activation and levels of PGC1α would also be important in characterising these cells antioxidant defence control. Further investigation into the interaction of NO with complex IV and its role in signalling and coordinating endothelial cells defences will also be important.

An alternative method of measuring GSH and GSSG described by Vergani et al (Vergani, Floreani et al. 2004) is more precise than the one used in this work and

would be utilised to confirm the existing results. If the GSH/GSSG ratio is confirmed to be reduced in future work it would be important to perform further experiments to confirm whether this is a true reflection of increased antioxidant defences, due to increased stress or both. Alternatively the reduced ratio could be due to the cells inability to reduce GSSG back to GSH as a result of insufficient NADPH, if this were the case it would be important to ascertain whether this is due to a problem with the pentose phosphate pathway.

Further studies to fully characterise the non-mitochondrial sources of ROS production would be important. In particular studies to characterise the isoforms of NOX present in HUVEC and their relative contribution to ROS production would be important. Once the major isoforms of NOX known to be active in HUVEC were known then the proposed model could be tested experimentally. This could initially be done using pharmacological stimulators or inhibitors of NOX and therefore non-mtROS. However, ideally genetic approaches would be used to manipulate levels of NOX and thus non-mtROS. In WT HUVEC it would be expected that up-regulation, or pharmacological stimulation, of NOX would lead to an increased amount of stress-induced senescence for a given dose of a stressor (such as *t*BHP) and down-regulation, or pharmacological inhibition, of NOX would lead to increased resistance to stress-induced senescence. In Rho 0 HUVEC changes in NOX produced ROS would not be expected to change the cells resistance or susceptibility to stress-induced senescence although it may increase antioxidant defence levels, as discussed in section 6.8. Although NOX has been shown to be the major source of non-mtROS in endothelial cells it would be important to confirm this by studying the relative contribution of xanthine oxidase and eNOS in the same manner.

Future investigations

It would be interesting to see if BSO, which is known to deplete glutathione and has been shown to increase ROS production in WT but not Rho 0 HUVEC, induces stress-induced senescence in WT but not Rho 0 HUVEC. It will also be important to look at the effect of antioxidants on the prevention of stress-induced senescence. Further work should look at levels of p16 and p14ARF (alternate reading frame), both cell cycle regulators that have been shown to be markers of senescence (Krishnamurthy, Torrice et al. 2004).

Using Rho 0 cells created by genetic means it would be interesting to study replicative senescence in Rho 0 HUVEC, by passaging them until they become senescent to see if they are more or less prone to replicative senescence compared to wild type cells. A genetic model of Rho 0 HUVEC would avoid the potential mutagenic problems of long term exposure of cells to low dose ethidium bromide, which could be a confounding factor in any such experiments. Given that telomere length has been shown to play a crucial role in replicative senescence it would be important to study telomere length, as well as other telomere dynamics such as the single stranded telomere overhang length (measured with the T-OLA assay) and telomerase levels.

8 References

4S-investigators (1994). "Randomised trial of cholesterol lowering in 4444 patients with coronary heart disease: the Scandinavian Simvastatin Survival Study (4S)." Lancet **344**(8934): 1383-9.

Adams, J. M. and S. Cory (1998). "The Bcl-2 protein family: arbiters of cell survival." Science **281**(5381): 1322-6.

Ahluwalia, A., P. Foster, et al. (2004). "Antiinflammatory activity of soluble guanylate cyclase: cGMP-dependent down-regulation of P-selectin expression and leukocyte recruitment." Proc Natl Acad Sci USA **101**(5): 1386-91.

Andrews, N. P., A. Prasad, et al. (2001). "N-acetylcysteine improves coronary and peripheral vascular function." J Am Coll Cardiol **37**(1): 117-23.

Appleby, R. D., W. K. Porteous, et al. (1999). "Quantitation and origin of the mitochondrial membrane potential in human cells lacking mitochondrial DNA." Eur J Biochem **262**(1): 108-16.

Applegate, L. A., P. Luscher, et al. (1991). "Induction of heme oxygenase: a general response to oxidant stress in cultured mammalian cells." Cancer Res **51**(3): 974-8.

Armand, R., J. Y. Channon, et al. (2004). "The effects of ethidium bromide induced loss of mitochondrial DNA on mitochondrial phenotype and ultrastructure

in a human leukemia T-cell line (MOLT-4 cells)." Toxicol Appl Pharmacol **196**(1): 68-79.

Aruoma, O. I., B. Halliwell, et al. (1989). "The antioxidant action of N-acetylcysteine: its reaction with hydrogen peroxide, hydroxyl radical, superoxide, and hypochlorous acid." Free Radic Biol Med **6**(6): 593-7.

Aviram, M., M. Rosenblat, et al. (1998). "Paraoxonase inhibits high-density lipoprotein oxidation and preserves its functions. A possible peroxidative role for paraoxonase." J Clin Invest **101**(8): 1581-90.

Azzolin, L., S. von Stockum, et al. (2010). "The mitochondrial permeability transition from yeast to mammals." FEBS Lett **584**(12): 2504-9.

Barja, G. (1999). "Mitochondrial oxygen radical generation and leak: sites of production in states 4 and 3, organ specificity, and relation to aging and longevity." J Bioenerg Biomembr **31**(4): 347-66.

Barja, G. and A. Herrero (2000). "Oxidative damage to mitochondrial DNA is inversely related to maximum life span in the heart and brain of mammals." Faseb J **14**(2): 312-8.

Beckman, K. B. and B. N. Ames (1998). "The free radical theory of aging matures." Physiol Rev **78**(2): 547-81.

Bellomo, G., S. A. Jewell, et al. (1982). "Regulation of intracellular calcium compartmentation: studies with isolated hepatocytes and t-butyl hydroperoxide." Proc Natl Acad Sci USA **79**(22): 6842-6.

Bellomo, G., H. Thor, et al. (1984). "Increase in cytosolic Ca2+ concentration during t-butyl hydroperoxide metabolism by isolated hepatocytes involves NADPH oxidation and mobilization of intracellular Ca2+ stores." FEBS Lett **168**(1): 38-42.

Belmokhtar, C. A., J. Hillion, et al. (2001). "Staurosporine induces apoptosis through both caspase-dependent and caspase-independent mechanisms." Oncogene **20**(26): 3354-62.

Bennett, M. R., K. Macdonald, et al. (1998). "Cooperative interactions between RB and p53 regulate cell proliferation, cell senescence, and apoptosis in human vascular smooth muscle cells from atherosclerotic plaques." Circ Res **82**(6): 704-12.

Berge, U., J. Behrens, et al. (2007). "Sugar-induced premature aging and altered differentiation in human epidermal keratinocytes." Ann N Y Acad Sci **1100**: 524-9.

Bkaily, G., P. Pothier, et al. (1997). "The use of confocal microscopy in the investigation of cell structure and function in the heart, vascular endothelium and smooth muscle cells." Mol Cell Biochem **172**(1-2): 171-94.

Blackburn, E. H. (2000). "Telomere states and cell fates." Nature **408**(6808): 53-6.

Blanc, H., B. Dujon, et al. (1978). "Detection of specific DNA sequences in yeast by colony hybridization." Mol Gen Genet **161**(3): 311-5.

Blankenberg, F. G., P. D. Katsikis, et al. (1998). "In vivo detection and imaging of phosphatidylserine expression during programmed cell death." Proc Natl Acad Sci USA **95**(11): 6349-54.

Blasco, M. A. (2005). "Telomeres and human disease: ageing, cancer and beyond." Nat Rev Genet **6**(8): 611-22.

Boveris, A. and B. Chance (1973). "The mitochondrial generation of hydrogen peroxide. General properties and effect of hyperbaric oxygen." Biochem J **134**(3): 707-16.

Brand, M. D., C. Affourtit, et al. (2004). "Mitochondrial superoxide: production, biological effects, and activation of uncoupling proteins." Free Radic Biol Med **37**(6): 755-67.

Brandes, R. P., I. Fleming, et al. (2005). "Endothelial aging." Cardiovasc Res **66**(2): 286-94.

Brandt, R. and A. S. Keston (1965). "Synthesis of Diacetyldichlorofluorescin: A Stable Reagent for Fluorometric Analysis." Anal Biochem **11**: 6-9.

Bredt, D. S. (1999). "Endogenous nitric oxide synthesis: biological functions and pathophysiology." Free Radic Res **31**(6): 577-96.

Brown, J. R. and W. F. Doolittle (1997). "Archaea and the prokaryote-to-eukaryote transition." Microbiol Mol Biol Rev **61**(4): 456-502.

Brune, B. (2003). "Nitric oxide: NO apoptosis or turning it ON?" Cell Death Differ **10**(8): 864-9.

Buchet, K. and C. Godinot (1998). "Functional F1-ATPase essential in maintaining growth and membrane potential of human mitochondrial DNA-depleted rho degrees cells." J Biol Chem **273**(36): 22983-9.

Buchner, T., W. Dittrich, et al. (1971). "[Impulse cytophotometry of blood cells and bone marrow cells]." Verh Dtsch Ges Inn Med **77**: 416-8.

Cabassi, A., E. C. Dumont, et al. (2001). "Effects of chronic N-acetylcysteine treatment on the actions of peroxynitrite on aortic vascular reactivity in hypertensive rats." J Hypertens **19**(7): 1233-44.

Cai, H. and D. G. Harrison (2000). "Endothelial dysfunction in cardiovascular diseases: the role of oxidant stress." Circ Res **87**(10): 840-4.

Cai, J., D. C. Wallace, et al. (2000). "Separation of cytochrome c-dependent caspase activation from thiol-disulfide redox change in cells lacking mitochondrial DNA." Free Radic Biol Med **29**(3-4): 334-42.

Campisi, J. (2001). "From cells to organisms: can we learn about aging from cells in culture?" Experimental Gerontology **36**(4-6): 607-618.

Cao, C., S. Lu, et al. (2008). "SIRT1 confers protection against UVB- and H(2)O(2)-induced cell death via modulation of p53 and JNK in cultured skin keratinocytes." J Cell Mol Med **13**(9B):3632-43.

Cardoso, S. M., A. C. Rego, et al. (2004). "Apoptotic cell death induced by hydrogen peroxide in NT2 parental and mitochondrial DNA depleted cells." Neurochem Int **45**(5): 693-8.

Chandel, N. S., D. S. McClintock, et al. (2000). "Reactive oxygen species generated at mitochondrial complex III stabilize hypoxia-inducible factor-1alpha during hypoxia: a mechanism of O2 sensing." J Biol Chem **275**(33): 25130-8.

Chen, Q. and B. N. Ames (1994). "Senescence-like growth arrest induced by hydrogen peroxide in human diploid fibroblast F65 cells." Proc Natl Acad Sci USA **91**(10): 4130-4.

Chen, S. C. and C. H. Chen (1982). "Vascular endothelial cell effectors in fetal calf retina, vitreous, and serum." Invest Ophthalmol Vis Sci **23**(3): 340-50.

Chiaratti, M. R. and F. V. Meirelles (2006). "Increase in mitochondrial DNA quantity and impairment of oxidative phosphorylation in bovine fibroblast cells treated with ethidium bromide for 15 passages in culture." Genet Mol Res **5**(1): 55-62.

Cines, D. B., E. S. Pollak, et al. (1998). "Endothelial cells in physiology and in the pathophysiology of vascular disorders." Blood **91**(10): 3527-61.

Clark, J. E., R. Foresti, et al. (2000). "Dynamics of haem oxygenase-1 expression and bilirubin production in cellular protection against oxidative stress." Biochem J **348 Pt 3**: 615-9.

Clark, L. C., Jr., R. Wolf, et al. (1953). "Continuous recording of blood oxygen tensions by polarography." J Appl Physiol **6**(3): 189-93.

Clemmons, D. R., W. L. Isley, et al. (1983). "Dialyzable factor in human serum of platelet origin stimulates endothelial cell replication and growth." Proc Natl Acad Sci USA **80**(6): 1641-5.

Collins, K. and J. R. Mitchell (2002). "Telomerase in the human organism." Oncogene **21**(4): 564-79.

Colombo, S. L. and S. Moncada (2009). "AMPKalpha1 regulates the antioxidant status of vascular endothelial cells." Biochem J **421**(2): 163-9.

Cortopassi, G. A. and N. Arnheim (1990). "Detection of a specific mitochondrial DNA deletion in tissues of older humans." Nucleic Acids Res **18**(23): 6927-33.

Cummins, J. (1998). "Mitochondrial DNA in mammalian reproduction." Rev Reprod **3**(3): 172-82.

Dalby, B., S. Cates, et al. (2004). "Advanced transfection with Lipofectamine 2000 reagent: primary neurons, siRNA, and high-throughput applications." Methods **33**(2): 95-103.

Davies, K. J. (1995). "Oxidative stress: the paradox of aerobic life." Biochem Soc Symp **61**: 1-31.

Davis, H. E., M. Rosinski, et al. (2004). "Charged polymers modulate retrovirus transduction via membrane charge neutralization and virus aggregation." Biophys J **86**(2): 1234-42.

de Cavanagh, E. M., B. Piotrkowski, et al. (2003). "Enalapril and losartan attenuate mitochondrial dysfunction in aged rats." Faseb J **17**(9): 1096-8.

de Cavanagh, E. M., J. E. Toblli, et al. (2006). "Renal mitochondrial dysfunction in spontaneously hypertensive rats is attenuated by losartan but not by amlodipine." Am J Physiol Regul Integr Comp Physiol **290**(6): R1616-25.

De Mattia, G., M. C. Bravi, et al. (1998). "Reduction of oxidative stress by oral N-acetyl-L-cysteine treatment decreases plasma soluble vascular cell adhesion molecule-1 concentrations in non-obese, non-dyslipidaemic, normotensive, patients with non-insulin-dependent diabetes." Diabetologia **41**(11): 1392-6.

DeFrancesco, L., I. E. Scheffler, et al. (1976). "A respiration-deficient Chinese hamster cell line with a defect in NADH-coenzyme Q reductase." J Biol Chem **251**(15): 4588-95.

Denis, M. (1986). "Structure and function of cytochrome-c oxidase." Biochimie **68**(3): 459-70.

Denninger, J. W. and M. A. Marletta (1999). "Guanylate cyclase and the .NO/cGMP signaling pathway." Biochim Biophys Acta **1411**(2-3): 334-50.

Desjardins, P., E. Frost, et al. (1985). "Ethidium bromide-induced loss of mitochondrial DNA from primary chicken embryo fibroblasts." Mol Cell Biol **5**(5): 1163-9.

DiMauro, S. and E. A. Schon (2003). "Mitochondrial respiratory-chain diseases." N Engl J Med **348**(26): 2656-68.

Dimri, G. P., X. Lee, et al. (1995). "A biomarker that identifies senescent human cells in culture and in aging skin in vivo." Proc Natl Acad Sci USA **92**(20): 9363-7.

Dittrich, W. and W. Gohde (1969). "[Impulse fluorometry of single cells in suspension]." Z Naturforsch B **24**(3): 360-1.

Doughan, A. K., D. G. Harrison, et al. (2008). "Molecular mechanisms of angiotensin II-mediated mitochondrial dysfunction: linking mitochondrial oxidative damage and vascular endothelial dysfunction." Circ Res **102**(4): 488-96.

Drobinskaya, I. E., I. A. Kozlov, et al. (1978). "ATP-induced inhibition of mitochondrial ATPase by oligomycin." FEBS Lett **96**(1): 111-4.

Dumont, P., M. Burton, et al. (2000). "Induction of replicative senescence biomarkers by sublethal oxidative stresses in normal human fibroblast." Free Radic Biol Med **28**(3): 361-73.

Duncan, E. L., R. Wadhwa, et al. (2000). "Senescence and immortalization of human cells." Biogerontology **1**(2): 103-21.

Erusalimsky, J. D. and D. J. Kurz (2005). "Cellular senescence in vivo: Its relevance in ageing and cardiovascular disease." Exp Gerontol **40**(8-9):634-42.

Erusalimsky, J. D. and S. Moncada (2007). "Nitric oxide and mitochondrial signaling: from physiology to pathophysiology." Arterioscler Thromb Vasc Biol **27**(12): 2524-31.

Fadeel, B. and S. Orrenius (2005). "Apoptosis: a basic biological phenomenon with wide-ranging implications in human disease." J Intern Med **258**(6): 479-517.

Felgner, P. L., T. R. Gadek, et al. (1987). "Lipofection: a highly efficient, lipid-mediated DNA-transfection procedure." Proc Natl Acad Sci USA **84**(21): 7413-7.

Feng, G. and N. Kaplowitz (2002). "Mechanism of staurosporine-induced apoptosis in murine hepatocytes." Am J Physiol Gastrointest Liver Physiol **282**(5): G825-34.

Fenton, M., S. Barker, et al. (2001). "Cellular senescence after single and repeated balloon catheter denudations of rabbit carotid arteries." Arterioscler Thromb Vasc Biol **21**(2): 220-6.

Fenton, M., H. L. Huang, et al. (2004). "Early atherogenesis in senescence-accelerated mice." Exp Gerontol **39**(1): 115-22.

Ferraresi, R., L. Troiano, et al. (2008). "Resistance of mtDNA-depleted cells to apoptosis." Cytometry A **73**(6): 528-37.

Fire, A., S. Xu, et al. (1998). "Potent and specific genetic interference by double-stranded RNA in Caenorhabditis elegans." Nature **391**(6669): 806-11.

Fiske, C. H. and Y. SubbaRow (1929). "Phosphorous compounds of liver and muscle." Science **70**: 381-2.

Fliss, M. S., H. Usadel, et al. (2000). "Facile detection of mitochondrial DNA mutations in tumors and bodily fluids." Science **287**(5460): 2017-9.

Florey (1966). "The endothelial cell." Br Med J **2**(5512): 487-90.

Foecking, M. K. and H. Hofstetter (1986). "Powerful and versatile enhancer-promoter unit for mammalian expression vectors." Gene **45**(1): 101-5.

Forstermann, U. (2008). "Oxidative stress in vascular disease: causes, defense mechanisms and potential therapies." Nat Clin Pract Cardiovasc Med **5**(6): 338-49.

Fox, K. M. (2003). "Efficacy of perindopril in reduction of cardiovascular events among patients with stable coronary artery disease: randomised, double-blind, placebo-controlled, multicentre trial (the EUROPA study)." Lancet **362**(9386): 782-8.

Frankel, D., K. Mehindate, et al. (2000). "Role of heme oxygenase-1 in the regulation of manganese superoxide dismutase gene expression in oxidatively-challenged astroglia." J Cell Physiol **185**(1): 80-6.

Galkin, A. and S. Moncada (2007). "S-nitrosation of mitochondrial complex I depends on its structural conformation." J Biol Chem **282**(52): 37448-53.

Galustian, C., J. Dye, et al. (1995). "Actin cytoskeletal isoforms in human endothelial cells in vitro: alteration with cell passage." In Vitro Cell Dev Biol Anim **31**(10): 796-802.

Gao, L. and G. E. Mann (2009). "Vascular NAD(P)H oxidase activation in diabetes: a double-edged sword in redox signalling." Cardiovasc Res **82**(1): 9-20.

Garcia-Calvo, M., E. P. Peterson, et al. (1999). "Purification and catalytic properties of human caspase family members." Cell Death Differ **6**(4): 362-9.

Gerschenson, L. E. and R. J. Rotello (1992). "Apoptosis: a different type of cell death." Faseb J **6**(7): 2450-5.

Gifford, S. M., M. A. Grummer, et al. (2004). "Functional characterization of HUVEC-CS: Ca2+ signaling, ERK 1/2 activation, mitogenesis and vasodilator production." J Endocrinol **182**(3): 485-99.

Gimbrone, M. A., Jr., R. S. Cotran, et al. (1974). "Human vascular endothelial cells in culture. Growth and DNA synthesis." J Cell Biol **60**(3): 673-84.

Graham, F. L. and A. J. van der Eb (1973). "A new technique for the assay of infectivity of human adenovirus 5 DNA." Virology **52**(2): 456-67.

Grandgenett, D. P. and S. R. Mumm (1990). "Unraveling retrovirus integration." Cell **60**(1): 3-4.

Gregoire, M., R. Morais, et al. (1984). "On auxotrophy for pyrimidines of respiration-deficient chick embryo cells." Eur J Biochem **142**(1): 49-55.

Guzik, T. J. and D. G. Harrison (2006). "Vascular NADPH oxidases as drug targets for novel antioxidant strategies." Drug Discov Today **11**(11-12): 524-33.

Guzik, T. J., J. Sadowski, et al. (2004). "Systemic regulation of vascular NAD(P)H oxidase activity and nox isoform expression in human arteries and veins." Arterioscler Thromb Vasc Biol **24**(9): 1614-20.

Haendeler, J., J. Hoffmann, et al. (2004). "Antioxidants inhibit nuclear export of telomerase reverse transcriptase and delay replicative senescence of endothelial cells." Circ Res **94**(6): 768-75.

Harman, D. (1956). "Aging: a theory based on free radical and radiation chemistry." J Gerontol **11**(3): 298-300.

Harman, D. (1972). "The biologic clock: the mitochondria?" J Am Geriatr Soc **20**(4): 145-7.

Hayashi, T., H. Matsui-Hirai, et al. (2006). "Endothelial cellular senescence is inhibited by nitric oxide: Implications in atherosclerosis associated with menopause and diabetes." Proc Natl Acad Sci USA **103**(45): 17018-23.

Hayflick, L. (1965). "The Limited in Vitro Lifetime of Human Diploid Cell Strains." Exp Cell Res **37**: 614-36.

Hayflick, L. (1997). "Mortality and immortality at the cellular level. A review." Biochemistry (Mosc) **62**(11): 1180-90.

Heart-Protection-Study-Collaborative-Group (2002). "MRC/BHF Heart Protection Study of antioxidant vitamin supplementation in 20,536 high-risk individuals: a randomised placebo-controlled trial." Lancet **360**(9326): 23-33.

Heffelfinger, S. C., H. H. Hawkins, et al. (1992). "SK HEP-1: a human cell line of endothelial origin." In Vitro Cell Dev Biol **28A**(2): 136-42.

Heitzer, T., T. Schlinzig, et al. (2001). "Endothelial dysfunction, oxidative stress, and risk of cardiovascular events in patients with coronary artery disease." Circulation **104**(22): 2673-8.

Heller, R., A. Unbehaun, et al. (2001). "L-ascorbic acid potentiates endothelial nitric oxide synthesis via a chemical stabilization of tetrahydrobiopterin." J Biol Chem **276**(1): 40-7.

Herbette, S., P. Roeckel-Drevet, et al. (2007). "Seleno-independent glutathione peroxidases. More than simple antioxidant scavengers." Febs J **274**(9): 2163-80.

Herst, P. M. and M. V. Berridge (2007). "Cell surface oxygen consumption: a major contributor to cellular oxygen consumption in glycolytic cancer cell lines." Biochim Biophys Acta **1767**(2): 170-7.

Herst, P. M., A. S. Tan, et al. (2004). "Cell surface oxygen consumption by mitochondrial gene knockout cells." Biochim Biophys Acta **1656**(2-3): 79-87.

Heumuller, S., S. Wind, et al. (2008). "Apocynin is not an inhibitor of vascular NADPH oxidases but an antioxidant." Hypertension **51**(2): 211-7.

Ho, Y. S., Y. Xiong, et al. (2004). "Mice lacking catalase develop normally but show differential sensitivity to oxidant tissue injury." J Biol Chem **279**(31): 32804-12.

Hobbs, A. J., A. Higgs, et al. (1999). "Inhibition of nitric oxide synthase as a potential therapeutic target." Annu Rev Pharmacol Toxicol **39**: 191-220.

Hogrefe, H. H., C. J. Hansen, et al. (2002). "Archaeal dUTPase enhances PCR amplifications with archaeal DNA polymerases by preventing dUTP incorporation." Proc Natl Acad Sci USA **99**(2): 596-601.

Holland, J. J. (1963). "Effects of Puromycin on Rna Synthesis in Mammalian Cells." Proc Natl Acad Sci USA **50**: 436-46.

Holmgren, A. (1989). "Thioredoxin and glutaredoxin systems." J Biol Chem **264**(24): 13963-6.

Hong, Y., M. Quintero, et al. (2007). "Evidence against the involvement of nitric oxide in the modulation of telomerase activity or replicative capacity of human endothelial cells." Exp Gerontol **42**(9): 904-10.

Hudson, B., W. B. Upholt, et al. (1969). "The use of an ethidium analogue in the dye-buoyant density procedure for the isolation of closed circular DNA: the variation of the superhelix density of mitochondrial DNA." Proc Natl Acad Sci USA **62**(3): 813-20.

Invitrogen (2008). "pcDNA™4/TO Expression vector designed for use with the T-REx™ System." Invitrogen Ltd.

Itahana, K., J. Campisi, et al. (2007). "Methods to detect biomarkers of cellular senescence: the senescence-associated beta-galactosidase assay." Methods Mol Biol **371**: 21-31.

Itoh, K., N. Wakabayashi, et al. (1999). "Keap1 represses nuclear activation of antioxidant responsive elements by Nrf2 through binding to the amino-terminal Neh2 domain." Genes Dev **13**(1): 76-86.

Iwata, S., J. W. Lee, et al. (1998). "Complete structure of the 11-subunit bovine mitochondrial cytochrome bc1 complex." Science **281**(5373): 64-71.

Jacobson, M. D., J. F. Burne, et al. (1993). "Bcl-2 blocks apoptosis in cells lacking mitochondrial DNA." Nature **361**(6410): 365-9.

Jannasch, H. W., C. O. Wirsen, et al. (1992). "Comparative Physiological Studies on Hyperthermophilic Archaea Isolated from Deep-Sea Hot Vents with Emphasis on Pyrococcus Strain GB-D." Appl Environ Microbiol **58**(11): 3472-3481.

Jazayeri, M., A. Andreyev, et al. (2003). "Inducible expression of a dominant negative DNA polymerase-gamma depletes mitochondrial DNA and produces a rho0 phenotype." J Biol Chem **278**(11): 9823-30.

Jensen, P. K. (1966). "Antimycin-insensitive oxidation of succinate and reduced nicotinamide-adenine dinucleotide in electron-transport particles. I. pH dependency and hydrogen peroxide formation." Biochim Biophys Acta **122**(2): 157-66.

Jeong, S. Y. and D. W. Seol (2008). "The role of mitochondria in apoptosis." BMB Rep **41**(1): 11-22.

Jiang, F., S. J. Roberts, et al. (2006). "NO modulates NADPH oxidase function via heme oxygenase-1 in human endothelial cells." Hypertension **48**(5): 950-7.

Jiang, S., J. Cai, et al. (1999). "Cytochrome c-mediated apoptosis in cells lacking mitochondrial DNA. Signaling pathway involving release and caspase 3 activation is conserved." J Biol Chem **274**(42): 29905-11.

Kasprzak, J. D., M. Klosinska, et al. (2006). "Clinical aspects of assessment of endothelial function." Pharmacol Rep **58 Suppl**: 33-40.

Kerr, J. F., A. H. Wyllie, et al. (1972). "Apoptosis: a basic biological phenomenon with wide-ranging implications in tissue kinetics." Br J Cancer **26**(4): 239-57.

King, M. P. and G. Attardi (1988). "Injection of mitochondria into human cells leads to a rapid replacement of the endogenous mitochondrial DNA." Cell **52**(6): 811-9.

King, M. P. and G. Attardi (1989). "Human cells lacking mtDNA: repopulation with exogenous mitochondria by complementation." Science **246**(4929): 500-3.

King, M. P. and G. Attardi (1996). "Isolation of human cell lines lacking mitochondrial DNA." Methods Enzymol **264**: 304-13.

Klingbeil, A. U., S. John, et al. (2003). "Effect of AT1 receptor blockade on endothelial function in essential hypertension." Am J Hypertens **16**(2): 123-8.

Krebs, H. A. and W. A. Johnson (1937). "The role of citric acid in intermediate metabolism in animal tissues." Enzymologia **4**: 148-56.

Kresge, N., R. D. Simoni, et al. (2005). "Otto Fritz Meyerhof and the elucidation of the glycolytic pathway." J Biol Chem **280**(4): e3.

Krishnamurthy, J., C. Torrice, et al. (2004). "Ink4a/Arf expression is a biomarker of aging." J Clin Invest **114**(9): 1299-307.

Kurz, D. J., S. Decary, et al. (2000). "Senescence-associated (beta)-galactosidase reflects an increase in lysosomal mass during replicative ageing of human endothelial cells." J Cell Sci **113 (Pt 20)**: 3613-22.

Kurz, D. J., S. Decary, et al. (2004). "Chronic oxidative stress compromises telomere integrity and accelerates the onset of senescence in human endothelial cells." J Cell Sci **117**(Pt 11): 2417-26.

Lafuente, N., N. Matesanz, et al. (2008). "The deleterious effect of high concentrations of D-glucose requires pro-inflammatory preconditioning." J Hypertens **26**(3): 478-85.

Lambert, A. J. and M. D. Brand (2004). "Superoxide production by NADH:ubiquinone oxidoreductase (complex I) depends on the pH gradient across the mitochondrial inner membrane." Biochem J **382**(Pt 2): 511-7.

Larm, J. A., F. Vaillant, et al. (1994). "Up-regulation of the plasma membrane oxidoreductase as a prerequisite for the viability of human Namalwa rho 0 cells." J Biol Chem **269**(48): 30097-100.

Le, S. B., M. K. Hailer, et al. (2007). "Inhibition of mitochondrial respiration as a source of adaphostin-induced reactive oxygen species and cytotoxicity." J Biol Chem **282**(12): 8860-72.

Lee, M. S., J. Y. Kim, et al. (2004). "Resistance of rho(0) cells against apoptosis." Ann N Y Acad Sci **1011**: 146-53.

Lee, S. B., I. H. Bae, et al. (2006). "Link between mitochondria and NADPH oxidase 1 isozyme for the sustained production of reactive oxygen species and cell death." J Biol Chem **281**(47): 36228-35.

Li, J. M. and A. M. Shah (2002). "Intracellular localization and preassembly of the NADPH oxidase complex in cultured endothelial cells." J Biol Chem **277**(22): 19952-60.

Li, J. M. and A. M. Shah (2003). "Mechanism of endothelial cell NADPH oxidase activation by angiotensin II. Role of the p47phox subunit." J Biol Chem. **278**(14): 12094-100. Epub 2003 Jan 30.

Liao, J. K. (2002). "Beyond lipid lowering: the role of statins in vascular protection." Int J Cardiol **86**(1): 5-18.

Liao, S., J. A. Curci, et al. (2000). "Accelerated replicative senescence of medial smooth muscle cells derived from abdominal aortic aneurysms compared to the adjacent inferior mesenteric artery." J Surg Res **92**(1): 85-95.

Lin, J., C. Handschin, et al. (2005). "Metabolic control through the PGC-1 family of transcription coactivators." Cell Metab **1**(6): 361-70.

Lipman, F. (1941). "Metabolic generation and utilization of phosphate bond energy." Adv. Enzymol. **1**(99): 162.

Liu, D., C. Li, et al. (2004). "Nuclear import of proinflammatory transcription factors is required for massive liver apoptosis induced by bacterial lipopolysaccharide." J Biol Chem **279**(46): 48434-42.

Liu, X., C. N. Kim, et al. (1996). "Induction of apoptotic program in cell-free extracts: requirement for dATP and cytochrome c." Cell **86**(1): 147-57.

Lonn, E., J. Bosch, et al. (2005). "Effects of long-term vitamin E supplementation on cardiovascular events and cancer: a randomized controlled trial." Jama **293**(11): 1338-47.

Lundberg, K. S., D. D. Shoemaker, et al. (1991). "High-fidelity amplification using a thermostable DNA polymerase isolated from Pyrococcus furiosus." Gene **108**(1): 1-6.

Lyman, C. P., R. C. O'Brien, et al. (1981). "Hibernation and longevity in the Turkish hamster Mesocricetus brandti." Science **212**(4495): 668-70.

Maciag, T., J. Kadish, et al. (1982). "Organizational behavior of human umbilical vein endothelial cells." J Cell Biol **94**(3): 511-20.

Manconi, F., R. Markham, et al. (2000). "Culturing endothelial cells of microvascular origin." Methods Cell Sci **22**(2-3): 89-99.

Mann, G. E., D. L. Yudilevich, et al. (2003). "Regulation of amino acid and glucose transporters in endothelial and smooth muscle cells." Physiol Rev **83**(1): 183-252.

Martin, G. M. (2005). "Genetic modulation of senescent phenotypes in Homo sapiens." Cell **120**(4): 523-32.

Masaki, N., M. E. Kyle, et al. (1989). "Mitochondrial damage as a mechanism of cell injury in the killing of cultured hepatocytes by tert-butyl hydroperoxide." Arch Biochem Biophys **270**(2): 672-80.

Mass, H., B. Pirazzi, et al. (1995). "N-acetylcysteine diminishes injury induced by balloon angioplasty of the carotid artery in rabbits." Biochem Biophys Res Commun **215**(2): 613-8.

Matsumoto, T., V. D'Uscio L, et al. (2003). "Protective effect of chronic vitamin C treatment on endothelial function of apolipoprotein E-deficient mouse carotid artery." J Pharmacol Exp Ther **306**(1): 103-8.

Matthews, C., I. Gorenne, et al. (2006). "Vascular Smooth Muscle Cells Undergo Telomere-Based Senescence in Human Atherosclerosis. Effects of Telomerase and Oxidative Stress." Circ Res **99**(2): 156-64.

McBride, H. M., M. Neuspiel, et al. (2006). "Mitochondria: more than just a powerhouse." Curr Biol **16**(14): R551-60.

Michiels, C. (2003). "Endothelial cell functions." J Cell Physiol **196**(3): 430-43.

Michikawa, Y., F. Mazzucchelli, et al. (1999). "Aging-dependent large accumulation of point mutations in the human mtDNA control region for replication." Science **286**(5440): 774-9.

Miller, S. W., P. A. Trimmer, et al. (1996). "Creation and characterization of mitochondrial DNA-depleted cell lines with "neuronal-like" properties." J Neurochem **67**(5): 1897-907.

Minamino, T. and I. Komuro (2007). "Vascular Cell Senescence: Contribution to Atherosclerosis." Circ Res **100**(1): 15-26.

Minamino, T., H. Miyauchi, et al. (2002). "Endothelial cell senescence in human atherosclerosis: role of telomere in endothelial dysfunction." Circulation **105**(13): 1541-4.

Minsky, M. (1961). "Microscopy Apparatus." European patent office.

Moncada, S., J. F. Martin, et al. (1993). "Symposium on regression of atherosclerosis." Eur J Clin Invest **23**(7): 385-98.

Monteiro, P., A. I. Duarte, et al. (2005). "Valsartan improves mitochondrial function in hearts submitted to acute ischemia." Eur J Pharmacol **518**(2-3): 158-64.

Morais, R., P. Desjardins, et al. (1988). "Development and characterization of continuous avian cell lines depleted of mitochondrial DNA." In Vitro Cell Dev Biol **24**(7): 649-58.

Morgenstern, J. P. and H. Land (1990). "Advanced mammalian gene transfer: high titre retroviral vectors with multiple drug selection markers and a complementary helper-free packaging cell line." Nucleic Acids Res **18**(12): 3587-96.

Muller, F. L., M. S. Lustgarten, et al. (2007). "Trends in oxidative aging theories." Free Radic Biol Med **43**(4): 477-503.

Nagley, P. and A. W. Linnane (1970). "Mitochondrial DNA deficient petite mutants of yeast." Biochem Biophys Res Commun **39**(5): 989-96.

Nass, M. M. (1970). "Abnormal DNA patterns in animal mitochondria: ethidium bromide-induced breakdown of closed circular DNA and conditions leading to oligomer accumulation." Proc Natl Acad Sci USA **67**(4): 1926-33.

Nass, M. M. (1972). "Differential effects of ethidium bromide on mitochondrial and nuclear DNA synthesis in vivo in cultured mammalian cells." Exp Cell Res **72**(1): 211-22.

Nguyen, T., P. Nioi, et al. (2009). "The Nrf2-antioxidant response element signaling pathway and its activation by oxidative stress." J Biol Chem **284**(20): 13291-5.

Nirenberg, M. W. and J. F. Hogg (1958). "Inhibition of anaerobic glycolysis in Ehrlich ascites tumor cells by 2-deoxy-D-glucose." Cancer Res **18**(5): 518-21.

Nisoli, E., C. Tonello, et al. (2005). "Calorie restriction promotes mitochondrial biogenesis by inducing the expression of eNOS." Science **310**(5746): 314-7.

O'Donnell, B. V., D. G. Tew, et al. (1993). "Studies on the inhibitory mechanism of iodonium compounds with special reference to neutrophil NADPH oxidase." Biochem J **290 (Pt 1)**: 41-9.

O'Malley, Y., B. D. Fink, et al. (2006). "Reactive oxygen and targeted antioxidant administration in endothelial cell mitochondria." J Biol Chem **281**(52): 39766-75.

Ochi, T. and S. Miyaura (1989). "Cytotoxicity of an organic hydroperoxide and cellular antioxidant defense system against hydroperoxides in cultured mammalian cells." Toxicology **55**(1-2): 69-82.

Olofsson, A. M., M. Vestberg, et al. (1999). "Heparin-binding protein targeted to mitochondrial compartments protects endothelial cells from apoptosis." J Clin Invest **104**(7): 885-94.

Orlowski, M. and A. Meister (1970). "The gamma-glutamyl cycle: a possible transport system for amino acids." Proc Natl Acad Sci USA **67**(3): 1248-55.

Palacios-Callender, M., V. Hollis, et al. (2007). "Cytochrome c oxidase maintains mitochondrial respiration during partial inhibition by nitric oxide." J Cell Sci **120**(Pt 1): 160-5.

Palacios-Callender, M., V. Hollis, et al. (2007). "Cytochrome c oxidase regulates endogenous nitric oxide availability in respiring cells: a possible explanation for hypoxic vasodilation." Proc Natl Acad Sci USA **104**(47): 18508-13.

Palacios-Callender, M., M. Quintero, et al. (2004). "Endogenous NO regulates superoxide production at low oxygen concentrations by modifying the redox state of cytochrome c oxidase." Proc Natl Acad Sci USA **101**(20): 7630-5.

Palmer, R. M., A. G. Ferrige, et al. (1987). "Nitric oxide release accounts for the biological activity of endothelium-derived relaxing factor." Nature **327**(6122): 524-6.

Paolini, M., A. Sapone, et al. (2003). "Antioxidant vitamins for prevention of cardiovascular disease." Lancet **362**(9387): 920; author reply 921.

Papaiahgari, S., S. R. Kleeberger, et al. (2004). "NADPH oxidase and ERK signaling regulates hyperoxia-induced Nrf2-ARE transcriptional response in pulmonary epithelial cells." J Biol Chem **279**(40): 42302-12.

Park, K. S., K. J. Nam, et al. (2001). "Depletion of mitochondrial DNA alters glucose metabolism in SK-Hep1 cells." Am J Physiol Endocrinol Metab **280**(6): E1007-14.

Park, S. Y., I. Chang, et al. (2004). "Resistance of mitochondrial DNA-depleted cells against cell death: role of mitochondrial superoxide dismutase." J Biol Chem **279**(9): 7512-20.

Park, S. Y., B. Choi, et al. (2004). "Cellular aging of mitochondrial DNA-depleted cells." Biochem Biophys Res Commun **325**(4): 1399-405.

Park, S. Y., G. H. Choi, et al. (2005). "Depletion of mitochondrial DNA causes impaired glucose utilization and insulin resistance in L6 GLUT4myc myocytes." Journal of Biological Chemistry **280**(11): 9855-64.

Passos, J. F. and T. von Zglinicki (2005). "Mitochondria, telomeres and cell senescence." Exp Gerontol **40**(6): 466-72.

Passos, J. F., T. Zglinicki, et al. (2006). "Mitochondrial dysfunction and cell senescence: cause or consequence?" Rejuvenation Res **9**(1): 64-8.

Pearl, R. (1929). "The rate of living." New York, Alfred A. Knopf, Inc.

Pias, E. K., O. Y. Ekshyyan, et al. (2003). "Differential effects of superoxide dismutase isoform expression on hydroperoxide-induced apoptosis in PC-12 cells." J Biol Chem **278**(15): 13294-301.

Piconi, L., L. Quagliaro, et al. (2006). "Constant and intermittent high glucose enhances endothelial cell apoptosis through mitochondrial superoxide overproduction." Diabetes Metab Res Rev **22**(3): 198-203.

Pillarisetti, S. (2008). "A review of Sirt1 and Sirt1 modulators in cardiovascular and metabolic diseases." Recent Pat Cardiovasc Drug Discov **3**(3): 156-64.

Polyak, K., Y. Li, et al. (1998). "Somatic mutations of the mitochondrial genome in human colorectal tumours." Nat Genet **20**(3): 291-3.

Poot, M., Y. Z. Zhang, et al. (1996). "Analysis of mitochondrial morphology and function with novel fixable fluorescent stains." J Histochem Cytochem **44**(12): 1363-72.

QIAGEN (2005). "QIAprep® Miniprep Handbook." QIAGEN Ltd.

Quintero, M., S. L. Colombo, et al. (2006). "Mitochondria as signaling organelles in the vascular endothelium." Proc Natl Acad Sci USA **103**(14): 5379-84.

Rasola, A. and P. Bernardi (2007). "The mitochondrial permeability transition pore and its involvement in cell death and in disease pathogenesis." Apoptosis **12**(5): 815-33.

Ray, R. and A. M. Shah (2005). "NADPH oxidase and endothelial cell function." Clin Sci (Lond). **109**(3): 217-26.

Rich, P. R. (2003). "The molecular machinery of Keilin's respiratory chain." Biochem Soc Trans **31**(Pt 6): 1095-105.

Riley, P. A. (1994). "Free radicals in biology: oxidative stress and the effects of ionizing radiation." Int J Radiat Biol **65**(1): 27-33.

Rina, M., C. Pozidis, et al. (2000). "Alkaline phosphatase from the Antarctic strain TAB5. Properties and psychrophilic adaptations." Eur J Biochem **267**(4): 1230-8.

Roche (2004). "Colorimetric immunoassay for the quantification of cell proliferation, based on the measurement of BrdU incorporation during DNA synthesis. Instruction manual." Roche Ltd.

Ropp, P. A. and W. C. Copeland (1996). "Cloning and characterization of the human mitochondrial DNA polymerase, DNA polymerase gamma." Genomics **36**(3): 449-58.

Rosenkranz, A. R., S. Schmaldienst, et al. (1992). "A microplate assay for the detection of oxidative products using 2',7'-dichlorofluorescin-diacetate." J Immunol Methods **156**(1): 39-45.

Rouzer, C. A., W. A. Scott, et al. (1981). "Depletion of glutathione selectively inhibits synthesis of leukotriene C by macrophages." Proc Natl Acad Sci USA **78**(4): 2532-6.

Rustin, P. and A. Rotig (2002). "Inborn errors of complex II--unusual human mitochondrial diseases." Biochim Biophys Acta **1553**(1-2): 117-22.

Sablina, A. A., A. V. Budanov, et al. (2005). "The antioxidant function of the p53 tumor suppressor." Nat Med **11**(12): 1306-13.

Sanz, A., R. Pamplona, et al. (2006). "Is the mitochondrial free radical theory of aging intact?" Antioxid Redox Signal **8**(3-4): 582-99.

Sato, A., K. Nakada, et al. (2006). "Mitochondrial dynamics and aging: Mitochondrial interaction preventing individuals from expression of respiratory deficiency caused by mutant mtDNA." Biochim Biophys Acta **1763**(5-6): 473-81.

Scaffidi, C., S. Fulda, et al. (1998). "Two CD95 (APO-1/Fas) signaling pathways." Embo J **17**(6): 1675-87.

Scandalios, J. G. (2005). "Oxidative stress: molecular perception and transduction of signals triggering antioxidant gene defenses." Braz J Med Biol Res **38**(7): 995-1014.

Schauen, M., D. Spitkovsky, et al. (2006). "Respiratory chain deficiency slows down cell-cycle progression via reduced ROS generation and is associated with a reduction of p21CIP1/WAF1." J Cell Physiol **209**(1): 103-12.

Schultz, B. E. and S. I. Chan (2001). "Structures and proton-pumping strategies of mitochondrial respiratory enzymes." Annu Rev Biophys Biomol Struct **30**: 23-65.

Schumann, J., F. Ehring, et al. (1971). "[Pulse cytophotometry of DNA in skin tumours]." Arch Klin Exp Dermatol **239**(4): 377-89.

Scott, I. D. and D. G. Nicholls (1980). "Energy transduction in intact synaptosomes. Influence of plasma-membrane depolarization on the respiration and membrane potential of internal mitochondria determined in situ." Biochem J **186**(1): 21-33.

Sekhar, K. R., P. A. Crooks, et al. (2003). "NADPH oxidase activity is essential for Keap1/Nrf2-mediated induction of GCLC in response to 2-indol-3-yl-methylenequinuclidin-3-ols." Cancer Res **63**(17): 5636-45.

Serrano, M. and M. A. Blasco (2001). "Putting the stress on senescence." Curr Opin Cell Biol **13**(6): 748-53.

Shen, J., N. Khan, et al. (2003). "Oxygen consumption rates and oxygen concentration in molt-4 cells and their mtDNA depleted (rho0) mutants." Biophys J **84**(2 Pt 1): 1291-8.

Shepherd, J., S. M. Cobbe, et al. (1995). "Prevention of coronary heart disease with pravastatin in men with hypercholesterolemia. West of Scotland Coronary Prevention Study Group." N Engl J Med **333**(20): 1301-7.

Simons, J. M., B. A. Hart, et al. (1990). "Metabolic activation of natural phenols into selective oxidative burst agonists by activated human neutrophils." Free Radic Biol Med **8**(3): 251-8.

Singh, K. K. (2006). "Mitochondria damage checkpoint, aging, and cancer." Ann N Y Acad Sci **1067**: 182-90.

Skyrme-Jones, R. A., R. C. O'Brien, et al. (2000). "Vitamin E supplementation improves endothelial function in type I diabetes mellitus: a randomized, placebo-controlled study." J Am Coll Cardiol **36**(1): 94-102.

Sohal, R. S., R. J. Mockett, et al. (2002). "Mechanisms of aging: an appraisal of the oxidative stress hypothesis." Free Radic Biol Med **33**(5): 575-86.

Sokal, A. and G. Bartosz (1998). "Uncouplers of mitochondrial oxidative phosphorylation are not substrates of the erythrocyte glutathione-S-conjugate pump." Arch Biochem Biophys **349**(1): 113-21.

Sorescu, D., D. Weiss, et al. (2002). "Superoxide production and expression of nox family proteins in human atherosclerosis." Circulation **105**(12): 1429-35.

Spector, A., W. Ma, et al. (2002). "The effect of H2O2 and tertiary butyl hydroperoxide upon a murine immortal lens epithelial cell line, alphaTN4-1." Exp Eye Res **75**(5): 573-82.

St-Pierre, J., S. Drori, et al. (2006). "Suppression of reactive oxygen species and neurodegeneration by the PGC-1 transcriptional coactivators." Cell **127**(2): 397-408.

Stocker, R. and M. A. Perrella (2006). "Heme oxygenase-1: a novel drug target for atherosclerotic diseases?" Circulation **114**(20): 2178-89.

Stratagene (2004). "QuikChange® II XL Site-Directed Mutagenesis Kit Instruction Manual." Stratagene Ltd.

Subramanian, V. A., Y. Hernandez, et al. (1986). "Prostacyclin production by internal mammary artery as a factor in coronary artery bypass grafts." Surgery **100**(2): 376-83.

Susin, S. A., H. K. Lorenzo, et al. (1999). "Molecular characterization of mitochondrial apoptosis-inducing factor." Nature **397**(6718): 441-6.

Tesauro, M., W. C. Thompson, et al. (2005). "Effect of staurosporine-induced apoptosis on endothelial nitric oxide synthase in transfected COS-7 cells and primary endothelial cells." Cell Death Differ **13**(4): 597.

The Office for National Statistics (2003). "Review of the Registrar General on deaths by cause, sex and age, in England and Wales, 2002." Her Majesty's Sationary Office.

Thierbach, G. and H. Reichenbach (1981). "Myxothiazol, a new antibiotic interfering with respiration." Antimicrob Agents Chemother **19**(4): 504-7.

Thierbach, G. and H. Reichenbach (1981). "Myxothiazol, a new inhibitor of the cytochrome b-c1 segment of th respiratory chain." Biochim Biophys Acta **638**(2): 282-9.

Tian, W. N., L. D. Braunstein, et al. (1998). "Importance of glucose-6-phosphate dehydrogenase activity for cell growth." J Biol Chem **273**(17): 10609-17.

Tietze, F. (1969). "Enzymic method for quantitative determination of nanogram amounts of total and oxidized glutathione: applications to mammalian blood and other tissues." Anal Biochem **27**(3): 502-22.

Toussaint, O., E. E. Medrano, et al. (2000). "Cellular and molecular mechanisms of stress-induced premature senescence (SIPS) of human diploid fibroblasts and melanocytes." Exp Gerontol **35**(8): 927-45.

Trifunovic, A., A. Wredenberg, et al. (2004). "Premature ageing in mice expressing defective mitochondrial DNA polymerase." Nature **429**(6990): 417-23.

Tsuneki, H., N. Sekizaki, et al. (2007). "Coenzyme Q10 prevents high glucose-induced oxidative stress in human umbilical vein endothelial cells." Eur J Pharmacol **566**(1-3): 1-10.

Turkseven, S., A. Kruger, et al. (2005). "Antioxidant mechanism of heme oxygenase-1 involves an increase in superoxide dismutase and catalase in experimental diabetes." Am J Physiol Heart Circ Physiol **289**(2): H701-7.

Tuzcu, E. M., S. R. Kapadia, et al. (2001). "High prevalence of coronary atherosclerosis in asymptomatic teenagers and young adults: evidence from intravascular ultrasound." Circulation **103**(22): 2705-10.

Unterluggauer, H., B. Hampel, et al. (2003). "Senescence-associated cell death of human endothelial cells: the role of oxidative stress." Exp Gerontol **38**(10): 1149-60.

Vaheri, A. and J. S. Pagano (1965). "Infectious poliovirus RNA: a sensitive method of assay." Virology **27**(3): 434-6.

Valle, I., A. Alvarez-Barrientos, et al. (2005). "PGC-1alpha regulates the mitochondrial antioxidant defense system in vascular endothelial cells." Cardiovasc Res **66**(3): 562-73.

van der Loo, B., M. J. Fenton, et al. (1998). "Cytochemical detection of a senescence-associated beta-galactosidase in endothelial and smooth muscle cells from human and rabbit blood vessels." Exp Cell Res **241**(2): 309-15.

Vanderkooi, J. M., M. Erecinska, et al. (1991). "Oxygen in mammalian tissue: methods of measurement and affinities of various reactions." Am J Physiol **260**(6 Pt 1): C1131-50.

Vara, J. A., A. Portela, et al. (1986). "Expression in mammalian cells of a gene from Streptomyces alboniger conferring puromycin resistance." Nucleic Acids Res **14**(11): 4617-24.

Vasa, M., K. Breitschopf, et al. (2000). "Nitric oxide activates telomerase and delays endothelial cell senescence." Circ Res **87**(7): 540-2.

Vaux, D. L., S. Cory, et al. (1988). "Bcl-2 gene promotes haemopoietic cell survival and cooperates with c-myc to immortalize pre-B cells." Nature **335**(6189): 440-2.

Vergani, L., M. Floreani, et al. (2004). "Antioxidant defences and homeostasis of reactive oxygen species in different human mitochondrial DNA-depleted cell lines." Eur J Biochem **271**(18): 3646-56.

Verlangieri, A. J. and M. J. Bush (1992). "Effects of d-alpha-tocopherol supplementation on experimentally induced primate atherosclerosis." J Am Coll Nutr **11**(2): 131-8.

Vermes, I., C. Haanen, et al. (1995). "A novel assay for apoptosis. Flow cytometric detection of phosphatidylserine expression on early apoptotic cells using fluorescein labelled Annexin V." J Immunol Methods **184**(1): 39-51.

Vermeulen, K., D. R. Van Bockstaele, et al. (2005). "Apoptosis: mechanisms and relevance in cancer." Ann Hematol **84**(10): 627-39.

von Zglinicki, T., G. Saretzki, et al. (1995). "Mild hyperoxia shortens telomeres and inhibits proliferation of fibroblasts: a model for senescence?" Exp Cell Res **220**(1): 186-93.

Voyta, J. C., D. P. Via, et al. (1984). "Identification and isolation of endothelial cells based on their increased uptake of acetylated-low density lipoprotein." J Cell Biol **99**(6): 2034-40.

Wagener, F. A., J. L. da Silva, et al. (1999). "Differential effects of heme oxygenase isoforms on heme mediation of endothelial intracellular adhesion molecule 1 expression." J Pharmacol Exp Ther **291**(1): 416-23.

Wang, C., M. W. Wang, et al. (2005). "IL-1beta acts in synergy with endogenous IL-1beta in A375-S2 human melanoma cell apoptosis through mitochondrial pathway." J Korean Med Sci **20**(4): 555-61.

Wang, H. and J. A. Joseph (1999). "Quantifying cellular oxidative stress by dichlorofluorescein assay using microplate reader." Free Radic Biol Med **27**(5-6): 612-6.

Wang, W., H. Fang, et al. (2008). "Superoxide flashes in single mitochondria." Cell **134**(2): 279-90.

Warnholtz, A., G. Nickenig, et al. (1999). "Increased NADH-oxidase-mediated superoxide production in the early stages of atherosclerosis: evidence for involvement of the renin-angiotensin system." Circulation **99**(15): 2027-33.

Weber, C., W. Erl, et al. (1994). "Antioxidants inhibit monocyte adhesion by suppressing nuclear factor-kappa B mobilization and induction of vascular cell adhesion molecule-1 in endothelial cells stimulated to generate radicals." Arterioscler Thromb **14**(10): 1665-73.

Weiss, B., A. Jacquemin-Sablon, et al. (1968). "Enzymatic breakage and joining of deoxyribonucleic acid. VI. Further purification and properties of polynucleotide ligase from Escherichia coli infected with bacteriophage T4." J Biol Chem **243**(17): 4543-55.

Weissberg, P. L. (2000). "Atherogenesis: current understanding of the causes of atheroma." Heart **83**(2): 247-52.

Wilson, M. T., C. Greenwood, et al. (1975). "Kinetic studies on the reaction between cytochrome c oxidase and ferrocytochrome c." Biochem J **147**(1): 145-53.

Wong, T. K. and E. Neumann (1982). "Electric field mediated gene transfer." Biochem Biophys Res Commun **107**(2): 584-7.

Xu, D., R. Neville, et al. (2000). "Homocysteine accelerates endothelial cell senescence." FEBS Lett **470**(1): 20-4.

Yamawaki, H., J. Haendeler, et al. (2003). "Thioredoxin: a key regulator of cardiovascular homeostasis." Circ Res **93**(11): 1029-33.

Yang, E. and S. J. Korsmeyer (1996). "Molecular thanatopsis: a discourse on the BCL2 family and cell death." Blood **88**(2): 386-401.

Yang, L., S. Quan, et al. (1999). "Retrovirus-mediated HO gene transfer into endothelial cells protects against oxidant-induced injury." Am J Physiol **277**(1 Pt 1): L127-33.

Yet, S. F., M. D. Layne, et al. (2003). "Absence of heme oxygenase-1 exacerbates atherosclerotic lesion formation and vascular remodeling." Faseb J **17**(12): 1759-61.

Yu, R., C. Chen, et al. (2000). "Activation of mitogen-activated protein kinase pathways induces antioxidant response element-mediated gene expression via a Nrf2-dependent mechanism." J Biol Chem **275**(51): 39907-13.

Yusuf, S., P. Sleight, et al. (2000). "Effects of an angiotensin-converting-enzyme inhibitor, ramipril, on cardiovascular events in high-risk patients. The Heart Outcomes Prevention Evaluation Study Investigators." N Engl J Med **342**(3): 145-53.

Zafarullah, M., W. Q. Li, et al. (2003). "Molecular mechanisms of N-acetylcysteine actions." Cell Mol Life Sci **60**(1): 6-20.

Zemojtel, T., M. Kolanczyk, et al. (2006). "Mammalian mitochondrial nitric oxide synthase: characterization of a novel candidate." FEBS Lett **580**(2): 455-62.

Zylber, E., C. Vesco, et al. (1969). "Selective inhibition of the synthesis of mitochondria-associated RNA by ethidium bromide." J Mol Biol **44**(1): 195-204.